CORA Cork Open Research Archive
Cartlann Taighde Oscailte Chorcaí

Title	Identification of the molecular pathways that mediate cytokine induced immunopathology of the gut epithelium
Authors	Saini Rokade, Nisha
Publication date	2020
Original Citation	Saini Rokade, N. 2020. Identification of the molecular pathways that mediate cytokine induced immunopathology of the gut epithelium. PhD Thesis, University College Cork.
Type of publication	Doctoral thesis
Rights	© 2020, Nisha Saini Rokade. - https://creativecommons.org/licenses/by-nc-nd/4.0/
Download date	2026-11-12 12:18:30
Item downloaded from	https://hdl.handle.net/10468/12014

UCC
University College Cork, Ireland
Coláiste na hOllscoile Corcaigh

Ollscoil na hÉireann, Corcaigh

National University of Ireland, Cork



Identification of the Molecular Pathways that Mediate Cytokine induced Immunopathology of the Gut Epithelium

Thesis presented by:

Nisha Saini Rokade, M.Sc.

for the degree of

Doctor of Philosophy

University College Cork

School of Biochemistry and Cell Biology

Head of School: Prof. Rosemary O'Connor

Supervisor: Dr. Ken Nally

2020

Table of Contents

Table of Contents ii
Author's Declaration: vi
Data Attribution: vi
List of Conference Presentations and Publications vii
Journal Article vii
Poster Presentations viii
List of abbreviations: ix
General Abstract xxii
1. Chapter I: Literature Review Crosstalk between IFN-γ & TNF-α Signalling Pathways and Contribution to Cell Death 23
1.1. Interferon-gamma (IFN-γ) 24
1.1.1. IFN-γ gene 24
1.1.2. IFN-γ Protein 24
1.1.3 IFN-γ receptors (IFNGR) 25
1.1.3. JAK-STAT signalling pathway 26
1.1.4. Nuclear translocation of STAT1 28
1.1.5. Post-translational modifications of STATs 31
1.1.6. Role of unphosphorylated STATs 32
1.1.7. Feedback regulation of the JAK-STAT pathway 33
1.1.8. Clinical targeting of JAK-STAT pathway 34
1.1.9. Effects of IFN-γ on Immune Cell Activation 38
1.1.10. Anti-Microbial activities 40
1.1.11. Dual Roles of IFN- γ in Cancer 41
1.1.12. IFN-γ in regulation of epithelial homeostasis 45
1.2. Tumour necrosis factor alpha 48
1.2.1. TNF-α gene 48
1.2.2. TNF-α protein: 48
1.2.3. TNF receptors (TNFR) family 49
1.2.4. TNFR1 Signalling by Complex-1 50
1.2.5. TNFR1 Signalling by Complex-II 54
1.2.6. Dual role of TNF in cancer 59
1.2.7. TNF-α in regulation of intestinal homeostasis and inflammation 60
1.3. IFN-γ and TNF-α cross talk in signalling 62
1.4. IFN-γ and TNF-α transcriptional cross talk 65
1.5. IFN-γ and TNF-α Crosstalk and Cell death 68

1.6. References 73
2. Chapter 2: IFN-γ and TNF-α synergise to kill intestinal epithelial cells through a JAK1/2 dependent pathway 108
2.1. Abstract: 109
2.2. Introduction 110
2.3. Methods and Materials 114
2.3.1. Cell culture 114
2.3.2. Reagents 115
2.3.3. CRISPR/Cas9 knockout cell lines 115
2.3.4. Cell death assays 116
2.3.5. Human Kinome RNAi screen 117
2.3.6. Drug library screen 117
2.3.7. Transfections, RNAi, and RT-qPCR 118
2.3.8. Cell lysis and immunoblotting 120
2.3.9. Cellular and mitochondrial ROS measurement 121
2.3.10. Human Colonic Organoids 121
2.3.11. Statistical analysis 123
2.4. Results 124
2.4.1. IFN-γ and TNF-α synergise to induce cell death in colorectal cancer cells 124
2.4.2. IFN-γ and TNF-α synergise to induce cell death in colorectal cancer cells in a JAK1 and JAK2 dependent manner 129
2.4.3. IFN-γ + TNF-α induced killing is independent of TNFR1 associated apoptotic and necroptotic pathways 139
2.4.4. IFN-γ + TNF-α induced killing is caspase-8-dependent but independent of caspase-8 enzymatic activity 144
2.4.5. IFN-γ+TNF-α induced synergistic cell death is independent of the BCL2 family members BAK and BAX 149
2.4.6. IFN-γ/TNF-α synergize to induce cell death in human colonic organoids in a JAK1/2 dependent manner 153
2.5. Discussion 157
2.6. References 162
3. Chapter 3: Identification of the Mechanisms Underpinning Concentration Dependent Effects of IFN-γ and TNF-α on Epithelial Cell Death Decisions 175
3.1. Abstract 176
3.2. Introduction 178
3.3. Methods and material 181
3.3.1. Cell culture 181
3.3.2. Reagents 181
3.3.3. Cell death assays 182

3.3.4. CXCL-10 chemokine analysis 182
3.3.5. RNA isolation and quantitative RT-PCR 183
3.3.6. Cell lysis and immunoblotting 184
3.3.7. Homogeneous Time Resolved Fluorescence (HTRF assay) 185
3.3.8. Cellular fractionation experiments 186
3.3.9. Total RNA extraction and RNA-Sequencing 186
3.3.10. RNA-Seq data analysis 187
3.3.11. Principal Component Analysis 187
3.3.12. Differential Expression (DE) Analysis 188
3.3.13. Pathway analysis 188
3.3.14. Statistical Analysis 189
3.4. Results 190
3.4.1. IFN-γ and TNF-α synergise to induce cell death in colorectal cancer cell lines in a concentration-dependent manner. 190
3.4.2. IFN-γ and TNF-α induced expression of pro-inflammatory and pro-apoptotic genes in a concentration dependent manner 194
3.4.3. JAK1/2-STAT1 signalling induced by the combination of IFN-γ + TNF-α follows a dose-to-duration pattern. 198
3.4.4. The combination of IFN-γ + TNF-α at high concentrations induced sustained activation of STAT1 in both the cytoplasm and nucleus of colorectal cancer cells 203
3.4.5. Sustained activation of JAK1/2-STAT1 pathway is essential for the induction of cell death in HT-29 cells 205
3.4.6. RNA-Seq analysis identifies differentially expressed genes which are associated with the concentration of cytokines and the duration of cytokine treatment 209
3.4.7. The cytotoxic concentration of cytokines induced the differential expression of a unique set of genes at later time points post-cytokine treatment 217
3.4.8. IFN-γ and TNF-α induced late genes are associated with the induction of multiple cell death pathways 220
3.5. Discussion 246
3.6. References 254
4. Chapter 4: Phospho-tyrosine Proteomics Analysis Identifies JAK 1/2 Substrates in Cytokine Treated Intestinal Epithelial Cells 265
4.1. Abstract 266
4.2. Introduction 268
4.3. Methods and material 271
4.3.1. Cell culture 271
4.3.2. Reagents 271
4.3.3. Cell death assays 272
4.3.4. Cell lysis and immunoblotting 272
4.3.5. Homogeneous Time Resolved Fluorescence (HTRF) assay 273

4.3.6. Phospho-tyrosine Post-translational Modification (p-Y PTM) Proteomics 273
4.3.7. PTM Scan data analysis 274
4.3.8. Gene Ontology (GO) analysis and pathway analysis 275
4.3.9. Statistical Analysis 275
4.4. Results 276
4.4.1. Sustained activation of the JAK1/2-STAT1 pathway is required for cytokine-induced cell death of colorectal cancer cells 276
4.4.2. IFN-γ + TNF-α dependent synergistic cell death is dependent on the sustained and late phase kinase activity of JAK1 and JAK2 280
4.4.3. Blocking JAK1 and JAK2 kinase activity results in rapid dephosphorylation of STAT1 p-Y701 282
4.4.4. Identification of “late phase” JAK1/2 target substrates by phospho-tyrosine post-translational modification (p-Y PTM) proteomics 285
4.4.5. Functional analysis of “late phase” JAK1/2 target substrates identifies their role in cellular integrity and cell-cell interaction 297
4.4.6. Identification of pathways dependent on late kinase activity of JAK1 and JAK2 in IFN-γ+TNF-α treated cells 303
4.5. Discussion 306
4.6. References 311
5. Chapter 5: General Discussion and Future Perspectives 321
5.1. General Discussion and future perspectives: 322
5.2. References 329
Acknowledgment 333

Author's Declaration:

I hereby declare that this thesis is my own work and effort and that it has not been submitted anywhere for any other award. Where other sources of information have been used, they have been acknowledged.

Data Attribution:

The Human kinome RNAi screens and drug repurposing screens were performed at the Functional Genomics Core Facility, Sandford Burnham Prebys Medical Discovery Institute, La Jolla, CA, USA. RNA-sequencing was performed at Edinburgh Genomics, University of Edinburgh, U.K. PhosphoScan phosphorylation proteomics was performed by Cell Signaling Technology, Danvers, MA, USA. The parental, CASP8, CASP10, RIPK1 and RIPK3 knockout HT-29 cell lines were a kind gift from Professor John Silke at the Walter and Eliza Hall Institute of Medical Research, Parkville, Victoria, Australia. RNA-Seq data was analysed by bioinformatician from our group Dr. Janaki Velmurugan. Human colonic organoid lines were generated by Dr. Peter Flood from our group. Dr. Agnieszka Skowyra from our group advised and assisted with generation of JAK1, JAK2 and STAT1 knockout DLD1 cell lines.

Nisha Saini Rokade, M.Sc.

List of Conference Presentations and Publications

Journal Article

TNF-a Synergises with IFN-g to Induce Caspase-8-JAK1/2-STAT1-dependent Cell Death of Intestinal Epithelial Cells. **N. Saini**, J.A. Woznicki, P. Flood, S. Rajaram, C.M. Lee, P. Stamou, A. Skowyra, M. Bustamante-Garrido, S.A. Zulquernain, J. McCarthy, F. Shanahan, K. Nally (Accepted in Cell death and disease - August 2021)

Poster Presentations

1. **Irish Society for Immunology meeting, 2018, Dublin, Ireland**. *IFN-γ AND TNF-α synergise to kill intestinal epithelial cells through a jak1/2 dependent pathway*. **N. Saini**, P. Stamou, M. Bustamante-Garrido, P. Flood, S. Rajaram, J. A. Woznicki, P. Aza-blanc, K. Nally (Oral presentation)
2. **International cytokine and interferon society (ICIS) 2018, Boston, USA**: *IFN-gamma and TNF-αlpha synergise to kill intestinal epithelial cells through a JAK1/2 dependent pathway* **N. Saini**, P. Stamou, M. Bustamante-Garrido, P. Flood, S. Rajaram, J. A. Woznicki, P. Aza-blanc, K. Nally (Poster presentation)
3. **IBD meeting, 2019, Taos, NM USA** *IFN-gamma and TNF-αlpha synergise to kill intestinal epithelial cells through a jak1/2 dependent pathway* **N. Saini**, P. Stamou, M. Bustamante-Garrido, P. Flood, S. Rajaram, J. A. Woznicki, P. Aza-blanc, K. Nally (Poster presentation)
4. **APC SYMPOSIUM: Weird cell death in the gut, 2019**, **Cork Ireland** IFN-γ and TNF-α Synergise to Kill Intestinal Epithelial Cells through a Non-Canonical Caspase-8-JAK1/2-STAT1-Dependent Pathway. **N. Saini**, J.A. Woznicki, P. Flood, S. Rajaram, C.M. Lee, P. Stamou, A. Skowyra, M. Bustamante-Garrido, K. Regazzoni, S.A. Zulquernain, J. McCarthy, F. Shanahan, K. Nally (Oral and poster presentation)

List of abbreviations:

AFDN	Afadin
ADAM-17	ADAM metallopeptidase domain 17
AJC	Apical junctional complex
AJs	Adherens junctions
AKT	Protein kinase B
AMPK	Monophosphate-activated protein kinase
AP-1	Activator protein 1
AP-2	Activator protein 2
ATCC	American Type Culture Collection
ATG16	Autophagy-related 16
ATG3	Autophagy-related 3
ATG7	Autophagy-related 7
ATP	Adenosine triphosphate
AVLs	Antigen-loss variants
BAD	BCL2 associated agonist of cell death
BAG3	BAG family molecular chaperone regulator 3
BAK	Bcl-2 homologous antagonist/killer
BAM32	B lymphocyte adaptor molecule
BARI	Baricitinib
BAX	Bcl2 associated x
BCA	Bicinchoninic acid

BCL-2	B cell lymphoma 2
BCL-XL	B-cell lymphoma-extra large
BID	BH3 interacting domain death agonist
BMDCs	Bone marrow–derived dendritic cells
BSA	Bovine serum albumin
CD2AP	CD2-associated protein
c-FLIP	FADD-like IL-1β-converting enzyme
CHEK1	Checkpoint kinase 1
CHIC2	Cysteine-rich hydrophobic domain-containing protein 2
ChIP-seq	Chromatin immunoprecipitation sequencing
CHST8	Carbohydrate sulfotransferase 8
CHX	Cycloheximide
cIAP	Inhibitors of apoptosis protein
CIITA	Class II trans activator
CLDN1	Claudin-1
CRC	Colorectal cancer
CRE	cAMP responsive element
CSNK1A1	Casein kinase 1 alpha
CSNK2A1	Casein kinase 2 alpha
CST	Cell Signalling Technology
CTG	Cell titer-glo
CTLs	Cytotoxic T lymphocytes
CXCL10	C-x-c motif chemokine ligand 10

CXCL11	C-x-c motif chemokine ligand 11
CXCL9	C-x-c motif chemokine ligand 9
CXCR3	C-x-c motif chemokine receptor 3
CYLD	Cylindromatosis
DAMPs	Damage-associated molecular patterns
DAPP1	Dual adapter for phosphotyrosine
DD	Death domain
DDX60L	Dexd/H-Box 60 Like
DE	Differential expression
DEAD	ATP-dependent RNA helicase dead
DISC	Death-inducing signalling complex
DMSO	Dimethyl sulfoxide
DNA	Deoxyribonucleic acid
DR	Death receptors
DSG2	Desmoglein-2
DSS	Dextran sulphate sodium
DUBs	Different deubiquitinating enzymes
Duox2	Dual oxidase 2
DuoxA2	Dual oxidase a2
ECACC	European Collection of Authenticated Cell Cultures
EGF	Epidermal growth factor
EPB41L2	Erythrocyte membrane protein band 4.1 like 2
EPLIN	LIM domain and actin binding 1

ERBB2	Erb-b2 receptor tyrosine kinase 2
ErbB4	Erb-b2 receptor tyrosine kinase 2
ERK	Extracellular regulated MAP kinase
ESI-HCD	Electrospray ionising Higher-energy collisional dissociation
FACS	Fluorescence-activated cell sorting
FADD	Fas associated via death domain
FAK	Focal adhesion kinase
FAS	Fas cell surface death receptor
FBS	Fetal bovine serum
FDA	Food drug and administration
FDR	False discovery rate
FLOT2	Flotillin-2
FLVCR1	Feline leukaemia virus subgroup C receptor-related protein 1; Isoform 1
Fos	Fos proto-oncogene
FTL	Ferritin light chain
FUS3	Mitogen-activated serine/threonine-protein kinase FUS3
GALK1	Galactokinase
GalNAc	N-acetyl galactosamine
GAPDH	Glyceraldehyde-3-phosphate dehydrogenase
GAS	Gamma activated sequence
GATA3	GATA binding protein 3
GDNF	Glial cell derived neurotrophic factor
GEFs	Guanine-nucleotide-exchange factors

GPEC	Gene Prioritization by Evidence Counting
GPX4	Glutathione peroxidase 4
GVHD	Graft versus host disease
HB	Heparin-binding
HBV	Hepatitis B virus
HCV	Hepatitis C virus
HDACi	Histone deacetylase inhibitor
HLA-DOA	Major histocompatibility complex, class II, DO Alpha
HOG	Human oligodendroglioma
HRP	Horseradish peroxidase
HRS	Hepatocyte growth factor regulated tyrosine kinase substrate
HSG	Human salivary gland cell line
HSP90AA	Heat shock protein-90
HSV-1	herpes simplex virus
HTRF	Homogeneous time resolved fluorescence
IBD	Inflammatory bowel disease
ICAM1	Intercellular adhesion molecule 1
IDO	Indoleamine 2,3-dioxygenase
IECs	Intestinal epithelial cells
IFNGR	Interferon gamma receptors
IFN-γ	Interferon gamma
IFNGR1	Interferon gamma receptor 1
IFNGR2	Interferon gamma receptor 2

IKK	Inhibitor of nuclear factor kappa-B kinase
IL-10	Interleukin-10
IL-1β	Interleukin -1β
IL-6	Interleukin-6
ILCs	Innate lymphoid cells
iNOS	Inducible nitric oxide synthase
INPP5D	Inositol polyphosphate-5-phosphatase D
INPPL1	Inositol polyphosphate phosphatase like 1
IRF-1	Interferon regulatory factor 1
ISC	Intestinal stem cell
ISGs	Interferon stimulated genes
ISRE	Interferon stimulated response elements
JAK	Janus kinase
JAK1	Janus kinase 1
JAK2	Janus kinase 2
JAKinibs	JAK inhibitors
JAM	Junctional adhesion molecules
JNK	c-Jun N-terminal kinases
KEGG	Kyoto Encyclopedia of Genes and Genomes
KIR	Kinase inhibitory region
LIGHT	Tumour necrosis factor superfamily member 14
LIMA1	LIM domain and actin binding 1
LMO7	LIM domain only protein 7

LMP-2	Low molecular mass polypeptide
LPS	Lipopolysaccharide
LUBAC	Linear ubiquitin chain assembly complex
MAF	Macrophage activation factor
MAPK	Mitogen-activated protein kinase
MCL-1	Myeloid cell leukemia 1
MCMV	Murine cytomegalovirus
MEFs	Murine embryonic fibroblasts
MHC	Major histocompatibility complex
MISP	Mitotic interactor and substrate of PLK1
MLKL	Mixed lineage kinase domain like pseudokinase
MLLT4	Myeloid/lymphoid or mixed-lineage leukemia
MOMP	Outer membrane permeabilization of mitochondria
MS	Mass spectroscopy
MS	Multiple sclerosis
MSD	Meso scale discovery
MVBs	Multivesicular body
NAC	N-acetyl-L-cysteine
NADPH	Nicotinamide adenine dinucleotide phosphate
NBD	Nucleotide-binding domain
NCF2	Neutrophil cytosolic factor-2
NCF4	Neutrophil cytosolic factor-4
NEC	Necrotizing enterocolitis

NEF	Nucleotide-exchange factor
NF-κB	Nuclear factor kappa B
NK	Natural killer
NLS	Nuclear localization sequence
NO	Nitric oxide
NOD	Non-obese diabetic
NOS	Nitric oxide synthase
NOXA	Phorbol-12-myristate-13-acetate-induced protein 1
OAS2	2'-5'-oligoadenylate synthetase
OCLN	Occludin
OGM	Organoid growth media
OMM	Outer mitochondrial membrane
PARP	Poly-(ADP-ribose) polymerase
PBS	Phosphate buffer saline
PCA	Principal component analysis
PCR	Polymerase chain reaction
PDL1	Programmed death-ligand 1
PDX1	Pancreatic and duodenal homeobox 1
PI3K	Phosphatidylinositol 3-kinase
PIAS	Protein inhibitor of activated STAT
PKD	Protein kinase D
PKR	Protein kinase R
PLEKHA7	Pleckstrin homology domain-containing family A member 7

PLK1	Polo like kinase 1
PRDX1	Peroxiredoxin-1
PRDX2	Peroxiredoxin-2
PRMT1	Protein arginine methyltransferase 1
PRRSV	Porcine reproductive and respiratory syndrome virus
PTM	Post translational modification
PTP1	protein tyrosine phosphatase 1
PTPN11	protein tyrosine phosphatase non-receptor type 11
PUMA	P53-upregulated modulator of apoptosis
PVDF	polyvinylidene difluoride
PXN	Paxillin
p-Y PTM	Phospho-tyrosine post-translational modification
PYGB	Glycogen phosphorylase
RA	Rheumatoid arthritis
RAG	Recombination activating gene
RANBP1	RAN binding protein 1
RAPH1	Ras association (RalGDS/AF-6) and pleckstrin homology domains 1
RIPA	Radioimmunoprecipitation assay buffer
RIPK1	Receptor-interacting protein kinase 1
RIPK3	Receptor-interacting protein kinase 3
RNA-seq	RNA-sequencing
RNI	Reactive nitrogen intermediates
RORgt	RAR-related orphan receptor gamma

ROS	Reactive oxygen species
RT-qPCR	Quantitative reverse transcription PCR
RUXO	Ruxolitinib
SAT1	Spermidine/spermine N1-acetyltransferase 1
SAT2	Spermidine/spermine N1-acetyltransferase family member-2
SBD	Substrate-binding domain
SEPTIN2	Septin-2
SFTPA1	Surfactant protein-A1
SH2	Src homology-2
SHANK	SH3 and multiple ankyrin repeat domains 2
SHARPIN	SHANK-associated RH domain interacting protein
SHIP	inositol polyphosphate-5-phosphatase D
SHIP-2	Inositol polyphosphate phosphatase like 1
SINV	Sindbis virus
SLC	Solute carrier
SLC25A	Solute carrier family 25-member 25a
SLC39	Solute carrier family 39 member
SLC3A2	Solute carrier family 3-member 2
SLC40	Solute carrier family 39 member
SLC7A11	Solute carrier family 7-member 11
SMAC	Second mitochondria-derived activator of caspase
SNAP23	Synaptosomal-associated protein 23
SNCG	Synuclein gamma

SOCS	Suppressor of cytokine signalling
SOCS3	Suppressor of cytokine signalling 3
SODD	Silencer protein called silencer of death domain
SRC	Src proto-oncogene
SS	Sjögren's syndrome
STAM2	Signal Transducing Adaptor Molecule 2
STAT	Signal transducer and activator of transcription
STAT3	Signal transducer and activator of transcription 3
STAT5B	Signal transducer and activator of transcription 5B
STAT6	Signal transducer and activator of transcription 6
SUMO	Small ubiquitin-like modifier
T1DM	Type 1 diabetes mellites
TAB2	TAK1-binding protein 2
TACE	Tumour necrosis factor-α-converting enzyme
TAK1	Transforming growth factor beta-activated kinase 1
T-bet	Transcription factor T-box expressed in T cells
TBST	Tris-buffered saline with tween-20
TC45	T cell protein tyrosine phosphatase
TCA	Tricarboxylic acid cycle
TC-PTP	T-cell protein tyrosine phosphatases
TGF-β	Transforming growth factor beta 1
TH-1	T helper type-1
TICAM	Toll like receptor adaptor molecule 1

TJP1 Tight junction protein 1

TJP2 Tight junction protein 2

TJs Tight junctions

TLR-2 Toll like receptor-2r

TNBS 2,4,6-Trinitrobenzenesulfonic acid solution

TNFR TNF receptor

TNFRSF TNF receptor superfamily

TNFSF TNF superfamily

TNF-α Tumour necrosis factor alpha

TOLLIP Toll-interacting protein

TPD52L2 Tumour protein D52 like 2

TPM Transcripts per million

TPPP3 Tubulin polymerization-promoting protein family member 3

TRADD TNFRSF1A associated via death domain

TRAF2 TNF receptor-associated factor-2

TRAIL TNF superfamily member 10

TRPM7 Transient receptor potential melastatin related-7

TWEAK TNF superfamily member 12

TYK2 Tyrosine kinase 2

UBE2F Ubiquitin conjugating enzyme E2 F

UC Ulcerative colitis

U-NF-κB Unphosphorylated NF-κB

UPA Upadacitinib

USP2a	Ubiquitin-specific cysteine protease 2a
U-STAT	Unphosphorylated STAT
VDAC	Voltage-dependent anion channel
VSD	Viral surveillance and diagnosis
VSP4	Vacuolar protein sorting 4
WEE1	Wee 1 kinase
Wnt	Wingless-int
XIAP	X-linked inhibitor of apoptosis protein
ZDHHC5	zinc finger DHHC-type palmitoyltransferase 5
ZNF185	Zinc finger protein 185
ZO	Zona occludens
ZYX	Zyxin

General Abstract

Although the phenomenon of synergistic cell death induced by the combination of IFN-γ and TNF-α has been known for more than 30 years, the underlying mechanisms are still not clear. The main aim of my PhD was to identify the mechanisms which are required for the killing of human intestinal epithelial cells (Chapter-I) by this cytokine combination. A human kinome RNAi screen and a drug repurposing screen identified the Janus kinases (JAKs) JAK1 and JAK2 as the major kinases required for IFN-γ + TNF-α dependent synergistic cell death. While TNF receptor-1 (TNFR1) was also required, there was no direct dependency of cell death on TNFR1-downstream canonical apoptotic and necroptotic signalling pathways. Furthermore, we identified a non-canonical role for caspase-8 and receptor-interacting serine/threonine-protein kinase 3 (RIPK3) in the cell death signalling pathway (Chapter-II). For the first time we report that IFN-γ and IFN-γ + TNF-α induced JAK1/2-STAT1 signalling followed a dose-to-duration pattern of activation whereby increasing concentration of cytokines resulted in sustained JAK-STAT signalling leading to epithelial cell death. This dose-to-duration signalling pattern allowed cells to respond appropriately to increasing levels of inflammatory cytokines. RNA-sequencing revealed that sustained activation of the JAK1/2-STAT1 pathway resulted in the expression of a unique set of 'late' genes associated with different cell death pathways (Chapter-III). Phosphoproteomics identified potential target substrates for sustained JAK1 and JAK2 kinase activity. These JAK1/2 substrate proteins are associated with epithelial junctions, cell adhesion and cell-cell interactions, highlighting the importance of JAK1/2-STAT1 signalling in regulating the integrity of the epithelial barrier. Overall, our results identify the central underlying mechanisms underpinning IFN-γ + TNF-α induced cell death of intestinal epithelial cells and disruption of the intestinal epithelial barrier during intestinal inflammatory diseases.

1. Chapter I: Literature Review

Crosstalk between IFN-γ & TNF-a Signalling Pathways and Contribution to Cell Death

1.1. Interferon-gamma (IFN-γ)

IFN-γ is a pro-inflammatory cytokine associated with the regulation of many important biological activities such as co-ordinating innate and adaptive immunity to bacterial and viral pathogens, metabolism, tissue homeostasis, inflammatory responses and tumour immunosurveillance[1]. IFN-γ was first discovered by Wheelock et al. in 1965 from fresh human leukocytes[2]. IFN-γ is the sole member of type-II interferon family. Primarily, IFN-γ is secreted by immune cells such as T helper 1 (TH1) cells and $CD8^+$ cytotoxic T lymphocytes (CTLs) natural killer (NK) cells and innate lymphoid cells (ILCs)[3].

1.1.1. IFN-γ gene

Mouse and Human *IFNG* both are encoded by a 6 kb gene located on chromosome 10 and 12 respectively[4,5]. IFN-γ is composed of four exons and three introns[5]. Even though there are structural similarities between mouse and human IFN-γ, they share only 60% sequence homology[6]. The expression of the IFN-γ gene is controlled by regulatory elements present 2.3 kb upstream and 1 kb downstream of the IFN-γ gene, containing binding sites for several transcription factors including: GATA Binding Protein 3 (GATA3), Fos, Jun, Nuclear factor kappa B (NF-κB) and T-bet[6].

1.1.2. IFN-γ Protein

IFN-γ is made up of two 17 kDa polypeptide chains, non-covalently linked in an antiparallel fashion to form a homodimer[7]. As the two chains are non-covalently bound, the IFN-γ molecule is sensitive to temperature and pH. Each polypeptide chain contains approximately 160 amino acids and is glycosylated to form a 50 kDa homodimer[7]. Even though the glycosylation of polypeptide chains does not directly contribute to IFN-γ activity, it is essential for its protection from proteasomal degradation[7]. Studies performed using enzymatic

cleavage of amino or carboxy terminal ends of the protein identified that both the amino and carboxy terminus of IFN-γ are required for its interaction with IFN-γ receptor[8,9]. Also, blocking of either the amino or carboxyl termini using blocking antibodies also inhibited the binding of IFN-γ with its receptor, as well as IFN-γ signalling[8,9].

1.1.3 IFN-γ receptors (IFNGR)

IFN-γ signals through binding to the interferon gamma receptors (IFNGR). IFN-γ receptor belongs to the class-II cytokine receptor family and is composed of subunits - two ligand binding alpha chains (IFNGR1) and two ligand binding beta chains (IFNGR2). IFNGR1 is constitutively expressed in almost all cell types, while IFNGR2 expression is limited to certain cell populations and based on state of their differentiation. Due to the limited expression level of IFNGR2, the responsiveness of cells towards IFN-γ exposure is highly dependent upon IFNGR2 levels[10]. For instance, the level of IFNFR2 is observed to be lower in TH1 cell population compared to TH2 type population. The low expression of IFNGR2 makes TH1 cells unresponsive towards IFN-γ signalling supports the transition of T cells from Th2 to Th1 phenotype during differentiation to avoid growth inhibitory and pro-apoptotic effects.. [10, 11].

IFNGR1 is a 90 kDa protein and acts as the major ligand binding unit[12]. IFNGR1 consists of four regions: signal sequence with amino acids position 1 to 17 (1-17aa), extracellular domain (18-245 aa), transmembrane region (246-266 aa) and intracellular domain (267-487aa). IFNGR2 is a 62 kDa protein containing extracellular domain (28-247 aa), transmembrane region (248-268 aa) and intracellular domain (269-337 aa)[6]. Both, IFNGR1 and IFNGR2 are translated on the endoplasmic reticulum and are highly glycosylated[13]. Immunoprecipitation studies performed in untreated and IFN-γ treated cells identified that the two receptors are not tightly associated in the absence of IFN-γ, and that interaction strength between the receptors increases with IFN-γ binding[14]. Neither IFNGR1 or IFNGR2 contain any

intrinsic tyrosine phosphorylation activity. Deletion/mutation studies identified two important sequences associated with IFNGR1, one is present on the intracellular domain (aa-266LPKS269) containing proline at 267 aa position[15]. This sequence represents the attachment site for Janus kinase 1 (JAK1). The second functionally important sequence is present close to carboxy terminal of IFNGR1 (aa- 440YDKPH444) with an essential tyrosine residue at 440 position[16]. Phosphorylation of Y440 is required for the binding of the Src homology-2 (SH2) domain of the recruited transcription factor called signal transducer and activator of transcription 1 (STAT1)[16]. IFNGR2 also contains two sequences (263PPSIP267 and 270IEEYL274) associated with recruitment and attachment of JAK2 with IFNGR2[11]. Stoichiometry experiments showed the binding of IFN-γ to IFNGR in 1:2 ratio, indicating binding of 1 IFN-γ molecule with two receptors. The interaction of IFN-γ with IFNGR1 was further confirmed by x-ray crystallography[17].

1.1.3. JAK-STAT signalling pathway

The IFN-γ-IFNGR1-IFNGR2 signalling pathway is mainly dependent on two families of proteins: JAKs and STATs[3]. Immunoprecipitation experiments performed in IFN-γ treated cells identified that JAK1 binds to the intracellular domain of IFNGR1, while JAK2 binds to the intracellular domain of IFNGR2. Even in the absence of IFN-γ, JAK1 and JAK2 are bound to their corresponding receptors, but are enzymatically inactive[14]. Binding of IFN-γ to the receptors induces strong interaction and association of the receptors with each other triggering their reorientation. This reorientation of IFNGR1 and IFNGR2 brings JAK1 and JAK2 into close proximity of each other[14,18]. This close proximity facilitates the autophosphorylation and transphosphorylation of JAK1 and JAK2 and also their functional activation[18]. Once activated JAK1 phosphorylates IFNGR1 chains at tyrosine-440 and forms a docking site for the SH2 domain of STAT1[19,20]. After recruitment of STAT1 to IFNGR1, JAK2 phosphorylates STAT1 at

701 amino acid position (phospho-Y701 or pY701), facilitating homodimerization of STAT1 and inducing dissociation of the STAT1 homodimer from the receptor, which then translocates to the nucleus and binds with Gamma activated sequence (GAS) in the promoter regions of Interferon stimulated genes (ISGs)[21] [Figure 1.1]. In addition to STAT1 pY701, the C-terminal transactivation domain of STAT1 also contains one serine-727 (pS727) phosphorylation site that is essential for maximum transcription of STAT1 target genes[22]. Gene-targeted mutant mice expressing a serine727-alanine mutation in Stat1 showed reduced expression of IFN-γ regulated genes, macrophage activation and increased mortality with *Listeria monocytogenes* infection[23]. It highlighted the role of STAT1 serine 727 phosphorylation in macrophage activation and to IFN-gamma-dependent immune responses [23]. Several stimuli including Type I and II IFNs, TNF-α, Interleukin (IL)-12, IL-2 and lipopolysaccharides (LPS) can induce S-727 phosphorylation.[22] Chromatin-associated cyclin dependent kinase 8 (CDK8) is reported to be a kinase which directly phosphorylates STAT1 pS727[24,25]. LPS induces STAT1 pS727 phosphorylation independent of STAT1 pY701 phosphorylation in macrophages[26]. The major transcription factor induced by STAT1 signalling is interferon regulatory factor 1 (IRF-1). IRF-1 leads to the transcription of many secondary response genes by activation of interferon stimulated response elements (ISRE)[3,27]. A chromatin immunoprecipitation sequencing (ChIP-seq) experiment performed in human breast cancer cell line, H3396 to identify genome-wide targets of IRF-1, identified more than 17,000 binding sites associated with IFN-γ treatment[28]. Functional characterisation of these binding sites correlated their role with DNA damage, apoptosis, and immune processes. Notably, the data suggested an important role of IRF-1 in tumour suppression and anti-cancer apoptotic pathways[28].

1.1.4. Nuclear translocation of STAT1

STAT1 pY701 phosphorylation and dimer formation is required for STAT1 nuclear translocation[29]. The studies performed with blocking STAT1 dimerization or STAT Y701F mutants showed reduced translocation of STAT1 into the nucleus[30,31]. The nuclear translocation of STAT1 requires identification of STAT1 dimer by importin-α family member-importin α5[32][Figure 1.1]. Importin α5 only recognizes tyrosine-phosphorylated STAT1 dimers and binds directly to the DNA binding domain of STAT1 without any bridging adaptor, allowing the STAT1-importin α5 complex to enter into the nucleus[29]. The binding of Importin α5 with STAT1 is different than its binding with other nuclear localization sequence (NLS). STAT1 interacts with the C terminus of importin α5 containing Arms 8 to 10, whereas other classical NLS sequences interact with Arms 2, 3, 4, 7 and 8 of importin α5[29]. The entry of STAT1 dimer allows its binding to the GAS sites at enhancer and promoter elements throughout the genome to regulate transcription. STAT1 pY701 phosphorylation and nuclear transport in response to IFN-γ is transient and STAT1 is redistributed to the cytoplasm after a few hours[33]. The nuclear export of STAT1 is dependent upon its STAT1 pY701 dephosphorylation and dissociation of STAT1 homodimer[34].

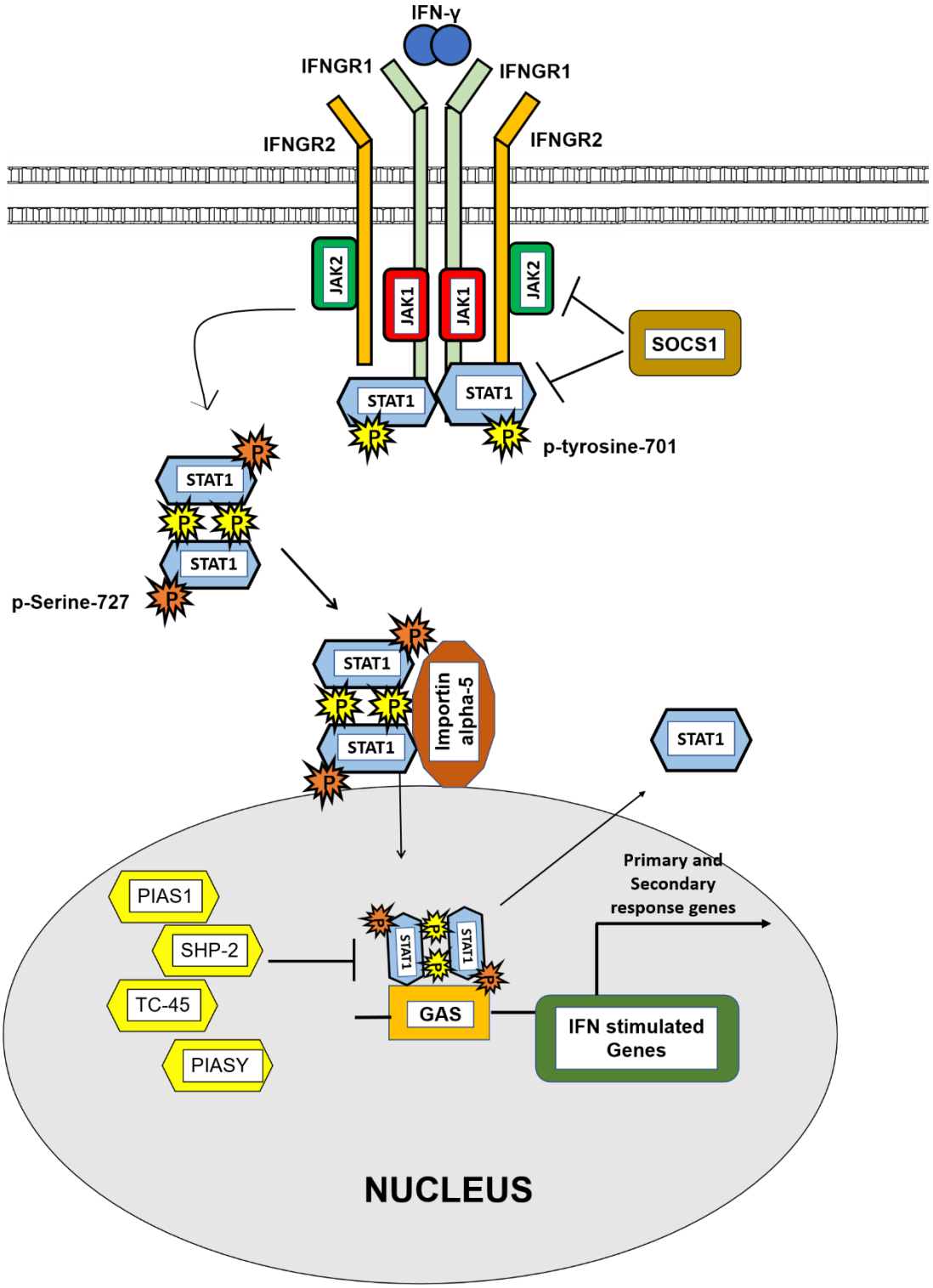


Figure 1.1 IFN-γ signal transduction via JAK-STAT signalling pathway

IFN-γ binds to IFNGR (composed of IFNGR1 and IFNGR2) causing autophosphorylation of JAK2 kinase. This allows activation of JAK1 by JAK2. Functionally active JAK1 phosphorylates IFNGR1 at tyrosine-440 residue to form docking site for SH2 domain of latent STAT1. Receptor recruited STAT1 is phosphorylated at tyrosine 701 residue to form a homodimer and dissociates

from the receptor. STAT1 homodimer travels to the nucleus with the help of importin-α5 and binds with GAS elements to regulate expression of IFN-γ regulated genes. In the nucleus STATs are dephosphorylated by protein tyrosine phosphatases such as SHP-2, TC-45. and PIAS. Unphosphorylated STATs are shuttled back to the cytoplasm. SOCS1 negatively regulates IFN-γ signalling by blocking JAKs and STAT1 activity.

Abbreviations are as follows: IFN-γ, Interferon gamma; IFNGR, Interferon gamma receptor; JAK, Janus kinase; STAT1, Signal transducer and activator of transcription; GAS, ; SOCS1, Suppressor of cytokine signalling1; SHP-2, SH2 domain- containing PTP-1; PIAS, protein inhibitors of activated STATs; TC-45, ; Modified from: Schroder et al. 2004, Staab et al 2013

1.1.5. Post-translational modifications of STATs

As discussed, STAT1 pY701 and STAT1 pS727 phosphorylation play an important role in its nuclear translocation and transcriptional activation, respectively. In addition to STAT1 pY701 and STAT1 S727 phosphorylation there are other post-translational modifications which regulate the transcriptional activity of STAT1. Methylation, acetylation, ubiquitination and SUMOylation have all been reported to regulate the amount of STAT1 in the nucleus by controlling the tyrosine phosphorylation status of STAT1 pY701[35]. The N-terminal region of STAT1 has been reported to be the most important for STAT1 activity and it is homologous among different STATs and contains a conserved arginine residue (Arg-31)[36]. A deletion of the N-terminal region of STAT1 results in decreased phosphorylation at STAT1 pY701 upon stimulation. Methylation of the arg-31 residue at the N-terminal end of STAT1 by methyltransferase- protein arginine methyltransferase 1 (PRMT1) blocks the association of STATs with protein inhibitors of activated STATs (PIAS) and increases the transcriptional activity of STAT1[36]. A mutational analysis performed by substituting arginine 31 with alanine showed no methylation and decreased STAT1 transcriptional activity[36]. A STAT1 phosphorylation-acetylation switch was suggested as a central mechanism for regulation of STAT1 phosphorylation in the nucleus however this mechanism has been disputed by another group[37]. An inhibitor study performed by using the histone deacetylase inhibitor (HDACi) identified lysine 410 and Lys 413 as sites for STAT1 acetylation and STAT1 acetylation was shown to decrease STAT1 phosphorylation and nuclear import[38]. The substitution of STAT1 Lys 410 and Lys 413 to glutamine or alanine amino acids showed an acetylation dependent decrease in STAT1 activity[38]. Conversely, another study showed that a histone deacetylase inhibitor did not affect STAT1 activation and Lys 410 and Lys 413 were irrelevant for STAT1 phosphorylation[39]. Thus, the effect of the acetylation of Lys 410 and Lys 413 on STAT1 activity

is contested. Ubiquitination of STAT has also been shown to repress STAT1 phosphorylation at pY701. While total STAT1 protein levels were reported to be less affected by ubiquitination, STAT1 pY701 was down regulated by proteasomal degradation[40,41,42] and inhibition of proteasomal degradation increased STAT1 phosphorylation significantly[42]. In addition, the deubiquitinase ubiquitin-specific cysteine protease 2a (USP2a) has been reported to stabilise STAT1 pY701 phosphorylation by removing K-48 ubiquitin chain[42]. Another modification which has been reported to affect STAT1 is SUMOylation. The addition of small ubiquitin-like modifier (SUMO) has been reported to decrease the transcriptional activity of STAT1. SUMOylation has been shown to occur at Lys 703 position of STAT1[43]. This site is conserved in STAT1 but not in other STATs. As both Tyr 701 and Lys 703 are close to each other SUMOylation and phosphorylation events are proposed to be mutually exclusive for STAT1. SUMOylation has been proposed to only affect unphosphorylated STATs and does not affect transcriptionally active STATs[43]. SUMOylation solubilises para-crystals and leads to the dephosphorylation of STAT1 at both STAT1 pY701 and STAT1 pS727 positions which results in decreased transcription of STAT1 target genes, thus making cells insensitive to IFN-γ[44].

1.1.6. Role of unphosphorylated STATs

Even though there is plenty of evidence highlighting the importance of STAT1 tyrosine phosphorylation for its nuclear localization and induction of gene expression, some studies also show transcriptional roles for unphosphorylated (non-pY701 phosphorylated) STATs (U-STAT)[45]. Both U-STAT1 and U-STAT3 have been reported to induce the expression of a specific set of genes even in the absence of tyrosine phosphorylation (STAT1 pY701 or STAT3 pY705) when provided with appropriate signals[45]. In response to IL-6 signalling, it has been shown that there was an accumulation of a high level of U-STAT3 in cells which formed a complex with

unphosphorylated NF-κB (U-NF-κB) and activated a specific set of NF-κB regulated genes[46]. The role of unphosphorylated STAT1 was first discovered in a study of Kumar et al where they analysed and reported on the role of STAT1 in TNF-α induced cell death in fibroblasts[47]. TNF-α along with cycloheximide induced cell death and caspase expression in 2fTGH fibroblast cell line in STAT1 dependent manner[47]. Even though *STAT1*$^{-/-}$ U3A cell line was resistant to TNF-α induced cell death, STAT1 Y701F mutant cell line did not rescue the cell death, suggesting the pY701 independent role of STAT1 in TNF-α induced cell death and caspase expression[47]. In another example, the expression of IFN-γ inducible gene low molecular mass polypeptide (LMP-2) required the presence of both STAT1 and IRF1[48]. Even though *STAT1*$^{-/-}$ and *IRF1*$^{-/-}$ cell lines did not express LMP-2, cell lines with STAT1 Y701F expression plasmid could express LMP-2, confirming STAT1 -pY701 independent role in LMP-2 expression[49].

1.1.7. Feedback regulation of the JAK-STAT pathway

The JAK-STAT pathway is highly tuned and tightly controlled by different feedback regulation mechanisms. The key regulators of the JAK1/2-STAT1 pathway involves two main phosphatases; T-cell protein tyrosine phosphatases (TC-PTP), and SH2 domain- containing PTP-2 (SHP-2)[35 50]. TC-PTP also known as CD45 or TC45, is a member of the phospho-tyrosine phosphatase family. It is a transmembrane protein and is involved in the dephosphorylation of JAK1 and JAK3 in human cells and all JAKs in murine cells[51 52]. $CD4^+$ T cells lacking TC-45 showed increased anti-viral activity upon treatment with interferon alpha supporting the hyperactivation of the JAK-STAT pathway in the absence of TC-45[53]. It has also been shown that cell density, extracellular matrix proteins and modification to actin cytoskeletons increased the activation of TC-45 and in turn dephosphorylation of STAT1[54]. Another phosphatase, SHP-2 is well studied in terms of JAK-STAT signalling[55]. SHP-2 performs multiple regulatory functions on the JAK-STAT pathway. For instance, SHP-2 deficient$^-$ mouse

fibroblasts had elevated STAT1 and STAT2 phosphorylation and this was reversed by overexpression of SHP-2 in fibroblasts derived from the knockout mice[56]. Prominent feedback regulators for JAK-STAT signalling include the SOCS family of proteins[57]. SOCS1 and SOCS3 contain an N-terminal domain known as Kinase inhibitory region (KIR) which acts as a pseudo-substrate for JAKs and contributes to their negative regulation.[58] The C-terminal domain of SOCS proteins contain a 40 amino acid domain called 'SOCS Box' and can interact with ubiquitin ligation machinery causing polyubiquitylation of key signalling proteins such as JAKs resulting in their proteasomal degradation[57]. The SH-2 domain of SOCS1 can interact at the pY1007 position of JAK2.[59] Mice lacking *Socs1* gene did not survive more than 3 weeks due to excessive IFN-γ signalling and showed defects in acquired and innate immune system[58]. *Socs1*$^{-/-}$ mice were characterised by a reduction of eosinophils, lymphocytes and platelets and an increase in neutrophils[60]. Treatment with IFN-γ neutralization antibodies protected *Socs1*$^{-/-}$ mice from disease. Other than that, the mice with *Socs1*$^{-/-}$*Ifng*$^{-/-}$ double knockout phenotype also remained healthy or showed minor signs of haematological diseases[60] .

1.1.8. Clinical targeting of JAK-STAT pathway

The JAK-STAT pathway was initially identified as a major pathway for the induction of antiviral activity by interferons[61]. But now it is known to act as a communication node for the immune system and acts downstream of signalling pathways for more than 50 cytokines and growth hormones[62]. Different knock out studies and GWAS have shown that any mutation including both loss or gain of function in JAKs and STATs can lead to different malignancies and immunological diseases[63]. Furthermore, the successful application of JAK inhibitors (JAKinibs) in the treatment of different disorders justifies the importance of the JAK-STAT pathway in disease pathogenesis (table 1.1). For example, Ruxolitinib was the first drug approved for

myofibrilosis neoplasm targeting both JAK1 and JAK2[64]. Now it has been used in the treatment of several other diseases such as polycythaemia vera, RH and in clinical trial for ulcerative colitis[65,66]. Tofacitinib was the second JAK inhibitor approved by FDA for Rheumatoid arthritis[67], majorly as JAK1 and JAK3 inhibitor, but it also targets JAK2 to a lesser extent [68]. There are many more other JAK inhibitors that were approved later by the FDA for the treatment of different diseases both in human and other animals (e.g. Oclacitinib for dermatitis in dogs)[69].

Even though the JAK-STAT pathway is the major pathway associated with STAT1 activation and IFN-γ signalling, there are alternative pathways associated with the IFN-γ signalling cascade which phosphorylate STAT1 on its transactivation domain. For instance, IFN-γ can signal through the mitogen-activated protein kinase (MAPK) pathway, protein kinase C, and Phosphatidylinositol 3-kinase (PI3K)/protein kinase B (AKT) pathway to positively regulate STAT1 transcriptional activity[70]. In certain circumstances IFN-γ can also induce STAT1 independent signalling by transcription factors like STAT3, STAT5, NF-κB and AP-1 (activator protein-1)[71–74].

Table 1.1: Small molecule drugs targeting JAKs in different stages of pre-clinical and clinical development.

JAKinib	Target JAK	Disease	Stage
Ruxolitinib	JAK1/2	P. Vera	Clinic
		RA	Clinic
		Myelofibrosis	Clinic
		UC	Phase-III
Tofacitinib	JAK3>JAK1/2	UC	Clinic
		RA	Clinic
		Psoriasis	Phase-III
Fedratinib	JAK2	Myelofibrosis	Phase-III
Decemotinib	JAK1/2/3, TYK2	RA	Phase-II
Peficitinib	JAK1/2/3	RA	Phase-III
CEP-33779	JAK2	Colorectal Cancer	Mice
AG-490	JAK2	RA	Mice
Momelotinib	JAK1/2	Myelofibrosis	Phase-I/II
Cerdulatinib	JAK1/2/3, TYK2	CLL/ B-cell	Phase-I
Filgotinib	JAK1> JAK2/3	RA	Phase-II
		CD and UC	Phase-II/III
Pacritinib	JAK1/2/3	Myelofibrosis	Phase-III/Terminated
		RA	Phase-III
		Psoriasis	Phase-II
Gandotinib	JAK2	Myeloproliferative Neoplasm	Phase-II
Baricitinib	JAK1/2	RA	Clinic
		Psoriasis	Phase-II
TG101209	JAK2	Lung Cancer	Mice

XL019	JAK2>JAK1/2, TYK2	Myelofibrosis	Phase-I
AT9283	JAK2/3	Multiple myeloma	Phase-II
AZD1480	JAK1/2	Solid Tumours	Phase-I
NVP-BSK805	JAK2	P. Vera	Mice
INCB018424	JAK1/2	Myelofibrosis	Phase-II
CEP-701	JAK2	Myelofibrosis	Phase-II
Upadacitinib	JAK1	CD	Phase-III
		UC	Phase-III
Solcitinib	JAK1	Psoriasis	Phase-II/Terminated
		UC	Phase-II/Terminated

Table 1.1 includes JAK inhibitors (JAKinibs) that are FDA-approved, in pre-clinical studies or in clinical trials, for the treatment of autoimmune diseases. JAK- Janus kinase, Jakinib- JAK inhibitor, Stage- status in clinical study; Terminated- removed from the study (failed); P. Vera- Polycythaemia Vera; RA- Rheumatoid arthritis, UC- Ulcerative Colitis; CD- Crohn's disease. Adapted from [66] [63]

1.1.9. Effects of IFN-γ on Immune Cell Activation

IFN-γ is an essential pro-inflammatory cytokine associated with defence against intracellular pathogens and tumour control[1]. In order to generate innate and adaptive immune responses IFN-γ induces activation of several immune cells including macrophages, antigen presenting cells, B cells, $CD4^+$ T cells, $CD4^+$ regulatory T cells and $CD8^+$ cytotoxic T cells. In fact, IFN-γ can induce the expression of a core set of 290 genes in peripheral blood cells including genes encoding cytokines, chemokines, chemokine receptors, MHC proteins, cell adhesion molecules and other signalling mediators[75]. Classically, IFN-γ was identified as an activator of macrophage cells, therefore IFN-γ was previously named as macrophage activation factor (MAF)[76]. The *in vivo* studies performed in mice treated with neutralising antibodies against IFN-γ showed a reduced resistance in mice against bacterial infections, suggesting the role of IFN-γ in macrophage activation[77,78,79]. IFN-γ mediates the polarisation of macrophages to a hyper-inflammatory M1 phenotype and increases the production of pro-inflammatory cytokines TNF, IL-1β, IL-12, IL-18, and IL-23 by macrophages in response to pathogen-associated molecular patterns (PAMPs) such as bacterial lipopolysaccharides (LPSs) also known as endotoxin[1,6]. In addition, IFN-γ induces the upregulation of the major histocompatibility complex (MHC) molecules, upregulation of antigen processing and presentation machinery and increases expression and activity of the proteasome[76]. IFN-γ also upregulates the expression of MHC class II trans activator (CIITA) for increased expression of MHC class II molecules[80 81]. IFN-γ primes macrophages for a rapid and stronger response to LPS and other toll like receptor (TLR) agonists through various epigenetic and transcriptional mechanisms[1]. IFN-γ induces activation of several enzymes including NADPH-dependent phagocyte oxidase system (Respiratory burst), inducible nitric oxide synthase (iNOS) for nitric oxide (NO) production, tryptophan depletion and by up-regulation of lysosomal enzymes[82]. The

microbicidal activity of macrophages primarily depends on the production of reactive oxygen species (ROS) and reactive nitrogen intermediates (RNI) by induction of NADPH oxidase system and iNOS. The inhibition of iNOS using specific inhibitors or mutated iNOS gene decreases the bacterial killing ability of phagocytic cells[83]. In addition, IFN-γ signalling also modulates immune-regulation by promoting differentiation of Th1 ($CD4^+$ helper T cells) type cell and inhibiting the differentiation of Th2 and Th17 T cell lineages. Even though IL-12 is the major cytokine associated with Th1 cell activation, IFN-γ signalling is important for maximum IL-12 production from phagocytes. IL-4/STAT6 signalling is required for the activation and differentiation of Th2 type cells[76,84,85]. IFN-γ inhibited the IL-4/STAT6 activation by inducing the upregulation of SOCS1 thereby blocking IL-4 receptor signalling in human monocytes[86]. Also, Th1 T cells generated in mice lacking IFN-γ gene continued to produced IL-4 (a Th2 cytokine), suggesting the important role of IFN-γ for the complete polarisation of Th1 cells[84]. The IFN-γ-induced transcription factor- T-box expressed in T cells (T-bet) increases the production IL-12 to support Th1 cell differentiation, but also inhibits Th2 differentiation by interfering with the IL-4 associated transcription factor GATA3[87]. In addition, T-bet also inhibits the differentiation of precursor T cells into Th17 cells by blocking the expression of transcription factor RORgt[88] .Classically, IFN-γ has been considered as a pro-inflammatory cytokine and can affect different inflammatory and anti-inflammatory signalling pathways and responses. It antagonizes TGF-β and IL-10 signalling[89,90,91]. It also blocks regulatory $CD4^+$ T cell (Treg) cell differentiation and functions[92,93]. In contrast, IFN-γ has also been reported to be tissue protective by increasing the number of T-reg cells during chronic inflammatory conditions[94]. Thus, IFN-γ can have pleiotropic context dependent temporal effects and induces a negative feedback loop to minimise its own detrimental effect.

1.1.10. Anti-Microbial activities

IFN-γ exerts its antiviral effects by regulating the expression of genes to induce direct anti-viral responses in infected cells and can in parallel activate immune cells (e.g. macrophages, dendritic cells, NK cells etc.) required for co-ordinating inflammatory, adaptive immune and antiviral functions[95–98]. IFN-γ can elucidate its direct antiviral responses either by blocking viral entry, replication, gene expression or transmission[99]. For instance, in the case of Hepatitis C virus (HCV), Measles virus, hepatitis B virus (HBV), West Nile virus and, Sindbis virus (SINV) infections, IFN-γ has been reported to exert non-cytolytic antiviral activities by reducing the expression of receptors required for viral entry[100–104]. HCV requires several receptors such as CD81, claudin-1 (CLDN1), and occludin (OCLN), scavenger receptor class B type I (SR-BI) to enter the cells. IFN-γ treatment decreased the expression of CLDN1 and distribution of CD81 and SR-BI receptors on the surface of liver cells to reduce HCV infections[104,105]. Protein kinase R (PKR) is a common antiviral protein used by interferons against viruses to reduce viral replication[106]. In case of porcine reproductive and respiratory syndrome virus (PRRSV), IFN-γ reduces viral replication by induction of (PKR) dependent inhibition of viral synthesis[107]. In the case of HCV infections in Huh cells, IFN-γ decreased viral entry and replication by blocking protein synthesis of HCV virus in a DExD/H box helicase DEAD box polypeptide 60-like (DDX60L) dependent manner[108]. IFN-γ inhibited vaccinia viral infection and virion production by production of nitric oxide in murine macrophages[109]. In the case of murine cytomegalovirus (MCMV) infection, IFN-γ inhibits the expression of MCMV transcripts and proteins in bone marrow derived macrophages[110]. Furthermore, IFN-γ inhibits HIV-1 and HSV-1 viral infections by reducing virus release and transmission in cells. For example, HIV-1 exits out of the cell by formation of Gag-CD63 complex. IFN-γ treatment of cells decreases the expression of Gag significantly, disrupting the Gag-CD63 complex and blocking HIV-1 release from the cells[111].

Similarly, in the case of HSV-1 infection, IFN-γ treatment of neuronal cells blocked the axonal transmission of HSV -1 infection, inhibiting spread of HSV-1[112]. IFN-γ also mediates its antiviral responses by increasing the expression of indoleamine 2,3-dioxygenase (IDO) and iNOS which results into depletion of tryptophan and production of nitric oxide (NO) to produce antiviral responses[113,114].

1.1.11. Dual Roles of IFN- γ in Cancer

Historically, IFN-γ has been considered a central player in anti-tumour immunity[27]. The anti-tumour properties of IFN-γ were discovered during studies using MethA fibrosarcoma cells in a syngeneic mouse model which lacked responsiveness to IFN-γ. These cells showed enhanced tumorigenicity compared to control cells, suggesting the direct effect of IFN-γ in tumour elimination[115]. Furthermore, the role of IFN-γ was further supported by experiments performed in 129/SV mice, lacking STAT1 and IFNGR1 and were IFN-γ insensitive. These mice developed rapid and more frequent sarcomas compared to wild-type counterparts[116]. Similarly, C57BL/6 mice with *Ifng*$^{-/-}$ phenotype were more susceptibile to development of primary and metastatic tumours compared to wild type mice[117] [118]. Additional studies performed mice models with either *Ifng*$^{-/-}$ phenotype or mice lacking recombination activating gene (RAG) protein (lacking mature B and T lymphocytes) developed Methylcholanthrene (MCA)-induced sarcomas to similar incidence level, suggesting the involvement of T cell–IFN-γ axis in tumour surveillance[119].

IFN-γ elucidates its anti-tumour properties by directly acting on tumour cells and by activating immune effector cells[120]. For instance, IFN-γ increases the expression of MHC class-I molecules on the surface of tumour cells and increases antigen presentation, resulting in their recognition by cytotoxic immune cells[121]. Additionally, IFN-γ induces the activation of NK cells and CTLs in the tumour microenvironment[121,122]. Direct anti-tumour actions of IFN-γ include,

induction of cell cycle arrest in tumour cells, induction of tumour cell death and generation of reactive oxygen species in these cells[120]. IFN-γ induces the activation p21 and p27 tumour suppressors to inhibit cell cycle progression and cell proliferation[123]. IFN-γ induced cell death in in cancer cells is associated with increased expression of both caspase-8. IFN-γ also induces cell death via death receptor pathways by increasing the expression of TNF family members (Fas, TRAIL, TNF-α etc)[124]. For instance, IFN-γ increased the expression of Fas and Fas ligand in a STAT1 dependent manner to induce cell death of HT-29 human colon adenocarcinoma cell line[125]. IFN-γ inhibited NF-κB mediated upregulation of XIAP to sensitize MIN6N8 insulinoma cells towards TNF-α- induced apoptosis[126]. IFN-γ sensitized osteosarcoma cells to Fas-induced apoptosis by up-regulating Fas receptors and caspase-8[127] [128]. IFN-γ also sensitized cells for different cell death ligands and chemotherapeutic drugs. IFN-γ increased the chemotherapeutic response of cisplatin in ovarian cancer cells.[129] In addition, the administration of type-I and type-II interferons in MCF-7 and Hela cells activated STAT1/3 phosphorylation to increase mitochondrial respiratory complex formation and reactive oxygen species (ROS) production, resulting in cellular apoptosis[130]. Also, in pancreatic cancer cells, IFN-γ increased the expression of Dual Oxidase 2 (Duox2)/ Dual Oxidase 2A (DuoxA2)expression in a JAK-STAT dependent manner to increase the production intracellular ROS and extracellular H_2O_2.[131]

In addition to cancer cell apoptosis, several studies have described the role of IFN-γ in activation of necrosis or necroptosis of cancer cells[132]. IFN-γ induced Receptor-interacting protein kinase 1 (RIPK1)/RIPK3 mediated necrosis in mouse embryonic fibroblasts, which required the activation of RNA-responsive kinase (PKR)[133]. IFN-γ treatment increased the expression of PKR which interacted with RIPK1 and induced its phosphorylation resulting in necrosis of MEFs. This IFN-γ/PKR mediated necrosis was negatively regulated by Fas

Associated Via Death Domain (FADD) and caspases[133]. IFN-γ synerised with Smac mimetic-BV6 to induce necroptosis in apoptosis resistant cell lines in an IRF-1 dependent manner[134]. Another study performed in colonic epithelial cell lines reported synergism between IFN-γ and Smac mimetics to increase expression of caspase 10 and RIPK1 to induce cell death independent of caspase 8, RIPK3 and Mixed Lineage Kinase Domain Like Pseudokinase (MLKL)[135]. IFN-γ induced the transcriptional activation of MLKL in different cancer cell lines[136]. IRF-1 or STAT1 knock down significantly attenuated the expression of MLKL, suggesting the IFN-γ dependent regulation of MLKL transcription[136]. The interaction of MLKL trimer with phosphatidylserine of the plasma membrane is required for the initiation of necroptosis. IFN-γ has been shown to increase the cell surface exposure of phosphatidylserine by activating MLKL in the absence of caspase-8 activity[137]. Recent studies have shown the involvement of IFN-γ into ferroptosis[138]. Ferroptosis is a unique iron catalysed mechanism of cell death, induced by either an increase in the intracellular iron pool or deactivation of Glutathione peroxidase 4 (GPX4) by depletion of the intracellular glutathione (GSH)[139]. A study from Wang et al. reported that IFN-γ released from infiltrating T-cells downregulated the expression of subunits of cystine/glutamate antiporter (Solute carrier (SLC) - SLC3A2 and SLC7A11) in cancer cells, causing the depletion of intracellular GSH, resulting in ferroptosis in tumour cells[140].

IFN-γ plays an important role in co-ordinating the activation of the effector immune system in tumour microenvironment[6]. IFN-γ secreted by T cells present in the tumour microenvironment of murine neuroblastoma model induced the M1-polarisation of macrophages resulting in increased immunogenicity and increased phagocytosis of cancer cells[66]. Consistently, IFN-γ also upregulated the expression of CIITA in multiple myeloma and melanoma cells, to increase the expression of their MHC II molecules[80 81]. Despite of the known role of IFN-γ in the development of immunosuppressive Treg cells, recent studies have shown

the role of IFN-γ in enhancing anti-tumour immunity by removal of T-reg cells[141]. Furthermore, studies with loss of active IFN-γ pathway components have confirmed the critical role of IFN-γ signalling in tumour killing and immunotherapy. A study from Weider et al suggested an important role of IFN-γ in triggering dormancy of tumour cells by triggering cell cycle arrest and senescence of cancer cells[142].

Recent evidence also implicates IFN-γ and IFN-γ pathway associated genes in acquired resistance to immunotherapy, which suggests a critical role of IFN-γ in mediating pro-tumour activities[143]. For example, IFN-γ has the ability to induce activation of PD-L1 expression in cancer, stromal and myeloid cells[144]. Prolonged activation of IFN-γ signalling in cancer cells has been associated with the induction of PD-L1 dependent and independent resistance immune checkpoint blockade[145,146]. As stated earlier, IFN-γ is potent activator of MHC class-I antigen presentation in cancer cells to increase their immunogenicity. But prolonged exposure of tumour cells to IFN-γ leads to a decrease in the expression of MHC-class I genes resulting in decrease antigen presentation[147,148]. A similar mechanism was observed in M14 melanoma and CT26 colon cancer cell lines where exposure of cancer cells to IFN-γ resulted in downregulation of antigen presentation, leading to immune evasion[149,150].

In summary, these studies suggest a dual role of IFN-γ in regulation of tumour immunity, demonstrating both anti-tumour and pro-tumour activities. IFN-γ influences tumour cells directly and indirectly by activation of immune cells. The broad range of IFN-γ actions depends on the IFN-γ-signalling intensity and duration, context of tumour specificity and other microenvironment conditions[151, 152,76].

1.1.12. IFN-γ in regulation of epithelial homeostasis

The regulation of intestinal homeostasis depends on the crosstalk between intestinal epithelial cells, microbiota and local immune cells[153,154]. The intestinal epithelial barrier plays an important role in the maintenance of this intestinal homeostasis and its disruption can lead to inflammatory bowel disease[155]. IFN-γ is one of the major cytokines reported to be elevated during IBD and has been reported to contribute to disease pathogenesis by increasing cell death in epithelial cells and Paneth cells, inducing dysregulation of cell structural proteins, and impairment of epithelial barrier functions[156–160]. The involvement of IFN-γ in the pathogenesis of intestinal disease is supported by studies in murine IBD model where mice lacking *Ifng*$^{-/-}$ were protected from DSS induced colitis[161]. IFN-γ has been reported to induce apoptosis in intestinal epithelial cells either itself or in combination of other cytokines[162–164]. In addition, IFN-γ can increase the permeability of the epithelial barrier by inducing the disassembly of tight junctions[165]. Cell culture and animal studies have shown the effect of proinflammatory cytokines on the regulation of tight junction (TJ) proteins, induction of epithelial apoptosis and enhanced bacterial translocation, as observed both in CD and UC[166,167]. IFN-γ reduced the expression ZO-1 and occluden-1 by adenosine monophosphate-activated protein kinase (AMPK)- dependent pathway in T84 intestinal epithelial cells[168]. IFN-γ also regulated the distribution of tight junction molecules on the cell surface[169]. For instance IFN-γ induced the down regulation of barrier forming claudin-1, -5 and -7 and increased the expression of pore forming claudin-2 in a rat colon[169]. IFN-γ induced the internalisation of tight junction proteins by the process of micropinocytosis[170]. The blockade of micropinocytosis by inhibitors blocked the internalisation of tight junction proteins[170]. IFN-γ induced the cleavage of intracellular desmoglein-2 to sensitize epithelial cells to apoptosis in response to pro-inflammatory cytokines[171]. Along with regulating junctional proteins, IFN-γ also regulated the ion transport

functions of epithelial barrier[172]. IFN-γ treatment decreased the Na^+K^+ ATPase activity of T84 cells resulting into increased intracellular Na^+ concentration in the cells and dysfunctional epithelium[172].

Paneth cells in the small intestine play an important role in the regulation of intestinal homeostasis by secreting antimicrobial peptides and maintaining the intestinal stem cell niche (ISC)[173–175]. Several studies have demonstrated a role for IFN-γ in enteropathies through induction of excessive cell death and injury of ISC[176]. Mouse crypts enteroids cultured with activated T cells showed excessive cell death of Paneth cells by activation of caspase 3/7 and loss of enteroid integrity[177]. Enteroids lacking IFN-γ receptor were not responsive to activated T cells, furthermore the treatment with JAK1/2 inhibitor ruxolitinib rescued Paneth cells confirming the role of IFN-γ in destruction of intestinal epithelium[177]. A ex vivo co-culture performed with epithelial organoids cultured with infiltrated T cells (performed to mimic bone marrow transplant) showed a JAK1-STAT1 mediated increase in pro-apoptotic gene expression and intestinal stem cell death[178]. The blockade of JAK-STAT pathway by JAK inhibitors, depletion of IFN-γ receptor from Paneth cell surface or dysregulation of T cell activation could protect the Paneth cells and the intestinal stem cell niche[178].

Even though IFN-γ has been associated with a proinflammatory role in IBD, there is mounting evidence suggesting the protective role of IFN-γ in disease models. For instance, a study from Nava *et al*. shows that IFN-γ regulated both proliferation and apoptosis and in intestinal epithelial cells through two different (serine-threonine protein kinase AKT-β-catenin and Wing- less-Int (Wnt)-β-catenin) signalling pathways[179]. They showed that a short exposure to IFN-γ induced the proliferation of epithelial cells while prolonged exposure to IFN-γ resulted in apoptosis of epithelial cells[179]. Also, IFN-γ induces the expression of IDO in epithelial cells[180]. TNBS colitis models show an increased level of IDO production compared to normal colon, in

response to increased IFN-γ level[180]. In addition, IFN-γ induced IL-10 receptor expression in intestinal epithelial cells and was required for the apical localisation of IL-10 in cells, suggesting a complex role of IFN-γ in support of intestinal homeostasis[181].

1.2. Tumour necrosis factor alpha

TNF-α is a pleiotropic multifunctional pro-inflammatory cytokine that plays vital role in immunity, inflammation, proliferation, differentiation, tissue homeostasis and cell death[182]. TNF-α was first described by Carswell et al in 1975 for its cytotoxic nature and induction of tumour necrosis[183]. Aggarwal et al in 1984 performed the isolation and characterisation of TNF-α and identified structural similarities of TNF-α with Lymphotoxin-α.

1.2.1. TNF-a gene

The gene encoding TNF-α is located in the class III region of the major histocompatibility complex on chromosome 6 (6p21.32) between the HLA-B and HLA-DR genes[184]. The TNF-α gene is around 3 kb long with four exons interspersed with three introns. The first and second exons code only the leading sequence of the nascent peptide, while the fourth exon of the gene encodes than 80% of protein[182]. Several regulatory sites with consensus sequences for transcription factors (NF-κB), AP-1, AP-2 and cAMP responsive element (CRE) are present at the 5'end of the TNF-α gene[182]. So far several genetic polymorphisms have been identified in the promotor region of TNF-α specifically related to the transcription start site-–1031 (T/C), −863 (C/A), −857 (C/A), −851 (C/T), −419 (G/C), −376 (G/A), −308 (G/A), −238 (G/A), −162 (G/A), and −49 (G/A). These polymorphism in the locus of TNF-α has been suggested to alter the production and bioactivity of TNF-α[185].

1.2.2. TNF-a protein:

TNF-α is a type-II transmembrane protein, produced in two forms: transmembrane TNF-α (tm TNF-α) and soluble TNF-α (sTNF-α). Initially, TNF-α is expressed as a 26 kDa transmembrane protein and is converted into a 17 kDa soluble form by a matrix metalloproteinase TNF-α converting enzyme (TACE) or ADAM metallopeptidase domain 17 (ADAM-17)[186]. Both,

transmembrane and soluble forms of TNF-α are active as homotrimers with each monomer of TNF-α containing two packed β-pleated sheets, assembled as eight anti-parallel β-strands arranged in a β-jellyroll topology[187]. The sTNF-α and tmTNF-α show differences in their biological activities, where the tmTNF-α form is more active than the sTNF- a form[188].

1.2.3. TNF receptors (TNFR) family

The TNF superfamily (TNFSF) consists of 19 structurally related proteins which interact with one or more receptors of the TNF receptor superfamily (TNFRSF) — consisting of 29 structurally similar receptors[189]. TNF-α exerts its biological functions by binding to two different receptors: TNF receptor 1 (TNFR1) and TNF receptor 2 (TNFR2)[190]. The *TNFR1* gene is localised on chromosome 12 (at locus12p13.31) and consists of 10 exons coding for a 55-60 kDa transmembrane receptor[191]. The *TNFR2* gene also consists of 10 exons and is located on chromosome 1 (locus 1p36.22) and codes for a 75-80 kDa protein[192]. A characteristic feature of the TNFR superfamily, is that the extracellular ligand binding domain of both TNFR1 and TNFR2 contains cysteine rich subdomains with a sequence homology of 28%, but the intracellular domain of TNFR1 and TNFR2 do not share any sequence homology[193,182]. TNFR1 is ubiquitously expressed on the surface of almost all cell types (except erythrocytes), while TNFR2 is mostly located on the surface of immune and endothelial cells[194]. A recent review from Fischer et al. references that in animal disease models the ablation of *TNFR1* reduces the disease status while the deletion of *TNFR2* exacerbates disease, suggesting the role of TNF-α/TNFR1 in activation of pro-apoptotic and inflammatory responses while TNFR2 is associated with immune regulation and tissue regeneration[195].

TNFR1 belongs to a family of death receptors (DR) each containing a characteristic death domain (DD) of 80 aa. In the absence of a stimulus, the death domain of TNFR1 is blocked by a silencer protein called silencer of death domain (SODD) which prevents the

activity of DD. Binding of TNF homotrimer to TNFR1 triggers the removal of SODD from the DD and results into the recruitment of TRADD to the DD of TNFR1[182,196]. This facilitates the context-dependent assembly of different signalling complexes (I, IIa, IIb and IIc) downstream of TNFR1 to give different functional outcomes such as cell survival, inflammation and cell death[197]. In contrast, TNFR2 expression is restricted to immune cells, endothelial cells and neurons[194]. It lacks a DD to facilitate interaction with TRADD hence programmed cell death cannot be induced by TNFR2 but it can activate the NF-κB pathway by interacting with TRAF1 and TRAF2[198].

1.2.4. TNFR1 Signalling by Complex-1

TNF-α signalling conventionally activates TNFR1 associated complex-1, which is composed of TRADD, FADD, TNF receptor-associated factor-2 (TRAF2), inhibitor of apoptosis proteins 1 (cIAP1), cIAP2 and RIPK1. Binding of TNF-α to TNFR1 induces homotrimerization of TNFR1 and mediates the association of TRADD with TNFR1 resulting in the binding of RIPK1 and TRAF2[199,200]. TRAF2 further recruits cIAP1 and cIAP2 to the complex[190,200]. A structural and signalling scaffold formed by a network of polyubiquitin chains is very important for the assembly and activation of TNFR1 complex-1[199]. TRAF2 along with cIAP1 or cIAP2 mediates Lys11, Lys48 and Lys63 linked polyubiquitination of complex-1. Different components of complex-1, including RIPK1, are conjugated with ubiquitin through this network[201,202]. This allows further recruitment of Linear ubiquitin chain assembly complex (LUBAC) which adds both complexity and stability to the complex-I[201,203,204]. LUBAC is composed of haem-oxidized IRP-2 ubiquitin ligase 1 (HOIL 1), HOIL 1 interacting protein (HOIP) and SHANK-associated RH domain interactor (SHARPIN), which adds M1-linked polyubiquitin chains to the complex. Recent studies show that the ubiquitination mediated scaffolding is a stepwise process.[197] (Figure 1.2)

This membrane-bound TNFR1 complex-1 allows activation of two signalling complexes: TGF beta-activated kinase 1 (TAK1) complex and inhibitor of kB (IkB) kinase (IKK) complex. Both the TAK1 and the IKK complex contain three subunits; the TAK1 complex is composed of TAK1, TAK1-binding protein 2 (TAB2) and TAB3 and the IKK complex consists of IKKα, IKKβ and NEMO (NF-κB modulator or IKKγ)[205]. There is a ubiquitin-binding domain present in both TAB2/3 (binds to K-63 chains) and NEMO (binds to M1-linked chains)[206 204 207]. A report suggests that K63/M1-linked polyubiquitin allows close proximity between TAK1 and IKK complex facilitating TAK1 induced phosphorylation of the IKK complex[207]. Phosphorylation of IKKβ mediates phosphorylation of IκBα (Inhibitor of NF-κB) at a specific serine residue which targets it for subsequent proteasomal degradation. Degradation of IkBα allows translocation of NF-κB p50/p65 heterodimer to the nucleus, leading to the expression of NF-κB and AP-1 target genes[200,208]. In order to fine-tune the activity of complex-1 there are different deubiquitinating enzymes (DUBs), associated with complex-1 which dismantle the ubiquitin network and repress the downstream activation of NF-κB. Another ubiquitin editing enzyme A20 downregulates the NF-κB signalling pathway by substituting the K63 linked ubiquitin chain of RIPK1 with K48 linked chain resulting in proteasomal degradation of RIPK1[209]. Another DUB, cylindromatosis (CYLD) was reported to remove K63 and M1-linked polyubiquitin chains from several components of complex-I including NEMO, RIPK1 and TRAF2[210 211]. Complex I regulates cell death, first by phosphorylating RIPK1 to inhibit its death-signalling function, and subsequently by phosphorylating IκB to activate NF-κB which induces the expression of pro-survival genes[197].

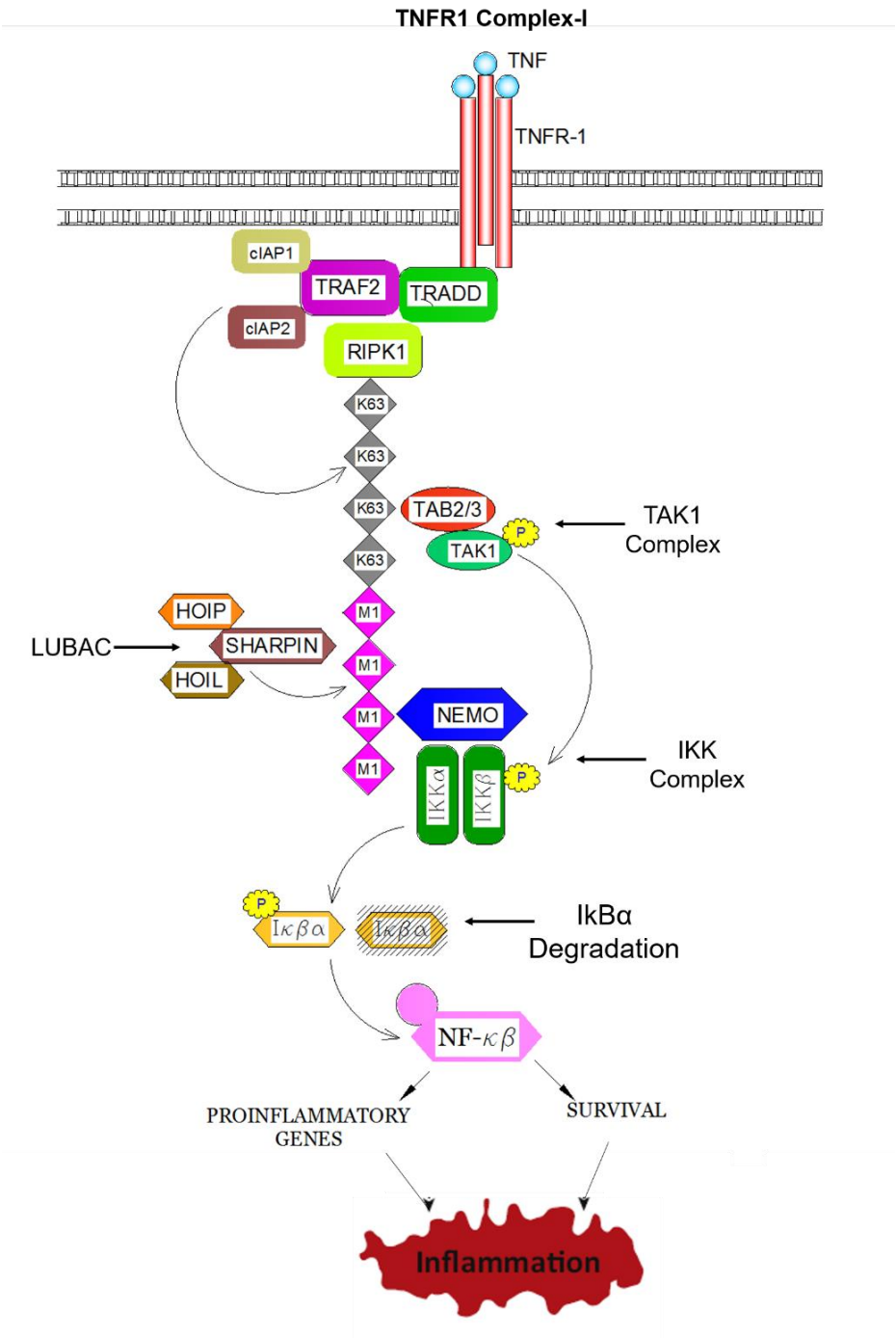


Figure 1.3. TNF signalling via TNFR1-Complex I

The binding of TNF-α to TNFR1 allows the formation of a macromolecular complex formed of TNFR1, TRADD, RIPK1, TRAF2, cIAP1/2, LUBAC, TAB2/3- TAK1 and NEMO-IKKα/IKKβ The recruitment of TRAF2-cIAP1/2 and LUBAC to TRADD results into K-63 and M1 ubiquitination of RIPK1, which acts as a platform for the recruitment of the TAK1 complex (TAB2/3-TAK1) and IKK complex (NEMO-

IKKα/IKKβ). The recruitment to the polyubiquitin chain allows proximity to TAK1 and IKK complex resulting in phosphorylation of IKKβ via TAK1. p-IKKβ phosphorylates IκBα and its proteasomal degradation. Degradation of IκBα allows translocation of NF-κB heterodimer to the nucleus, leading to the activation of NF-κB signalling pathway and survival and pro-inflammatory signalling.

Abbreviations are as follows: TNFR1, TNF receptor 1; TRADD, TNFR1 associated death domain protein; RIPK1, receptor interacting protein-1; TRAF2, TNF receptor-associated factor-2; cIAP, inhibitor of apoptosis proteins 1; LUBAC, Linear ubiquitin chain assembly complex; HOIL1, haem-oxidized IRP-2 ubiquitin ligase 1; HOIP, HOIL 1 interacting protein; SHAPRIN, SHANK-associated RH domain interactor; TAK1, TGF-β-activated kinase 1; TBP2, TAK1-binding protein 2; IκBα, inhibitor of κB alpha; IKK, (IκB) kinase; NEMO, NF-κB modulator

Modified from[197,212]

1.2.5. TNFR1 Signalling by Complex-II

TNFR1 signalling is tightly regulated to induce pro-inflammatory and pro-survival signals. But in the case of sensitized cells, disruption of signalling complex-I can lead to the formation of alternative TNFR1 signalling complexes which can result in apoptosis (complexes IIa & IIb) or necroptosis (complex IIc).[200] Unlike complex-I, complex IIa, IIb and IIc are assembled in the cytoplasm[213]. Formation of complex-II is a slow and transient process. Release of TRADD from complex 1 allows its association with FADD (Fas-associated via death domain) which acts as a platform for the recruitment and activation of caspase 8 and induction of apoptosis. This TRADD-FADD-Caspase 8 dependent apoptotic complex is termed TNFR1 complex-II-a[182]. NF-κB induces the expression of a gene called *CFLAR* which encodes FLICE-like inhibitory protein (c-FLIP) protein. c-FLIP is a homolog of caspase 8 and acts as a competitor for FADD binding. When NF-κB is transcriptionally active, c-FLIP levels are high and complex II is blocked. But when NF-κB activity is suppressed, caspase 8 activity increases due to the low level of c-FLIP[214]. RIPK1 ubiquitination also plays a crucial role in the complete activation of the NF-κB pathway. Cells with a mutation in RIPK1 at the ubiquitin acceptor site (K377R) underwent apoptosis after TNF-α stimulation[215] [216]. This was further supported by the observation that depletion of cIAP1/2 or LUBAC resulted in perturbation of RIPK1 ubiquitylation and increased sensitivity towards TNF-α induced cell death[216]. There are several reports showing that TNF-a stimulation of cells lacking IAPs, treated with Smac mimetics (IAP inhibitors), or in TAK1 or NEMO deficient cells can lead to a formation of cytoplasmic complex-IIb which is composed of TRADD-FADD-RIPK1 and caspase-8. This complex results into RIPK1 kinase activity dependent apoptosis.[212] The relative level of caspase-8 is an important factor contributing to the activity of this complex. Caspase-8 also mediates cleavage of RIPK1 and RIPK3 which inhibits the formation of a necroptosis complex thereby promoting apoptosis.[217] [218] A higher level of RIPK3 and MLKL in

the cells can reduce or block caspase 8 activity which leads to the formation of TNFR1 associated complex IIc- composed of RIPK1-RIPK3 -MLKL (necrosome)[212]. CYLD enzyme can also remove the ubiquitin chain of RIPK1 and favours necrosome formation[219]. C-FLIP is a crucial protein controlling the transition between apoptosis and necroptosis. A relatively high level of c-FLIP can lead to the formation of a Caspase-8-FLIP heterodimer. This heterodimer can assemble in complex-IIb but is not catalytical active and does not process into cleaved caspase 8. Thus, FADD-Caspase 8-$FLIP_L$ mediated control can prevent apoptosis.[220] This also explains why most of the studies on necroptosis use a combination of complex 1 inhibitors (smac mimetics, TAK1 inhibitor, IKK inhibitors) along with the caspase inhibitor z-VAD-fmk (carbobenzoxy-valyl-alanyl-aspartyl-[O-methyl]-fluoromethylketone) to establish the necrosome.[135] Addition of the transcriptional inhibitor Actinomycin D or the protein synthesis inhibitor cycloheximide along with the caspase 8 inhibitor can also result in necroptosis.[212]

Suppression of RIPK1 by complex I caspase-8 activity protects the cells from unnecessary cell death mediated by both complex IIb and complex IIc[221]. Some studies have shown both catalytic and non-catalytic activities of RIPK3. Catalytic inactive RIPK3 supported RIPK1 dependent apoptosis while active RIPK3 has been shown to induce necroptosis[222].

As discussed, the kinase activity of RIPK1, RIPK3 and blocking of caspase 8 activity is required for necrosome formation.[223] So far, the only relevant substrate known for RIPK1 and RIPK3 associated necroptosis is mixed lineage kinase domain-like protein (MLKL)[224]. The role of MLKL in necroptosis was identified by treatment of human cells with an inhibitor of necroptosis called necro sulphonamide (MLKL inhibitor)[225]. RNAi mediated knockdown of RIPK1 could also achieve a similar response in blocking necroptosis[226]. MLKL is a direct phosphorylation target of RIPK3 and serine phosphorylation of RIPK3 is crucial for stabilisation of MLKL in the complex. The location of MLKL in the cell is also important for necroptosis. At the early phase of

necroptosis, trimerized MLKL is translocated to the plasma membrane and interacts with membrane lipids [227] [228]. It facilitates the influx of positively charged ions $Ca2^{+}$, K^{+} and Na^{+} as an early event of necroptosis [227] [228].

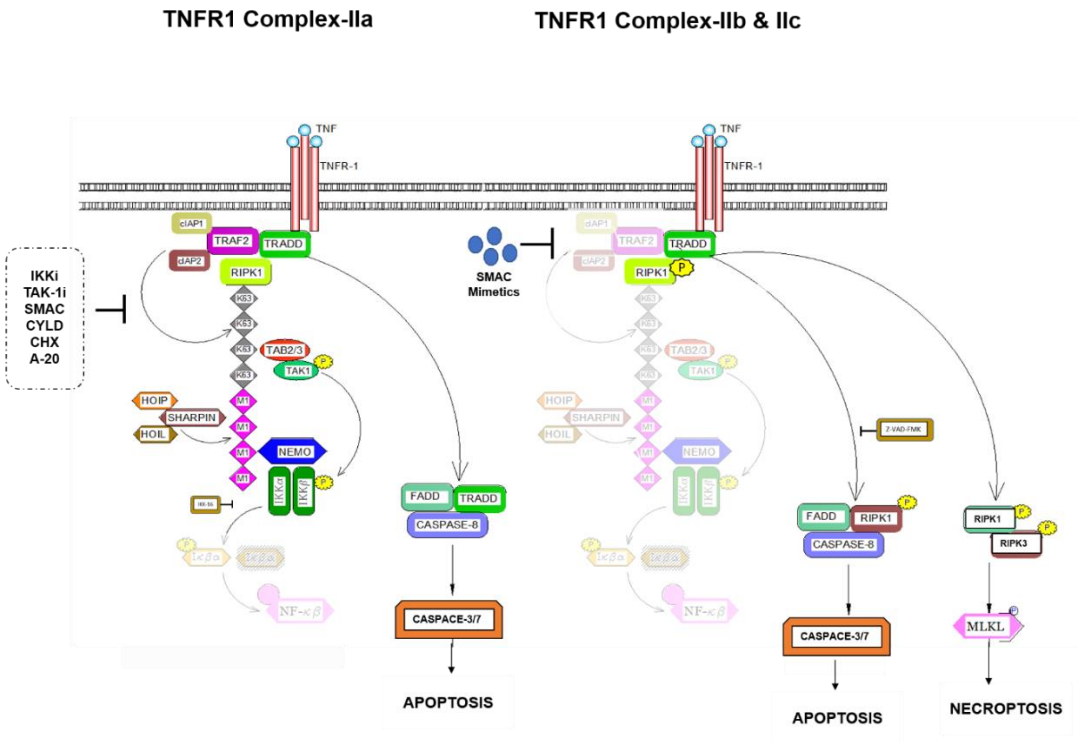


Figure 1.4 TNF signalling via TNFR1-Complex II

If NF-κB activity is blocked (e.g. in CHX or IKK inhibitor treated cells), a cytosolic complex containing TRADD, FADD and caspase-8 is formed, called complex-IIa. It allows autocatalysis of caspase-8 and activation of execution caspase 3/7 to induce apoptosis. The activity of complex-II-a is independent of kinase activity of RIPK1. Disruption of Complex-I (e.g. Smac mimetic, CYLD or TAK1 inhibitor), forms cytoplasmic complex-IIb, made up of FADD, RIPK1 and caspase-8, resulting in caspase 8 dependent apoptosis involving RIPK1 kinase activity. In addition of blocking complex-I activity, if caspase 8 is blocked (e.g. Z-VAD-FMK) complex Iic or the necrosome is formed, consisting of RIPK1, RIPK3 and MLKL. It activates RIPK1 kinase activity and RIPK3-kinase-activity-dependent necroptosis.

Abbreviations are as follows: TNFR1, TNF receptor 1; TRADD, TNFR1 associated death domain protein; RIPK1, receptor interacting protein-1; RIPK3, receptor interacting protein-3 TRAF2, TNF receptor-associated factor-2; cIAP, inhibitor of apoptosis proteins 1; LUBAC, Linear ubiquitin chain assembly complex; HOIL1, haem-oxidized IRP-2 ubiquitin ligase 1; HOIP, HOIL 1 interacting protein; SHAPRIN, SHANK-associated RH domain interactor; TAK1, TGF beta-activated kinase 1; TBP2, TAK1-binding protein 2; IκBα, inhibitor of kB alpha; IKK, (IkB)

kinase; NEMO, NF-κB modulator; CHX, cycloheximide; CYLD, Cylindromatosis; MLKL, mixed lineage kinase domain-like. Modified from[197,212]

1.2.6. Dual role of TNF in cancer

As discussed in the previous section, TNF-α induces the activation of both cell survival and cell death signalling depending upon the cellular context[200]. It plays a paradoxical role in the case of cancer biology by performing both anti-tumour and pro-tumour activities[229]. Initially TNF-α was isolated from the serum of mice treated with endotoxin and was able to induce tumour necrosis[230]. Following that numerous studies have investigated the role of TNF-α into cancer immunotherapy[229,231–234]. Interestingly, TNF-α can bind to the surface of almost all cell types, allowing its systemic administration and toxicity even at low concentration in various cancer models[190]. Therefore, several clinical trials conducted in 1980s and 1990s, used TNF-α for treatment of cancer by itself or along with other therapies (chemotherapy and radiotherapy), but results of these studies were a bit disappointing as there was massive toxicity due to systemic administration of TNF-α[235]. Later studies also showed that the cytotoxic effect of TNF-α is limited to specific cells lines[236]. However, studies performed with TNF-α in combination with actinomycin D, cycloheximide or IFN-γ showed cytotoxicity of TNF-α towards malignant cells[237 238].

In 1993, Komori et al. first discovered role of TNF-α in directly contributing to both oncogene activation and DNA damage in cancer cells[239]. The group reported that the long-term use of low dose of TNF-α on mouse 3T3 cell lines rendered them capable of forming tumours in mice[239]. High doses of TNF-α were also able to induce direct DNA damage in *Trp53*$^{-/-}$ cancer cells and also in genetically normal lung epithelial cells[240]. Furthermore, low level of TNF-α production by cancer cells in a B16 mouse melanoma model, increased infiltration of myeloid cells into the tumour vascularisation and growth, suggesting an important role of TNF-α dose on its anti-tumour or pro-tumour properties[241]. In an ovarian cancer murine model, $CD4^+$ T cells expressing TNFR1 were able to secrete IL-17 and and promoted infiltration of myeloid

cells to promote tumour progression[242]. Arnott et al suggested the role of both TNFR1 and TNFR2 expression in development of skin cancer[243]. In a DMBA/TPA induced skin carcinoma murine model both receptor TNFR1 and TNFR2 deficiency inhibited the papilloma growth significantly[243,233]. Some groups also reported reduced lung and liver metastases in *Tnfr1*$^{-/-}$ mice compared to wild type[244,245]. Blocking the activity of TNF-α or TNFR1 signalling using neutralising antibodies increased the level of $CD8^+$ T cells in tumour microenvironment and delayed cancer growth[246]. Moreover, studies also describe the role of TNF-α in epithelial-to-mesenchymal transition (EMT) in different cancer models including lung, breast, and renal cell carcinoma[247–250]. In summary, the role of TNF-α in cancer biology is very complex. TNF-α has the potential to activate both cell death processes and cell survival. The two opposing actions of TNF-α are also dependent on its levels in the tumour environment.

1.2.7. TNF-a in regulation of intestinal homeostasis and inflammation

TNF-α plays an important role in the maintenance of intestinal integrity but elevated levels of TNF-α can contribute to the pathogenesis of intestinal inflammation[253]. In mice and patients with chronic gut inflammation, TNF-α is produced at increased levels from multiple cell types in gut mucosal tissue[254–257]. Also, mice with overproduction of TNF-α due to a lack of AU-rich elements (ERE) in the 3'-untranslated region (3'-UTR) of the TNF-α mRNA transcript developed Crohn's like inflammation in their small intestine[258]. In addition, increased levels of TNF-α production in the intestinal mucosa is also a characteristic of murine models of intestinal inflammation induced by Dextran Sulphate Sodium (DSS), 2,4,6-trinitrobenzenesulfonic acid (TNBS) or in *Il10*$^{-/-}$ null mice [259–262]. However, while *Tnf-α*$^{-/-}$ mice were not sensitive to TNBS induced colitis *Tnf-α* overexpressing mice were more susceptible to intestinal inflammation[262,260]. Interestingly, in a murine model with DSS induced acute colitis, blocking

TNF-α activity using anti-TNF-α antibodies or *TNF-α* gene knock out, aggravated inflammation, suggesting a tissue protective homeostatic role of TNF-α in the case of acute inflammation[263].

Several studies have reported a role of TNF-α in the disruption of epithelial barrier functions. Epithelial cell shedding at the intestinal villus tip is part of regular homeostatic epithelial renewal and is highly regulated by tight junction protein complex to maintain barrier integrity[264,265]. Elevated levels of TNF-α were shown to alter the assembly of tight junction complexes and increased epithelial permeability and promoted massive epithelial cell shedding at the tip of villus[266–268]. In addition, altered tight junction profile and dysregulated epithelial cell shedding were also observed in the intestinal mucosa of patients with IBD.[269,270]. Mice deficient for NF-κB signalling in intestinal epithelial cells were characterised by increased levels of TNF-α, increased apoptotic cell death, disrupted epithelial barrier function with infiltration of bacteria inside the bowel wall and severe inflammation[271]. This disease phenotype was mediated by TNFR-1 signalling[271].

Interestingly, an in vitro model system also suggested differential effects of TNF-α concentration on wound healing phenotype where low concentration of TNF-α promoted wound healing in a TNFR2 dependent manner while a high concentration of TNF-α reduced prolieration[274,275]. Collectively, these studies suggest that optimal TNF-α levels are key player in maintaining intestinal homeostasis. In different contexts, TNF-α can exert beneficial or harmful functions, underlining its pleiotropic role in gut homeostasis.

1.3. IFN-γ and TNF-α cross talk in signalling

The conventional IFN-γ signalling pathway involves binding of IFN-γ to IFNGR leading to the activation of the JAK1/2-STAT1 signalling pathway and conventional TNF-α signalling involves signalling through TNFR1 for activation of the NF-κB and MAPK pathways[62,199]. However, studies in different model systems have described interactions between components of the IFN-γ/JAK1/2-STAT1 pathway and TNF-α /TNFR1 associated pathways. In 1997, Stark *et al*. described a novel mechanism underpinning TNF-α /CHX induced cell death that was dependent on the JAK1/2-STAT1 pathway and caspase activation in the murine fibroblast 2fTGH cell line[47]. While the parental 2fTGH cell line was sensitive to TNF-α /CHX treatment and cell death the *Stat1*$^{-/-}$ U3A cell line was resistant[47]. The study also suggested a crucial role of STAT1 pS727 in this TNF-α /CHX induced cell death[47]. Another study from Gua *et al.* reported the regulation of the JAK1/2-STAT1 pathway by TNF-α through TNFR1 signalling[276]. TNF-α was also reported to induce the phosphorylation and activation of JAKs (JAK1, JAK2 and Tyk2) specific STATs (STAT1, STAT3 and STAT5) in 3T3-L1 murine adipocyte cells by interaction with TNFR1[276]. The radiolabelling of JAKs and immunoprecipitation of TNFR1 confirmed the interaction of JAKs with TNFR1[276].

As discussed earlier, TNF-α signalling through TNFR1 allows its association with TRADD forming complex-I to activate the NF-κB pathway for inflammatory and cell survival signalling[277]. Wang *et al.* reported the formation of a unique complex which consisted of an association of STAT1 with both TRADD and FADD leading to the formation of a TNFR1-TRADD-STAT1 complex in Hela cells[278]. Furthermore, the same study also highlighted the role of STAT1 and the TNFR1-TRADD-STAT1 complex in the negative regulation of NF-κB activation in response to TNF-α treatment[278]. SOCS1 is one of the major negative feedback regulators for

JAK-STAT signalling pathway[58]. A study from Morito *et al.* reported that SOCS1 could supress TNF-α induced cell death in murine embryonic fibroblasts cells by blocking p38/MAPK pathway activation[279]. They showed that fibroblasts cells derived from *Socs1*$^{-/-}$ mice were very sensitive to TNF-α treatment and underwent accelerated apoptosis[279]. In addition, overexpression of SOCS1 in the TNF-α sensitive L929 murine fibroblast cell line made them resistant to TNF-α induced cell death[279]. Furthermore, SOCS1 was also reported to supress TNF-α induced cell death in murine embryonic fibroblast cells by blocking JAKs and caspase-8 activity[280]. Additionally, a study from Wesemann *et al.* also reported interaction of components of the IFN-γ signalling pathway with TNFR1 and other components of complex-1 in RAW264.7 macrophage cells[278]. The study showed that IFN-γ treatment induced the formation of TRADD-STAT1 complex in macrophage cells[278]. IFN-γ also mediated the nuclear translocation of this TRADD-STAT1 complex which negatively regulated the DNA binding ability and transcriptional potential of STAT1 in the nucleus[278]. However, there was no reported evidence of formation of STAT1-TRADD complex with TNF-α stimulation[278].

Furthermore, IFN-γ has also been reported to regulate RIPK1 and MLKL activity affecting necroptosis in different model systems[135,281,136]. NF-κB activation negatively regulated the IFN-γ induced necrosis in MEFs and mice model[282]. MEFs with compromised NF-κB activity or NF-κB knockout mice induced a RIPK1 and JAK1 dependent accumulation of ROS resulting in necrosis and inflammation[282]. There is also evidence of IFN-γ induced necroptosis in the absence of caspase-8. Upon IFN-γ treatment, MEFs lacking caspase 8 and RIPK3 showed an increased expression of *MLKL* and increased exposure of phosphatidylcholine on the plasma membrane. This allowed more interaction of MLKL trimer with plasma membrane resulting into necroptosis[137]. Also, in HT-29 *CASP8*$^{-/-}$ cell line, IFN-γ synergised with smac mimetics to induce cell death in a RIPK1 and caspase-10 dependent manner[135]. A study from Cekay *et al.*

also confirmed the role synergism between IFN-γ and smac mimetics to trigger necroptosis in apoptosis-resistant cancer cell lines[134].

Concanavalin A (ConA) is a lectin known to induce inflammatory liver injury by activation of immune cells[283] A study by Gruther *et al.* reported that the treatment of hepatocytes with ConA stimulated T cells to activate IFN-γ induced necroptosis[284]. This necroptosis involved an IFN-γ mediated activation of STAT1 to increase the expression level of MLKL to induce necroptosis[284]. This IFN-γ supported necroptosis was independent of RIPK3 mediated phosphorylation of MLKL[284]. Another study in hepatocytes suggested IFN-γ and ConA dependent necrotic cell death caused by autophagic flux and increased lysosomal membrane permeabilization[285]. The cooperativity of IFN-γ and TNF-α can also be explained by the increased expression of corresponding receptors in response to the individual and co-operating cytokines[286-290]. IFN-γ has been shown to also upregulate the level of TNFR1 and TNFR2 in the Caco-2 cell line[291]. In addition, the upregulation of TNFR2 by IFN-γ was shown to sensitize the cells for response to TNF-α and downstream effects on epithelial barrier function[291].

Altogether, the evidence suggests that there is a high degree of cross-talk between the IFN-γ and TNF-α signalling pathways which provides possible mechanisms underpinning the synergism between both cytokines for both gene regulation and induction of epithelial cell death. But the synergism is not limited to signalling crosstalk at the receptor level and at the level of downstream signalling pathway components. IFN-γ and TNF-α also synergise to regulate gene expression through epigenetic and transcriptional mechanisms that are not completely understood.

1.4. IFN-γ and TNF-α transcriptional cross talk

Compelling evidence suggests that the inflammatory effects of IFN-γ and TNF-α involves their transcriptional synergism for macrophage activation, antigen presentation, chemotaxis, antiviral responses and cell death[292–295]. In order to perform these functions, both cytokines synergistically regulate the activity of major transcription factors like NF-κB, STAT1, IRF-1 and CIITA [296–301]. NF-κB is the key transcription factor activated by the TNF-α signalling pathway and STAT1 and IRF1 are major transcription factors involved with IFN-γ signalling pathway[277,302]. There is also evidence of synergism between the primary transcription factors STAT1 and NF-κB to induce diverse responses[303-306]. In 1997, Ohmori et al showed that while TNF-α alone induced transient activation of NF-κB through the degradation of IκBα, IFN-γ and TNF-α synergistically induced prolonged activation of the NF-κB pathway by triggering the degradation of both IκBα and IκB-β promoting translocation of NF-κB to the nucleus[303]. In hepatic pancreatic cells IFN-γ and TNF-α synergistically increased ROS production, and loss of mitochondrial membrane potential by STAT1 overexpression, promoting apoptosis and liver injury induced by LPS/D-galactosamine (D-GalN)[307]. In IFN-γ and TNF-α treated fibroblast cell lines there was cooperative transcriptional regulation of proinflammatory genes mediated by co-operating downstream transcription factors by NF-κB and STAT1[303].

IFN-γ and TNF-α synergism plays an important role in providing immunity against infectious diseases[308]. The synergistic regulation of antiviral response by IFN-γ and TNF-α was first discovered by Wong et al 1986, demonstrating that the coadministration of the two cytokines can block viral replication for both RNA and DNA viruses[309]. The antiviral activity of IFN-γ and TNF-α was associated with synergistic upregulation of 2'-5'-oligoadenylate synthetase (OAS2) [309]. After that, the synergistic regulation of anti-viral response was

confirmed for several viruses including Epstein Barr virus, Herpes simplex virus-2, Varicella zoster and SARS[293]. One of the mechanisms hypothesised for IFN-γ and TNF-α synergism in terms of mediating an antimicrobial response is the regulation of cellular tryptophan stores. IFN-γ and TNF-α synergistically regulate the transcription of IDO[310,311], an enzyme required for tryptophan catabolism and required for generation of antimicrobial responses[312]. IFN-γ and TNF-α also mediate their antiviral responses by increasing the expression of IFN-β.

In response to infections, IFN-γ and TNF-α increase the activation of macrophages to elucidate a robust inflammatory and microbiocidal effector phenotype[295,313]. IFN-γ and TNF-α synergistically increased the expression of transcription of the transcription factor CIITA which regulates the increase in the expression of MHC class-II genes and molecules in macrophages[301,314]. Another mechanism underpinning activation of macrophages by IFN-γ and TNF-α involves increased expression of iNOS which is required for the ROS generation to eradicate bacterial or viral [292,299,315].

To activate the adaptive arm of the immune response IFN-γ and TNF-α synergistically increase the expression levels of chemokine and adhesion molecules to promote the trafficking of different immune cells into the site of inflammation[316]. Specifically, CXCL10 (IFN-γ -induced protein 10, IP-10) is the major chemokine associated with the influx of $CD4^+$ and $CD8^+$ T cells for production of different inflammatory cytokines[317] and for effective anti-viral and anti-tumour adaptive immune responses. The perturbation of CXCL-10 reduced the influx of $CD4^+$ and $CD8^+$ T cells and the severity of colitis in *Il10*$^{-/-}$ mice by decreasing the production of cytokines. Even though IFN-γ itself is a potent regulator of CXCL-10 production, CXCL10 is synergistically regulated by both IFN-γ and TNF-α under inflammatory conditions in many different cell types. A study in NIH3T3 cells showed that the

CXCL-10 promoter has one binding motif for ISRE and two sites for NF-κB binding[318]. Although, IFN-γ and TNF-α independently regulated the interaction of transcription factors with these binding motifs disruption of either binding motif blocked the synergistic induction of CXCL-10[318]. IFN-γ and TNF-α synergistically regulated *CX3CL1* expression and post-transcriptional stabilisation of CX3CL1 in vascular endothelial cells[319]. Moreover, a study by Wang *et al.* showed that IFN-γ and TNF-α synergistically increased the expression of *ICAM1* in an NF-κB-dependent manner to increase the cytotoxicity.

Furthermore, IFN-γ and TNF-α also support the signalling crosstalk between both pathways by increasing the expression of genes encoding each other's cell surface receptors. IFN-γ has been reported to increase the expression level of TNFR1 and TNFR2 to increase cancer cell death[290]. In Caco-2 cell line, treatment with IFN-γ increased the expression level of both TNFR1 and TNFR2[291]. In a study from Li et al, TNF-α enhanced the IFN-γ signalling pathway by increasing the expression level of IFNGR1 in HCC cells, which supported the expression of B7-H1 molecules in tumour cells to develop immune resistance[286].

1.5. IFN-γ and TNF-α Crosstalk and Cell death

Pro-inflammatory cytokines such as IFN-γ and TNF-α play an important role in the development of an immunogenic microenvironment and therefore are main players in mediating immunopathology and an anti-tumour immune response. A study from Hermelink *et al.* suggested that both TNFR and IFNGR signalling were essential for the anti-tumour effects IFN-γ and TNF-α. In the presence of IFN-γ and TNF-α receptors on pancreatic cells, T cells induced tumour supressing effect while Absence of either receptor (IFNGR or TNFR) on the surface of pancreatic cancer cell, same T cell pancreatic promoted cell proliferation and angiogenesis in resulting in islet carcinoma, further supporting the co-operative anti-tumour effect of IFN-γ and TNF-α[320].

The role of IFN-γ and TNF-α synergism in tumour cell death is well described *in vivo* and *in vitro* studies[321]. As early as 1983, Williamson *et al.* identified that IFN-γ and TNF-α synergised to induce cell death in transformed B-cells. Since then several studies have demonstrated the role of IFN-γ and TNF-α synergism in anti-proliferative and cell death activities. So far, several mechanisms have been identified for the regulation of IFN-γ and TNF-α induced cell death in different model systems. In colon cancer cells, TNF-α and IFN-γ accelerated NF-κB- mediated apoptosis through increased of expression of Fas ligand In the HT-29 colon cancer cell line, IFN-γ and TNF-α activated apoptotic pathways by activation of PI3K dependent signalling and nitric oxide expression[322]. In a human salivary gland cell line (HSG) IFN-γ sensitized the cells for TNF-α mediated activation of apoptotic pathways[323]. Feng *et al.* reported , that upon exposure to low dose of x-ray radiation or ultraviolet radiation, bone marrow-derived mesenchymal stromal cells (BM-MSCs) mediated an anti-tumour effect by secreting IFN-γ and TNF-α, which inhibited the proliferation and induced apoptosis of

colorectal cancer cells[324]. Shen *et al.* described a combination therapy with tumour vasculature homing peptide (TCP)- 1/TNF-α and TCP- 1/IFN-γ to inhibit colorectal tumour growth by inducing targeted tumour cell necrosis[325].

Other than inducing direct apoptotic effects, IFN-γ and TNF-α also promoted other immune cells for induction of cell death in cancer cells[321]. For instance, a study from Zhang *et al.* showed that IFN-γ and TNF-α produced by cytotoxic T lymphocytes (CTLs) were crucial for the irradication of mouse tumours[295]. The IFN-γ and TNF-α secreted by CTLs promoted perforin mediating killing of all stromal cells, including antigen-loss variants (ALVs) and tumour destruction[295]. Moreover, IFN-γ and TNF-α synergistically enhanced cytotoxicity of NK cells by up-regulation of ICAM-1 expression in an NF-κB dependent manner[326]. The upregulated ICAM1 facilitated direct interaction between target cells and NK cells to promote target cell cytolysis[326]. Also, in human and murine breast cancer cell lines IFN-γ and TNF-α induced apoptosis, reduced proliferation and reduced the surface expression of (HER2) protein[327]. Other than promoting cell death in cancer cells IFN-γ and TNF-α also inhibit cancer progression by mediating cell cycle arrest and inducing tumour dormancy[320,328,329].

Even though IFN-γ+TNF-α induced synergistic cell death plays an important role in mediating anti-tumour immunity, excessive cell death induced by two cytokines can contribute to immunopathology in chronic inflammatory diseases and autoimmune diseases including rheumatoid arthritis, Type-1 diabetes mellites, psoriasis, graft versus host disease and inflammatory bowel disease [330,331]. Type 1 diabetes mellites (T1DM) is a common autoimmune disease characterised by destruction of insulin-secreting pancreatic beta cells with consequent immune deficiency [332]. For a long time IFN-γ+TNF-α synergism had been proposed as the critical death mediators in β-cell destruction[333]. Administration of IFN-γ and TNF-α in NOD mice induced caspase dependent apoptosis of insulinoma and pancreatic cells

in a STAT1/IRF-1 dependent manner [334]. The treatment of these NOD mice with anti-TNF antibodies inhibited cell death and prevented the development of diabetes[334]. *Stat1*$^{-/-}$ NOD mice were resistant to IFN-γ+TNF-α induced cell death and this confirmed the role of STAT1 in IFN-γ+TNF-α synergistic β-cell apoptosis and type 1 diabetes[335] Furthermore, Chang *et al.* described a novel mechanism of IFN-γ+TNF-α induced cell death via regulation of cytosolic Ca^{2+} concentration[336]. The treatment of insulinoma (MIN6N8) cells with IFN-γ+TNF-α increased the cytosolic Ca^{2+} concentration resulting in activation of intracellular events leading to mitochondria dependent apoptosis[336]. The blocking of Ca^{2+} downstream signalling by inhibitor FK506 could rescue this cell death[336]. Another study suggested that IFN-γ+TNF-α synergistic cell death was mediated by activation of the JNK/SAPK pathway, p53 activation and ROS production[337]. Barthsom and collegues, reported the activation of BCL-2 interacting protein (DP5), p53 up-regulated modulator of apoptosis (PUMA) and Bim in rodent β-cells upon IFN-γ+TNF-α treatment. Furthermore, Kim *et al.* suggested that XIAP was an important modulator for pancreatic cell death and that a decrease in XIAP levels could induce pancreatic β-cell apoptosis[126]. They showed that IFN-γ+TNF-α regulated the cell death by controlling the level of XIAP in the cells. , Where TNF-α induced the expression of XIAP in a NF-κB dependent manner while IFN-γ supressed the XIAP activation in NF-κB independent manner[126].

IFN-γ and TNF-α are two main cytokines known for disruption of epithelial homeostasis and immunopathology of IBD[158]. The measurement of IFN-γ and TNF-α levels from biopsy samples obtained from non-inflamed and inflamed intestine using spot-ELISA identified elevated level of IFN-γ and TNF-α in the inflamed biopsies, supporting the role of these cytokines in disease[338,157] Extensive studies over the past three decades have shown that IFN-γ and TNF-α regulate epithelial barrier function through molecular mechanisms including triggering of epithelial cell death and disruption of tight junction proteins[339]. In the INT-407 epithelial cell

line, IFN-γ and TNF-α induced epithelial cell death via caspase 8 activation which further activated BAX and caspase 9 for activation of executioner caspase-3 and apoptosis.[163] In colon cancer cell lines short-term stimulation (less than 2 days) with TNF-α or IFN-γ caused cell growth arrest and sensitized the epithelial cells to CD95 (Fas/Apo-1)-mediated cell death. while long-term cytokine exposure attenuated the cell death responses[340]. There are also evidence showing synergistic induction of cell death in small intestinal crypts cell in a Fas-dependent manner by IFN-γ and TNF-α[163]. IFN-γ and TNF-α also disrupted gut barrier function by damaging the apical junctional complex (AJC) mediated by increased internalization of TJs and and increasing membrane permeability by redistribution of Junctional Adhesion Molecule (JAM-1) [165]. IFN-γ and TNF-α together damaged the basement membrane molecules, laminin required for epithelial cell proliferation and differentiation.[341]. Even though the cytokines synergistically induced cell death via apoptosis, blocking apoptosis could not rescue the cell death of intestinal cells suggesting that the cell death happens by an apoptosis-independent mechanism.[341] Other than that, T-cell derived cytokines IFN-γ and TNF-α also regulate intestinal homeostasis by regulating Paneth cell death and disruption of the stem cell niche[178,342,343]. Sjögren's syndrome (SS) is an autoimmune disorder characterized by the destruction of salivary and lachrymal glands by pro-inflammatory cytokines. Hairy cell leukaemia was reported to extremely sensitive to IFN-γ. Kulkarni et al reported that IFN-γ can sensitizes the HSG (human salivary gland cell line) to TNF-α- induced apoptosis[323]. The exposure of hairy cells to IFN-γ resulted in a significant increase in TNF-α secretion resulting in caspase-8 and caspase--9 activation to induce apoptosis[323]. Multiple sclerosis (MS) is a chronic inflammatory disorder of the central nervous system characterized by destruction of myelin sheaths and oligodendrocytes. IFN-γ and TNF-α are reported to target cell death and tissue injury in MS. IFN-γ and TNF-α synergized to induce apoptosinin and apoptosis after 24 hours

of incubation in oligodendroglia cell lines - human oligodendroglioma (HOG) and MO3.13[344]. There are also evidence showing involvement of cytokine synergism in relapse of the MS[345,346]. In summary, the association of IFN-γ and TNF-α synergism with both cancer and autoimmune diseases makes them very clinically relevant immune effector molecules. A mechanistic understanding of the synergistic co-operation between IFN-γ and TNF-α may help in the discovery of new biology and targets for treatment of cancer and autoimmune diseases.

1.6. References

1. Ivashkiv, L. B. IFNγ: signalling, epigenetics and roles in immunity, metabolism, disease and cancer immunotherapy HHS Public Access. Nat Rev Immunol 18, 545–558 (2018).
2. Ozgür A, Xiang Z, Radev DR, He Y. Literature-Based Discovery of IFN-γ and Vaccine-Mediated Gene Interaction Networks. J. Biomed. Biotechnol. 2010, 2–4 (2010)
3. Schroder, K., Hertzog, P. J., Ravasi, T. & Hume, D. A. Interferon gamma orchestrates : an overview of signals , mechanisms and functions. J. Leukoc. Biol. 75, 163–189 (2004).
4. Trent, J. M., Olson, S. & Lawn, R. M. Chromosomal localization of human leukocyte, fibroblast, and immune interferon genes by means of in situ hybridization. Proc. Natl. Acad. Sci. U. S. A. (1982).
5. Naylor, S. L. et al. Human immune interferon gene is located on chromosome 12. J. Exp. Med. (1983).
6. Alspach, E., Lussier, D. M. & Schreiber, R. D. Interferon γ and its important roles in promoting and inhibiting spontaneous and therapeutic cancer immunity. Cold Spring Harb. Perspect. Biol. 11, (2019).
7. Ealick, S. E. et al. Three-dimensional structure of recombinant human interferon-γ. Science (80-86). (1991).
8. Hogrefe, H. H. et al. Amino terminus is essential to the structural integrity of recombinant human interferon-γ. J. Biol. Chem. (1989).
9. Zavodny, P. J., Petro, M. E., Chiang, T. R., Narula, S. K. & Leibowitz, P. J. Alterations of the Amino Terminus of Murine Interferon-γ: Expression and Biological Activity. J. Interferon Res. (1988).
10. Pernis, A. et al. Lack of interferon gamma receptor beta chain and the prevention of

interferon gamma signaling in TH1 cells. Science (80-.). 269, 245–7 (2006).

11. Bach, E. A. et al. Ligand-induced autoregulation of IFN-γ receptor β chain expression in T helper cell subsets. Science (80-.). (1995).

12. Fountoulakis, M. et al. A 25-kDa stretch of the extracellular domain of the human interferon γ receptor is required for full ligand binding capacity. J. Biol. Chem. (1991).

13. Hershey, G. K. K. & Schreiber, R. D. Biosynthetic analysis of the human interferon-γ receptor. Identification of N-linked glycosylation intermediates. J. Biol. Chem. (1989).

14. Bach, E. A. et al. Ligand-induced assembly and activation of the gamma interferon receptor in intact cells. Mol. Cell. Biol. (1996).

15. Igarashi, K. I. et al. Interferon-γ induces tyrosine phosphorylation of interferon-γ receptor and regulated association of protein tyrosine kinases, Jak1 and Jak2, with its receptor. J. Biol. Chem. (1994).

16. Greenlund, A. C. et al. Stat recruitment by tyrosine-phosphorylated cytokine receptors: An ordered reversible affinity-driven process. Immunity (1995).

17. Walter, M. R. et al. Crystal structure of a complex between interferon-γ and its soluble high-affinity receptor. Nature (1995).

18. Bach, E. A., Aguet, M. & Schreiber, R. D. The IFN gamma receptor: a paradigm for cytokine receptor signaling. Annu. Rev. Immunol. (1997).

19. Greenlund, A. C., Farrar, M. A., Viviano, B. L. & Schreiber, R. D. Ligand-induced IFN gamma receptor tyrosine phosphorylation couples the receptor to its signal transduction system (p91). EMBO J. 13, 1591–600 (1994).

20. Heim, M., Kerr, I., Stark, G. & Darnell, J. Contribution of STAT SH2 groups to specific interferon signaling by the Jak-STAT pathway. Science (80-.). 267, 1347–1349 (1995).

21. Decker, T., Lew, D. J., Mirkovitch, J., Darnell, J. E. & Jr. Cytoplasmic activation of GAF, an

IFN-gamma-regulated DNA-binding factor. EMBO J. 10, 927–32 (1991).

22. Wen, Z., Zhong, Z. & Darnell, J. E. Maximal activation of transcription by Stat1 and Stat3 requires both tyrosine and serine phosphorylation. Cell 82, 241–50 (1995).

23. Varinou, L. et al. Phosphorylation of the Stat1 transactivation domain is required for full-fledged IFN-gamma-dependent innate immunity. Immunity 19, 793–802 (2003).

24. Putz, E. M. et al. STAT1-S727 - the license to kill STAT1-S727 - the license to kill. 49–52 (2017).

25. Staab, J. et al. CDK8 as the STAT1 serine 727 kinase? 3996, (2017).

26. Kovarik, P. et al. Stress-induced phosphorylation of STAT1 at Ser727 requires p38 mitogen-activated protein kinase whereas IFN-uses a different signaling pathway.

27. Castro, F., Cardoso, A. P., Gonçalves, R. M., Serre, K. & Oliveira, M. J. Interferon-gamma at the crossroads of tumor immune surveillance or evasion. Front. Immunol. 9, 1–19 (2018).

28. Rettino, A. & Clarke, N. M. Genome-wide Identification of IRF1 Binding Sites Reveals Extensive Occupancy at Cell Death Associated Genes. J. Carcinog. Mutagen. (2013).

29. McBride, K. M. & Reich, N. C. The Ins and Outs of STAT1 Nuclear Transport. Sci. Signal. 2003, re13–re13 (2003).

30. Improta, T. et al. Transcription factor ISGF-3 formation requires phosphorylated Stat91 protein, but Stat113 protein is phosphorylated independently of Stat91 protein. Proc. Natl. Acad. Sci. U. S. A. 91, 4776–80 (1994).

31. Mowen, K. & David, M. Role of the STAT1-SH2 domain and STAT2 in the activation and nuclear translocation of STAT1. J. Biol. Chem. 273, 30073–6 (1998).

32. Sekimoto, T., Imamoto, N., Nakajima, K., Hirano, T. & Yoneda, Y. Extracellular signal-dependent nuclear import of Stat1 is mediated by nuclear pore-targeting complex

formation with NPI-1, but not Rch1. EMBO J. 16, 7067–77 (1997).

33. Köster, M. & Hauser, H. Dynamic redistribution of STAT1 protein in IFN signaling visualized by GFP fusion proteins. Eur. J. Biochem. 260, 137–44 (1999).

34. McBride, K. M., McDonald, C. & Reich, N. C. Nuclear export signal located within theDNA-binding domain of the STAT1transcription factor. EMBO J. 19, 6196–206 (2000).

35. Mechanisms and consequences of Jak–STAT signaling in the immune system. (2017). doi:10.1038/ni.3691

36. Mowen, K. A. et al. Arginine Methylation of STAT1 Modulates IFNα/β-Induced Transcription. Cell 104, 731–741 (2001)

37. Krämer, O. H. & Heinzel, T. Phosphorylation–acetylation switch in the regulation of STAT1 signaling. Mol. Cell. Endocrinol. 315, 40–48 (2010).

38. Krä Mer, O. H. et al. A phosphorylation-acetylation switch regulates STAT1 signaling (2011).

39. Antunes, F., Marg, A. & Vinkemeier, U. STAT1 signaling is not regulated by a phosphorylation-acetylation switch. Mol. Cell. Biol. 31, 3029–37 (2011).

40. Precious, B., Childs, K., Fitzpatrick-Swallow, V., Goodbourn, S. & Randall, R. E. Simian Virus 5 V Protein Acts as an Adaptor, Linking DDB1 to STAT2, To Facilitate the Ubiquitination of STAT1. J. Virol. 79, 13434–13441 (2005).

41. Guo, H., Mi, Z., Bowles, D. E., Bhattacharya, S. D. & Kuo, P. C. Osteopontin and protein kinase C regulate PDLIM2 activation and STAT1 ubiquitination in LPS-treated murine macrophages. J. Biol. Chem. 285, 37787–96 (2010)

42. Ren, Y. et al. Deubiquitinase USP2a Sustains Interferons Antiviral Activity by Restricting Ubiquitination of Activated STAT1 in the Nucleus. PLoS Pathog. 12, 1–27 (2016).

43. Begitt, A., Droescher, M., Knobeloch, K.-P. & Vinkemeier, U. SUMO conjugation of STAT1 protects cells from hyperresponsiveness to IFN. (2011).

44. Droescher, M., Begitt, A. & Vinkemeier, U. Paracrystals of STAT proteins and their dissolution by SUMO: How reduced transcription factor solubility increases cytokine signaling. Oncotarget 2, 527–528 (2015).

45. Yang, J. & Stark, G. R. Roles of unphosphorylated STATs in signaling. Cell Res. 18, 443–451 (2008).

46. Yang, J. et al. Unphosphorylated STAT3 accumulates in response to IL-6 and activates transcription by binding to NFkappaB. Genes Dev. 21, 1396–408 (2007).

47. Kumar, A., Commane, M., Flickinger, T. W., Horvath, C. M. & Stark, G. R. Defective TNF-α-induced apoptosis in STAT1-null cells due to low constitutive levels of caspases. Science 278, 1630–1632 (1997).

48. White, L. C. et al. Regulation of LMP2 and TAP1 genes by IRF-1 explains the paucity of CD8+ T cells in IRF-1-/- mice. Immunity 5, 365–76 (1996).

49. Chatterjee-Kishore, M., Wright, K. L., Ting, J. P. & Stark, G. R. How Stat1 mediates constitutive gene expression: a complex of unphosphorylated Stat1 and IRF1 supports transcription of the LMP2 gene. EMBO J. 19, 4111–22 (2000).

50. Xu, D. & Qu, C.-K. Protein tyrosine phosphatases in the JAK/STAT pathway. Front. Biosci. 13, 4925–32 (2008).

51. Irie-Sasaki, J. et al. CD45 is a JAK phosphatase and negatively regulates cytokine receptor signalling. Nature 409, 349–354 (2001).

52. Yamada, T., Zhu, D., Saxon, A. & Zhang, K. CD45 controls interleukin-4-mediated IgE class switch recombination in human B cells through its function as a Janus kinase phosphatase. J. Biol. Chem. 277, 28830–5 (2002).

53. Fleming, H. E., Milne, C. D. & Paige, C. J. CD45-Deficient Mice Accumulate Pro-B Cells Both In Vivo and In Vitro. J. Immunol. 173, 2542–2551 (2004).

54. Zhimin Chen, Xiuquan Ma, Haohao Zhang, Xiaoxiao Sun, Shensi Shen, Ying Li, Yuan Gu, Ying Wang, Shoushen Yan, Qiang Yu, Negative regulation of interferon-γ/STAT1 signaling through cell adhesion and cell density-dependent STAT1 dephosphorylation, Cellular Signalling, (2011).

55. Neel, B. G., Gu, H. & Pao, L. The 'Shp'ing news: SH2 domain-containing tyrosine phosphatases in cell signaling. Trends Biochem. Sci. 28, 284–93 (2003).

56. You, M., Yu, D. H. & Feng, G. S. Shp-2 tyrosine phosphatase functions as a negative regulator of the interferon-stimulated Jak/STAT pathway. Mol. Cell. Biol. 19, 2416–24 (1999).

57. Kershaw, N. J., Murphy, J. M., Lucet, I. S., Nicola, N. A. & Babon, J. J. Regulation of Janus kinases by SOCS proteins. Biochem. Soc. Trans. 41, 1042–1047 (2013).

58. Larkin, J., Ahmed, C. M., Wilson, T. D. & Johnson, H. M. Regulation of interferon gamma signaling by suppressors of cytokine signaling and regulatory T cells. Front. Immunol. 4, 1–8 (2013).

59. Croker, B. A., Kiu, H. & Nicholson, S. E. SOCS regulation of the JAK/STAT signalling pathway. Semin. Cell Dev. Biol. 19, 414–22 (2008).

60. Yoshimura, A., Naka, T. & Kubo, M. SOCS proteins, cytokine signalling and immune regulation. Nat. Rev. Immunol. 7, 454–465 (2007).

61. Majoros, A. et al. Canonical and Non-Canonical Aspects of JAK–STAT Signaling: Lessons from Interferons for Cytokine Responses. Front. Immunol. 8, 29 (2017).

62. Villarino, A. V., Kanno, Y., Ferdinand, J. R. & O'Shea, J. J. Mechanisms of Jak/STAT Signaling in Immunity and Disease. The Journal of Immunology 194, 21–27 (2015).

63. Bousoik, E. & Montazeri Aliabadi, H. “Do We Know Jack” About JAK? A Closer Look at JAK/STAT Signaling Pathway. Front. Oncol. 8, 1–20 (2018).

64. Harrison, C. & Vannucchi, A. M. Ruxolitinib: a potent and selective Janus kinase 1 and 2 inhibitor in patients with myelofibrosis. An update for clinicians. Ther. Adv. Hematol. 3, 341–54 (2012).

65. Raedler, L. A. Jakafi (Ruxolitinib): First FDA-Approved Medication for the Treatment of Patients with Polycythemia Vera. Am. Heal. drug benefits 8, 75–9 (2015).

66. JAK-inhibitors. New players in the field of immune-mediated diseases, beyond rheumatoid arthritis.

67. Dhillon, S. Tofacitinib: A Review in Rheumatoid Arthritis. Drugs 77, 1987–2001 (2017).

68. Hodge, J. A. et al. The mechanism of action of tofacitinib - an oral Janus kinase inhibitor for the treatment of rheumatoid arthritis. Clin. Exp. Rheumatol. 34, 318–28

69. Gonzales, A. J. et al. Oclacitinib (APOQUEL ®) is a novel Janus kinase inhibitor with activity against cytokines involved in allergy. J. Vet. Pharmacol. Ther. 37, 317–324 (2014).

70. Choudhury, G. G. A linear signal transduction pathway involving phosphatidylinositol 3-kinase, protein kinase Cepsilon, and MAPK in mesangial cells regulates interferon-gamma-induced STAT1alpha transcriptional activation. J. Biol. Chem. 279, 27399–409 (2004).

71. Qing, Y. & Stark, G. R. Alternative Activation of STAT1 and STAT3 in Response to Interferon-. J. Biol. Chem. 279, 41679–41685 (2004).

72. Meinke, A., Barahmand-Pour, F., Wöhrl, S., Stoiber, D. & Decker, T. Activation of different Stat5 isoforms contributes to cell-type-restricted signaling in response to interferons. 16, (1996).

73. Deb, A., Haque, S. J., Mogensen, T., Silverman, R. H. & Williams, B. R. RNA-dependent protein kinase PKR is required for activation of NF-kappa B by IFN-gamma in a STAT1-independent pathway. J. Immunol. 166, 6170–80 (2001).

74. Lewis, M., Amento, E. P. & Unemori, E. N. Transcriptional inhibition of stromelysin by interferon-gamma in normal human fibroblasts is mediated by the AP-1 domain. J. Cell. Biochem. 72, 373–86 (1999).

75. Waddell, S. J. et al. Dissecting interferon-induced transcriptional programs in human peripheral blood cells. PLoS One 5, e9753 (2010).

76. Castro, F. et al. Interferon-gamma at the crossroads of tumor immune surveillance or evasion. Front. Immunol. 9, 1–19 (2018).

77. Askenase, M. H. et al. Bone-Marrow-Resident NK Cells Prime Monocytes for Regulatory Function during Infection. Immunity (2015).

78. Prencipe, G. et al. Neutralization of IFN-γ reverts clinical and laboratory features in a mouse model of macrophage activation syndrome. J. Allergy Clin. Immunol. 141, 1439–1449 (2018)

79. Leopold Wager, C. M. et al. IFN-γ immune priming of macrophages in vivo induces prolonged STAT1 binding and protection against Cryptococcus neoformans. PLoS Pathog. 14, (2018)

80. Zhao, M. et al. MHC class II transactivator (CIITA) expression is upregulated in multiple myeloma cells by IFN-γ. Mol. Immunol. 44, 2923–2932 (2007)

81. Deffrennes, V. et al. Constitutive expression of MHC class II genes in melanoma cell lines results from the transcription of class II transactivator abnormally initiated from its B cell-specific promoter. J. Immunol. 167, 98–106 (2001)

82. Decker, T., Stockinger, S., Karaghiosoff, M., Müller, M. & Kovarik, P. IFNs and STATs in

innate immunity to microorganisms. J. Clin. Invest. 109, 1271–7 (2002).

83. MacMicking, J., Xie, Q. & Nathan, C. NITRIC OXIDE AND MACROPHAGE FUNCTION. Annu. Rev. Immunol. 15, 323–350 (1997)

84. Zhang, Y. et al. Interferon γ stabilizes the T helper cell type 1 phenotype. J. Exp. Med. (2001). doi:10.1084/jem.194.2.165

85. Schulz, E. G., Mariani, L., Radbruch, A. & Höfer, T. Sequential Polarization and Imprinting of Type 1 T Helper Lymphocytes by Interferon-γ and Interleukin-12. Immunity (2009). doi:10.1016/j.immuni.2009.03.013

86. Dickensheets, H. L., Venkataraman, C., Schindler, U. & Donnelly, R. P. Interferons inhibit activation of STAT6 by interleukin 4 in human monocytes by inducing SOCS-1 gene expression. Proc. Natl. Acad. Sci. U. S. A. 96, 10800–10805 (1999).

87. Hwang, E. S., Szabo, S. J., Schwartzberg, P. L. & Glimcher, L. H. T helper cell fate specified by kinase-mediated interaction of T-bet with GATA-3. Science 307, 430–3 (2005).

88. Lazarevic, V. et al. T-bet represses TH 17 differentiation by preventing Runx1-mediated activation of the gene encoding RORγt. Nat. Immunol. (2011).

89. Herrero, C. et al. Reprogramming of IL-10 activity and signaling by IFN-gamma. J. Immunol. 171, 5034–41 (2003).

90. Hu, X. et al. IFN-gamma suppresses IL-10 production and synergizes with TLR2 by regulating GSK3 and CREB/AP-1 proteins. Immunity 24, 563–74 (2006).

91. Park, I.-K., Letterio, J. J. & Gorham, J. D. TGF-beta 1 inhibition of IFN-gamma-induced signaling and Th1 gene expression in CD4+ T cells is Smad3 independent but MAP kinase dependent. Mol. Immunol. 44, 3283–90 (2007).

92. Olalekan, S. A., Cao, Y., Hamel, K. M. & Finnegan, A. B cells expressing IFN-γ suppress Treg-cell differentiation and promote autoimmune experimental arthritis. Eur. J.

Immunol. 45, 988–998 (2015).

93. Caretto, D., Katzman, S. D., Villarino, A. V., Gallo, E. & Abbas, A. K. Cutting Edge: The Th1 Response Inhibits the Generation of Peripheral Regulatory T Cells. J. Immunol. 184, 30–34 (2010).

94. Wang, Z. et al. Role of IFN-gamma in induction of Foxp3 and conversion of CD4+ CD25- T cells to CD4+ Tregs. J. Clin. Invest. 116, 2434–41 (2006).

95. Hwang, S. et al. Nondegradative role of Atg5-Atg12/Atg16L1 autophagy protein complex in antiviral activity of interferon gamma. Cell Host Microbe (2012).

96. Weizman, O. El et al. ILC1 Confer Early Host Protection at Initial Sites of Viral Infection. Cell (2017).

97. Changotra, H. et al. Type I and Type II Interferons Inhibit the Translation of Murine Norovirus Proteins. J. Virol. (2009).

98. Upton, J. W. & Chan, F. K. M. Staying alive: Cell death in antiviral immunity. Mol. Cell 54, 273–280 (2014).

99. Kang, S., Brown, H. M. & Hwang, S. Direct antiviral mechanisms of interferon-gamma. Immune Network 18, (2018).

100. Zhang, M. et al. Anti-West Nile virus activity of in vitro expanded human primary natural killer cells. BMC Immunol. (2010).

101. Seeger, C. & Mason, W. S. Molecular biology of hepatitis B virus infection. Virology (2015).

102. Patterson, C. E., Lawrence, D. M. P., Echols, L. A. & Rall, G. F. Immune-Mediated Protection from Measles Virus-Induced Central Nervous System Disease Is Noncytolytic and Gamma Interferon Dependent. J. Virol. (2002).

103. Burdeinick-Kerr, R. & Griffin, D. E. Gamma Interferon-Dependent, Noncytolytic

Clearance of Sindbis Virus Infection from Neurons In Vitro. J. Virol. (2005).

104. Wei, X. et al. Inhibition of hepatitis C virus infection by interferon-γ through downregulating claudin-1. J. Interf. Cytokine Res. (2009). doi:10.1089/jir.2008.0040

105. Reynolds, G. M. et al. Hepatitis C virus receptor expression in normal and diseased liver tissue. Hepatology (2008).

106. García, M. A. et al. Impact of Protein Kinase PKR in Cell Biology: from Antiviral to Antiproliferative Action. Microbiol. Mol. Biol. Rev. (2006).

107. Rowland, R. R. R. et al. Inhibition of porcine reproductive and respiratory syndrome virus by interferon-gamma and recovery of virus replication with 2-aminopurine. Arch. Virol. (2001).

108. Grünvogel, O. et al. DDX60L Is an Interferon-Stimulated Gene Product Restricting Hepatitis C Virus Replication in Cell Culture. J. Virol. (2015).

109. Harris, N., Buller, R. M. & Karupiah, G. Gamma interferon-induced, nitric oxide-mediated inhibition of vaccinia virus replication. J. Virol. (1995).

110. Kropp, K. et al. Reversible inhibition of MCMV replication by IFNγ in primary macrophages involves a primed type I IFN signaling sub-network for full establishment of an immediate-early antiviral-state. J. Virol. (2011).

111. Kubo, Y. et al. Gamma-interferon-inducible, lysosome/endosome-localized thiolreductase, GILT, has anti-retroviral activity and its expression is counteracted by HIV-1. Oncotarget 7, 71255–71273 (2016).

112. Mikloska, Z. & Cunningham, A. L. Alpha and Gamma Interferons Inhibit Herpes Simplex Virus Type 1 Infection and Spread in Epidermal Cells after Axonal Transmission. J. Virol. (2001).

113. Kane, M. et al. Identification of Interferon-Stimulated Genes with Antiretroviral Activity.

Cell Host Microbe (2016).

114. Becerra, A. et al. Increased activity of indoleamine 2,3-dioxygenase in serum from acutely infected dengue patients linked to gamma interferon antiviral function. J. Gen. Virol. (2009).

115. Dighe, A. S., Richards, E., Old, L. J. & Schreiber, R. D. Enhanced in vivo growth and resistance to rejection of tumor cells expressing dominant negative IFNγ receptors. Immunity (1994).

116. Kaplan, D. H. et al. Demonstration of an interferon γ-dependent tumor surveillance system in immunocompetent mice. Proc. Natl. Acad. Sci. U. S. A. (1998).

117. Street, S. E. A., Cretney, E. & Smyth, M. J. Perforin and interferon-γ activities independently control tumor initiation, growth, and metastasis. Blood (2001).

118. Street, S. E. A., Trapani, J. A., MacGregor, D. & Smyth, M. J. Suppression of lymphoma and epithelial malignancies effected by interferon γ. J. Exp. Med. (2002).

119. Shankaran, V. et al. IFNγ, and lymphocytes prevent primary tumour development and shape tumour immunogenicity. Nature (2001).

120. Zaidi, M. R. The Interferon-Gamma Paradox in Cancer (2019).

121. Martini, M. et al. IFN-γ-mediated upmodulation of MHC class I expression activates tumor-specific immune response in a mouse model of prostate cancer. Vaccine (2010).

122. Vigneron, N. Human Tumor Antigens and Cancer Immunotherapy. BioMed Research International (2015).

123. Laphanuwat, P. & Jirawatnotai, S. Immunomodulatory Roles of Cell Cycle Regulators. Front. Cell Dev. Biol. 7, 23 (2019).

124. Kim, K.-B. et al. Potentiation of Fas- and TRAIL-mediated apoptosis by IFN-gamma in A549 lung epithelial cells: enhancement of caspase-8 expression through IFN-response

element. Cytokine 20, 283–8 (2002).

125. Xu, X., Fu, X. Y., Plate, J. & Chong, A. S. FN-gamma induces cell growth inhibition by Fas-mediated apoptosis: requirement of STAT1 protein for up-regulation of Fas and FasL expressioIn. Cancer Res. 58, 2832–7 (1998).

126. Kim, H. S., Kim, S. & Lee, M.-S. IFN-gamma sensitizes MIN6N8 insulinoma cells to TNF-alpha-induced apoptosis by inhibiting NF-kappaB-mediated XIAP upregulation. Biochem. Biophys. Res. Commun. 336, 847–53 (2005).

127. Inaba, H., Glibetic, M., Buck, S., Ravindranath, Y. & Kaplan, J. Interferon-? sensitizes osteosarcoma cells to fas-induced apoptosis by up-regulating fas receptors and caspase-8. Pediatr. Blood Cancer 43, 729–736 (2004).

128. Adachi, Y. et al. Apoptosis of colorectal adenocarcinoma induced by 5-FU and/or IFN-gamma through caspase 3 and caspase 8. Int. J. Oncol. 15, 1191–6 (1999).

129. Barton, C., Davies, D., Balkwill, F. & Burke, F. Involvement of both intrinsic and extrinsic pathways in IFN-γ-induced apoptosis that are enhanced with cisplatin. Eur. J. Cancer 41, 1474–1486 (2005).

130. Wang, Y. et al. The STAT-ROS cycle extends IFN-induced cancer cell apoptosis. Int. J. Oncol. 52, 305–313 (2018).

131. Wu, Y. et al. Up-regulation and sustained activation of Stat1 are essential for interferon-γ (IFN-γ)-induced dual oxidase 2 (Duox2) and dual oxidase A2 (DuoxA2) expression in human pancreatic cancer cell lines. J. Biol. Chem. 286, 12245–12256 (2011).

132. Balachandran, S. & Adams, G. P. Interferon-γ-Induced Necrosis: An Antitumor Biotherapeutic Perspective. J. Interf. Cytokine Res. 33, 171–180 (2013).

133. Thapa, R. J. et al. Interferon-induced RIP1/RIP3-mediated necrosis requires PKR and is licensed by FADD and caspases. Proc. Natl. Acad. Sci. U. S. A. 110, E3109–E3118 (2013).

134. Cekay, M. J. et al. Smac mimetics and type II interferon synergistically induce necroptosis in various cancer cell lines. Cancer Lett. 410, 228–237 (2017).

135. Tanzer, M. C. et al. Combination of IAP antagonist and IFNγ activates novel caspase-10- and RIPK1-dependent cell death pathways. Cell Death Differ. 24, 481–491 (2017).

136. Knuth, A. K. et al. Interferons Transcriptionally Up-Regulate MLKL Expression in Cancer Cells. Neoplasia (United States) 21, 74–81 (2019).

137. Chen, J., Kuroki, S., Someda, M. & Yonehara, S. Interferon-g induces the cell surface exposure of phosphatidylserine by activating MLKL in the absence of caspase-8 activity. J. Biol. Chem. jbc.RA118.007161 (2019).

138. Zitvogel, L. & Kroemer, G. Interferon-Î3 induces cancer cell ferroptosis.

139. Tang, D., Kang, R., Berghe, T. Vanden & Vandenabeele, P. The molecular machinery of regulated cell death. Cell Res. (2019).

140. Wang, W. et al. CD8+ T cells regulate tumour ferroptosis during cancer immunotherapy. Nature 569, 270–274 (2019).

141. Overacre-Delgoffe, A. E. et al. Interferon-γ Drives Treg Fragility to Promote Anti-tumor Immunity. Cell (2017).

142. Wieder, T., Brenner, E., Braumüller, H., Bischof, O. & Röcken, M. Cytokine-induced senescence for cancer surveillance. Cancer and Metastasis Reviews 36, 357–365 (2017).

143. Gao, J. et al. Loss of IFN-γ Pathway Genes in Tumor Cells as a Mechanism of Resistance to Anti-CTLA-4 Therapy. Cell (2016).

144. Abiko, K. et al. IFN-γ from lymphocytes induces PD-L1 expression and promotes progression of ovarian cancer. Br. J. Cancer (2015).

145. Benci, J. L. et al. Tumor Interferon Signaling Regulates a Multigenic Resistance Program

to Immune Checkpoint Blockade. Cell (2016).

146. Wang, X. B., Zheng, C. Y., Giscombe, R. & Lefvert, A. K. Regulation of surface and intracellular expression of CTLA-4 on human peripheral T cells. Scand. J. Immunol. (2001).

147. Shankaran, V. et al. IFNgamma and lympohcytes prevent primary tomour development and shape tomour immunogenicity. Nature (2001).

148. Koebel, C. M. et al. Adaptive immunity maintains occult cancer in an equilibrium state. Nature (2007).

149. Beatty, G. L. & Paterson, Y. IFN-γ Can Promote Tumor Evasion of the Immune System In Vivo by Down-Regulating Cellular Levels of an Endogenous Tumor Antigen. J. Immunol. (2000).

150. Le Poole, I. C. et al. Interferon-γ reduces melanosomal antigen expression and recognition of melanoma cells by cytotoxic T cells. Am. J. Pathol. (2002).

151. Zaidi, M. R. et al. Interferon-γ 3 links ultraviolet radiation to melanomagenesis in mice. Nature (2011).

152. Kosmidis, C. et al. Interferon-γ and colorectal cancer: An up-to date. Journal of Cancer (2018).

153. De Mey, J. R. & Freund, J.-N. Understanding epithelial homeostasis in the intestine. Tissue Barriers 1, e24965 (2013).

154. Maloy, K. J. & Powrie, F. Intestinal homeostasis and its breakdown in inflammatory bowel disease. Nature 474, 298–306 (2011).

155. Koch, S. & Nusrat, A. The Life and Death of Epithelia During Inflammation: Lessons Learned from the Gut. Annu. Rev. Pathol. Mech. Dis. 7, 35–60 (2012).

156. Neurath, M. F. Cytokines in inflammatory bowel disease. Nat. Rev. Immunol. 14, 329–

342 (2014).

157. Vitale, S. et al. Cytokine production profile in intestinal mucosa of paediatric inflammatory bowel disease. (2017).

158. Lechuga, S. & Ivanov, A. I. Disruption of the epithelial barrier during intestinal inflammation: Quest for new molecules and mechanisms. Biochim. Biophys. Acta - Mol. Cell Res. 1864, 1183–1194 (2017).

159. Farin, H. F. et al. Paneth cell extrusion and release of antimicrobial products is directly controlled by immune cell-derived IFN-γ. J. Exp. Med. (2014).

160. Lee, S. H. Intestinal Permeability Regulation by Tight Junction: Implication on Inflammatory Bowel Diseases. Intest. Res. 13, 11 (2015).

161. Ito, R. et al. Interferon-gamma is causatively involved in experimental inflammatory bowel disease in mice. Clin. Exp. Immunol. (2006).

162. Jarry, A. et al. Mucosal IL-10 and TGF-beta play crucial roles in preventing LPS-driven, IFN-gamma-mediated epithelial damage in human colon explants. J. Clin. Invest. 118, 1132–42 (2008).

163. Mukherjee, S. & Biswas, T. Activation of TOLLIP by porin prevents TLR2-associated IFN-γ and TNF-α-induced apoptosis of intestinal epithelial cells. Cell. Signal. 26, 2674–2682 (2014).

164. Woznicki, J. A. et al. Human BCL-G regulates secretion of inflammatory chemokines but is dispensable for induction of apoptosis by IFN-γ and TNF-α in intestinal epithelial cells.

165. Bruewer, M. et al. Proinflammatory cytokines disrupt epithelial barrier function by apoptosis-independent mechanisms. J. Immunol. 171, 6164–72 (2003).

166. Lee, S. H. Intestinal permeability regulation by tight junction: implication on inflammatory bowel diseases. Intest. Res. 13, 11–8 (2015).

167. Chelakkot, C., Ghim, J. & Ryu, S. H. Mechanisms regulating intestinal barrier integrity and its pathological implications. Experimental and Molecular Medicine 50, (2018).

168. Scharl, M., Paul, G., Barrett, K. E. & McCole, D. F. AMP-activated protein kinase mediates the interferon-γ-induced decrease in intestinal epithelial barrier function. J. Biol. Chem. (2009).

169. Amasheh, S. et al. Tight junction proteins as channel formers and barrier builders: Claudin-2, -5, and -8. Ann. N. Y. Acad. Sci. (2009).

170. Bruewer, M. et al. Interferon-γ induces internalization of epithelial tight junction proteins via a macropinocytosis-like process. FASEB J. 19, 923–933 (2005).

171. Yulis, M., Quiros, M., Hilgarth, R., Parkos, C. A. & Nusrat, A. Intracellular Desmoglein-2 cleavage sensitizes epithelial cells to apoptosis in response to pro-inflammatory cytokines. Cell Death Dis. 9, 389 (2018).

172. Sugi, K., Musch, M. W., Field, M. & Chang, E. B. Inhibition of NA+,K+-ATPase by interferon γ down-regulates intestinal epithelial transport and barrier function. Gastroenterology 120, 1393–1403 (2001).

173. Lueschow, S. R. & McElroy, S. J. The Paneth Cell: The Curator and Defender of the Immature Small Intestine. Frontiers in Immunology 11, 587 (2020).

174. Bevins, C. L. & Salzman, N. H. Paneth cells, antimicrobial peptides and maintenance of intestinal homeostasis. Nat. Rev. Microbiol. 9, 356–368 (2011).

175. Roth, S. et al. Paneth cells in intestinal homeostasis and tissue injury. PLoS One 7, (2012).

176. Fu, Y. Y. et al. T Cell Recruitment to the Intestinal Stem Cell Compartment Drives Immune-Mediated Intestinal Damage after Allogeneic Transplantation. Immunity 51, 90-103.e3 (2019).

177. Eriguchi, Y. et al. Essential role of IFN-γ in T cell-associated intestinal inflammation. JCI insight 3, (2018).

178. Takashima, S. et al. T cell-derived interferon-γ programs stem cell death in immune-mediated intestinal damage. Sci. Immunol. (2019).

179. Nava, P. et al. Interferon-γ Regulates Intestinal Epithelial Homeostasis through Converging β-Catenin Signaling Pathways. Immunity 32, 392–402 (2010).

180. Gurtner, G. J., Newberry, R. D., Schloemann, S. R., McDonald, K. G. & Stenson, W. F. Inhibition of Indoleamine 2,3-Dioxygenase Augments Trinitrobenzene Sulfonic Acid Colitis in Mice. Gastroenterology 125, 1762–1773 (2003).

181. Kominsky, D. J. et al. IFN-γ–Mediated Induction of an Apical IL-10 Receptor on Polarized Intestinal Epithelia. J. Immunol. 192, 1267–1276 (2014).

182. Zelová, H. & Hošek, J. TNF-α signalling and inflammation: Interactions between old acquaintances. Inflamm. Res. 62, 641–651 (2013).

183. Carswell, E. A. et al. An endotoxin induced serum factor that cuases necrosis of tumors. Proc. Natl. Acad. Sci. U. S. A. 72, 3666–3670 (1975).

184. El-Tahan, R. R., Ghoneim, A. M. & El-Mashad, N. TNF-α gene polymorphisms and expression. (2016).

185. Elahi, M. M., Asotra, K., Matata, B. M. & Mastana, S. S. Tumor necrosis factor alpha -308 gene locus promoter polymorphism: An analysis of association with health and disease. Biochimica et Biophysica Acta - Molecular Basis of Disease (2009).

186. Black, R. A. et al. A metalloproteinase disintegrin that releases tumour-necrosis factor-α from cells. Nature 385, 729–733 (1997).

187. Eck, M. J. & Sprang, S. R. The structure of tumor necrosis factor-α at 2.6 Å resolution. Implications for receptor binding. J. Biol. Chem. (1989). doi:10.2210/pdb1tnf/pdb

188. Wajant, H., Pfizenmaier, K. & Scheurich, P. Tumor necrosis factor signaling. Cell Death Differ. 10, 45–65 (2003).

189. Croft, M., Benedict, C. A. & Ware, C. F. Clinical targeting of the TNF and TNFR superfamilies. Nat. Rev. Drug Discov. 12, 147–168 (2013).

190. Holbrook, J., Lara-Reyna, S., Jarosz-Griffiths, H. & McDermott, M. Tumour necrosis factor signalling in health and disease F1000Research 8, (2019).

191. Fuchs, P., Strehl, S., Dworzak, M., Himmler, A. & Ambros, P. F. Structure of the human TNF receptor 1 (p60) gene (TNRF1) and localization to chromosome 12p13. Genomics (1992).

192. Santee, S. M. & Owen-Schaub, L. B. Human tumor necrosis factor receptor p75/80 (CD120b) gene structure and promoter characterization. J. Biol. Chem. (1996).

193. Ledgerwood, E. C., Pober, J. S. & Bradley, J. R. Recent advances in the molecular basis of TNF signal transduction. Lab. Invest. 79, 1041–50 (1999).

194. Faustman, D. & Davis, M. TNF receptor 2 pathway: drug target for autoimmune diseases. Nat. Rev. Drug Discov. 9, 482–493 (2010).

195. Fischer, R., Kontermann, R. E. & Pfizenmaier, K. Selective Targeting of TNF Receptors as a Novel Therapeutic Approach. Frontiers in Cell and Developmental Biology 8, 401 (2020).

196. Ihnatko, R. & Kubes, M. TNF signaling: early events and phosphorylation. Gen. Physiol. Biophys. 26, 159–67 (2007).

197. Ting, A. T. & Bertrand, M. J. M. More to Life than NF-κB in TNFR1 Signaling. Trends Immunol. 37, 535–545 (2016).

198. Wajant, H. & Siegmund, D. TNFR1 and TNFR2 in the Control of the Life and Death Balance of Macrophages. Front. Cell Dev. Biol. 7, 91 (2019).

199. Kalliolias, G. D. & Ivashkiv, L. B. TNF biology, pathogenic mechanisms and emerging therapeutic strategies. Nat. Rev. Rheumatol. 12, 49–62 (2016).

200. Brenner, D., Blaser, H. & Mak, T. W. Regulation of tumour necrosis factor signalling: live or let die. Nat. Rev. Immunol. 15, 362–374 (2015).

201. De Almagro, M. C., Goncharov, T., Newton, K. & Vucic, D. Cellular IAP proteins and LUBAC differentially regulate necrosome-associated RIP1 ubiquitination. Cell Death Dis. 6, (2015).

202. Tokunaga, F. Linear ubiquitination-mediated NF-κB regulation and its related disorders. Journal of Biochemistry 154, 313–323 (2013).

203. Haas, T. L. et al. Recruitment of the Linear Ubiquitin Chain Assembly Complex Stabilizes the TNF-R1 Signaling Complex and Is Required for TNF-Mediated Gene Induction. Mol. Cell 36, 831–844 (2009).

204. Rahighi, S. et al. Specific Recognition of Linear Ubiquitin Chains by NEMO Is Important for NF-κB Activation. Cell 136, 1098–1109 (2009).

205. Aggarwal, B. B., Gupta, S. C. & Kim, J. H. Historical perspectives on tumor necrosis factor and its superfamily: 25 years later, a golden journey. Blood 119, 651–665 (2012).

206. Kanayama, A. et al. TAB2 and TAB3 Activate the NF-κB Pathway through Binding to Polyubiquitin Chains. Mol. Cell 15, 535–548 (2004).

207. Emmerich, C. H. et al. Activation of the canonical IKK complex by K63/M1-linked hybrid ubiquitin chains. Proc. Natl. Acad. Sci. U. S. A. 110, 15247–52 (2013).

208. Hayden, M. S. & Ghosh, S. Regulation of NF-κB by TNF family cytokines. Semin. Immunol. 26, 253–266 (2014).

209. Wertz, I. E. et al. De-ubiquitination and ubiquitin ligase domains of A20 downregulate NF-κB signalling. Nature 430, 694–699 (2004).

210. Brummelkamp, T. R., Nijman, S. M. B., Dirac, A. M. G. & Bernards, R. Loss of the cylindromatosis tumour suppressor inhibits apoptosis by activating NF-κB. Nature 424, 797–801 (2003).

211. Kovalenko, A. et al. The tumour suppressor CYLD negatively regulates NF-κB signalling by deubiquitination. Nature 424, 801–805 (2003).

212. Pasparakis, M. & Vandenabeele, P. Necroptosis and its role in inflammation. Nature 517, 311–320 (2015).

213. Micheau, O. & Tschopp, J. Induction of TNF receptor I-mediated apoptosis via two sequential signaling complexes. Cell 114, 181–90 (2003).

214. Tsuchiya, Y. et al. FLIP the Switch: Regulation of Apoptosis and Necroptosis by cFLIP. Int. J. Mol. Sci. 16, 30321–30341 (2015).

215. O'Donnell, M. A., Legarda-Addison, D., Skountzos, P., Yeh, W. C. & Ting, A. T. Ubiquitination of RIP1 Regulates an NF-κB-Independent Cell-Death Switch in TNF Signaling. Curr. Biol. 17, 418–424 (2007).

216. Li, H., Kobayashi, M., Blonska, M., You, Y. & Lin, X. Ubiquitination of RIP is required for tumor necrosis factor alpha-induced NF-kappaB activation. J. Biol. Chem. 281, 13636–43 (2006).

217. Lin, Y., Devin, A., Rodriguez, Y. & Liu, Z. G. Cleavage of the death domain kinase RIP by caspase-8 prompts TNF-induced apoptosis. Genes Dev. 13, 2514–26 (1999).

218. Feng, S. et al. Cleavage of RIP3 inactivates its caspase-independent apoptosis pathway by removal of kinase domain. Cell. Signal. 19, 2056–67 (2007).

219. Lork, M., Verhelst, K. & Beyaert, R. CYLD, A20 and OTULIN deubiquitinases in NF-κB signaling and cell death: So similar, yet so different. Cell Death and Differentiation 24, 1172–1183 (2017).

220. Tummers, B. & Green, D. R. Caspase-8; regulating life and death. Immunol. Rev. 277, 76–89 (2017).

221. Newton, K. et al. Cleavage of RIPK1 by caspase-8 is crucial for limiting apoptosis and necroptosis. Nature 574, 428–431 (2019).

222. Orozco, S. & Oberst, A. RIPK3 in cell death and inflammation: the good, the bad, and the ugly. Immunological Reviews 277, 102–112 (2017).

223. Cho, Y. S. et al. Phosphorylation-driven assembly of the RIP1-RIP3 complex regulates programmed necrosis and virus-induced inflammation. Cell 137, 1112–23 (2009).

224. Weber, K., Roelandt, R., Bruggeman, I., Estornes, Y. & Vandenabeele, P. Nuclear RIPK3 and MLKL contribute to cytosolic necrosome formation and necroptosis. Commun. Biol. 1, 6 (2018).

225. Gong, Y. N., Guy, C., Crawford, J. C. & Green, D. R. Biological events and molecular signaling following MLKL activation during necroptosis. Cell Cycle 16, 1748–1760 (2017).

226. Zhao, J. et al. Mixed lineage kinase domain-like is a key receptor interacting protein 3 downstream component of TNF-induced necrosis. Proc. Natl. Acad. Sci. U. S. A. 109, 5322–7 (2012).

227. Cai, Z. et al. Plasma membrane translocation of trimerized MLKL protein is required for TNF-induced necroptosis. Nat. Cell Biol. 16, 55–65 (2014).

228. Chen, X. et al. Translocation of mixed lineage kinase domain-like protein to plasma membrane leads to necrotic cell death. Cell Res. 24, 105–121 (2014).

229. Montfort, A. et al. The TNF paradox in cancer progression and immunotherapy. Frontiers in Immunology (1993). doi:10.3389/fimmu.2019.01818

230. Carswell, E. A. et al. An endotoxin-induced serum factor that causes necrosis of tumors

(activated macrophage). Immunology (1075).

231. Probst, B. L. et al. Smac mimetics increase cancer cell response to chemotherapeutics in a TNF-α-dependent manner. Cell Death Differ. 17, 1645–1654 (2010).

232. Robaye, B., Mosselmans, R., Fiers, W., Dumont, J. E. & Galand, P. Tumor necrosis factor induces apoptosis (programmed cell death) in normal endothelial cells in vitro. Am. J. Pathol. (1991).

233. Moore, R. J. et al. Mice deficient in tumor necrosis factor-α are resistant to skin carcinogenesis. Nat. Med. (1999).

234. Waters, J. P., Pober, J. S. & Bradley, J. R. Tumour necrosis factor and cancer. Journal of Pathology (2013).

235. Roberts, N. J., Zhou, S., Diaz, L. A. & Holdhoff, M. Systemic use of tumor necrosis factor alpha as an anticancer agent. Oncotarget (2011).

236. Beissert, S. et al. Regulation of tumor necrosis factor gene expression in colorectal adenocarcinoma: In vivo analysis by in situ hybridization. Proc. Natl. Acad. Sci. U. S. A. (1989).

237. Pajak, B., Gajkowska, B. & Orzechowski, A. Cycloheximide-mediated sensitization to TNF-alpha-induced apoptosis in human colorectal cancer cell line COLO 205; role of FLIP and metabolic inhibitors. J. Physiol. Pharmacol. 56 Suppl 3, 101–18 (2005).

238. Cao, Z. et al. Caspase-3 is Involved in IFN-γ- and TNF-α-Mediated MIN6 Cells Apoptosis via NF-κB/Bcl-2 Pathway. Cell Biochem. Biophys. 67, 1239–1248 (2013).

239. Komori, A. et al. Tumor necrosis factor acts as a tumor promoter in BALB/3T3 cell transformation. Cancer Res. 53, 1982–5 (1993).

240. Babbar, N. & Casero, R. A. Tumor necrosis factor-α increases reactive oxygen species by inducing spermine oxidase in human lung epithelial cells: A potential mechanism for

inflammation-induced carcinogenesis. Cancer Res. (2006).

241. Li, B. et al. Low levels of tumor necrosis factor α increase tumor growth by inducing an endothelial phenotype of monocytes recruited to the tumor site. Cancer Res. (2009).

242. Charles, K. A. et al. The tumor-promoting actions of TNF-α involve TNFR1 and IL-17 in ovarian cancer in mice and humans. J. Clin. Invest. (2009).

243. Arnott, C. H. et al. Expression of both TNF-α receptor subtypes is essential for optimal skin tumour development. Oncogene (2004).

244. Tomita, Y. et al. Spontaneous regression of lung metastasis in the absence of tumor necrosis factor receptor p55. Int. J. Cancer (2004).

245. Kitakata, H. et al. Essential roles of tumor necrosis factor receptor p55 in liver metastasis of intrasplenic administration of colon 26 cells. Cancer Res. (2002).

246. Bertrand, F. et al. Blocking tumor necrosis factor α enhances CD8 T-cell-dependent immunity in experimental melanoma. Cancer Res. (2015).

247. Bates, R. C. & Mercurio, A. M. Tumor Necrosis Factor-Stimulates the Epithelial-to-Mesenchymal Transition of Human Colonic Organoids. Mol. Biol. Cell 14, 1790–1800 (2003).

248. Ho, M. Y. et al. TNF-α induces epithelial-mesenchymal transition of renal cell carcinoma cells via a GSK3β-dependent mechanism. Mol. Cancer Res. (2012).

249. Li, C. W. et al. Epithelial-mesenchymal transition induced by TNF-α requires NF-κB-mediated transcriptional upregulation of Twist1. Cancer Res. (2012).

250. Liao, S. J. et al. TGF-β1 and TNF-α synergistically induce epithelial to mesenchymal transition of breast cancer cells by enhancing TAK1 activation. J. Cell Commun. Signal. (2019).

251. Reinhardt, J. et al. MAPK signaling and inflammation link melanoma phenotype

switching to induction of CD73 during immunotherapy. Cancer Res. (2017).

252. Zingg, D. et al. The Histone Methyltransferase Ezh2 Controls Mechanisms of Adaptive Resistance to Tumor Immunotherapy. Cell Rep. (2017).

253. Ruder, B., Atreya, R. & Becker, C. Tumour necrosis factor alpha in intestinal homeostasis and gut related diseases. Int. J. Mol. Sci. 20, (2019).

254. Reinecker, H. C. et al. Enhanced secretion of tumour necrosis factor-alpha, IL-6, and IL-1 beta by isolated lamina propria mononuclear cells from patients with ulcerative colitis and Crohn's disease. Clin. Exp. Immunol. (1993).

255. Reimund, J. M. et al. Increased production of tumour necrosis factor-α, interleukin-1β, and interleukin-6 by morphologically normal intestinal biopsies from patients with Crohn's disease. Gut (1996).

256. REINECKER, H.-C. et al. Enhand secretion of tumour necrosis factor-alpha, IL-6, and IL-1β by isolated lamina ropria monouclear cells from patients with ulcretive cilitis and Crohn's disease. Clin. Exp. Immunol. (2008).

257. Dionne, S., Hiscott, J., D'Agata, I., Duhaime, A. & Seidman, E. G. Quantitative PCR analysis of TNF-α and IL-1β mRNA levels in pediatric IBD mucosal biopsies. Dig. Dis. Sci. (1997).

258. Kontoyiannis, D., Pasparakis, M., Pizarro, T. T., Cominelli, F. & Kollias, G. Impaired on/off regulation of TNF biosynthesis in mice lacking TNF AU- rich elements: Implications for joint and gut-associated immunopathologies. Immunity (1999).

259. Arrieta, M. C., Madsen, K., Doyle, J. & Meddings, J. Reducing small intestinal permeability attenuates colitis in the IL10 gene-deficient mouse. Gut 58, 41–48 (2009).

260. Noti, M., Corazza, N., Mueller, C., Berger, B. & Brunner, T. TNF suppresses acute intestinal inflammation by inducing local glucocorticoid synthesis. J. Exp. Med. (2010).

261. Yan, Y. et al. Temporal and spatial analysis of clinical and molecular parameters in dextran sodium sulfate induced colitis. PLoS One (2009).

262. Neurath, M. F. et al. Predominant pathogenic role of tumor necrosis factor in experimental colitis in mice. Eur. J. Immunol. (1997).

263. Wirtz, S. et al. Chemically induced mouse models of acute and chronic intestinal inflammation. Nat. Protoc. (2017).

264. Bullen, T. F. et al. Characterization of epithelial cell shedding from human small intestine. Lab. Investig. (2006).

265. Williams, J. M. et al. Epithelial Cell Shedding and Barrier Function: A Matter of Life and Death at the Small Intestinal Villus Tip. Vet. Pathol. (2015).

266. Al-Sadi, R., Guo, S., Ye, D. & Ma, T. Y. TNF-α modulation of intestinal epithelial tight junction barrier is regulated by ERK1/2 activation of Elk-1. Am. J. Pathol. (2013).

267. Ma, T. Y., Boivin, M. A., Ye, D., Pedram, A. & Said, H. M. Mechanism of TNF-α modulation of Caco-2 intestinal epithelial tight junction barrier: Role of myosin light-chain kinase protein expression. Am. J. Physiol. - Gastrointest. Liver Physiol. 288, (2005).

268. Marchiando, A. M. et al. The epithelial barrier is maintained by in vivo tight junction expansion during pathologic intestinal epithelial shedding. Gastroenterology (2011).

269. Kiesslich, R. et al. Local barrier dysfunction identified by confocal laser endomicroscopy predicts relapse in inflammatory bowel disease. Gut (2012).

270. Schmitz, H. et al. Altered tight junction structure contributes to the impaired epithelial barrier function in ulcerative colitis. Gastroenterology (1999). doi:10.1016/S0016-5085(99)70126-5

271. Nenci, A. et al. Epithelial NEMO links innate immunity to chronic intestinal inflammation. Nature (2007).

272. Günther, C. et al. Caspase-8 regulates TNF-α-induced epithelial necroptosis and terminal ileitis. Nature (2011).

273. Wittkopf, N. et al. Cellular FLICE-like inhibitory protein secures intestinal epithelial cell survival and immune homeostasis by regulating caspase-8. Gastroenterology (2013).

274. Corredor, J. et al. Tumor necrosis factor regulates intestinal epithelial cell migration by receptor-dependent mechanisms. Am. J. Physiol. - Cell Physiol. (2003).

275. Kaiser, G. C. & Polk, D. B. Tumor necrosis factor α regulates proliferation in a mouse intestinal cell line. Gastroenterology (1997).

276. Guo, D., Dunbar, J. D., Yang, C. H., Pfeffer, L. M. & Donner, D. B. Induction of Jak/STAT signaling by activation of the type 1 TNF receptor. J. Immunol. 160, 2742–2750 (1998).

277. Kondylis, V., Kumari, S., Vlantis, K. & Pasparakis, M. The interplay of IKK, NF-κB and RIPK1 signaling in the regulation of cell death, tissue homeostasis and inflammation. Immunological Reviews 277, 113–127 (2017).

278. Wesemann, D. R., Qin, H., Kokorina, N. & Benveniste, E. N. TRADD interacts with STAT1-α and influences interferon-γ signaling. Nat. Immunol. 5, 199–207 (2004).

279. Morita, Y. et al. Signals transducers and activators of transcription (STAT)-induced STAT inhibitor-1 (SSI-1)/suppressor of cytokine signaling-1 (SOCS-1) suppresses tumor necrosis factor alpha -induced cell death in fibroblasts. Proc. Natl. Acad. Sci. 97, 5405–5410 (2000).

280. Kimura, A., Naka, T., Nagata, S., Kawase, I. & Kishimoto, T. SOCS-1 suppresses TNF-α-induced apoptosis through the regulation of Jak activation. Int. Immunol. 16, 991–999 (2004).

281. Hitomi, J. et al. Identification of a molecular signaling network that regulates a cellular necrotic cell death pathway by a genome wide siRNA screen.

282. Thapa, R. J. et al. NF- B Protects Cells from Gamma Interferon-Induced RIP1-Dependent Necroptosis. Mol. Cell. Biol. 31, 2934–2946 (2011).

283. Tiegs, G., Hentschel, J. & Wendel, A. A T cell-dependent experimental liver injury in mice inducible by concanavalin A. J. Clin. Invest. 90, 196–203 (1992).

284. Günther, C. et al. The pseudokinase MLKL mediates programmed hepatocellular necrosis independently of RIPK3 during hepatitis. J. Clin. Invest. 126, 4346–4360 (2016).

285. Chang, C.-P., Yang, M.-C. & Lei, H.-Y. Concanavalin A/IFN-Gamma Triggers Autophagy-Related Necrotic Hepatocyte Death through IRGM1-Mediated Lysosomal Membrane Disruption. PLoS One 6, e28323 (2011).

286. Li, N. et al. Cross-talk between TNF-α and IFN-γ signaling in induction of B7-H1 expression in hepatocellular carcinoma cells. Cancer Immunol. Immunother. 67, 271–283 (2018).

287. Tannenbaum, C. S., Major, J. A. & Hamilton, T. A. IFN-gamma and lipopolysaccharide differentially modulate expression of tumor necrosis factor receptor mRNA in murine peritoneal macrophages. J. Immunol. 151, (1993).

288. Ruggiero, V., Tavernier, J., Fiers, W. & Baglioni, C. Induction of the synthesis of tumor necrosis factor receptors by interferon-gamma. J. Immunol. 136, 2445–2450 (1986).

289. Tsujimoto, M., Yip, Y. K. & Vilcek, J. Interferon-gamma enhances expression of cellular receptors for tumor necrosis factor. J. Immunol. 136, (1986).

290. Tsujimoto, M. & Vilcek, J. Tumor necrosis factor receptors in HeLa cells and their regulation by interferon-gamma. J. Biol. Chem. 261, 5384–8 (1986).

291. Fengjun Wang1,2,§, Brad T. Schwarz2,§, W. Vallen Graham2, Yingmin Wang2, L. S. IFN-γ-induced TNFR2 Upregulation is Required for TNFdependent Intestinal Epithelial Barrier Dysfunction.pdf.

292. Salim, T., Sershen, C. L. & May, E. E. Investigating the role of TNF-α and IFN-γ activation on the dynamics of iNOS gene expression in lps stimulated macrophages. PLoS One 11, (2016).

293. Bartee, E. & McFadden, G. Cytokine synergy: An underappreciated contributor to innate anti-viral immunity. Cytokine 63, 237–240 (2013).

294. Liao, F. et al. (IP-10) Chemokines by Human Neutrophils-Inducible Protein-10 γ (I-TAC), and IFN-Chemoattractant α IFN-Inducible T Cell (MIG), γ Monokine Induced by IFN-Gene Expression and Production of the. J Immunol References (2019).

295. Zhang, B., Karrison, T., Rowley, D. A. & Schreiber, H. IFN-gamma- and TNF-dependent bystander eradication of antigen-loss variants in established mouse cancers. J. Clin. Invest. 118, 1398–404 (2008).

296. Kim, W. H. et al. Apamin inhibits TNF-α- and IFN-γ-induced inflammatory cytokines and chemokines via suppressions of NF-κB signaling pathway and STAT in human keratinocytes. Pharmacol. Reports 69, 1030–1035 (2017).

297. Yang, J. H. et al. Jageum-Jung improves 2,4-dinitrochlorobenzene-induced atopic dermatitis-like skin lesions in mice and suppresses pro-inflammatory chemokine production by inhibiting TNF-α/IFN-γ-induced STAT-1 and NFκB signaling in HaCaT cells. J. Ethnopharmacol. 221, 48–55 (2018).

298. Cheshire, J. L. & Baldwin, A. S. Synergistic activation of NF-kappaB by tumor necrosis factor alpha and gamma interferon via enhanced I kappaB alpha degradation and de novo I kappaBbeta degradation. Mol. Cell. Biol. 17, 6746–54 (1997).

299. Ganster, R. W., Guo, Z., Shao, L. & Geller, D. A. Differential effects of TNF-α and IFN-γ on gene transcription mediated by NF-κB-Stat1 interactions. J. Interf. Cytokine Res. (2005). doi:10.1089/jir.2005.25.707

300. Yarilina, A., Park-Min, K.-H., Antoniv, T., Hu, X. & Ivashkiv, L. B. TNF activates an IRF1-dependent autocrine loop leading to sustained expression of chemokines and STAT1-dependent type I interferon–response genes. Nat. Immunol. 9, 378–387 (2008).

301. Hang, D. T. T., Song, J. Y., Kim, M. Y., Park, J. W. & Shin, Y. K. Involvement of NF-κB in changes of IFN-γ-induced CIITA/MHC-II and iNOS expression by influenza virus in macrophages. Mol. Immunol. 48, 1253–1262 (2011).

302. Morris, R., Kershaw, N. J. & Babon, J. J. The molecular details of cytokine signaling via the JAK/STAT pathway. Protein Science 27, 1984–2009 (2018).

303. Ohmori, Y., Schreiber, R. D. & Hamilton, T. A. Synergy between Interferon-and Tumor Necrosis Factor-in Transcriptional Activation Is Mediated by Cooperation between Signal Transducer and Activator of Transcription 1 and Nuclear Factor B*. Journal of Biological Chemistry 272, (1997).

304. Wienerroither, S. et al. Cooperative Transcriptional Activation of Antimicrobial Genes by STAT and NF-κB Pathways by Concerted Recruitment of the Mediator Complex. Cell Rep. 12, 300–312 (2015).

305. Farlik, M. et al. Nonconventional initiation complex assembly by STAT and NF-κB transcription factors regulates nitric oxide synthase expression. Immunity (2010).

306. Barbosa Lima, L. E. et al. STAT1-NFκB crosstalk triggered by interferon gamma regulates noradrenaline-induced pineal hormonal production. J. Pineal Res. 67, (2019).

307. Lee, H. J. et al. The Role of STAT1/IRF-1 on Synergistic ROS Production and Loss of Mitochondrial Transmembrane Potential during Hepatic Cell Death Induced by LPS/d-GalN. J. Mol. Biol. 369, 967–984 (2007).

308. Amemiya, K. et al. Dysregulation of TNF-α and IFN-γexpression is a common host immune response in a chronically infected mouse model of melioidosis when

comparing multiple human strains of Burkholderia pseudomallei. BMC Immunol. 21, 1–22 (2020).

309. Wong, G. H. W. & Goeddel, D. V. Tumour necrosis factors α and β inhibit virus replication and synergize with interferons. Nature (1986). doi:10.1038/323819a0

310. Robinson, C. M., Hale, P. T. & Carlin, J. M. The Role of IFN-γ and TNF-α-Responsive Regulatory Elements in the Synergistic Induction of Indoleamine Dioxygenase.

311. Robinson, C. M., Shirey, K. A. & Carlin, J. M. Synergistic Transcriptional Activation of Indoleamine Dioxygenase by IFN-g and Tumor Necrosis Factor-a. JOURNAL OF INTERFERON & CYTOKINE RESEARCH 23, (2003).

312. Schmidt, S. V. & Schultze, J. L. New insights into IDO biology in bacterial and viral infections. Front. Immunol. 5, 1–12 (2014).

313. Ray, J. C. J., Wang, J., Chan, J. & Kirschner, D. E. The timing of TNF and IFN-γ signaling affects macrophage activation strategies during Mycobacterium tuberculosis infection. J. Theor. Biol. 252, 24–38 (2008).

314. Girdlestone, J. Synergistic induction of HLA class I expression by RelA and CIITA. Blood 95, 3804–8 (2000).

315. Hsiao, H. Y. et al. TNF-α/IFN-γ-induced iNOS expression increased by prostaglandin E2 in rat primary astrocytes via EP2-evoked cAMP/PKA and intracellular calcium signaling. Glia 55, 214–223 (2007).

316. Neurath, M. F. Targeting immune cell circuits and trafficking in inflammatory bowel disease. Nature Immunology (2019).

317. Antonelli, A. et al. Chemokine (C–X–C motif) ligand (CXCL)10 in autoimmune diseases. Autoimmun. Rev. 13, 272–280 (2014).

318. Ohmori, Y. & Hamilton, T. A. The interferon-stimulated response element and a kappa

B site mediate synergistic induction of murine IP-10 gene transcription by IFN-gamma and TNF-alpha. J. Immunol. 154, 5235–44 (1995).

319. Yoshida, H. et al. Regulation of CX3CL1 in Post-Transcriptional α for TNF-Role Vascular Endothelial Cells: An Essential in γ and IFN-α CX3CL1/Fractalkine by TNF-Characterization of Synergistic Induction of. J Immunol Ref. 184, 4205–4214 (2010).

320. Müller-Hermelink, N. et al. TNFR1 Signaling and IFN-γ Signaling Determine whether T Cells Induce Tumor Dormancy or Promote Multistage Carcinogenesis. Cancer Cell 13, 507–518 (2008).

321. Shen, J. et al. Anti-cancer therapy with TNFα and IFNγ: A comprehensive review. Cell Prolif. 51, e12441 (2018).

322. Wright, K., Kolios, G., Westwick, J. & Ward, S. G. Cytokine-induced apoptosis in epithelial HT-29 cells is independent of nitric oxide formation. Evidence for an interleukin-13-driven phosphatidylinositol 3-kinase-dependent survival mechanism. J. Biol. Chem. (1999).

323. Kulkarni, K., Selesniemi, K. & Brown, T. L. Interferon-gamma sensitizes the human salivary gland cell line, HSG, to tumor necrosis factor-alpha induced activation of dual apoptotic pathways. Apoptosis 11, 2205–15 (2006).

324. Feng, H. et al. Bone marrow-derived mesenchymal stromal cells promote colorectal cancer cell death under low-dose irradiation. Br. J. Cancer 118, 353–365 (2018).

325. Shen, J. et al. Vascular-targeted TNFα and IFNγ inhibits orthotopic colorectal tumor growth. J. Transl. Med. 14, 1–13 (2016).

326. Wang, R., Jaw, J. J., Stutzman, N. C., Zou, Z. & Sun, P. D. Natural killer cell-produced IFN-γ and TNF-α induce target cell cytolysis through up-regulation of ICAM-1. J. Leukoc. Biol. 91, 299–309 (2012).

327. Namjoshi, P., Showalter, L., Czerniecki, B. J. & Koski, G. K. T-helper 1-type cytokines induce apoptosis and loss of HER-family oncodriver expression in murine and human breast cancer cells. Oncotarget 10, 6006–6020 (2019).

328. Brenner, E. et al. Cancer immune control needs senescence induction by interferon-dependent cell cycle regulator pathways in tumours. Nat. Commun. (2020).

329. Israeli, E. T helper-1 cell cytokines drive cancer into senescence. Isr. Med. Assoc. J. (2013).

330. Kunz, M. & Ibrahim, S. M. Cytokines and Cytokine Profiles in Human Autoimmune Diseases and Animal Models of Autoimmunity. Artic. ID 979258, 20 (2009).

331. Palucka, A. K., Blanck, J. P., Bennett, L., Pascual, V. & Banchereau, J. Cross-regulation of TNF and IFN-α in autoimmune diseases. Proc. Natl. Acad. Sci. U. S. A. 102, 3372–3377 (2005).

332. Cnop, M. et al. Mechanisms of pancreatic beta-cell death in type 1 and type 2 diabetes: many differences, few similarities. Diabetes 54 Suppl 2, S97-107 (2005).

333. Campbell, I. L., Iscaro, A. & Harrison, L. C. IFN-gamma and tumor necrosis factor-alpha. Cytotoxicity to murine islets of Langerhans. J. Immunol. 141, 2325–9 (1988).

334. Suk, K. et al. IFN- /TNF- Synergism as the Final Effector in Autoimmune Diabetes: A Key Role for STAT1/IFN Regulatory Factor-1 Pathway in Pancreatic Cell Death. J. Immunol. (2001).

335. Kim, S. et al. Essential role for signal transducer and activator of transcription-1 in pancreatic β-cell death and autoimmune type 1 diabetes of nonobese diabetic mice. Diabetes (2007).

336. Chang, I. et al. - Role of Calcium in Pancreatic Islet Cell Death by IFN- /TNF. J. Immunol. 172, 7008–7014 (2014).

337. Kim, W. H., Lee, J. W., Gao, B. & Jung, M. H. Synergistic activation of JNK/SAPK induced by TNF-α and IFN-γ: Apoptosis of pancreatic β-cells via the p53 and ROS pathway. Cell. Signal. 17, 1516–1532 (2005).

338. Macdonald, T. T., Hutchings, P., Choy, M.-Y., Murch, S. & Cooke, A. Tumour necrosis factor-alpha and interferon-gamma production measured at the single cell level in normal and inflamed human intestine. Clin. exp. Immunol 81, (1990).

339. Nayden G. Naydenov, 1, * somesh Baranwal, 1 & shadab Khan, 2 alex Feygin, 1 pooja Gupta1 and andrei I. Ivanov1, 3, 4. Novel mechanism of cytokine-induced disruption of epithelial barriers:Janus kinase and protein kinase D-dependent downregulation of junction protein expression. (2013).

340. Seidelin, J. B., Jäättelä, M. & Nielsen, O. H. Continuous interferon-γ or tumor necrosis factor-α exposure of enterocytes attenuates cell death responses. Cytokine 27, 113–119 (2004).

341. Francoeur, C., Escaffit, F., Vachon, P. H. & Beaulieu, J.-F. Proinflammatory cytokines TNF-α and IFN-γ alter laminin expression under an apoptosis-independent mechanism in human intestinal epithelial cells. Am. J. Physiol. Liver Physiol. 287, G592–G598 (2004).

342. Eriguchi, Y. et al. Essential role of IFN-γ in T cell-associated intestinal inflammation. JCI insight (2018).

343. Van Hauwermeiren, F. et al. TNFR1-induced lethal inflammation is mediated by goblet and Paneth cell dysfunction. Mucosal Immunol. 8, 828–840 (2015).

344. Buntinx, M. et al. Cytokine-induced cell death in human oligodendroglial cell lines: I. Synergistic effects of IFN-? and TNF-? on apoptosis. J. Neurosci. Res. 76, 834–845 (2004).

345. Simpson, S. et al. Stimulated PBMC-produced IFN- and TNF- are associated with

altered relapse risk in multiple sclerosis: results from a prospective cohort study. J. Neurol. Neurosurg. Psychiatry 86, 200–207 (2015).

346. Zhou, Y. et al. Genetic variation in PBMC-produced IFN-γ and TNF-α associations with relapse in multiple sclerosis. J. Neurol. Sci. 349, 40–44 (2015).

2. Chapter 2: IFN-γ and TNF-α synergise to kill intestinal epithelial cells through a JAK1/2 dependent pathway

2.1. Abstract:

Dysregulation of host cytokine networks is a key molecular feature associated with immunopathology in inflammatory bowel disease (IBD). The T helper type-1 (Th1) cytokines IFN-γ and TNF-α are important drivers of disease pathogenesis, potentially due to their ability to both independently and synergistically regulate inflammatory gene expression and induce cell death of intestinal epithelial cells (IECs). However, the mechanisms underpinning these synergistic effects are less well understood. Here, we investigated the molecular mechanisms underpinning the killing of IECs by the combination of IFN-γ and TNF-α. Specifically, we performed a human kinome RNAi screen and a drug library repurposing screen in HT-29 colorectal cancer (CRC) cells to identify underlying mechanisms. Both the screens and the follow-up validation work identified Janus kinase 1 (JAK1) and Janus kinase 2 (JAK2) as the main modulators of IFN-γ + TNF-α induced killing. We further investigated the role of TNF Receptor-1 (TNFR1) and canonical TNFR1-associated signalling complexes (Complex I & II) in IFN-γ + TNF-α induced killing. We also assessed the involvement of the Bcl-2 family and mitochondria in the cell death. Our results show that inhibition of caspase activation, necroptosis or perturbation of *BAK/BAX* expression did not block IFN-γ + TNF-α induced killing. In addition, we show that IFN-γ + TNF-α synergised to induce cell death of primary human colonic organoids which was blocked by JAK inhibitors (JAKinibs). Collectively, these data demonstrate that IFN-γ and TNF-α synergise to kill intestinal epithelial cells through a JAK1/2-STAT1 dependent pathway independently of canonical TNF-α-death receptor pathways and Bcl-2 family members BAK and BAX. Our findings provide a mechanism of action for the synergistic killing effects of IFN-γ and TNF-α on epithelial cells during intestinal inflammation and highlight the importance of JAK inhibitors (JAKinibs) as new therapeutics for IBD.

2.2. Introduction

IBD is a chronic inflammatory disorder affecting between 0.3% to 0.5% of the population in North America, Northern and Western Europe, New Zealand and several other western countries[1]. Several interacting factors such as environment, reduced diversity of the gut microbiota, genetics, diet and the immune system have been shown to influence disease susceptibility[2–5]. However, dysregulation of cytokine networks represents one of the main hallmarks and drivers of pathogenesis in IBD[6,7]. Patients with IBD exhibit gut inflammation resulting from infiltration of several immune cell populations including B and T lymphocytes, macrophages and dendritic cells that produce proinflammatory cytokines, chemokines and other inflammatory mediators in the intestinal mucosa[8–10]. In particular, the Th1 cytokines - IFN-γ and TNF-α - are known to be elevated during IBD and negatively regulate epithelial barrier integrity by disrupting epithelial tight junctions and increasing epithelial cell death.[8,11,12] TNF-α is a proinflammatory cytokine and a key therapeutic target in several chronic inflammatory diseases such as rheumatoid arthritis, psoriasis, multiple sclerosis and IBD[13]. Anti-TNF-α therapy has changed the paradigm of IBD treatment since 1998[14]. Infliximab was the first monoclonal antibody therapy approved by the Food Drug and Administration (FDA) against TNF-α for the treatment of Crohn's disease[14]. After that several other anti-TNF antibodies were approved for the treatment of IBD including Adalimumab and Certolizumab[15]. TNF-α is a pleiotropic cytokine and performs its biological functions by signalling through two receptors TNFR1 and TNFR2[16]. Initially, TNF-α is synthesised as a transmembrane protein which is cleaved into a soluble form by an enzyme called TNFα-converting enzyme (TACE). The TNF homotrimer interacts with homotrimeric TNFR1 and results into recruitment of the adaptor molecule TNFR1-associated death domain protein (TRADD) to the receptor. The

docking of TRADD to TNFR1 allows the assembly of different signalling complexes (Complex I, IIa, IIb and IIc) to give different functional outcomes; cell survival, inflammation or cell death[17]. Formation of TNFR1-complex-1 (TRADD, Receptor-interacting serine/threonine-protein kinase 1 (RIPK1), Inhibitors of apoptosis protein 1 (cIAP1), cIAP2, linear ubiquitin chain assembly complex (LUBAC)) allows activation of transforming growth factor beta-activated kinase 1 (TAK1) and inhibitor of nuclear factor kappa-B kinase (IKK) complexes to induce nuclear factor kappa light chain enhancer of activated B cells (NF-κB) activation, and mitogen-activated protein kinase (MAPK) signalling for activation of pro-survival and pro-inflammatory signalling and gene regulation[13]. But destabilisation of complex-1 or inhibition of NF-κB activation can lead to the formation of pro-apoptotic (IIa & IIb) complexes[18,19,20,21]. Complex-IIa is composed of TRADD-FADD (Fas associated death domain protein) - caspase-8; while complex-IIb contains RIPK1, RIPK3, FADD and caspase 8[22]. Caspase-8 is an important regulator of TNF signalling and acts as a checkpoint between cell survival and cell death decisions in multiple cell types.[23,24] Besides its involvement in activating death receptor-mediated apoptosis, caspase-8 performs pro-survival and anti-inflammatory functions by cleaving RIPK1, and blocking necroptosis[25,26]. The failure of caspase-8 to cleave RIPK1 can result in autoimmune diseases[27]. Other than blocking RIPK1, caspase-8 is also involved in cleavage of RIPK3 and CYLD Lysine 63 Deubiquitinase (CYLD)[28–31]. Disruption of complex-I in combination with blockade of caspase-8 activity results in the formation of complex-IIc or the necrosome which induces RIPK1, RIPK3 and Mixed Lineage Kinase Domain Like Pseudokinase (MLKL) dependent necroptosis[32,24]. RIPK1 also plays an important role in the regulation of both cell survival and cell death[33–36]. RIPK1 acts as an essential driver of NF-κB activation mediating cell survival, inflammation as well as caspse-8 dependent apoptosis[37,38]. Mice with *RIPK1*$^{-/-}$ genotype in IECs develop intestinal inflammation and caspase 8 dependent apoptosis of IECs,

leading to early death[39]. However, RIPK1 protein can result in ripoptocide (includes both apoptosis and necroptosis) leading to chronic inflammation, highlighting the potential involvement of RIPKs in IBD[40].

Similar to TNF-α, IFN-γ plays a crucial role in the regulation of homeostatic functions in the gut. IFN-γ induces its cellular responses by signalling through the JAK-STAT signalling pathway.[41,42] Binding of IFN-γ homodimer to IFN-γ receptor (IFNGR) mediates autophosphorylation of JAK2 and transactivation of JAK1[43]. JAK1 further phosphorylates IFNGR1 chain at tyrosine-440, forming a docking site for recruitment of STAT1. JAK2 phosphorylates STAT1 at tyrosine-701 residue leading to its homodimerization.[42] Phosphorylated STAT1 homodimer dissociates from the receptor, translocates to the nucleus, binds to gamma activated sequence (GAS) in the promoter region of interferon stimulated genes (ISGs) and induces gene expression to perform cellular functions[42]. IFN-γ contributes to gut epithelial barrier dysfunction by triggering the disassembly of tight junctions and by increasing cell death in intestinal epithelial stem cells and IECs[44–48]. T cell derived IFN-γ induces apoptosis in Paneth cells (specialised secretary epithelial cells), controlled release of antimicrobial products and stem cell death in intestinal tissues resulting into epithelial damage and inflammation[47–49] Dysregulation of T cell activation or inhibition of JAK/STAT pathway by JAK inhibitors prevents the Paneth cell death and stem cell impairment[47]. Furthermore, IFN-γ has been reported to induce the internalisation of tight junction proteins and rearrangement of actin cytoskeleton in intestinal epithelial cells[44,50,51]. This rearrangement of actin cytoskeleton promotes the cleavage of desmoglein-2 to regulate apoptosis of epithelial cells [52,53]. Moreover, IFN-γ regulates the cell proliferation and apoptosis of IECs through several pathways including Wingless-Int (Wnt)-β-catenin, serine-threonine protein kinase and AKT-β-catenin signalling[54]. There is evidence of an increase in IFN-γ induced epithelial cell death in response to parasite[55] and bacterial[56] infections. Recently, Justin *et al*.

has described a pyroptotic and programmed cell death independent mechanism of killing in murine IECs and fibroblasts upon IFN-γ treatment in cells infected with *Salmonella*[57].

Although both IFN-γ and TNF-α have the potential to induce cell death independently, they have also been shown to synergistically regulate both proliferation and apoptosis of epithelial cells to aggravate intestinal inflammatory disease cooperatively[8,6,58]. For a long time IFN-γ was known to sensitize different cell types to death receptor-triggered (TNF-R1, Fas/CD95/TRAIL) apoptosis[59–64]. IFN-γ has been reported to increase the expression and activation of caspase-8 and Fas ligand to mediate TNF-α induced apoptosis in IECs[65]. IFN-γ and TNF-α have been shown to activate caspase-9 and BAX dependent intrinsic apoptotic pathway along with downregulation of anti-apoptotic BCL-2 proteins[30]. IFN-γ has been reported to sensitise IECs to the effects of TNF-α by increasing the expression of the TNF-α receptor, TNFR2[66]. Even though there are several studies that have investigated and reported on potential mechanisms of IFN-γ and TNF-α synergism, the mechanism of cross talk between the two signalling pathways and the way they co-operate to trigger cell death still remains a mystery. Thus, a potential regulatory link between the two signalling pathways is yet to be thoroughly investigated. We report that IFN-γ and TNF-α induced synergistic cell death is dependent on JAK1/JAK2 and STAT1 in CRC cell lines and primary human colonic organoids. Indeed, TNFR1 plays a critical role in the progression of cell death, but TNFR1 receptor complexes I and II do not seem to have any involvement in the pathway. Furthermore, we show that cell death is independent of Bcl-2 family members- Bcl-2 homologous antagonist/killer (BAK) and BCL2 Associated X (BAX). Although, caspase-8 enzymatic activity is not essential for the cell death, caspase 8 was found to play a crucial role in the cell death pathway. These data reveal a caspase independent function of caspase 8 in IFN-γ/TNF-α induced cell death.

Collectively, our data provides a mechanism of action for synergism between IFN-γ and TNF-α in epithelial cell death. This cell death is primarily dependent on IFN-γ mediated JAK1/2-STAT1 signalling pathway where TNF-α boosts its killing effect. Even though IFN-γ/TNF-α induced cell death is independent of TNFR-1 canonical death complexes, our study suggests the possible involvement of a novel signalling complex downstream of IFN-γ/TNF-α signalling consisting of caspase 8/RIPK3 scaffold activity for the induction of intestinal epithelial cell death. This study reveals the molecular pathway which may underpin the efficacy of both anti-TNFs and JAKinibs in IBD.

2.3. Methods and Materials

2.3.1. Cell culture

Human colon adenocarcinoma cell lines- HT-29 (ATCC® HTB-38), DLD-1 (ATCC® CCL-221), LoVo (ATCC® CCL-229), RKO (ATCC® CRL-2577), Colo-205 (ATCC® CCL-222), HCT-15 (ATCC® CCL-225), HCT-116 (ATCC® CCL-247), SW-48 (ATCC® CCL-231) and SW-948 (ATCC® CCL-237) were obtained from American Type Culture Collection (ATCC) and HCA-7 (Cat no 06061902) was bought from European Collection of Authenticated Cell Cultures (ECACC). HT-29 and HCT-116 cells were cultured in McCoy's 5A medium (Sigma-Aldrich #M9309), DLD-1 cells were cultured in RPMI-1640 medium (Sigma-Aldrich #R8758), RKO and HCA-7 cells were grown in Dulbecco's modified Eagle's medium (Sigma-Aldrich #D5796). Kaighn's Modification of Ham's F-12 medium (ATCC #30-2004) was used to culture the LoVo cell line. All media were supplemented with 10% FBS (Sigma-aldrich) and 100 IU/mL penicillin (Sigma-aldrich) and 0.1 mg/mL streptomycin (Sigma-aldrich). SW-48 and SW-948 cell lines were grown in Hyclone Leibovitz's L-15 medium (Fisher Scientific #11566271) supplemented with 10% FBS, 100 IU/mL penicillin and 0.1 mg/mL streptomycin and 1500 mg/L sodium bicarbonate (Sigma-aldrich). All cell lines

were cultured in the incubators at 37ºC temperature and 5% CO2 conditions all the time. The cell lines were mycoplasma free and were tested for mycoplasma status every 2-4 months.

2.3.2. Reagents

Recombinant human IFN-γ (Peprotech # 300-02) and recombinant human TNF-α (Peprotech # 300-01A) were used for cell stimulations using 1 pg/mL - 100 ng/mL concentration of each. JAK inhibitors - Filgotinib (Selleckchem #S7605), Fedratinib (Selleckchem #S2736), Upadacitinib (Insight bio #HY-19569), BMS-911543 (Bertin Pharma #21088), Baricitinib (Selleckchem #S2851), Ruxolitinib (Selleckchem #S2851) and Tofacitinib (Bertin Pharma #T2398) were used as indicated. Caspase-8 Inhibitor Z-IETD-FMK (Biotechne #FMK007), caspase-9 inhibitor Z-LEHD-FMK (Biotechne #FMK008), caspase 10 inhibitor Z-AEVD (Bertin Pharma 14987) were used at 10 µM final concentration and pan-caspase inhibitor Z-VAD-FMK (Selleckchem #S8102) was used at 20 µM final concentration. IKK inhibitor- IKK-16 (Selleckchem #S2882), MLKL inhibitor necrosulphonamide (Bertin Pharma #S20844) and SMAC mimetic BV-6 (Selleckchem #S7597) were used at 1 µM concentration. RIPK1 inhibitor necrostatin-2 (Bertin Pharma #20924) and RIPK3 inhibitor GSK'872 (Calbiochem, Merck #530389) were used at 10 µM final concentration. Cycloheximide (Sigma #C7698) was used at 10 µg/mL final concentration.

2.3.3. CRISPR/Cas9 knockout cell lines

For the generation of CRISPR/Cas-9 DLD-1 *JAK1*$^{-/-}$, *JAK2*$^{-/-}$ and *STAT1*$^{-/-}$ cell lines, DLD-1 CRC cells were transfected with RNP complex consisting of guide RNA, ATTO-488 labelled Tracr-RNA and Cas9 nuclease (prepared as directed by IDT genome editing user guide) using Lipofectamine CRISPRMAX (Thermo Fisher # CMAX00015). After 24 hours of transfection, fluorescently labelled ATTO positive single cells were sorted using BD FACSAria™ Fusion Cell sorter into 96-well plates. Single cell colonies were expanded and validated for knock-out

phenotype by PCR, WB and exon sequencing for the target gene. HT-29 CRISPR/Cas9 *CASP8*$^{-/-}$, *CASP10*$^{-/-}$, *RIPK1*$^{-/-}$, *RIPK3*$^{-/-}$, *MLKL*$^{-/-}$ cell lines were obtained from Dr John Silke's lab (Melbourne, Australia) and cultured in RPMI-1640 medium supplemented with 10 % FBS and 100 IU/mL penicillin and 0.1 mg/mL streptomycin.

Table 2.3.1 Details of guide RNA used in preparation of DLD1-CRISPR/Cas9 cell lines

Gene Symbol	**PAM**	**Target Exon**	**Forward Primer (5'-3')**
JAK1	AGG	4	CGAGATATTCCATGCCGAT
JAK2	TGG	5	TCGAGATATTCCATGCCGAT
STAT1	AGG	10	TGTGATAGGGTCATGTTCGT

2.3.4. Cell death assays

Cell viability was measured by quantitation of ATP present in cells using CellTiter-Glo® luminescent assay (Promega # G7570) and caspase-3 and -7 activities were measured by using Caspase-Glo® 3/7 assay kit (Promega #G8091) according to the manufacturer's instructions. The luminescence was recorded using Synergy2, Biotek plate reader. Raw viability data were normalised to the control wells in the absence of any treatment. For crystal violet staining, cells were fixed with 100% methanol for 10 minutes at -20ºC and stained with 0.5% crystal violet stain (500 mg Crystal Violet, 25 mL methanol, 75 mL water for 100 mL solution) for 10 minutes. Plates were dried at room temperature overnight and scanned by using ODYSSEY system. ImageJ software was used to determine the intensity of cell staining. For cell death analysis by flow cytometry, cells were treated, harvested and washed. Cells were stained with fixable viability dye FVe660 (BD Biosciences# 564405) for 15 minutes protected from light and fixed with 100 ul of fixation/permeabilization buffer (BD Biosciences# 554714) for 30 minutes at 4ºC. Washed twice using 1X permeabilization/wash buffer (BD Biosciences# 554714).

Fixed/permeabilized cells were immuno-stained for active caspase-3 for 30 minutes at 4ºC by using anti-active caspase-3 antibody (BD Cat No# 561011) solution. Cells were washed twice using 1X permeabilization/wash buffer and resuspended in FACS buffer (PBS, 2% FBS, 5 mM EDTA). Cells were quantified using flow cytometry instrument- FACS Calibur 3CA (BD) and data were analysed using flow-jo software (version-10).

2.3.5. Human Kinome RNAi screen

The human kinome RNAi screen was performed in duplicate in 384-well format using Dharmacon's pooled human ON-TARGET plus (OTP) siRNA library – protein kinases at the Functional Genomics Core facility, Sanford Burnham Prebys Medical Discovery Institute, La Jolla, CA, USA. The library was spotted in black-clear bottom 384 well plates (Greiner 781092) together with positive and negative controls at 0.5 pmol/well and reverse transfected into HT-29 cells by adding 10 ul of Optimem : RNAimax (10:1, Life Technologies) and cells to a density of 1000 cells/well. Cells were incubated for 48 hours at 37^{o}C temperature & 5 % CO_2 conditions followed by treatment with a cocktail of TNF-α and IFN-γ (10 ng/mL or 100 ng/mL each) for 72 hours. Cell viability was measured using Cell Titer-Glo® assay (Promega). Raw viability data were normalized to non-silencing control wells in the absence of cytokines (NS) included in every plate and used to extract a normalized average and robust Z score (Z*) for each target.

2.3.6. Drug library screen

The drug library repurposing screen was performed in triplicate in 384-well format at the Functional Genomics Core facility, Sanford Burnham Prebys Medical Discovery Institute, La Jolla, CA, USA. HT-29 cells were seeded to a density of 5000 cells/well for 24hrs. Cells were pre-treated with 10 µM of each drug for 1 hour. A 10X cytokine cocktail of IFN-γ + TNF-α was added on top of each well to make a final concentration of 10 ng/mL of each cytokine. After 72 hr cell viability was measured using CellTiter-uGlo® assay (Promega). Raw viability data were

normalized to control wells in the absence of drugs and cytokines (NS) included in every plate and used to extract a normalized average and robust Z score (Z*) for each target.

2.3.7. Transfections, RNAi, and RT-qPCR

Cells were reverse transfected with 25 nM of siRNA for 48 hours using RNAiMax transfection reagent and McCoy's5A medium free from antibiotics penicillin and streptomycin. The knock-down level was measured by western blotting and/or reverse transcription quantitative polymerase chain reaction (RT-qPCR). For RT-qPCR, RNA was isolated using the RNeasy Mini Kit (Qiagen) according to the manufacturer's instructions. Reverse transcription was performed on 500 ng of total RNA using Transcriptor Reverse Transcriptase (Roche) and random hexamer primers (Roche) following the manufacturer's protocol. All qPCR assays were designed using the Universal Probe Library Assay Design Centre (Roche Applied Science). qPCR reactions containing 2×Sensi Mix II Probe Kit Reaction Mix (Bioline), 500 nM primers, 250 nM probe (Roche) and 0.5-1 ng of cDNA, were performed in a Light Cycler 480 instrument. Detailed information on siRNA sequences and PCR probe library assays are provided in Table 2.3.2 and Table 2.3.3.

Table 2.3.2 List of gene targets and PCR primers used in the study

Gene Symbol	Ensembl ID	Probe	Forward Primer (5'-3')	Reverse Primer (5'-3')
JAK1	ENSG00000162434	72	CAGTTCATGCTGCTGAAAACC	TCTCTACTTTCCAAAGCTACTTCAGAG
JAK2	ENSG00000096968	50	ACCTGGTGAAAGTCCCATATTC	AGGCCACAGAAAACTTGCTC
TNFRSF1A	ENSG00000067182	5	TCCAAATGCCGAAAGGAA	CAATAATGCCGGTACTGGTTC
TNFRSF1B	ENSG00000028137	23	CTCCTTCCTGCTCCCAATG	CACACCCACAATCAGTCCAA
CASPASE 8	ENSG00000026029	2	GGTCACTTGAACCTTGGGAAT	TTTCTGCTGAAGTCCATCTTTTT
CASPASE 10	ENSG00000003400	54	GGCAAAATAAGCATGCAGGTA	TGTTAGCAGATGCTCCTTGC
GAPDH	ENSG00000111640	60	AGCCACATCGCTCAGACAC	AGCCACATCGCTCAGACAC
ACTB	ENSG00000075624	11	ATTGGCAATGAGCGGTTC	CGTGGATGCCACAGGACT

Table 2.3.3 List of siRNAs used in the study

Gene Symbol	Ensembl ID	Source	siRNA Sequences
JAK1	ENSG00000162434	Dharmacon	1. CCACAUAGCUGAUCUGAAA 2. GACAUGAUAUUGAGAACGA 3. UUACAAGGAUGACGAAGGA 4. CGGAUGAGGUUCUAUUUCA
JAK2	ENSG00000096968	Dharmacon	1. CGAAUAAGGUACAGAUUUC 2. UUACAGAGGCCAACUCAUA 3. AAUCAAACCUUCUAGUCUU 4. GGAAUGGCCUGCCUUACGA
STAT1	ENSG00000115415	Dharmacon	1. AGAAAGAGCUUGACAGUAA 2. GAACCUGACUUCCAUGCGG 3. CUACGAACAUGACCCUAUC 4. GCACGAUGGGCUCAGCUUU
CSNK1A1	ENSG00000113712	Dharmacon	1. GCGAUGUACUUAAACAUU 2. GGAAUGAUUAGGAUAUGUU 3. AGAGUAACAUGAAAGGUUU 4 GGCUAAAGGCUGCAACAAA
CSNK2A1	ENSG00000101266	Dharmacon	1. CCAAGUGCAUGGAUGUGUA 2 GCAAUGAAUUGUUCUGUGA 3. GCAAGGAGACUUUGGUUAC 4. CAACCAGAGUGACCUGAUU
IKBKB	ENSG00000104365	Dharmacon	1. AUGAAUGCCUCUCGACUUA 2. GAAGAGGUGGUGAGCUUAA 3. GAGCUGUACGGAGACUAA 4. CCGAUAAGCCUGCCACUCA
GALK1	ENSG00000108479	Dharmacon	1. GCGCAAAUGUGAAGAAGUA 2. CCUUGGAAGUGGCCACGUA 3. GUGCUGUGCUUGUGAGGCA 4. GGGAACACACGGACUACAA
TNFRSF1A	ENSG00000067182	Ambion	1. AAAGUUGGGACAGUCACCG 2. UCAUUGUACAAGUAGGUUC
TNFRSF1B	ENSG00000028137	Ambion	1. UGAUGACACAGUUCACCAC 2. UUCUGUUCCCGAGUGCAGG
CASPASE 8	ENSG00000026029	Ambion	1. AAAGACCUCAAUUCUGAUC 2. UUGAUGAUCAGACAGUAUC
CASPASE 10	ENSG00000003400	Ambion	1. UGUCCUUUAAGUUCUCUGA 2. UGUCUUAACAUCUGUUUGG
BAK	ENSG00000030110	Dharmacon	1. CGACAUCAACCGACGCUAU 2. UAUGAGUACUUCACCAAGA 3. GACGGCAGCUCGCCAUCAU 4. AAUCAUGACUCCCAAGGGU
BAX	ENSG00000087088	Dharmacon	1. GUGCCGGAACUGAUCAGAA 2. ACAUGUUUUCUGACGGGCAA 3. CUGAGCAGAUCAUGAAGAC 4. UGGGCUGGAUCCAAGACCA
Control siRNA	NA	Dharmacon Ambion	ON-TARGETplus Non-targeting siRNA

2.3.8. Cell lysis and immunoblotting

Cells were stimulated with indicated treatments for indicated times and washed twice with ice-cold PBS (phosphate buffer saline) and lysed in RIPA buffer (50 mM Tris-HCl (pH 7.4), 1 %NP-40, 0.25 % Na deoxycholate, 150 mM NaCl, 1 mM EDTA) supplemented with broad spectrum serine protease inhibitor (AEBSF-HCl) (Stratech #S7378-SEL) and Halt™ protease & phosphatase cocktail inhibitor-100X (Thermo scientific #78446). Protein concentrations were determined with the Pierce™ BCA (bicinchoninic acid) protein assay kit (Thermo Fisher Scientific #23225). Electrophoresis was performed using 4-12 % Bis-Tris gradient gels (Thermo Fisher #NW04125BOX) and mini gel tanks as per manufacturers' instructions. Proteins were transferred to a 0.45-micron PVDF membrane (Millipore; Immobilon-FL) using mini bolt module (Thermo Fisher #B1000) as suggested by the manufacturer. Membranes were blocked in 1X TBST (Tris Buffer Saline, 0.1% Tween-20) containing 5% Bovine serum albumin (BSA) for 1 h at room temperature. Membranes were incubated with primary antibodies diluted in 5% BSA overnight at 4ºC. Secondary antibody incubation was performed for 1 h at room temperature. The blots were developed using Western Bright Quantum HRP substrate (Cat no# K-12042-D20) according to the manufacturer's instructions. Chemiluminescence detection was captured using Fujifilm LAS-3000 System.

Antibodies used for immunoblotting were as follow: anti-caspase 8 (mouse-mAb-1C12-CST #9746), anti-caspase 9 (mouse monoclonal C-9- CST #9508), anti-caspase 10 (mouse-4C1-MBL #M059-3), anti-caspase 3 (rabbit-CST #9662), anti-cleaved caspase 3 (rabbit-Asp175-CST #9661), anti-FADD (rabbit-CST #2782), anti-PARP (rabbit-CST #9542), anti-MLKL (rabbit-mAb EPR17514-Abcam #184718), anti-phospho-MLKL-S358 (rabbit-mAb-EPR9514-Abcam #187091), anti-RIPK1 (mouse-clone-38/RIPBD #610459), anti-RIPK3 (Sigma #AV31513), anti-LC3-II (rabbit-Sigma #L8918), anti-JAK1 (rabbit-CST #3332), anti-JAK2 (rabbit-CST #3230), anti-

STAT1 (CST #9172), anti-phospho-STAT1-Y701 (rabbit-clone-58D6-CST #9167), anti-CSNK1A1a (CST #2655), anti-CSNK2A1a (CST #2656), anti-GALK1 (sc-393356), anti-IKBKB (CST #2684), anti-BAK (CST #3814), anti-BAX (CST #2772), anti-GAPDH (Ambion, AM4300), anti-Beta actin (sc-47778), anti-mouse IgG (Sigma #A2554), anti-rabbit IgG (Sigma #A6154).

2.3.9. Cellular and mitochondrial ROS measurement

Cellular and mitochondrial reactive oxygen species (ROS) level were measured by using CM-H2DCFDA (Molecular probes #C6827) and MitoSox Red (Molecular probes #M36008) probes respectively. Probes were reconstituted in DMSO to make a stock concentration of 5 mM just before use and diluted into PBS (with Mg^{2+} and Ca^{2+}) to prepare a 5 µM working solution. HT-29 cells were reverse transfected with 25 µM of non-silencing siRNA or siBAK and siBAX siRNA smart pools for 48 hours and treated with IFN-γ/TNF-α +/- baricitinib for 16 hours. Cells were washed with PBS followed by incubation with diluted probes (500ul each well in 12 well plates) for 30 minutes in dark at 37^0C. Cells were harvested by trypsinisation and quantified for the staining using flow cytometry (FACS calibur 3CA, BD). The data was analysed using FLOW-JO software (BD Biosciences version 10).

2.3.10. Human Colonic Organoids

Protocols for crypt isolation and organoid culture were adapted from previously described methods[67,68]. Colonic pinch biopsies were obtained from an adult cohort of non-IBD patients and patients with Crohn's disease during routine colonoscopies. Biopsies were stored at 4°C in collection media (advanced DMEM/F12 (Gibco, 12634010) supplemented with 10% FBS, 100 U/mL penicillin, 100 µg/mL streptomycin, 10 mM HEPES (Gibco, 15630080), 2 mM Glutamax (Gibco, 35050061), 1X amphotericin B (HyClone™, 11526481) and 100 µg/mL gentamicin (Sigma-Aldrich, G1397)). For processing, biopsies were washed in cold 1X-PBS supplemented with 1X amphotericin B and 100 µg/mL gentamicin. Biopsies were dissociated with gentle cell

dissociation reagent (Stem Cell Technologies, #07174) supplemented with 1X amphotericin B and 200 µg/mL gentamicin for 20 minutes at room temperature with shaking at 180 RPM. Reagent activity was quenched using cold washing media (Advanced DMEM/F12 supplemented with 10% FBS, 100 U/mL penicillin, 100 µg/mL streptomycin, 10 mM HEPES and 2 mM Glutamax) and the suspension was passed through a 70 µm filter. The filtered solution was centrifuged at 200 RCF for 5 minutes and the supernatant was discarded. The pellet was re-suspended and transferred to a 1.5 mL tube and centrifuged at 400 RCF for 3 minutes. The supernatant was removed and the pellet containing the isolated crypts was re-suspended in reduced growth factor type 2 BME (Amsbio, 3533-010-02). 20 µl domes of crypt/BME solution were seeded in 48-well plates. Plates were placed in a cell culture incubator for 20 minutes to polymerise the BME. Once polymerised the domes were overlaid with 300 µl of Organoid Growth Media (OGM). OGM was prepared as follows: serum free media (advanced DMEM/F12 supplemented with 10 mM HEPES, 2 mM Glutamax (Gibco), 1X N2 supplement (Invitrogen, 17502-048), 1X B27 supplement (Invitrogen, 17504-044), 1 mM N-acetylcysteine (Sigma-Aldrich, A9165) and 50 ng/mL human recombinant EGF (PeproTech, AF-100-15)) was combined 1:1 with L-WRN conditioned media[69]. This 50 % L-WRN media was supplemented with 10 mM nicotinamide (Sigma-Aldrich, N0636), 10 µM Y-27632 (Selleckchem, S1049), 10 µM SB202190 (Sigma-Aldrich, S7067), 5 µM CHIR-99021 (Sigma-Aldrich, SML1046) and 500 nM A-83-01 (Sigma-Aldrich, SML0788), and filtered using the steriflip vacuum system (MerckMillipore, SE1M179M6). Culture media was replenished twice a week. For passaging, organoids were removed from BME and dissociated using Tryple Express (Gibco, 12604-013) supplemented with ROCK inhibitor Y-27632. Tryple Express was quenched with wash media. The cell solution was centrifuged at 400 RCF for 3 minutes and the supernatant removed. The pellet was re-suspended in fresh BME and seeded. Passaging was performed every 1–2 weeks,

using a 1:3 split ratio. For assays, cells were seeded in 96 well plates (5000/well) and left to recover for 2 days. Organoid lines selected for these experiments were used between passage numbers 4-10. Organoids were pre-treated for 1 hour with JAKinibs before stimulation with cytokines. Cell viability was measured by quantitation of ATP present in the cells using cell titre glo luminescent assay as per the manufacturer's instructions. Live light microscopy images were acquired using the EVOS FL (Life technologies).

2.3.11. Statistical analysis

Statistical analysis was performed using GraphPad Prism 7.0 (GraphPad Software, Inc., La Jolla, CA, USA). Data are presented as mean ± SEM, and statistical analysis of the data was performed by using 1-way-ANOVA or 2-way-ANOVA. Statistically significant differences were identified at p value < 0.05.

2.4. Results

2.4.1. IFN-γ and TNF-α synergise to induce cell death in colorectal cancer cells

The Th1 cytokines IFN-γ and TNF-α are known to induce cell death both independently and co-operatively in different cell types.[65,70–72] To investigate the role of IFN-γ and TNF-α on colonic epithelial cell death, HT-29 cells were treated with different concentrations (1 pg/mL – 100 ng/mL) of IFN-γ and TNF-α both individually and in combination for 72 hours and cell viability was measured (Figure 2.1A). The cells were moderately sensitive to IFN-γ induced cell death and the response was significantly increased in the presence of TNF-α co-treatment. But treatment of cells with TNF-α alone did not affect the viability. Maximum differences in cell viability between individual cytokine treatment and co-treatment was observed at 10 ng/mL concentration (Figure 2.1A), thus this cytokine concentration was chosen for further experiments. These results were further confirmed by crystal violet cell viability assay (Figure 2.1B & 2.1C) and by measuring active caspase-3 and cell viability by flow cytometry (Figure 2.1 D & 2.1E). A panel of nine additional CRC cell lines were then tested for their sensitivity to IFN-γ and TNF-α induced cell death (Figure 2.3). DLD1, HCT-15, SW-948, SW-48 and Colo-205 cell lines were sensitive towards IFN-γ + TNF-α induced cell death but to different extents (Figure 2.3A-E). HCT-116, RKO and HCA7 cell lines were resistant to cell death induced by either cytokine or the combination (Figure 2.3G-I). Interestingly, the LoVo cell line was uniquely sensitive to IFN-γ induced cell death and did not show additional killing with the co-treatment of IFN-γ + TNF-α (Figure 2.3F). To understand the cause of the phenotypic variability of cell lines toward IFN-γ + TNF-α, genomic mutation profiles of the sensitive and resistant cell lines were studied using Cell Model Passport database (https://cellmodelpassports.sanger.ac.uk/).

Although, all cancer cell lines have thousands of mutations recorded in their genome, the resistant cell lines were specifically mutated in *JAK* related genes, *STAT*s and different *TNFR* genes. For instance, HCT-116 cell line contains mutation in *STAT1* and *TNFRSF9* genes. RKO cell line has mutation in several TNF receptors (*TNFSF14, TNFSF8, TNFSF9, TNFSF12, TNFSF13*) and *STAT3*. Interestingly, RKO also had a observed in *CASP8* gene. While mutations in JAK-STAT and TNFR gene suggest an explanation of variable response of the cell lines, further studies are required to confirm the association of these mutations with the sensitivity of cell lines.

There are several studies reporting that IFN-γ + TNF-α can induce cell death through apoptotic pathways, [70,71,73] but IFN-γ and TNF-α are also known to be involved in triggering necroptosis[74–77]. Thus, to further understand the mode of cell death operational in IFN-γ + TNF-α treated cells, HT-29 cells were stimulated with IFN-γ, TNF-α or co-treated with both cytokines for a duration of 24 hours or 48 hours and protein lysates were immunoblotted for different markers of canonical cell death pathways. As shown in Figure 2.2A, IFN-γ + TNF-α triggered cell death of HT-29 cells with nearly 60% reduction in cell viability after 48 hours of cytokine treatment was associated with a significant activation of caspase 3 after 24 hours. Western blotting data demonstrated activation of caspase 8, 9, 10 and 3 confirming the involvement of both the extrinsic and intrinsic pathways of apoptosis (Figure 2.3B). There was also activation of MLKL and accumulation of cleaved microtubule-associated protein 1A/1B-light chain 3 (LC3-II) with combined treatment of IFN-γ + TNF-α, indicating that multiple cell death pathways may be triggered in response to IFN-γ + TNF-α treatment in colonic epithelial cells (Figure 2.3 B).

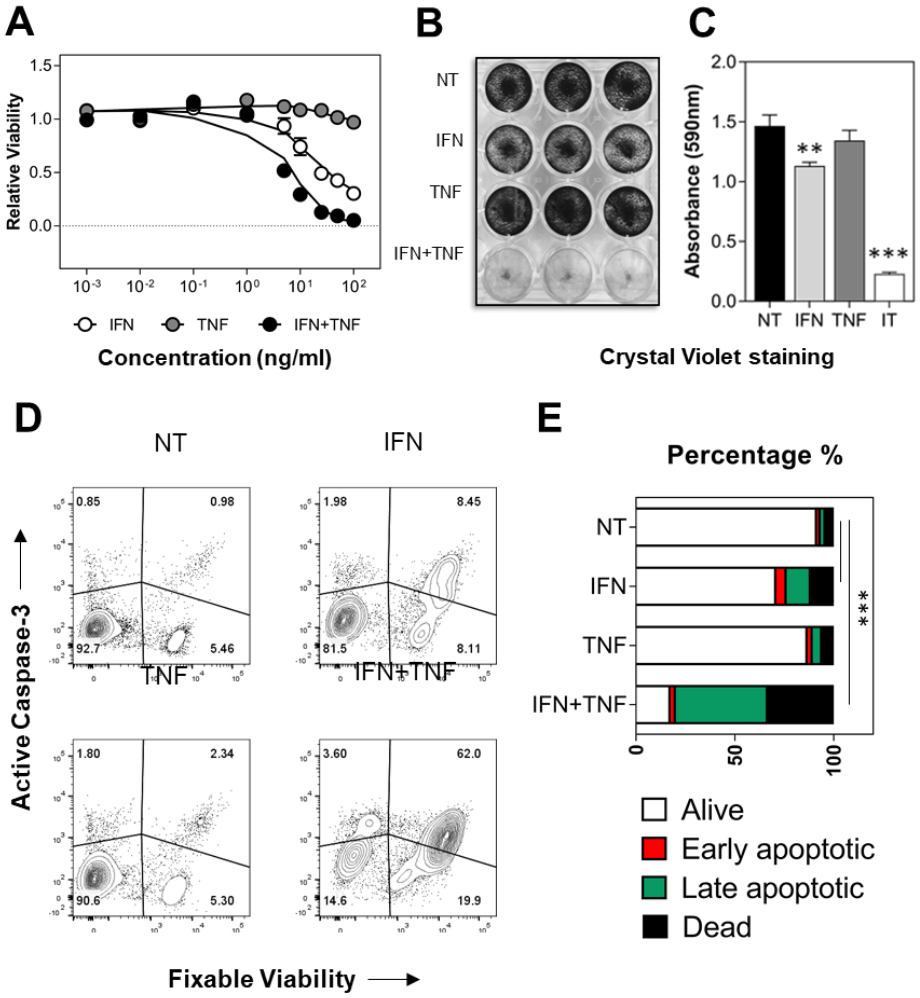


Figure 2.1 IFN-γ and TNF-α synergise to induce cell death in HT-29 colorectal cancer cells

(A) HT-29 cells were stimulated as indicated with 1 pg/mL - 100 ng/mL of IFN-γ, TNF-α or IFN-γ + TNF-α for 72 hours and relative cell viability was quantified using Cell Titre-Glo (Promega) assay. Data shown are the mean ± S.E.M of n = 3 independent experiments in triplicate. (B-E) HT-29 cells were treated with IFN-γ (10 ng/mL), TNF-α (10 ng/mL) or IFN-γ + TNF-α (10 ng/mL each) for 72 hours. (B) Crystal violet staining representing 1 of 3 experiments. (C) Bar graph representing estimation of intensity of crystal violet stain. Data shown are the mean ± S.E.M of n = 3 independent experiments in triplicate. (D) Cell death profile of HT29 cells stained for active caspase-3 and fixable viability dye FVS660. Data representing 1 out of 3 experiments. (E) graphical representation of cell death profile from (D). Data shown are the mean ± S.E.M of n = 3 independent experiments in duplicate. *p < 0.05, **p < 0.01 and ***p < 0.001

(two-way ANOVA followed by Tukey's multiple comparisons test vs. non-treated cells)

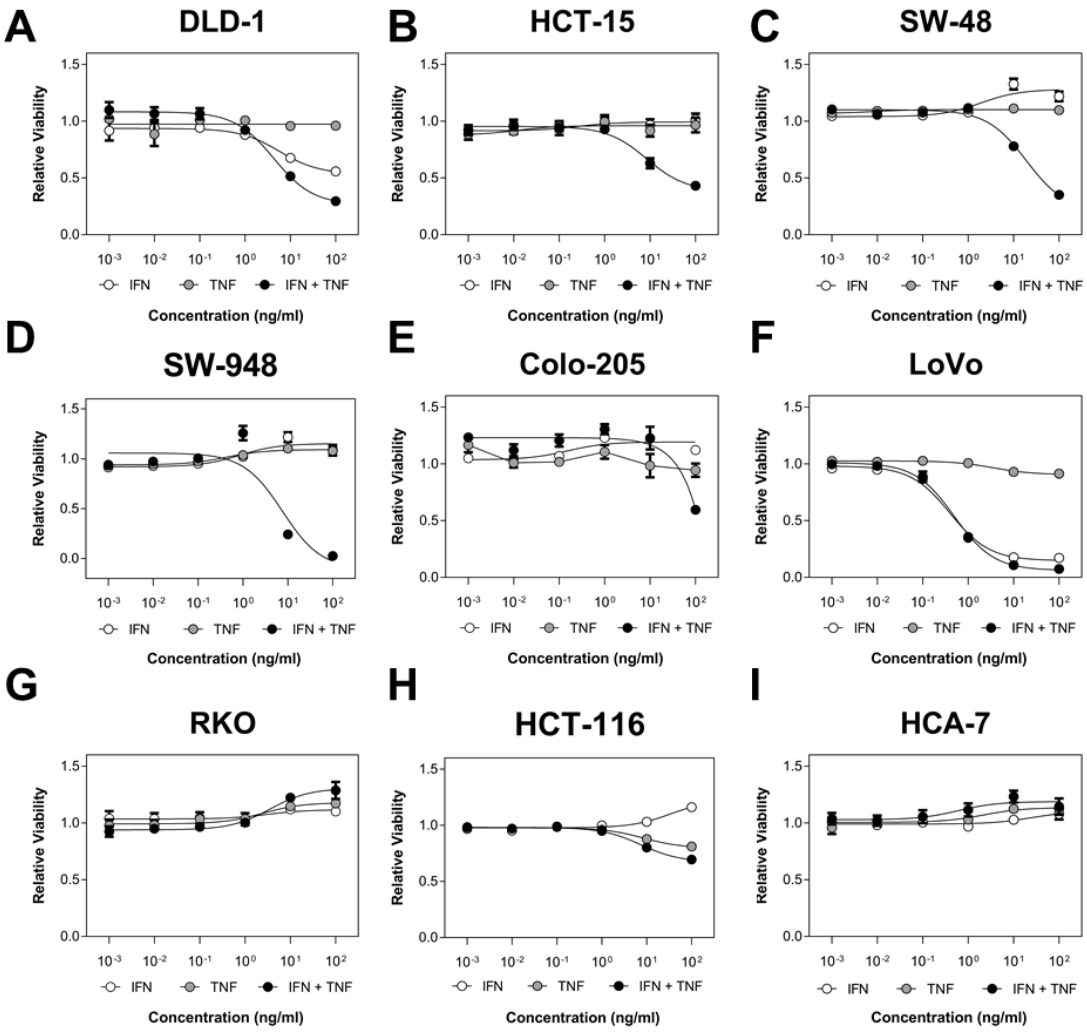


Figure 2.2 IFN-γ and TNF-α synergise to induce cell death in different colorectal cancer cell lines.

(A-I) Panel of 9 non-isogenic CRC cell lines (as labelled) were treated with IFN-γ (10 ng/mL), TNF-α (10 ng/mL) or IFN-γ + TNF-α (10 ng/mL of each) for 72 hours and assayed for relative cell viability by using Cell Titre-Glo (Promega) assay. (A-F) Cell lines sensitive to IFN-γ + TNF-α induced cell death (G-I) Cell lines resistant to IFN-γ + TNF-α induced cell death. Data shown are the mean ± S.E.M of n = 3 independent experiments in triplicates.

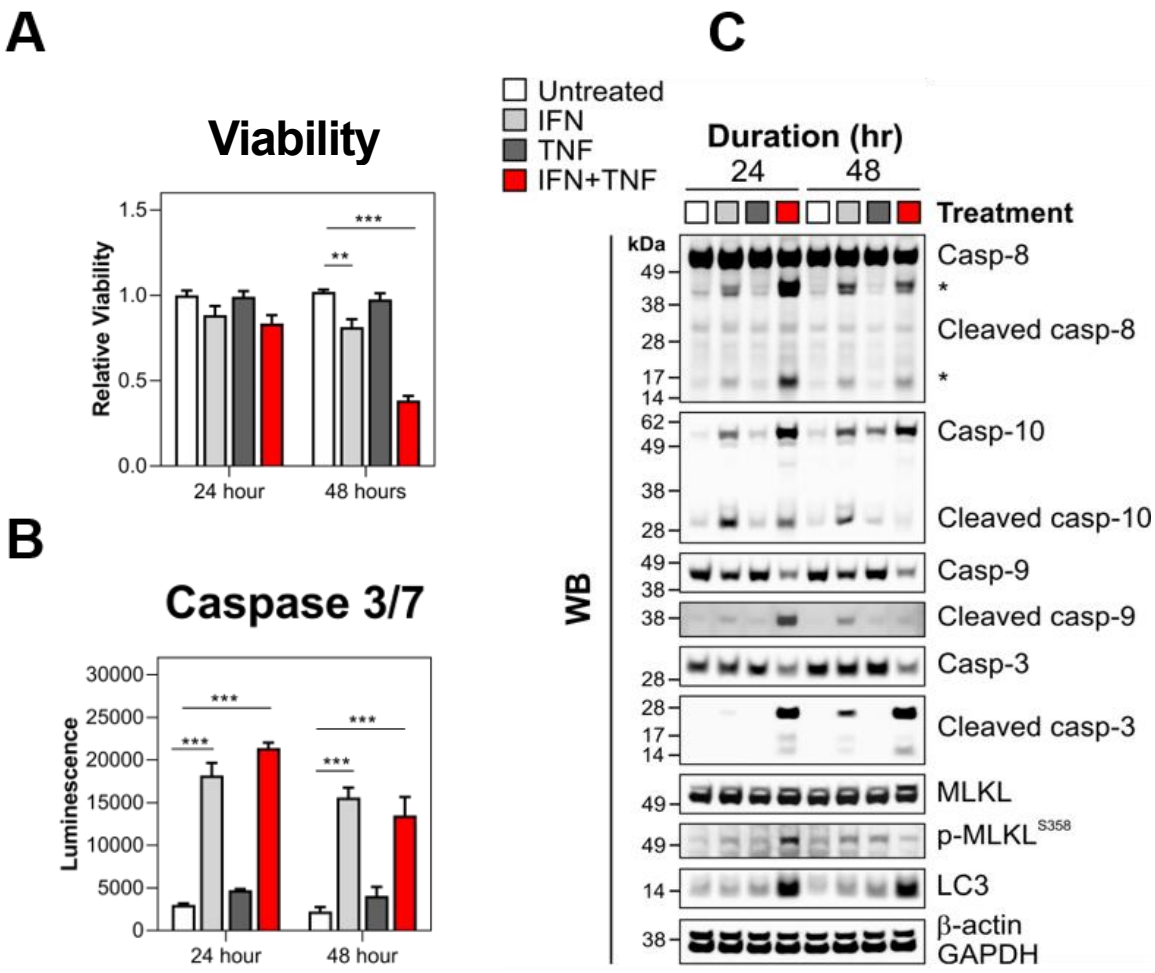


Figure 2.3 IFN-γ + TNF-α synergise to induce caspase activation in HT-29 cells

(A-C) HT-29 cells were stimulated with 10 ng/mL of IFN-γ, TNF-α or co-stimulated with both cytokines (A) Relative cell viability was estimated using CellTitre-Glo (Promega) assay (B) Active caspase-3/7 levels after 24 hours and 48 hours. Data shown is the mean ± S.E.M of n = 2 independent experiments in triplicates (C) Western blots showing activation of different cell death markers after 24 hours and 48 hours of IFN-γ + TNF-α treatment. The data shown is representative of one out of two experiments. $^{**}p < 0.01$ and $^{***}p < 0.001$ (two-way ANOVA followed by Tukey's multiple comparisons test as indicated). NT- non-treated cells

2.4.2. IFN-γ and TNF-α synergise to induce cell death in colorectal cancer cells in a JAK1 and JAK2 dependent manner

To identify kinases required for IFN-γ and TNF-α induced synergistic killing, a human kinome RNAi screen was performed. HT-29 cells were reverse transfected with a library of siRNAs (Dharmacon's pooled on Target-plus (OTP) siRNA-10nM each) against 768 human kinases for 48 hours and treated with 10 ng/mL of IFN-γ and TNF-α for 72 h and assayed for cell viability. The depletion of some kinases; Checkpoint Kinase 1 (*CHEK1),* Polo Like Kinase 1 *(PLK1*), and WEE1 G2 Checkpoint Kinase *(WEE1*) reduced the viability of cells in the absence of cytokine treatment and were essential for cell survival (Figure 2.5). Out of 768 human kinases screened, only knockdown of *JAK1* and *JAK2* could rescue the cells from IFN-γ and TNF-α induced killing (Figure 2.4 A). The screen also identified a few weaker hits; Casein kinase 1a (*CSNK1A1*), Casein kinase 2a (*CSNK2A1*), Galactokinase (*GALK1)* and Inhibitor of kappa light polypeptide gene enhancer (*IKBKB).* Surprisingly, none of the kinases associated with TNF-α cell death signalling pathways (*RIPK1, RIPK3, MLKL* etc) were hits in the RNAi screens.

We validated results from the kinome screen using separate siRNAs from the deconvoluted pools against the two major hits *JAK1* and *JAK2* and smart pools targeting the four weaker hits *GALK1, CSNK1A1, CSNK2A1* and *IKBKB* (Figure 2.7). Of these hits, only knockdown of JAK1 and JAK2 could rescue the cells from cytokine-induced cell death confirming their essential role in this cell death pathway. (Figure 2.7 A & B) Knocking down *GALK1, CSNK1A1, CSNK2A1, CSNK1A1/CSNK2A1* or *IKBKB* did not rescue viability of cells upon cytokine treatment (Figure 2.7 A). Perturbation of *STAT1*, the downstream transcription factor target of JAK1/JAK2-mediated phosphorylation also rescued cell death which further supported the central role of the JAK1/JAK2/STAT1 pathway in this cell death phenotype

(Figure 2.7A). Furthermore, CRISPR/Cas9 generated DLD1- JAK1, JAK2 and STAT1 knockout cell lines were resistant towards IFN-γ + TNF-α induced cell death (Figure 2.8).

In parallel to the kinome screen, a library of 2773 approved drugs (Micro-source FDA, Prestwick, NIH Clinical, and NCI Oncology libraries + 700 additional compounds) was screened to identify drugs that could potentially rescue the cells from IFN-γ/TNF-α induced killing (Figure 2.6). The major hits identified from the screen were JAK1 and JAK2 inhibitors, baricitinib (JAK1/2 inhibitor) and fedratinib (JAK2 inhibitor). To investigate and validate this further, a panel of six JAK inhibitors were tested in concentration-response experiments for their ability to inhibit the JAK1/2-STAT1 pathway and rescue cells from cytokine induced cell death (Figure 2.9). The JAK inhibitors upadacitinib (JAK1 inhibitor), fedratinib (JAK2 inhibitor), BMS-911543 (JAK2 inhibitors), baricitinib, ruxolitinib (JAK1/2 inhibitors) and tofacitinib (JAK3; JAK1&2 inhibitor) completely rescued the cells from IFN-γ and TNF-α induced killing at a concentration of ~1 μM. Fedratinib exhibited cytotoxicity at a concentration higher than 1 μM (Figure 2.9 B-G). The JAK inhibitory activity of JAKinibs was validated by western blotting for phosphorylated STAT1 pY701 at 1μM concentration of each inhibitor (Figure 2.9A). All JAKinibs except for filgotinib, were able to block or reduce STAT1 pY701 phosphorylation with maximum reduction of STAT1 pY701 by baricitinib. There was also a reduction in total STAT1 levels upon treatment of cells with BMS-911543, possibly due to some off-target effects. The activity of JAKinibs (Upadacitinib, BMS-911543, Baricitinib and Ruxolitinib) were further tested on different IFN-γ/TNF-α sensitive cell lines; HCT-15, DLD-1, SW-48 and SW-948 (Figure 2.10 A-D). All cell lines exhibit cell death upon IFN-γ+TNF-α treatment and could be rescued by the JAKinib treatments. Though HCT-15 showed only a partial rescue upon JAKinib treatment (Figure 2.10 B.)

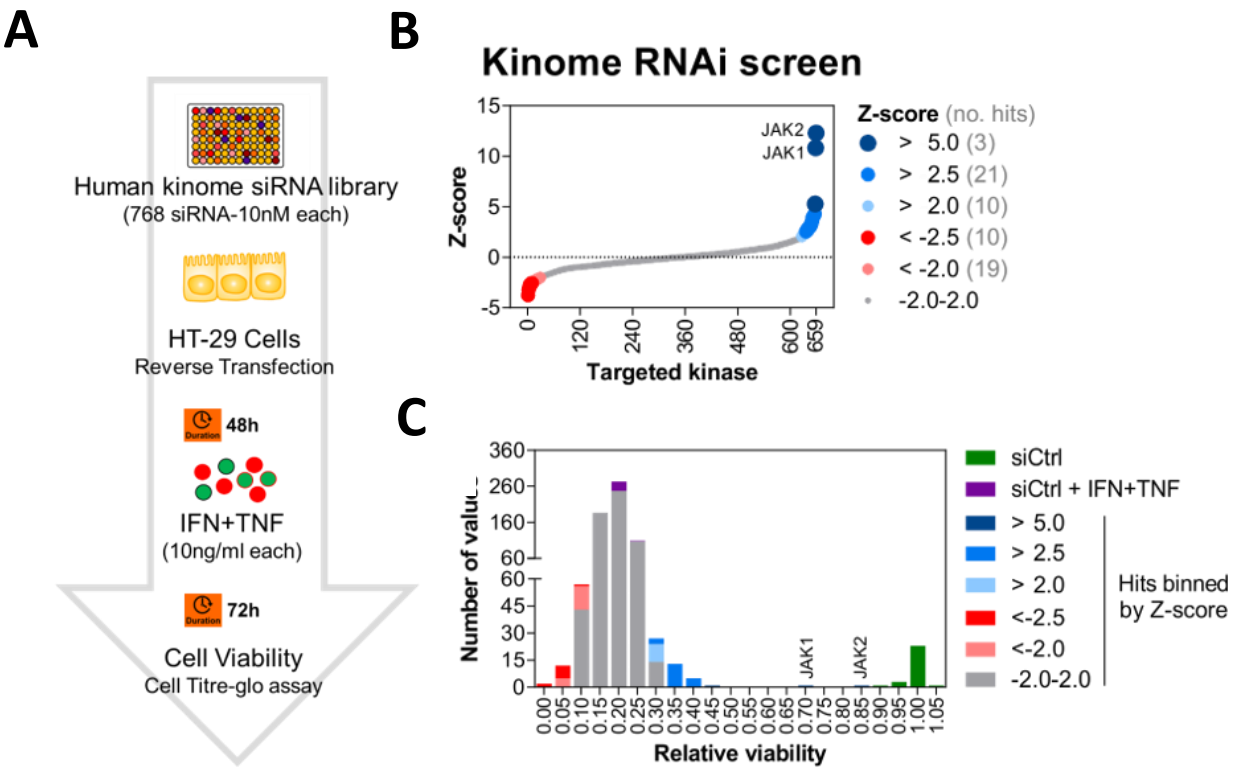


Figure 2.4 Human kinome RNAi screen identifies JAK1 and JAK2 as main modulators of cell death in cytokine treated HT-29 cells

(A) Workflow schematic of human kinome RNAi screens in HT-29 cells. (B-C) Overview of RNAi screen results. (B) The robust Z-score were determined for each targeted gene and Z-score was plotted against average relative viability for candidate genes with Z-score > 5.0 (C) Graph showing Frequency distribution of average relative viability across the kinome RNAi library. The viability of siCtrl cells were considered 100% viable with relative viability.

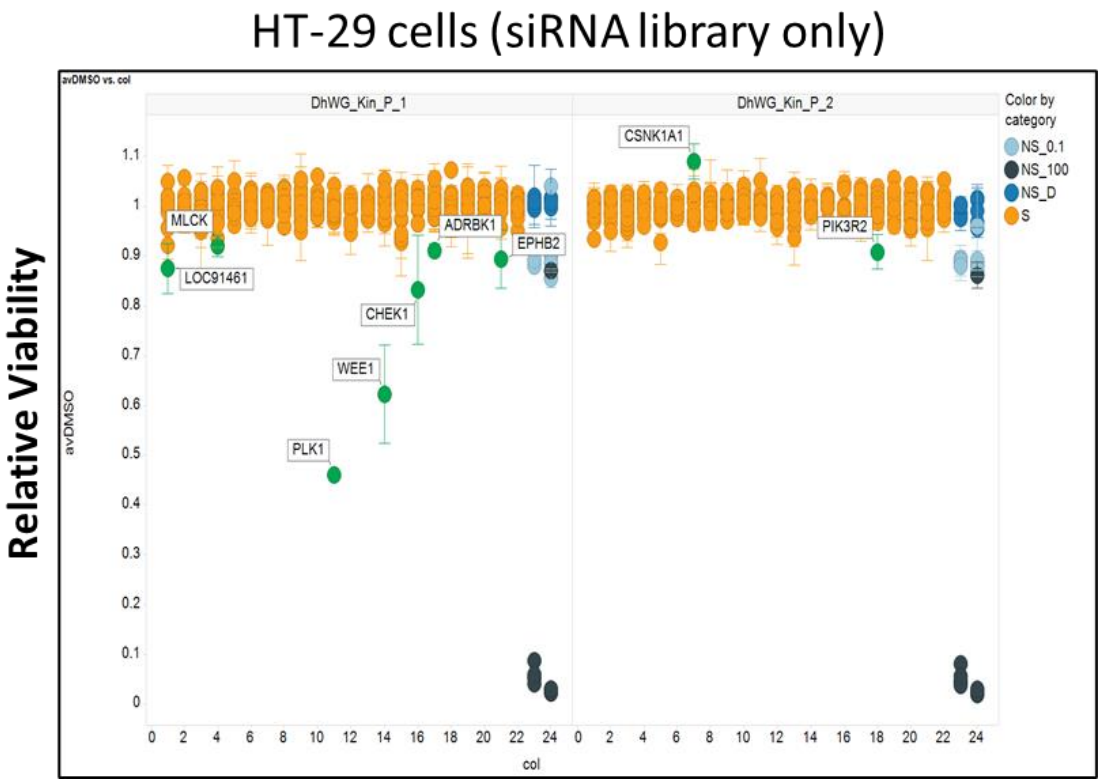


Figure 2.5 Human Kinome RNAi screen identifies genes required for cell survival

HT-29 cells were reverse transfected with RNAi library (siRNA against 768 kinases) for 48 hours and supplemented with culture media for 72 hours. Cell viability was estimated using cell titer glo assay and plotted for each condition. Blue circles (NS-D) represent average viability of control cells, Grey circles at the bottom represent average viability of cells treated with 10 ng/mL IFN-γ+TNF-α, Orange circles represent the average viability of cells for each targeted gene with Z score < 2.5 , Green circles, viability of cells with targeted gene with Z score > /= 2.5.

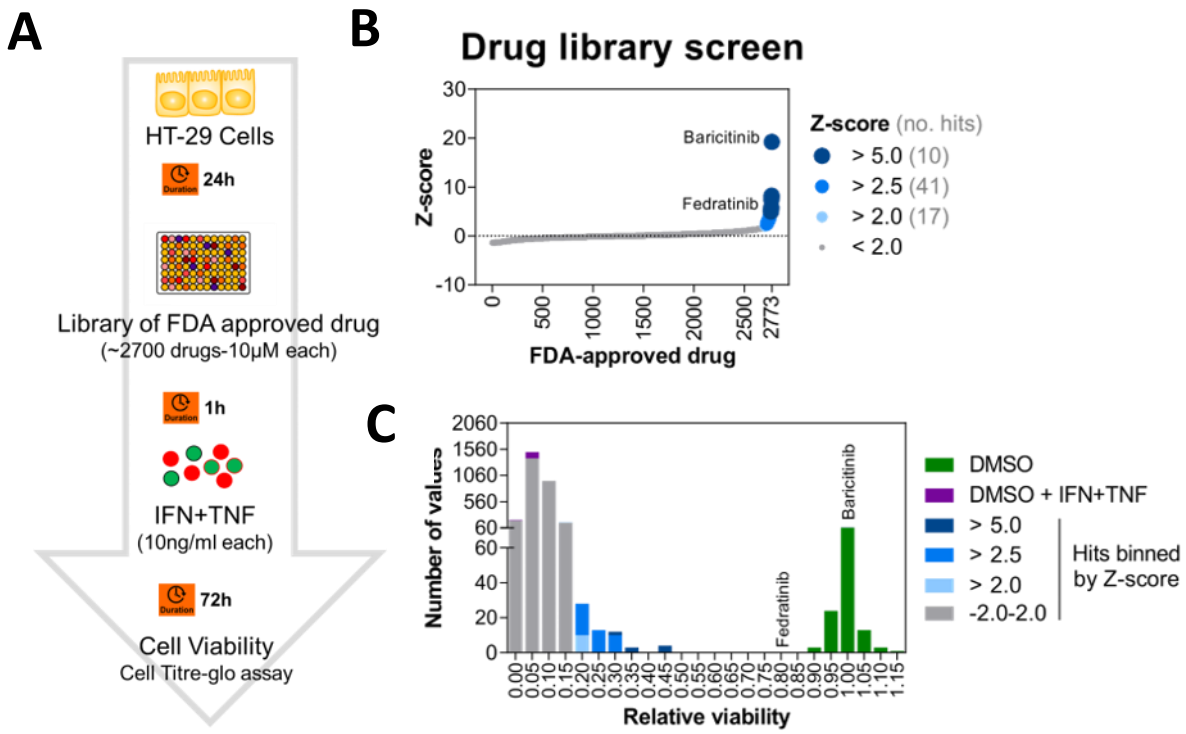


Figure 2.6 Drug repurposing screen identifies JAK1 and JAK2 as main modulators of cell death in cytokine treated HT-29 cells

(A) Workflow schematic of drug library screens in HT-29 cells. (B-C) Overview of Drug library screen results. (B) The robust Z-score were determined for each targeted gene and Z-score was plotted against Average relative viability for candidate drug treated cells with Z-score > 5.0 (C) Graph showing Frequency distribution of average relative viability across the drug library

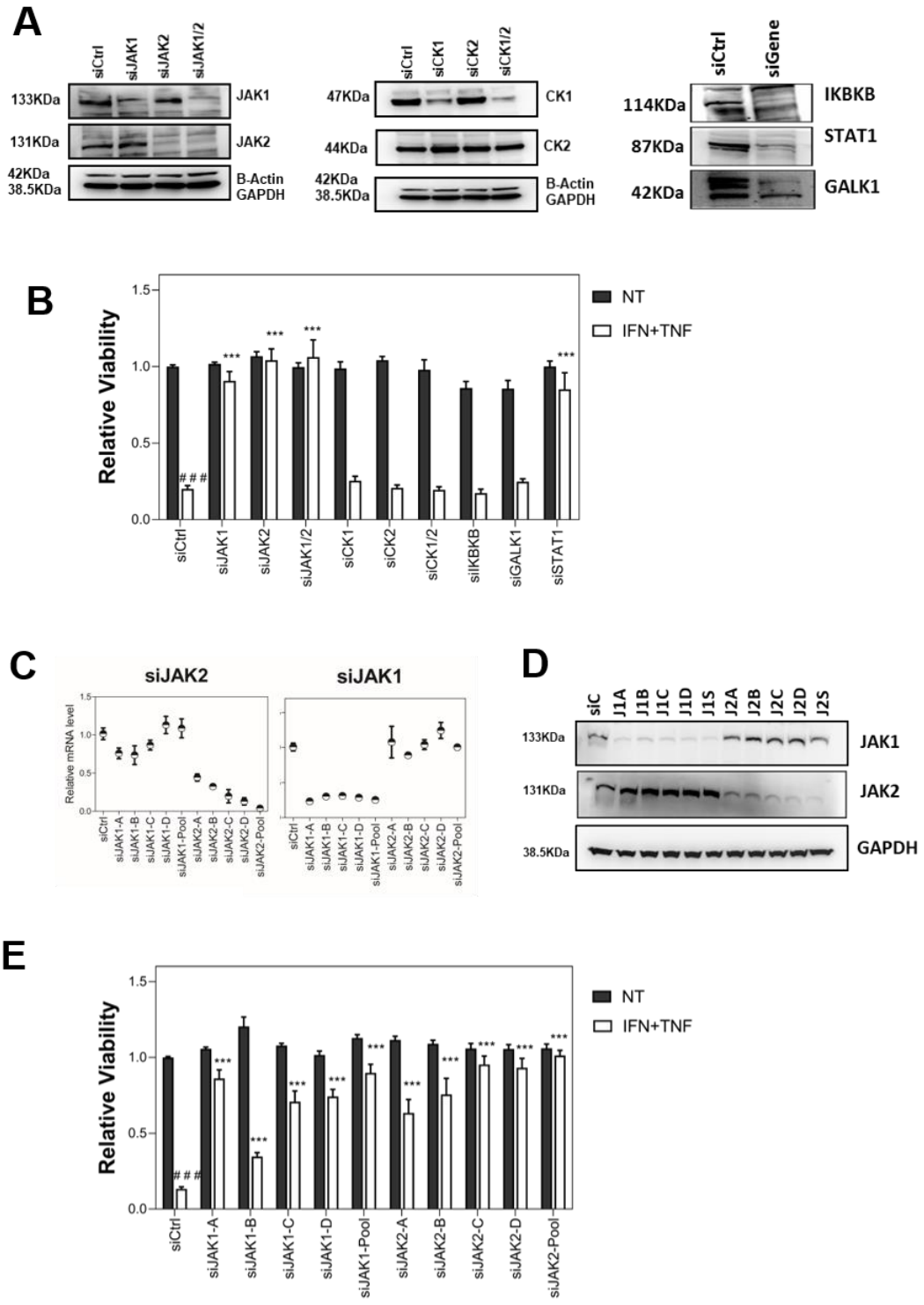


Figure 2.7 JAK1 and JAK2 are required for IFN-γ + TNF-α induced killing of colorectal cancer cells

(A-B) HT-29 cells were reverse transfected with non-targeting siRNA (siCTRL) or siRNA against *JAK1, JAK2, STAT1, CSNK1A1a, CSNK2A1a, GALK1 or IKBKB* (all siRNAs at 25nM) for 48 hours (A) RNAi knock down was confirmed by western

blot (B) Transfected cells were co-stimulated with IFN-γ and TNF-α (10 ng/mL each) for 72 hours and measured for cell viability. Data shown is the mean ± S.E.M of n = 3 independent experiments in triplicates. (C-E) HT-29 cells were reverse transfected for 48 hours with non-targeting siRNA or a panel of siRNA molecules against JAK1 and JAK2 (siJAK1 and JAK2 pool and deconvoluted, all siRNAs at 25 nM). (C) relative mRNA levels were estimated by RT-qPCR. Data shown is the mean ± S.E.M of n = 2 independent experiments in triplicates. (D) RNAi knock down was confirmed by western blot. Data shown is representative of 1 out of 2 independent runs. (E) Transfected cells were co-stimulated with IFN-γ and TNF-α (10 ng/mL each) for 72 hours and measured for cell viability using Cell Titre-Glo (Promega) assay. Data shown is the mean ± S.E.M of n = 3 independent experiments in triplicates *p < 0.05, **p < 0.01 and ***p < 0.001 (two-way ANOVA followed by Tukey's multiple comparisons test vs. IFN-γ+TNF-α) #p < 0.05, # #p < 0.01 and # # #p < 0.001 (two-way ANOVA followed by Tukey's multiple comparisons test vs. non-treated cells) NT- non cytokine treated cells

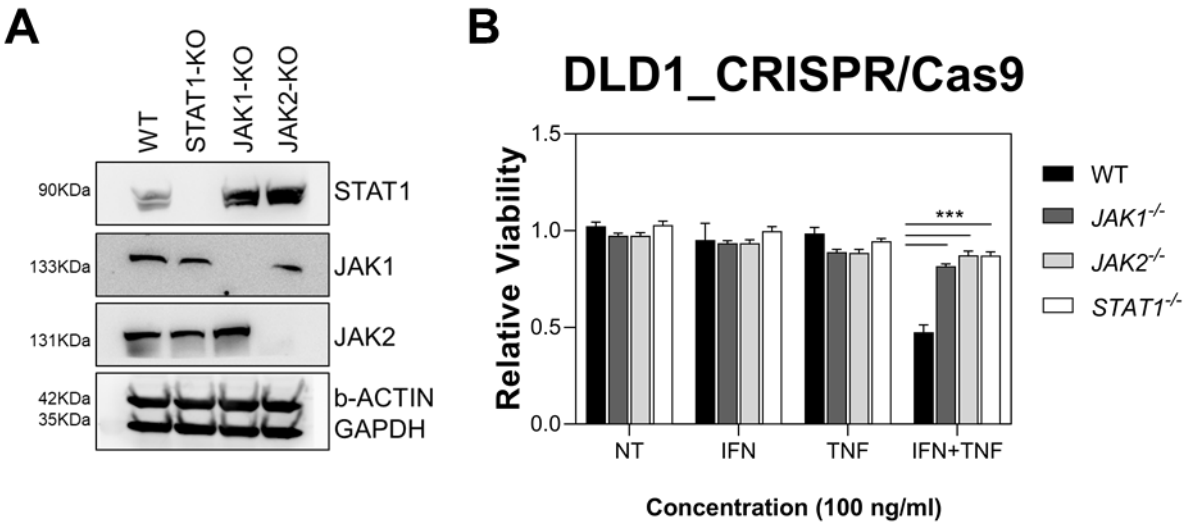


Figure 2.8 JAK1, JAK2 and STAT1 knockout DLD-1 cell lines are resistant to IFN-γ + TNF-α induced killing

(A) DLD1 parental wild type and DLD1 CRISPR/Cas9 *JAK1*$^{-/-}$, *JAK2*$^{-/-}$, *STAT1*$^{-/-}$ cell lines were tested for their knockout phenotype by western blotting (B) All cell lines were co-stimulated with IFN-γ + TNF-α (100 ng/mL of each) for 72 hours and estimated for cell viability by using CellTitre-Glo (Promega) assay. Data shown is the mean ± S.E.M of n = 3 independent experiments in triplicates. **p < 0.01 and ***p < 0.001 (two-way ANOVA followed by Tukey's multiple comparisons test as indicated). NT- non cytokine treated cells

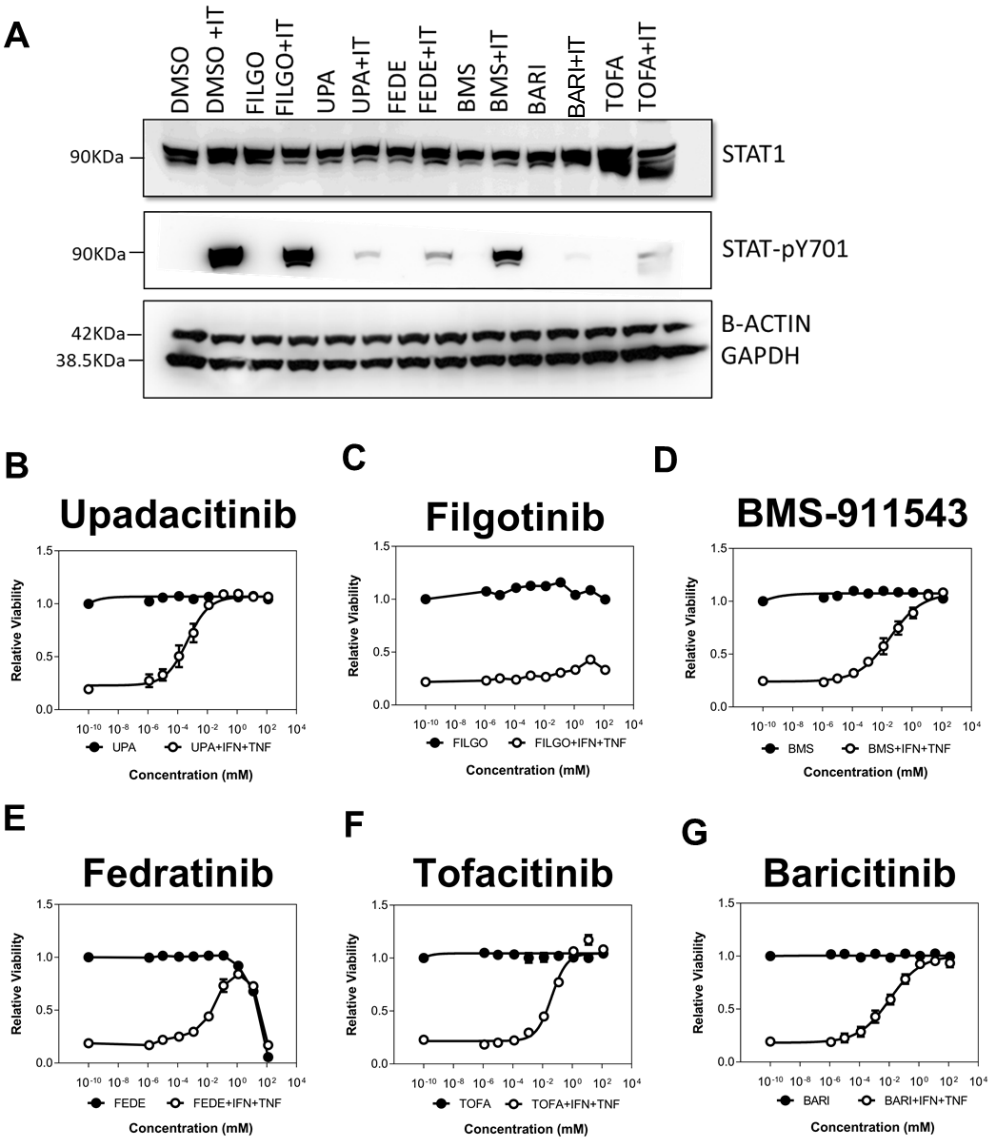


Figure 2.9 JAKinibs block IFN-γ+TNF-α induced cell death in HT-29 cells

(A) HT-29 cells were pre-treated with JAKinibs for 1 hour followed by co-treatment with IFN-γ+TNF-α for 1 hour. STAT1 and STAT1 pY701 levels were analysed by western blotting. Data shown is representative of 1 out of 2 independent experiments. (B) HT-29 cells were pre-treated with 1 pM – 10 μM of JAK1 inhibitor Upadacitinib (UPA), JAK2 inhibitor BMS-911543 (BMS), JAK1/2 inhibitor Baricitinib (BARI) and JAK1/3 inhibitor Tofacitinib (TOFA) for 1 hour followed by co-treatment with IFN-γ/ TNF-α (10 ng/mL of each) for 72 hours. Cell viability was estimated using using CellTitre-Glo (Promega) assay. Data shown is the mean ± S.E.M of n = 3 independent experiments in triplicate.

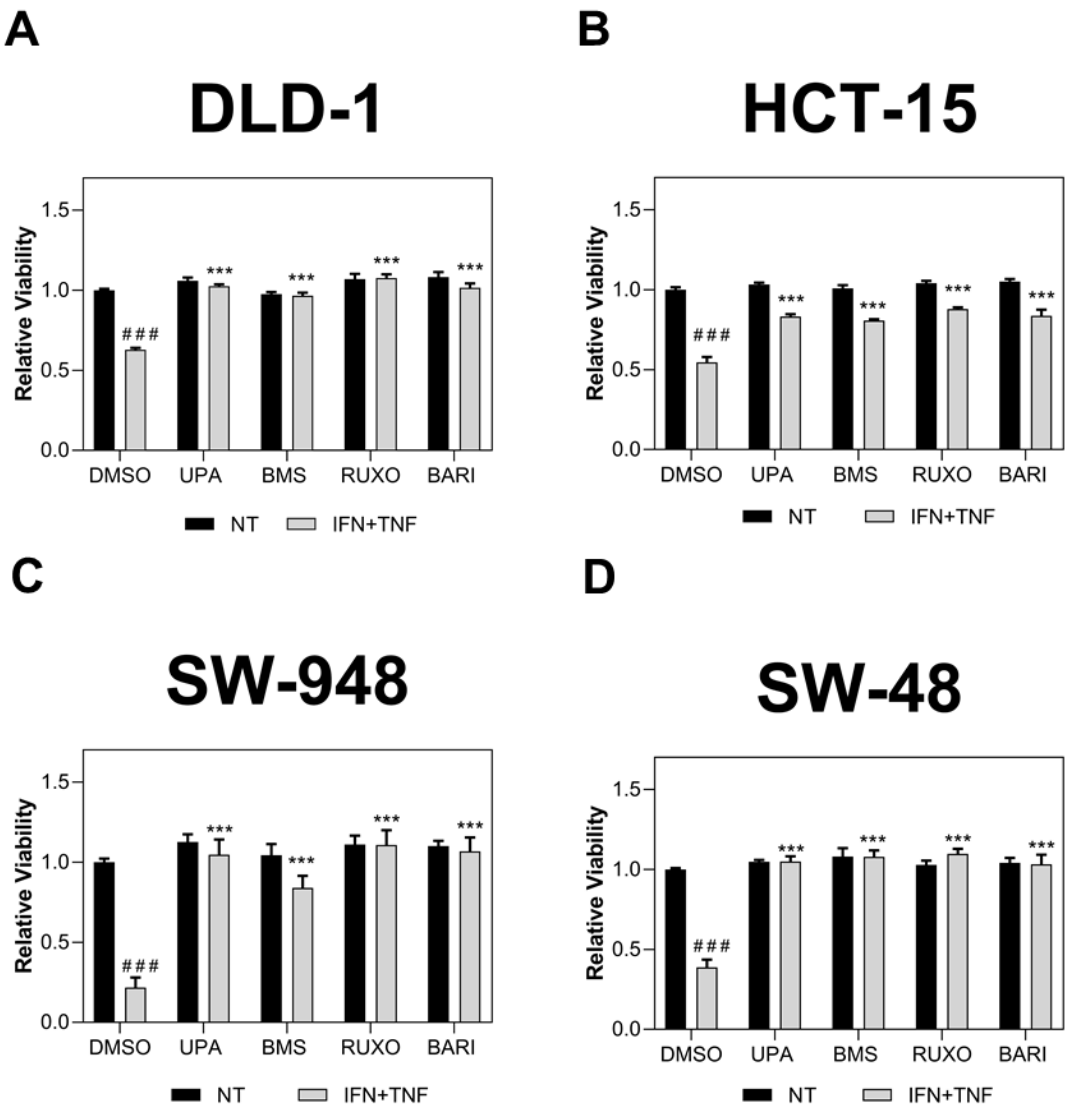


Figure 2.10 JAKinibs block IFN-γ/TNF-α induced cell death in multiple colorectal cancer cell lines

(A-D) DLD1, HCT-15, SW-48 and SW-948 CRC cell lines were pre-treated with 1 µM concentration of JAK1 inhibitors as indicated for 1 hour followed by co-treatment with 10 ng/mL of IFN-γ + TNF-α for 72 hours. Cell viability was measured using CellTitre-Glo (Promega) assay. Data shown are the mean ± S.E.M of n = 3 independent experiments in triplicates. *p < 0.05, **p < 0.01 and ***p < 0.001 (two-way ANOVA followed by Tukey's multiple comparisons test vs. IFN-γ+TNF-α) #p < 0.05, # #p < 0.01 and # # #p < 0.001 (two-way ANOVA followed by Tukey's multiple comparisons test vs. non-treated cells)

2.4.3. IFN-γ + TNF-α induced killing is independent of TNFR1 associated apoptotic and necroptotic pathways

TNF-α exerts its biological functions by interacting with two receptors; TNFR1 and TNFR2[78]. Both receptors have been reported to be involved in cell death, survival and proliferation processes[79]. Although several studies have described the role of TNF receptors and the death-inducing signaling complex (DISC) in IFN-γ + TNF-α induced cell death[65,80–82], Our kinome RNAi screen did not identify any kinases associated with TNFR1 mediated canonical cell death pathway (RIPK1, RIPK3)[17,39,83]. Thus, to understand the involvement of TNFR1 and TNFR2 in IFN-γ + TNF-α induced synergistic cell death TNFR1 and TNFR2 expression were perturbed using RNAi (Figure 2.11). The knockdown of TNFR1 in cells completely blocked cell death, while TNFR2 knockdown did not prevent the cell death phenotype thus confirming that IFN-γ + TNF-α induced cell death is TNFR1-dependent and TNFR2-independent (Figure 2.11).

TNFR1 signalling is mediated through activation of different signalling complexes (complex-1 or II) and can lead to different cellular outcomes - cell survival, apoptosis or necroptosis - depending on the particular complex activated[22]. In order to understand the involvement of TNFR1 signalling complexes in IFN-γ + TNF-α induced cell death, cell induced by the combination of IFN-γ and TNF-α was compared to cell death induced by TNFR1 associated apoptotic and necroptotic complexes[22,76,84]. Several compounds such as cycloheximide (CHX), BV-6 (IAP inhibitor) and IKK-16 (IKKα/β inhibitor) sensitize the cells to TNF induced apoptosis through complex IIa and complex IIb and treatment of the cells with these sensitizers in combination with z-vad-fmk (pan caspase inhibitor) switches the cell death to TNF-α induced necroptosis through complex II-c formation. Hence, three compounds cycloheximide, BV-6 and IKK-16 were used to sensitize to HT-29 cells to TNF-α induced apoptosis (-z-vad-fmk) and necroptosis (+z-vad-fmk) (Figure 2.12). Upon treatment with sensitizers (CHX, BV6 or IKK-16)

and TNF-α the cells underwent cell death. The addition of z-vad-fmk further increased the cell death which could be rescued by addition of necroptotic inhibitors Nec-2 (RIPK1 inhibitor), GSK'893 (RIPK3 inhibitor) and Necrosulphonamide (MLKL inhibitor), confirming the transition of TNFR1 cell death complex II-a/II-b to IIc (Figure 2.12 A-C). In comparison to TNF-α induced cell death mediated through apoptosis or necroptosis after sensitizing the cells to TNF-α with various inhibitors (CHX, BV-6 or IKK-16), IFN-γ + TNF-α induced synergistic cell death was very different and could not be rescued by either caspase inhibitor, necroptotic inhibitors or the combination of both (Figure 2.12 D). This suggests that IFN-γ + TNF-α induced cell death is unique and that there is no involvement of TNFR-1 associated apoptotic and necroptotic complexes in IFN-γ + TNF-α induced killing of CRC cells.

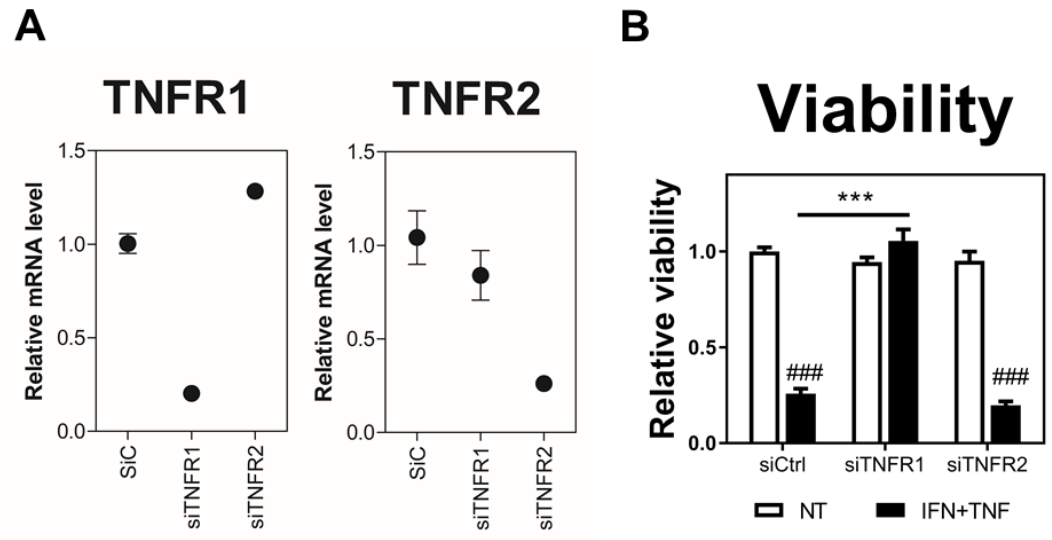


Figure 2.11 IFN-γ + TNF-α induced killing is TNFR1-dependent but independent of TNFR2

(A-B) HT-29 cells were reverse transfected for 48 hours with a non-targeting siRNA (siCtrl) or siRNA against TNFR1 or TNFR2 (all siRNAs at 25nM) (A) GAPDH and beta actin were used as reference genes for the normalisation of the data. Relative mRNA levels of *TNFR1* and *TNFR2* were estimated. Data shown is the mean ± S.E.M of n = 2 independent experiments in triplicate (B) HT-29 cells transfected with siRNAs co-treated with IFN-γ/TNF-α (10 ng/mL each) for 72 hr and measured for cell viability using CellTitre-Glo (Promega) assay. Data shown is the mean ± S.E.M of n = 3 independent experiments in triplicate # # #p < 0.001 (two-way ANOVA followed by Tukey's multiple comparisons test vs. non-treated cells) ***p < 0.001 (two-way ANOVA followed by Tukey's multiple comparisons test vs. IFN-γ+TNF-α) NT- non cytokine treated cells

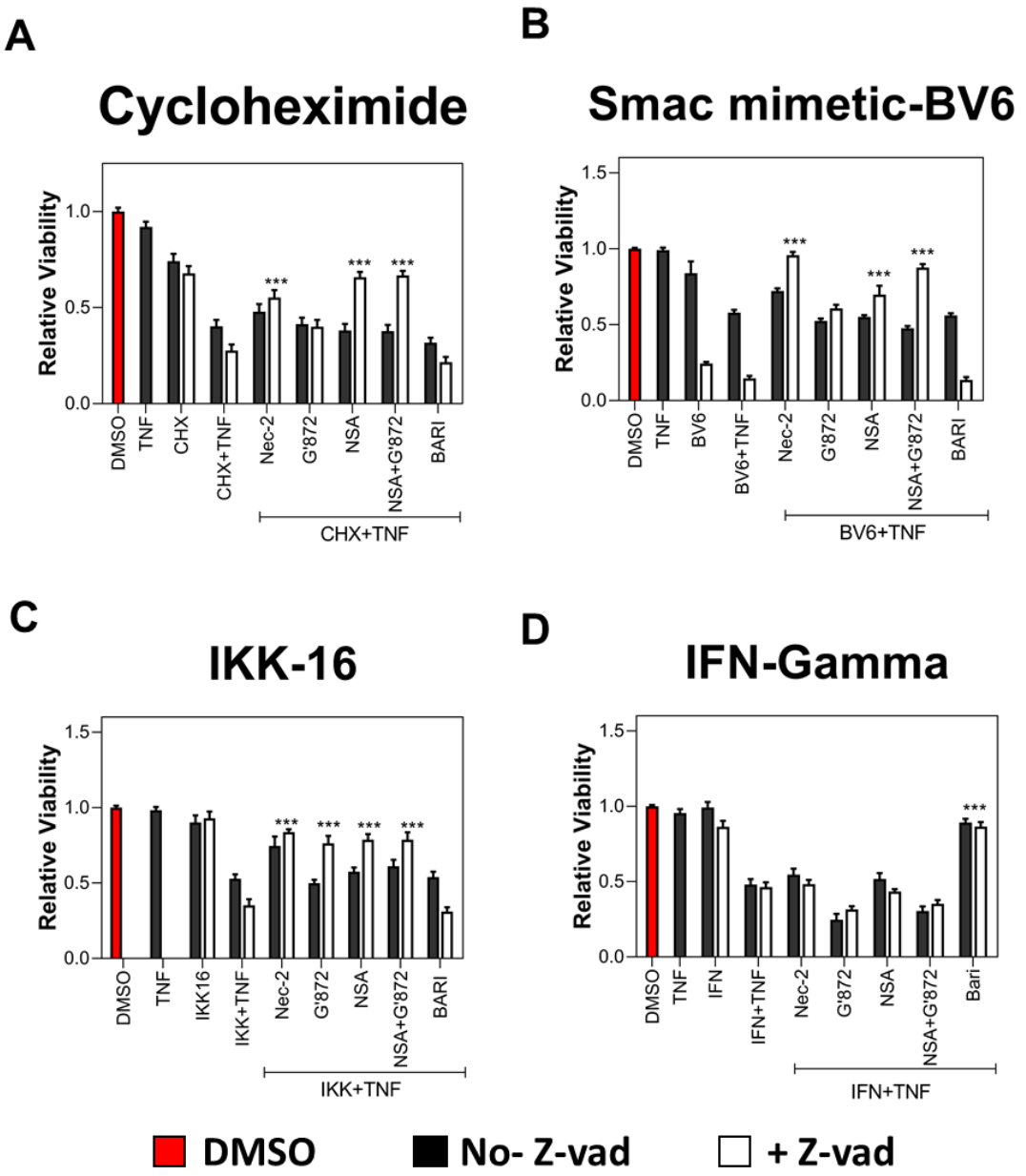


Figure 2.12 IFN-γ + TNF-α induced killing is TNFR1-dependent but independent of TNFR1-associated apoptotic and necroptotic pathways

(A-D) HT-29 cells were pre-treated with indicated inhibitors for 1 hour followed by treatment with TNF-α or co-treatment with IFN-γ+TNF-α, as specified. Cell viability was estimated after 72 hours after cytokine treatment using Cell Titre-Glo (Promega) assay. Data shown is the mean ± S.E.M of n = 3 independent experiments in triplicate. ***p < 0.001 (two-way ANOVA followed by Tukey's multiple comparisons test vs. TNF-α + X, X= CHX, BV6, IKK-16 or IFN) CHX-cycloheximide, IKK16= Inhibitor of IKK a/b, Nec-2 – RIPK1 inhibitorNeccrostatin-

2, NSA- MLKL inhibitor necrosulphonamide GSK'872- RIPK3 inhibitor GSK 985872 NT- non cytokine treated cells, Z-vad- Pan caspase inhibitor z-vad-fmk, Bari- JAK1/2 inhibitor baricitinib.

2.4.4. IFN-γ + TNF-α induced killing is caspase-8-dependent but independent of caspase-8 enzymatic activity

Previously, IFN-γ + TNF-α induced cell death has been reported to be associated with activation of both the intrinsic and extrinsic pathways of apoptosis[85, 86]. Even though HT-29 cells treated with IFN-γ/TNF-α showed activation of caspase-8, 9 and 10 as well as a very high caspase-3/7 activity (Figure 2.13A), blocking caspase activity using pan-caspase inhibitor Z-vad-fmk did not rescue cell death (Figure 2.13B). To further investigate this observation, HT-29 cells were pre-treated individually or in combination with caspase inhibitors selective for caspase-8, 9 and 10, and treated with IFN-γ/TNF-α for 72 hours (Figure 2.13 A-B). Inhibitor activity was monitored by measuring the relative levels of active caspase-3 and 7 in the cells. Even though, all caspase inhibitors tested were able to reduce caspase-3 and 7 activity to basal levels, none of them could rescue the cells from IFN-γ/TNF-α induced killing, confirming that this cell death is independent of caspase activity.

To further explore the role of caspases in cell death, caspase-8 and caspase-10 protein expression and activity were perturbed using RNAi and selective inhibitors (Figure 2.13 C-E). While blocking caspase-8 activity with a selective caspase-8 inhibitor did not rescue the cells RNAi-mediated depletion of caspase-8 protein significantly decreased cytokine-induced killing of HT-29 cells. On the other hand, depletion of caspase-10 protein did not show any rescue of cell viability (Figure 2.13 E). These data suggest a role for caspase-8 protein in the cytokine induced cell death pathway which is independent of its catalytic activity. These results were further confirmed using HT-29 CRISPR/Cas9 knock out cell lines for *CASP8, CASP10, RIPK1* and *RIPK3* genes (Figure 2.14). First, CRISPR/Cas9 cell lines were validated for their knockout phenotype by western blotting and exon sequencing (Figure 2.14 A). To test their sensitivity towards IFN-γ+TNF-α induced cell death, CRISPR/Cas9 mCherry (parental), *CASP8*$^{-/-}$, *CASP10*$^{-/-}$

, *RIPK1*$^{-/-}$ and *RIPK3*$^{-/-}$cell lines were treated with IFN-γ and TNF-α for 72 hours (Figure 2.14 B). CRISPR/Cas9 mcherry expressing HT-29 cells were sensitive to IFN-γ + TNF-α induced killing with a reduction of more than 50% cell viability after 72 hours of cytokine treatment. But cell death was not observed in the *CASP8*$^{-/-}$ cell lines. *CASP10*$^{-/-}$ cells exhibited a higher sensitivity towards synergistic cell death compared to wild type (Figure 2.14 B). *RIPK3*$^{-/-}$ cell line were also less sensitive to IFN-γ + TNF-α induced killing, and showed a partial recuse in response to the cytokine treatment compared to wild type cells. However, as previously described blocking RIPK3 activity with RIPK3 inhibitor GSK'872 did not rescue the cells from IFN-γ/TNF-α induced cell death (Figure 2.12 D). This suggested that similar to caspase-8, RIPK3 protein is required for IFN-γ+TNF-α induced cell death but that this cell death is independent of the kinase activity of RIPK3. The cells deficient for RIPK1 were sensitive to TNF-α induced cell death which further increased with the cytokine co-treatment (Figure 2.14 B & C). Treatment of cells with JAKinibs (Upadacitinib, BMS-911543, ruxolitinib and baricitinib) blocked cytokine induced cell death in all knock out cell lines. But the cell death in *RIPK1*$^{-/-}$ could be rescued only to level of TNF-α induced cell death (Fig 2.14 C). These data suggest that the synergistic cell death induced by IFN-γ/TNF-α is different than TNF-α induced cell death in RIPK1 deficient cells.

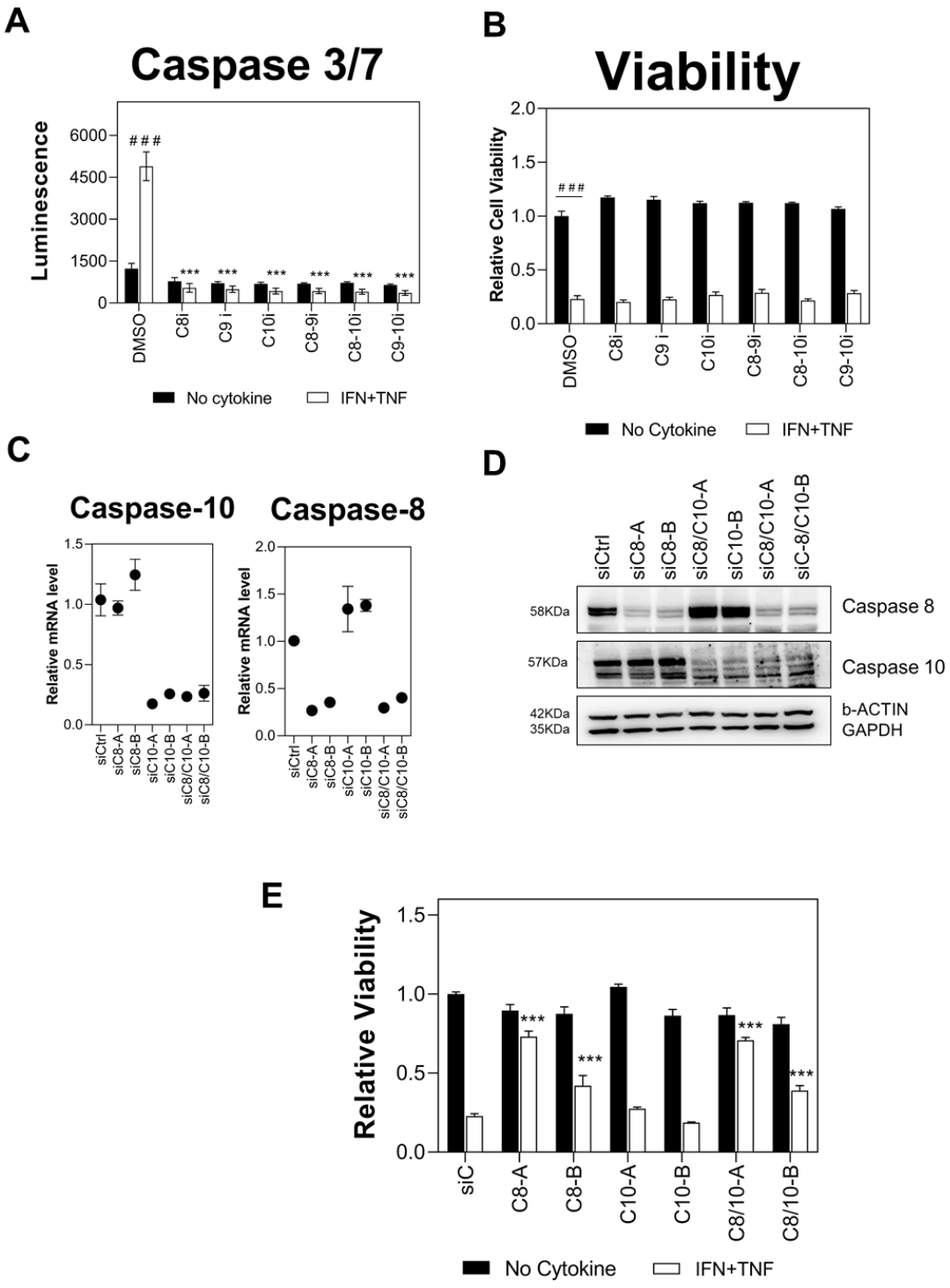


Figure 2.13 IFN-γ + TNF-α induced killing is caspase 8-dependent but independent of caspase-8 proteolytic activity

(A-B) HT-29 cells were pre-treated individually or in combination with 10 μM of selective inhibitors for caspase-8, 9 and 10 as indicated for 1 hour and co-treated IFN-γ + TNF-α (10 ng/mL of each). (A) Caspase-3/7 levels were estimated

after 24 hours of IFN-γ + TNF-α treatment. (B) Cell viability was measured after 72 hours of IFN-γ + TNF-α treatment. (C-E) HT-29 cells were reverse transfected with a non-targeting siRNA (siCTRL) or si*CASP8* and si*CASP10* (all siRNAs at 25nM) for 48 hour (C) The mRNA levels were estimated by RT-qPCR (D) Protein levels were measured by western blotting (A-D) Data shown is the mean ± S.E.M of n = 2 independent experiments in triplicate (E) Transfected cells were stimulated with IFN-γ + TNF-α (10ng/mL each) for 72 hours as indicated and measured for cell viability using CellTitre-Glo(Promega) assay. Data shown is the mean ± S.E.M of n = 3 independent experiments in triplicates ***p < 0.001 (two-way ANOVA followed by Tukey's multiple comparisons test vs IFN+TNF). ###p < 0.001 (two-way ANOVA followed by Tukey's multiple comparisons test vs control cells)

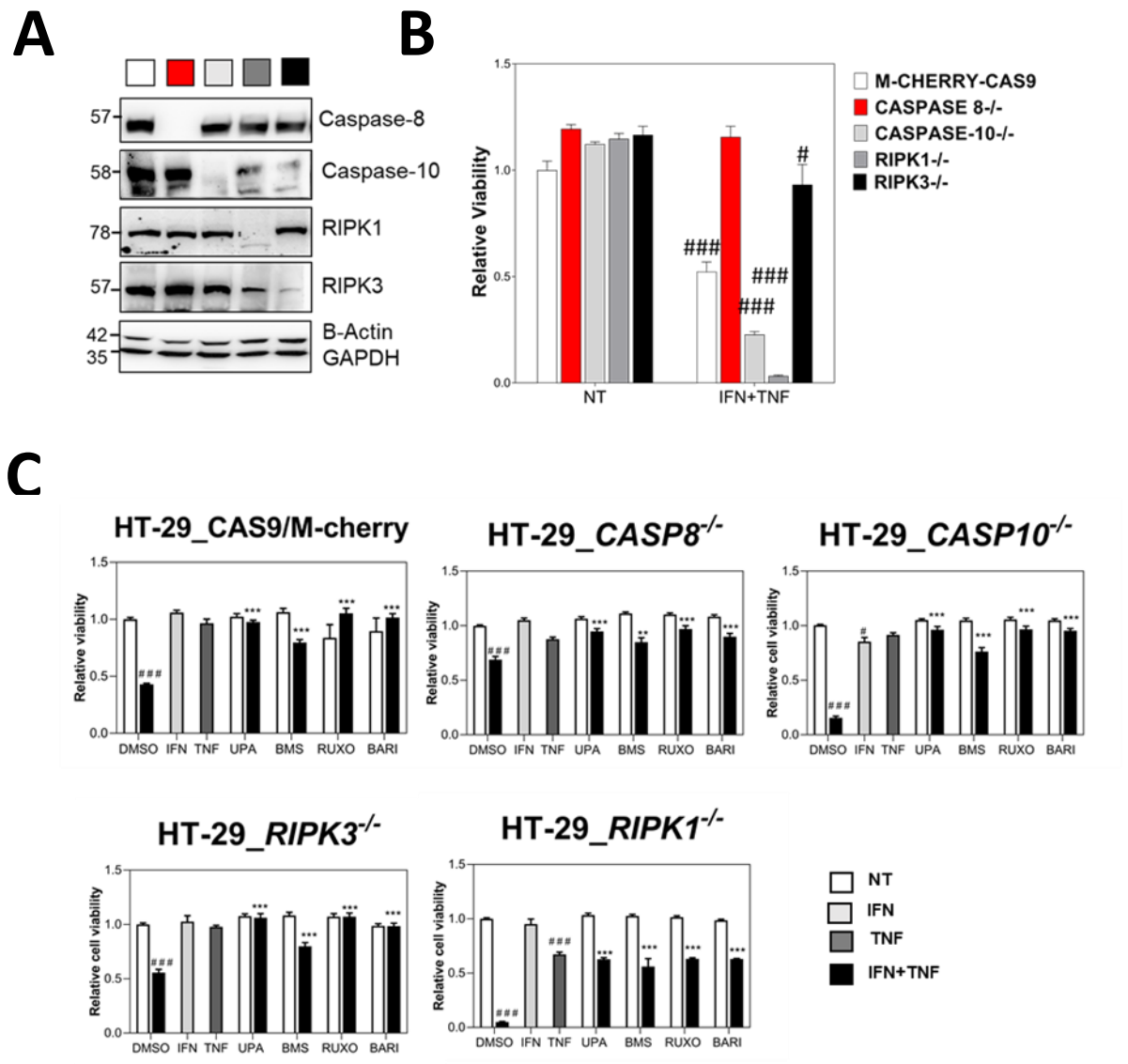


Figure 2.14 CASP8$^{-/-}$ and RIPK3$^{-/-}$ cells are resistant to IFN-γ+TNF-α induced killing

(A) Western blot confirming the knockout status of HT-29 CRISPR/Cas9 *CASP8*$^{-/-}$, *CASP10*$^{-/-}$, *RIPK1*$^{-/-}$, and *RIPK3*$^{-/-}$ HT-29 cell lines. (B) HT-29 knockout cell lines as indicated were co-treated with IFN-γ + TNF-α (10 ng/mL of each) for 72 hours and measured for the cell viability. (C) HT-29 knockout cell lines were pre-treated with JAKinibs as indicated for 1 hour and co-treated with 10 ng/mL of IFN-γ + TNF-α for 72 hours. Cell viability was estimated by measuring relative ATP levels in cells by using CellTitre-glo (Promega) assay. Data shown above is the mean ± S.E.M of n = 3 independent experiments in triplicate. #$p < 0.01$ and ###$p < 0.001$ (two-way ANOVA followed by Tukey's multiple comparisons test compared to NT). **$p < 0.01$ and ***$p < 0.001$ (two-way ANOVA followed by Tukey's multiple comparisons test, compared to IFN+TNF). NT: Cells untreated

with cytokines. Jakinibs: JAKinibs- Upadacitinib (UPA), BMS-911546 (BMS), baricitinib (BARI), Ruxolitinib (RUXO).

2.4.5. IFN-γ+TNF-α induced synergistic cell death is independent of the BCL2 family members BAK and BAX

The pro-apoptotic Bcl-2 family members BAK and BAX are the essential regulators of the intrinsic pathway of apoptosis[87,88]. When cells are treated with apoptotic stimuli, BAK and BAX proteins oligomerise and accumulate at the surface of the outer mitochondrial membrane. This causes the formation of pores on the outer mitochondrial membrane (OMM) and cause its permeabilization (MOMP) [87,88]. The permeable mitochondrial membrane allows the release of cytochrome C in the cells and generation of reactive oxygen species (ROS) and activation of caspase 9.

Previous studies have demonstrated the role of Bcl-2 family members as well as reactive oxygen species (ROS) production and apoptosis in IFN-γ + TNF-α induced synergistic cell death[73,89,90]. Due to the activation of caspase-9 (Figure 2.3B) by IFN-γ + TNF-α in HT-29 cells, we investigated the requirement for the Bcl-2 family members BAK and BAX and ROS production in cytokine induced cell death. HT-29 cells were transfected with siRNA against BAK and BAX protein and co-treated with IFN-γ and TNF-α. After perturbing BAK and BAX expression separately or together, the cells were still sensitive to IFN-γ + TNF-α induced killing (Figure 2.15B) and were successfully rescued by JAKinibs independent of BAK and BAX status, ruling out the role of these proteins in synergistic cell death (Figure 2.15C). Measurement of mitochondrial ROS production by MitoSOX fluorescent probes in the cells treated with IFN-γ + TNF-α did not show any significant increase in mitochondrial ROS accumulation independent of BAK/BAX status (Figure 2.16 A). The level of cytoplasmic ROS was measured by CM-

H2DCFDA probes. The cells treated with IFN-γ + TNF-α showed an increase in the level of cellular ROS production which could be rescued by treatment with JAK1/2 inhibitor baricitinib (Figure 2.16 B). Even though there was a significant cellular ROS production in the cells, blocking ROS generation by ROS inhibitor N-acetyl-L-cysteine (NAC) could not rescue the cell death (Figure 2.16C).

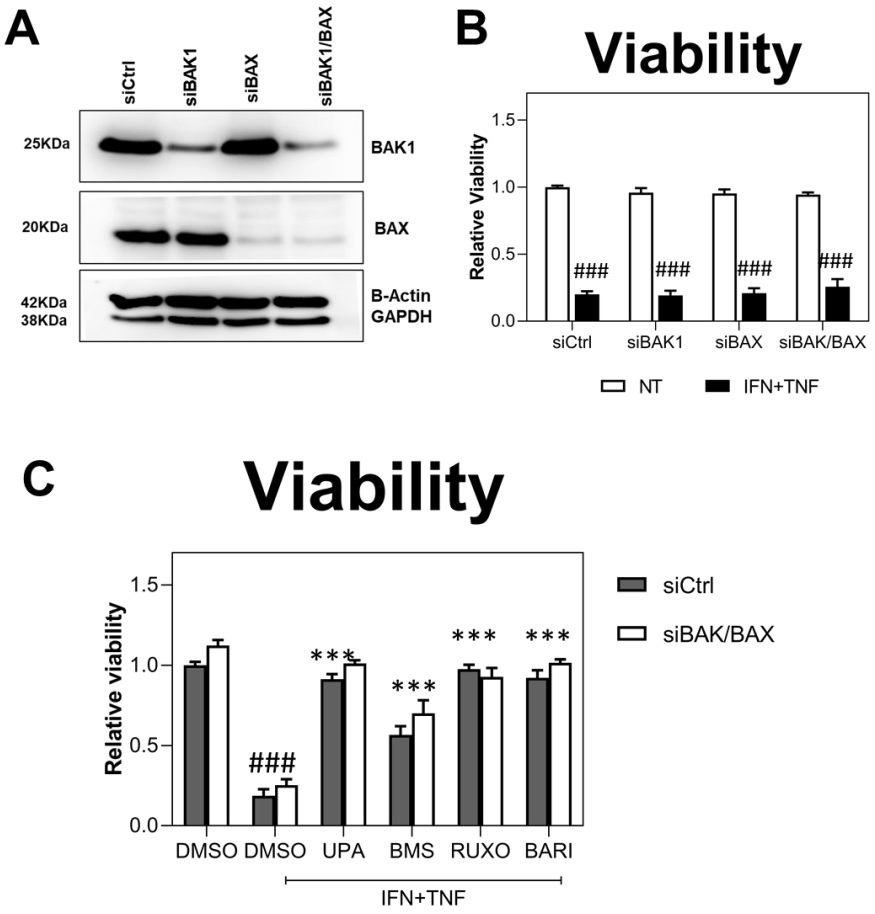


Figure 2.15 IFN-γ and TNF-α induced synergistic cell death is independent of pro-apoptotic BCL-2 family members BAX and BAK

(A-C) HT-29 cells were reverse transfected with 25nM of si*BAK* and si*BAX* siRNA smart pools as indicated for 48 hours. (A) Protein knock-down level were confirmed by western blotting. Data is representative of 2 experiments. (B) Transfected cells were treated with IFN-γ and TNF-α (10 ng/mL each) for 72 hours and measured for cell viability using cellTitr-glo (Promega) assay. Data shown are the mean ± S.E.M of n = 3 independent experiments in triplicates. (C) Transfected cells were pre-treated with JAKinibs as indicated for 1 hour and co-treated with IFNγ+ TNFα (10 ng/mL of each) for 72 hours. Cell viability was measured using cell Titre-glo (Promega) assay. Data shown are the mean ± S.E.M of n = 3 independent experiments in triplicate. ###$p < 0.001$ (two-way ANOVA followed by Tukey's multiple comparisons test vs non-cytokine treated control cells). **$p < 0.01$ and ***$p < 0.001$ (two-way ANOVA followed by Tukey's multiple comparisons test vs IFN+TNF). JAKinibs- Upadacitinib (UPA), BMS-911546 (BMS), baricitinib (BARI), Ruxolitinib (RUXO)

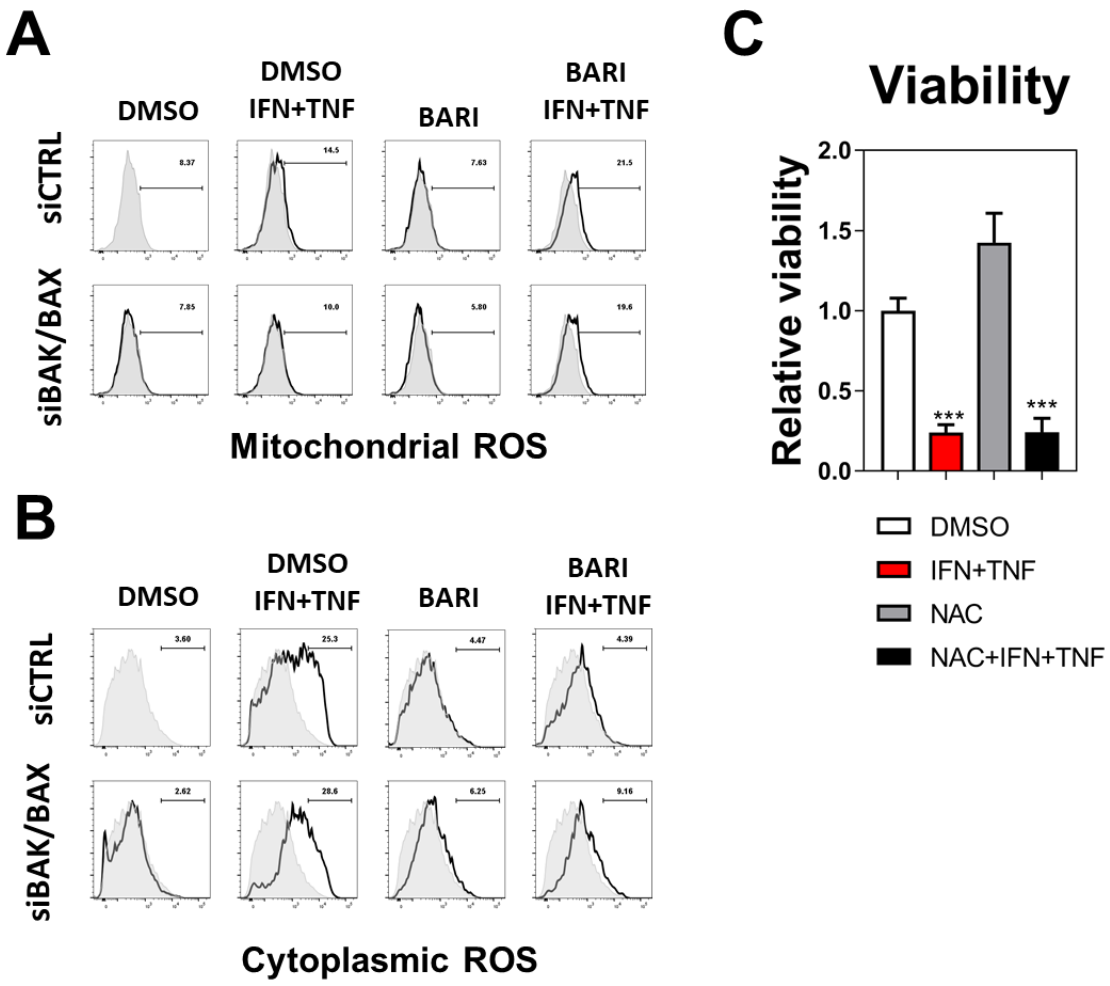


Figure 2.16 IFN-γ and TNF-α induced synergistic cell death is independent of mitochondria and cytoplasmic ROS production

(A-B) HT-29 cells were reverse transfected with 25nM of si*BAK* and si*BAX* siRNA smart pools as indicated for 48 hours and then pre-treated with DMSO or Baricitinib for 1 hour followed by co-treatment with IFNγ+TNFα (10 ng/mL of each) for 16 hours. (A) Mitochondrial ROS and cytoplasmic ROS levels were measured by flow cytometry (as indicated in methods and material section 2.3.8) Data from 1 experiment performed in duplicate (C) HT-29 cells were pre-treated with 10 mM of N-acetyl-L-cysteine (NAC) for 1 hour followed by treatment with IFN-γ + TNF-α (10ng/mL of each) for 72 hours and measured for cell viability using Cell Titre-glo (Promega). Data shown is the mean ± S.E.M of n = 3 independent experiments in triplicate. ***$p < 0.001$ (one-way ANOVA followed by Dunnett's multiple comparisons test as indicated).

2.4.6. IFN-γ/TNF-α synergize to induce cell death in human colonic organoids in a JAK1/2 dependent manner

To validate the findings from CRC cell lines further studies were performed in human primary colonic organoid lines. Colonic organoid lines were generated from colonic epithelial crypts isolated from colonic mucosal pinch biopsies obtained under informed consent from healthy individuals and patients with Crohn's disease as described in the Materials and Methods (section-2.3.9). These were treated with IFN-γ and TNF-α alone or in combination for 8 hour and 24 hour and cell viability was measured using CellTitre-Glo (Promega) assay (Figure 2.17A). Independent of disease status, both healthy and CD organoid lines showed a similar phenotype in terms of responsiveness towards IFN-γ and TNF-α (Figure 2.17A). Compared to cell lines, organoids were more sensitive towards cytokine induced killing and showed a high level of cell death within 8 hour of treatment which further increased at 24 hours. Colonic organoids did not show any sensitivity towards IFN-γ treatment alone, while moderate amount of cell death (20-30 %) could be observed in TNF-α treated organoids. Consistent with the CRC cell lines, IFN-γ and TNF-α synergised to induce cell death in colonic epithelial organoids. To test the JAK-STAT dependency of cytokine induced cell death in this system, colonic epithelial organoids obtained from patients with CD were pre-treated for 1 hour with 0.1, 1 and 10 µM concentration of JAKinibs (filgotinib, upadacitinib, baricitinib and tofacitinib) and treated with 10 ng/mL of IFN-γ + TNF-α for 2 hours to measure the STAT1 pY701 levels in the cells by HTRF assay (figure 2.17 B) and for 8 hours to estimate cell viability (Fig 2.11 D). After 2 hours of JAKinib and IFN-γ + TNF-α treatment the cells did not show any reduction in their viability (Figure 2.17 C). HTRF assay showed an increase in STAT1 pY701 levels in the cells treated with DMSO and cytokines in both IFN-γ and IFN-γ + TNF-α treatment group. The treatment with upadacitinib, tofacitinib and baricitinib reduced the STAT1 pY701 levels at 0.1

μM concentration which was further reduced to the same level as vehicle treated organoids at 1 μM and 10 μM concentration (Figure 2.17 E). Consistent with our observation in cell lines, filgotinib did not reduce STAT1 phosphorylation at lower concentrations but there was some reduction observed at 10 μM concentration. All JAKinibs except filgotinib rescued cytokine-iduced cell death at 1 and 10 μM concentration. Filgotinib alone exhibited some extent of cell death at 10 μM. The results confirmed that IFN-γ + TNF-α synergise to induce cell death in JAK1/2-STAT1 dependent manner in primary human colonic epithelial organoid lines.

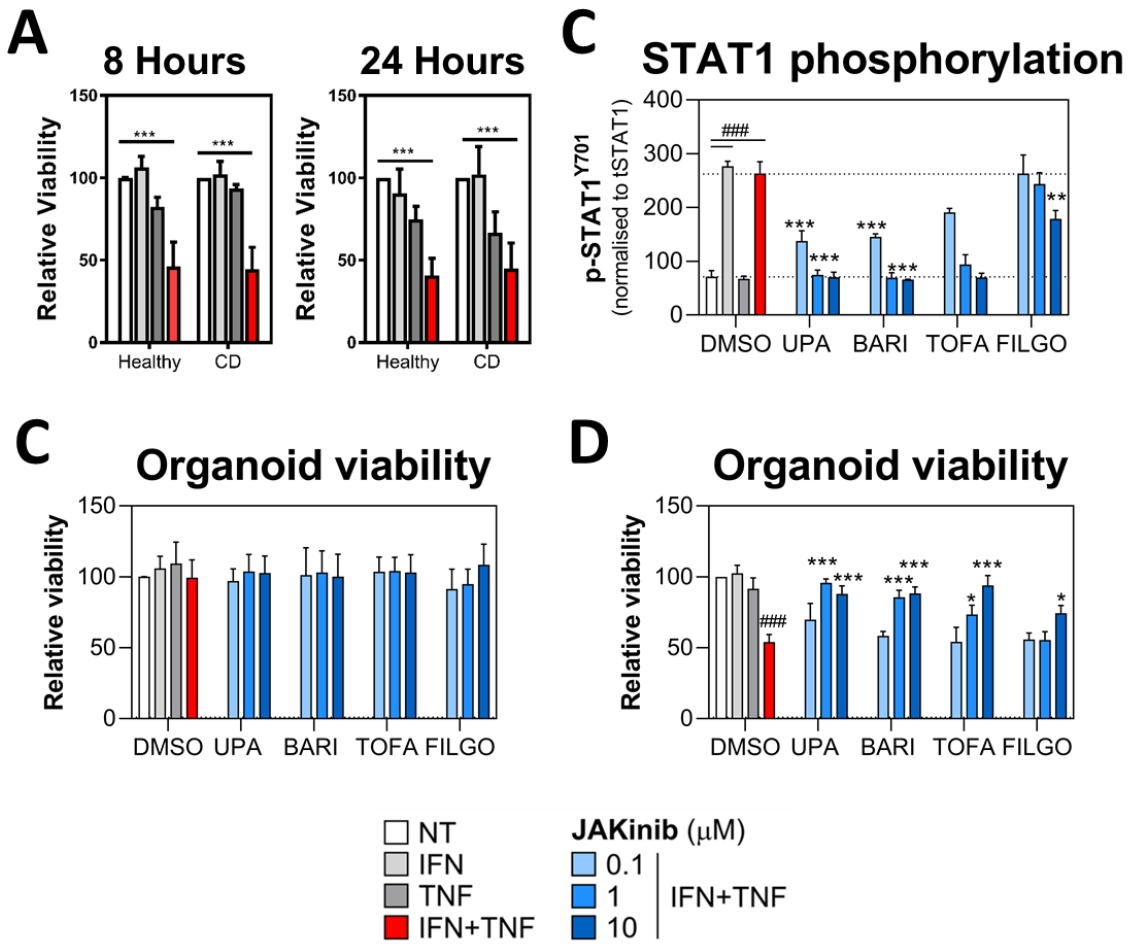


Figure 2.17 IFN-γ + TNF-α synergize to induce cell death in human colonic organoids in a JAK1/2 dependent manner

(A) Primary human colonic organoid lines (n=3) were treated with IFN-γ (10 ng/mL), TNF-α (10 ng/mL) or IFN-γ + TNF-α (10 ng/mL each) for the indicated time points. Relative organoid viability was measured at 8 hours and 24 hours in n = 3 healthy and CD organoid lines using Cell Titre-Glo (Promega) assay. (B-D) Colonic organoid lines (n=3) were pre-treated for 1 hour with specified concentration of JAKinibs and co-treated with IFN-γ (10 ng/mL) and TNF-α (10 ng/mL) for indicated duration. (B) STAT1 and STAT1 pY701 levels were measured using HTRF assay 2-hour post JAKinib and cytokine treatment across n=3 organoid lines. (C-D) Relative organoid viability measured 2 hr & 8 hr post JAKinib and cytokine treatment using Cell Titre-Glo (Promega) assay. Data shown are the mean ± S.E.M. ###$p < 0.001$ (two-way ANOVA followed by Tukey's multiple comparisons test compared with NT). **$p < 0.01$ and ***$p < 0.001$ (two-way ANOVA followed by Tukey's multiple comparisons test

compared with IFN+TNF). NT- Non-treated organoids, JAKinibs- Upadacitinib (UPA), baricitinib (BARI), tofacitinib (TOFA) & filgotinib (Filgo).

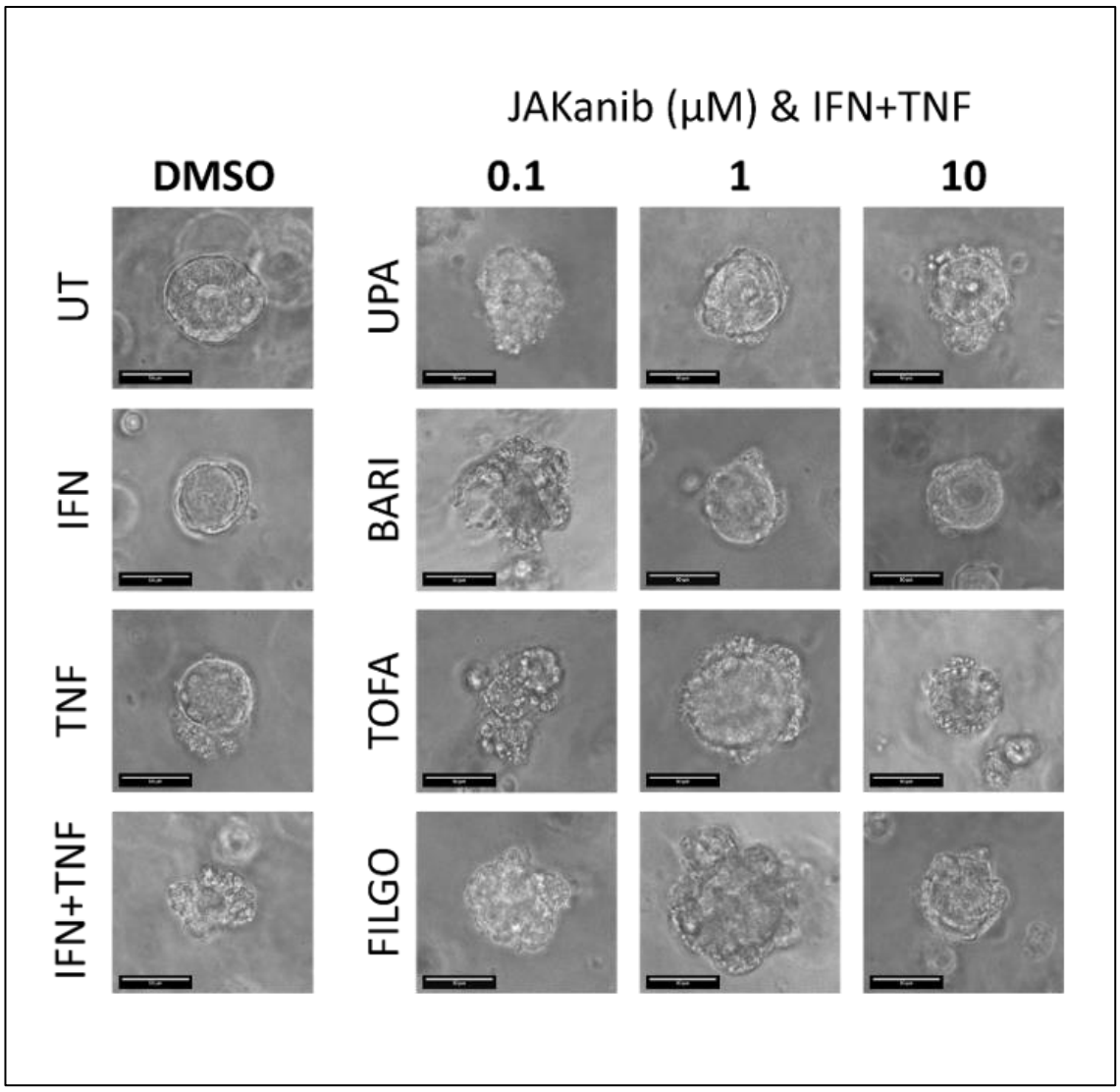


Figure 2.18 IFN-γ/TNF-α synergize to induce cell death in human colonic organoids in a JAK1/2 dependent manner

Colonic organoids were pre-treated with JAK1 inhibitor: filgotinib (Filgo), upadacitinib (UPA), JAK1/2 inhibitor: Baricitinib (BARI) and JAK1/3 inhibitor: Tofacitinib (TOFA) for 1 hour followed by co-treatment with IFN-γ (10 ng/mL) and TNF-α (10 ng/mL) for 8 hours. Cell morphology was analysed under microscope with 40X magnifying lens. Representative live images of 1 out of 3 organoid lines is used in panel. The scale represents a 50 μm length.

2.5. Discussion

IFN-γ and TNF-α are critical cytokine drivers of chronic inflammation and immunopathology in several diseases such as Type-1 diabetes, graft vs host disease, rheumatoid arthritis and Crohn's disease[87,92,93,94,95]. The success of drugs targeting TNF-α and IFN-γ signalling pathways for different diseases have confirmed the role of these cytokines in the field[96,97,98,99,100,101,102]. The phenomenon of IFN-γ and TNF-α synergism has been known for more than 30 years[103,104,105,106]. However, the effect and underlying mechanism of IFN-γ and TNF-α synergism in triggering intestinal epithelial cell death is not completely understood. In this study, we investigated the role of IFN-γ and TNF-α synergism on colonic epithelial cell death by using CRC cell lines and primary human colonic organoids as model systems.

Our results show that the combination of IFN-γ and TNF-α together induced significant killing compared to effects of treatment with individual cytokines, which is in agreement with previous studies performed in different cell lines[71,72]. This cell death has hallmarks of apoptosis (caspase activation) and necroptosis (MLKL phosphorylation)[89]. We further show that TNF-α synergizes with IFN-γ to induce cell death through the JAK1/2-STAT1 pathway in both CRC cell lines and human primary colonic organoids. However, the effect of TNF-α was independent of the TNFR1 associated canonical cell death pathways. IFN-γ + TNF-α synergistic cell death was RIPK3- and Caspase-8 -dependent but independent of their enzymatic activities. Also, IFN-γ +TNF induced synergistic cell death was independent of the BAX/BAK mitochondrial cell death pathway. We also showed that IFN-γ and TNF-α synergised to induce cell death in human primary 3D colonic organoid cultures. This IFN-γ + TNF-α induced synergistic cell death was blocked by JAK inhibitors (JAKinibs) in both cell lines and human primary 3D colonic organoid

cultures. Collectively these data provide a mechanistic basis for the therapeutic effects of both anti-TNFs and JAK inhibitors in the treatment of IBD

Identification of JAK1 and JAK2 as well as TNFR1 as the modulator of IFN-γ and TNF-α induced cell death suggested a possible crosstalk between the two signalling pathways. Several studies have previously described the interaction of components of IFN-γ signalling pathways and TNFR1 signalling pathways. There is evidence that STAT1 directly interacts with TNFR1 and TRADD[107,59,108]. IFN-γ has also been reported to sensitize different cell type for TNF-α induced DISC complex formation and apoptosis by increasing the expression of caspase 8 and Fas ligands.[62,70,109] Furthermore, there is also evidence of IFN-γ mediated necroptosis by regulation of RIPK1, RIPK3 and MLKL activity[77,110,111.].

Therefore, to understand the role of TNFR1 associated cell death complexes and to explore the involvement of IFN-γ as a sensitizer to TNF-α induced cell death, we induced cell death in HT-29 cells by treating with TNF-α and known sensitizers (BV6, cycloheximide and IKK16)[22,112] and compared it with IFN-γ + TNF-α induced cell death. Cell death induced by TNF-α and sensitizers (CHX, BV6 or IKK16) to canonical TNFR1-mediated cell death pathways could induce apoptosis, and on blocking caspase activity by pan-caspase inhibitor z-vad-fmk, the cells underwent necroptosis. This necroptosis could in turn be rescued by inhibitors of RIPK1, RIPK3 or MLKL[19,113,114]. In contrast, the synergistic cell death induced by IFN-γ and TNF-α could not be rescued by caspase inhibitors or inhibitors of necroptosis but was prevented by blocking JAK1/2 activity. These findings indicate that the role of TNFR1 in IFN-γ + TNF-α induced cell death is independent of TNFR1 associated canonical apoptotic and necroptotic complexes but is dependent on the JAK-STAT signalling pathway. It also indicates a significant degree of crosstalk between TNFR1 signalling and the JAK-STAT signalling pathway which has been reported by other groups in the past[115, 116,117,107]. In human fibroblast cells TNF-α induced cell

death and gene expression in a STAT1 dependent manner[118] TNF-α induced phosphorylation and activation of JAKs (JAK1, JAK2 and Tyk2) and STATs (STAT1, STAT3 and STAT5) downstream of TNFR1 in 3T3-L1 murine adipocytes[115]. Kishimoto et al, have reported the direct interaction of JAKs with TNFR1 and the role of SOCS1 in suppressing the TNF-α induced cell death in murine embryonic fibroblasts[119]. Thus, in line with the above studies, our results suggest a possible role of TNFR1 in activation of JAK-STAT signalling pathway directly or indirectly.

Another interesting observation in our study was the status of caspase 8 in cell death. Caspase 8 is an important signalling hub which determines the plasticity of cell death pathways and cell survival[120]. On one hand it induces apoptotic cell death downstream of death receptors; however, it also supresses necroptosis by regulating RIPK1 and MLKL[25,121–124]. Caspase 8 knockout mice die in their neonatal period due to activation of MLKL dependent necroptosis, while mice lacking both caspase 8 and MLKL are viable[125]. Another study showed that, caspase 8 mutant mice (with catalytically inactive caspase 8) lacking MLKL also died due to embryonic lethality, which demonstrates that a non-enzymatic role of caspase-8 in cell death. Consistent with these observations in mice, we report here that the role of caspase-8 protein in IFN-γ + TNF-α dependent cell death is independent of its proteolytic activity. The non-proteolytic scaffold function of caspase-8 has been described in the case of TRAIL induced activation of the NF-κB pathway. In TRAIL stimulated cells, caspase-8 either acted as a scaffold for the assembly of 'FADDosome' complex composed of caspase-8-FADD-RIPK1, leading to either NF-κB-dependent inflammation or as a protease promoting apoptosis[126]. The scaffold activity of caspase-8 may also provide a molecular explanation for the development of intestinal inflammation and immunodeficient disorders in patients with defective caspase-8[127,128].Even though IFN-γ +TNF-α induced cell death was dependent on the scaffold activity of caspase-8, there was no role of caspase-10 in the process. A further decrease in the viability was observed

in *CASP10*$^{-/-}$ cell lines, possibly due to the competitive behaviour of caspase 10 for its homologue caspase-8[129]. HT-29 *RIPK1*$^{-/-}$ cell lines were sensitive to TNF-α induced cell death which further increased with the co-treatment with IFN-γ. Intriguingly, the cell lines lacking RIPK3 protein could also partially rescue IFN-γ + TNF-α induced cell death while blocking kinase activity of RIPK3 did not rescue the cells, showing a possible role of RIPK3 in cell death independent of its kinase activity. A study from Moriwaki et al has suggested the role of RIPK3-Caspase 8 complex in activation of interleukin -1β (IL-1β) processing in bone marrow–derived dendritic cells (BMDCs)[130]. The study showed in BMDCs with mutant RIPK3 (RIPK3-K51A - which lacks catalytic activity), upon lipopolysaccharide (LPS) stimulation there was increased activation of caspase-8 to increase IL-1β secretion[130].

All the knockout cell lines in our study were rescued by JAKinib treatment, confirming the dependency of IFN-γ + TNF-α induced cell death on JAK1/2-STAT1 signalling pathway. Altogether, the non-enzymatic activity of caspase-8 and RIPK3 were required for the JAK-STAT dependent cell death in CRC cells. Our results suggest the formation of a novel signalling complex upon IFN-γ + TNF-α stimulation, consisting of scaffold activity of caspase-8/RIPK3 to boost JAK-STAT signalling pathway for the induction of cell death. Further immunoprecipitation studies are required for the confirmation and identification of components of this novel cell death complex.

We also investigated the role of the intrinsic apoptotic pathway and BCL-2 family members in IFN-γ + TNF-α induced cell death. Even though we observed activation of caspase-9 in IFN-γ and TNF-α treated cells blocking caspase-9 activity did not show any rescue in cell death. Depletion of either BAK or BAX individually or together did not show any rescue of cell death. Also, there was not any significant increase in the mitochondrial ROS level in the cells treated with IFN-γ and TNF-α, independent of BAK/BAX status. We also observed a significant increase

in the cellular ROS production in the cells treated with IFN-γ and TNF-α[104]. The ROS build-up could be blocked by baricitinib treatment confirming that this was a consequence of the JAK-STAT pathway. However, blocking the ROS built-up by N-acetyl-l-cysteine (NAC) did not block the cell death.

Collectively, our data reveals a novel signalling pathway and mechanism underpinning IFN-γ and TNF-α induced cell death in CRC cells. We show that IFN-γ + TNF-α induced cell death is JAK1/2-STAT1 dependent and is independent of TNFR1 associated canonical cell death complexes. Our study also suggests a role for caspase-8 and RIPK3 as a scaffold molecule serving as the base for activation of cell death through JAK1/2-STAT1 signalling.

2.6. References

1. Understanding and Preventing the Global Increase of Inflammatory Bowel Disease. (2017).
2. Ananthakrishnan, A. N. et al. Environmental triggers in IBD: a review of progress and evidence. Nat. Rev. Gastroenterol. Hepatol. 15, 39–49 (2018).
3. Plichta, D. R., Graham, D. B., Subramanian, S. & Xavier, R. J. Therapeutic Opportunities in Inflammatory Bowel Disease: Mechanistic Dissection of Host-Microbiome Relationships. Cell 178, 1041–1056 (2019).
4. Uhlig, H. H. & Muise, A. M. Clinical Genomics in Inflammatory Bowel Disease. Trends in Genetics 33, (2017).
5. Shivashankar, R. & Lewis, J. D. The Role of Diet in Inflammatory Bowel Disease. Curr. Gastroenterol. Rep. 19, 22 (2017).
6. Friedrich, M., Pohin, M. & Powrie, F. Review Cytokine Networks in the Pathophysiology of Inflammatory Bowel Disease. (2019).
7. Neurath, M. F. Cytokines in inflammatory bowel disease. Nat. Rev. Immunol. 14, 329–342 (2014).
8. Koch, S. & Nusrat, A. The Life and Death of Epithelia During Inflammation: Lessons Learned from the Gut. Annu. Rev. Pathol. Mech. Dis. 7, 35–60 (2012).
9. Vitale, S. et al. Cytokine production profile in intestinal mucosa of paediatric inflammatory bowel disease. (2017).
10. Neurath, M. F. Targeting immune cell circuits and trafficking in inflammatory bowel disease. Nature Immunology (2019).
11. Vitale, S. et al. Cytokine production profile in intestinal mucosa of paediatric

inflammatory bowel disease. (2017).

12. Bruewer, M. et al. Proinflammatory cytokines disrupt epithelial barrier function by apoptosis-independent mechanisms. J. Immunol. 171, 6164–72 (2003).

13. Brenner, D., Blaser, H. & Mak, T. W. Regulation of tumour necrosis factor signalling: live or let die. Nat. Rev. Immunol. 15, 362–374 (2015).

14. Samuel O. Adegbola 1,2, *, ID , Kapil Sahnan 1,2 ID , Janindra Warusavitarne 1,2, Ailsa Hart 1, 2 & and Philip Tozer 1, 2. Anti-TNF Therapy in Crohn's Disease.

15. Neurath, M. F. New targets for mucosal healing and therapy in inflammatory bowel diseases. Mucosal Immunol. 7, 6–19 (2014).

16. Ting, A. T. & Bertrand, M. J. M. More to Life than NF-κB in TNFR1 Signaling. Trends Immunol. 37, 535–545 (2016).

17. Kalliolias, G. D. & Ivashkiv, L. B. TNF biology, pathogenic mechanisms and emerging therapeutic strategies. Nat. Rev. Rheumatol. 12, 49–62 (2016).

18. Micheau, O. & Tschopp, J. Induction of TNF receptor I-mediated apoptosis via two sequential signaling complexes. Cell 114, 181–90 (2003).

19. De Almagro, M. C. et al. Coordinated ubiquitination and phosphorylation of RIP1 regulates necroptotic cell death. Cell Death Differ. 24, 26–37 (2017).

20. Pajak, B., Gajkowska, B. & Orzechowski, A. Cycloheximide-mediated sensitization to TNF-alpha-induced apoptosis in human colorectal cancer cell line COLO 205; role of FLIP and metabolic inhibitors. J. Physiol. Pharmacol. 56 Suppl 3, 101–18 (2005).

21. Totzke, J. et al. Takinib, a Selective TAK1 Inhibitor, Broadens the Therapeutic Efficacy of TNF-α Inhibition for Cancer and Autoimmune Disease. Cell Chem. Biol. 24, 1029–1039 (2017).

22. Pasparakis, M. & Vandenabeele, P. Necroptosis and its role in inflammation. Nature

517, 311–320 (2015).

23. Fritsch, M. et al. Caspase-8 is the molecular switch for apoptosis, necroptosis and pyroptosis. Nature (2019).

24. Tummers, B. & Green, D. R. Caspase-8; regulating life and death. Immunol. Rev. 277, 76–89 (2017).

25. Newton, K. et al. Cleavage of RIPK1 by caspase-8 is crucial for limiting apoptosis and necroptosis. Nature 574, 428–431 (2019).

26. Lalaoui, N. et al. Mutations that prevent caspase cleavage of RIPK1 cause autoinflammatory disease. Nature 577, 103–108 (2020).

27. Garcia-Carbonell, R., Yao, S.-J., Das, S. & Guma, M. Dysregulation of Intestinal Epithelial Cell RIPK Pathways Promotes Chronic Inflammation in the IBD Gut. Front. Immunol. 10, (2019).

28. Feltham, R., Vince, J. E. & Lawlor, K. E. Caspase-8: Not so silently deadly. Clinical and Translational Immunology 6, e124 (2017).

29. Feng, S. et al. Cleavage of RIP3 inactivates its caspase-independent apoptosis pathway by removal of kinase domain. Cell. Signal. 19, 2056–67 (2007).

30. O'Donnell, M. A. et al. Caspase 8 inhibits programmed necrosis by processing CYLD. Nat. Cell Biol. (2011).

31. Legarda, D. et al. CYLD Proteolysis Protects Macrophages from TNF-Mediated Auto-necroptosis Induced by LPS and Licensed by Type I IFN. Cell Rep. (2016). doi:10.1016/j.celrep.2016.05.032

32. Dickens, L. S., Powley, I. R., Hughes, M. A. & MacFarlane, M. The 'complexities' of life and death: Death receptor signalling platforms. Exp. Cell Res. 318, 1269–1277 (2012).

33. Filliol, A. et al. RIPK1 protects hepatocytes from death in Fas-induced hepatitis. Sci. Rep.

7, (2017).

34. Chan, F. K. A guardian angel of cell integrity. 1–3 (2014).

35. Dannappel, M. et al. RIPK1 maintains epithelial homeostasis by inhibiting apoptosis and necroptosis. Nature 513, 90–94 (2014).

36. Kondylis, V., Kumari, S., Vlantis, K. & Pasparakis, M. The interplay of IKK, NF-κB and RIPK1 signaling in the regulation of cell death, tissue homeostasis and inflammation. Immunological Reviews 277, 113–127 (2017).

37. Ofengeim, D. & Yuan, J. Regulation of RIP1 kinase signalling at the crossroads of inflammation and cell death. Nature Reviews Molecular Cell Biology (2013).

38. Festjens, N., Vanden Berghe, T., Cornelis, S. & Vandenabeele, P. RIP1, a kinase on the crossroads of a cell's decision to live or die. Cell Death and Differentiation (2007).

39. Takahashi, N. et al. RIPK1 ensures intestinal homeostasis by protecting the epithelium against apoptosis. Nature 513, 95–99 (2014).

40. Ang, R. L., Chan, M. & Ting, A. T. Ripoptocide – A Spark for Inflammation. Frontiers in Cell and Developmental Biology 7, (2019).

41. Majoros, A. et al. Canonical and Non-Canonical Aspects of JAK–STAT Signaling: Lessons from Interferons for Cytokine Responses. Front. Immunol. 8, 29 (2017).

42. Schroder, K., Hertzog, P. J., Ravasi, T. & Hume, D. A. Interferon gamma orchestrates : an overview of signals , mechanisms and functions. J. Leukoc. Biol. 75, 163–189 (2004).

43. Bach, E. A., Aguet, M. & Schreiber, R. D. THE IFNγ RECEPTOR:A Paradigm for Cytokine Receptor Signaling. Annu. Rev. Immunol. 15, 563–591 (1997).

44. Chiba, H., Kojima, T., Osanai, M. & Sawada, N. The significance of interferon-gamma-triggered internalization of tight-junction proteins in inflammatory bowel disease. Sci. STKE 2006, pe1 (2006).

45. Ferrier, L. et al. Stress-induced disruption of colonic epithelial barrier: role of interferon-γ and myosin light chain kinase in mice. Gastroenterology 125, 795–804 (2003).

46. Lechuga, S. & Ivanov, A. I. Disruption of the epithelial barrier during intestinal inflammation: Quest for new molecules and mechanisms. Biochim. Biophys. Acta - Mol. Cell Res. 1864, 1183–1194 (2017).

47. Takashima, S. et al. T cell-derived interferon-γ programs stem cell death in immune-mediated intestinal damage. Sci. Immunol. (2019). doi:10.1126/sciimmunol.aay8556

48. Eriguchi, Y. et al. Essential role of IFN-γ in T cell-associated intestinal inflammation. JCI insight (2018).

49. Farin, H. F. et al. Paneth cell extrusion and release of antimicrobial products is directly controlled by immune cell-derived IFN-γ. J. Exp. Med. (2014). doi:10.1084/jem.20130753

50. Bruewer, M. et al. Interferon-γ induces internalization of epithelial tight junction proteins via a macropinocytosis-like process. FASEB J. 19, 923–933 (2005).

51. Ivanov, A. I., Parkos, C. A. & Nusrat, A. Cytoskeletal regulation of epithelial barrier function during inflammation. American Journal of Pathology 177, 512–524 (2010).

52. Nava, P. et al. Desmoglein-2: a novel regulator of apoptosis in the intestinal epithelium. Mol. Biol. Cell 18, 4565–78 (2007).

53. Yulis, M., Quiros, M., Hilgarth, R., Parkos, C. A. & Nusrat, A. Intracellular Desmoglein-2 cleavage sensitizes epithelial cells to apoptosis in response to pro-inflammatory cytokines. Cell Death Dis. 9, 389 (2018).

54. Nava, P. et al. IFN gamma regulates intestinal epithelial homeostasis through converging Beta-catenin signaling pathways. Immunity 32, 392–402 (2010).

55. Raetz, M. et al. Parasite-induced T H 1 cells and intestinal dysbiosis cooperate in IFN-γ-

dependent elimination of Paneth cells. Nat. Immunol. (2013).

56. López-Yglesias, A. H., Burger, E., Araujo, A., Martin, A. T. & Yarovinsky, F. T-bet-independent Th1 response induces intestinal immunopathology during Toxoplasma gondii infection. Mucosal Immunol. (2018).

57. Ingram, J. P. et al. A Nonpyroptotic IFN-γ–Triggered Cell Death Mechanism in Nonphagocytic Cells Promotes Salmonella Clearance In Vivo . J. Immunol. 200, 3626–3634 (2018).

58. Capaldo, C. T. et al. IFN-γ and TNF-α-induced GBP-1 inhibits epithelial cell proliferation through suppression of β-catenin/TCF signaling. Mucosal Immunol. 5, 681–690 (2012).

59. Wesemann, D. R., Qin, H., Kokorina, N. & Benveniste, E. N. TRADD interacts with STAT1-α and influences interferon-γ signaling. Nat. Immunol. 5, 199–207 (2004).

60. Chang, Y.-H., Chao, Y., Hsieh, S.-L. & Lin, W.-W. Mechanism of LIGHT/interferon-?-induced cell death in HT-29 cells. J. Cell. Biochem. 93, 1188–1202 (2004).

61. Xu, X., Fu, X. Y., Plate, J. & Chong, A. S. FN-gamma induces cell growth inhibition by Fas-mediated apoptosis: requirement of STAT1 protein for up-regulation of Fas and FasL expressioIn. Cancer Res. 58, 2832–7 (1998).

62. Inaba, H., Glibetic, M., Buck, S., Ravindranath, Y. & Kaplan, J. Interferon-? sensitizes osteosarcoma cells to fas-induced apoptosis by up-regulating fas receptors and caspase-8. Pediatr. Blood Cancer 43, 729–736 (2004).

63. Kim, K.-B. et al. Potentiation of Fas- and TRAIL-mediated apoptosis by IFN-gamma in A549 lung epithelial cells: enhancement of caspase-8 expression through IFN-response element. Cytokine 20, 283–8 (2002).

64. Kulkarni, K., Selesniemi, K. & Brown, T. L. Interferon-gamma sensitizes the human salivary gland cell line, HSG, to tumor necrosis factor-alpha induced activation of dual

apoptotic pathways. Apoptosis 11, 2205–15 (2006).

65. Kimura, M. et al. TNF combined with IFN-α accelerates NF-κB-mediated apoptosis through enhancement of Fas expression in colon cancer cells. Cell Death Differ. 10, 718–728 (2003).

66. Fengjun Wang1,2,§, Brad T. Schwarz2,§, W. Vallen Graham2, Yingmin Wang2, L. S. IFN-γ-induced TNFR2 Upregulation is Required for TNFdependent Intestinal Epithelial Barrier Dysfunction.pdf.

67. Sato, T. et al. Long-term expansion of epithelial organoids from human colon, adenoma, adenocarcinoma, and Barrett's epithelium. Gastroenterology 141, 1762–1772 (2011).

68. VanDussen, K. L. et al. Development of an enhanced human gastrointestinal epithelial culture system to facilitate patient-based assays. Gut 64, 911–920 (2015).

69. Miyoshi, H. & Stappenbeck, T. S. In vitro expansion and genetic modification of gastrointestinal stem cells in spheroid culture. Nat. Protoc. 8, 2471–2482 (2013).

70. Kim, H. S., Kim, S. & Lee, M.-S. IFN-gamma sensitizes MIN6N8 insulinoma cells to TNF-alpha-induced apoptosis by inhibiting NF-kappaB-mediated XIAP upregulation. Biochem. Biophys. Res. Commun. 336, 847–53 (2005).

71. Cao, Z. et al. Caspase-3 is Involved in IFN-γ- and TNF-α-Mediated MIN6 Cells Apoptosis via NF-κB/Bcl-2 Pathway. Cell Biochem. Biophys. 67, 1239–1248 (2013).

72. Li, N. et al. Cross-talk between TNF-α and IFN-γ signaling in induction of B7-H1 expression in hepatocellular carcinoma cells. Cancer Immunol. Immunother. 67, 271–283 (2018).

73. Cao, Z. et al. STAT1-Mediated Down-Regulation of Bcl-2 Expression Is Involved in IFN-γ/TNF-α–Induced Apoptosis in NIT-1 Cells. PLoS One 10, e0120921 (2015).

74. Ballegeer, M. et al. Glucocorticoid receptor dimers control intestinal STAT1 and TNF-induced inflammation in mice. J. Clin. Invest. 128, 3265–3279 (2018).

75. Thapa, R. J., Nogusa, S. & Balachandran, S. Analysis of Cytokine- and Influenza A Virus-Driven RIPK3 Necrosome Formation. in Methods in molecular biology (Clifton, N.J.) 1857, 93–99 (2018).

76. Cekay, M. J. et al. Smac mimetics and type II interferon synergistically induce necroptosis in various cancer cell lines. Cancer Lett. 410, 228–237 (2017).

77. Jiancheng Chen ‡ §, Shunsuke Kuroki ‡ ¶, M. S. ‡ § & and Shin Yonehara ‡ § *. Interferon-g induces the cell surface exposure of phosphatidylserine by activating MLKL in the absence of caspase-8 activity.

78. Zelová, H. & Hošek, J. TNF-α signalling and inflammation: Interactions between old acquaintances. Inflamm. Res. 62, 641–651 (2013).

79. Croft, M., Benedict, C. A. & Ware, C. F. Clinical targeting of the TNF and TNFR superfamilies. Nat. Rev. Drug Discov. 12, 147–168 (2013).

80. Riccioli, A. et al. TNF-α and IFN-γ Regulate Expression and Function of the Fas System in the Seminiferous Epithelium. J. Immunol. 165, 743–749 (2000).

81. Li, J. H. et al. Interferon-γ augments CD95(APO-1/Fas) and pro-caspase-8 expression and sensitizes human vascular endothelial cells to CD95-mediated apoptosis. Am. J. Pathol. 161, 1485–1495 (2002).

82. Orvedahl, A. et al. Autophagy genes in myeloid cells counteract IFNγ-induced TNF-mediated cell death and fatal TNF-induced shock. Proc. Natl. Acad. Sci. U. S. A. 116, 16497–16506 (2019).

83. Pasparakis, M. Role of NF-κB in epithelial biology. Immunol. Rev. 246, 346–358 (2012).

84. De Almagro, M. C., Goncharov, T., Newton, K. & Vucic, D. Cellular IAP proteins and

LUBAC differentially regulate necrosome-associated RIP1 ubiquitination. Cell Death Dis. 6, (2015).

85. Woznicki, J. A. et al. Human BCL-G regulates secretion of inflammatory chemokines but is dispensable for induction of apoptosis by IFN-γ and TNF-α in intestinal epithelial cells.

86. Mukherjee, S. & Biswas, T. Activation of TOLLIP by porin prevents TLR2-associated IFN-γ and TNF-α-induced apoptosis of intestinal epithelial cells. Cell. Signal. 26, 2674–2682 (2014).

87. Barthson, J. et al. Cytokines tumor necrosis factor-α and interferon-γ induce pancreatic β-cell apoptosis through STAT1-mediated Bim protein activation. J. Biol. Chem. 286, 39632–43 (2011).

88. Cosentino, K. & García-Sáez, A. J. Bax and Bak Pores: Are We Closing the Circle? Trends in Cell Biology 27, 266–275 (2017).

89. Galluzzi, L. et al. Molecular mechanisms of cell death: Recommendations of the Nomenclature Committee on Cell Death 2018. Cell Death and Differentiation 25, 486–541 (2018).

90. Ho, S. et al. The role of Bcl-2 expression in EGF inhibition of TNF-α/IFN-γ-induced villous trophoblast apoptosis. Placenta 20, 423–430 (1999).

91. Kim, W. H., Lee, J. W., Gao, B. & Jung, M. H. Synergistic activation of JNK/SAPK induced by TNF-α and IFN-γ: Apoptosis of pancreatic β-cells via the p53 and ROS pathway. Cell. Signal. 17, 1516–1532 (2005).

92. Chang, I. et al. - Role of Calcium in Pancreatic Islet Cell Death by IFN- /TNF. J. Immunol. 172, 7008–7014 (2014).

93. Nalle, S. C. & Turner, J. R. Intestinal barrier loss as a critical pathogenic link between inflammatory bowel disease and graft-versus-host disease. Mucosal Immunology 8,

(2015).

94. Kim, E. Y. & Moudgil, K. D. Immunomodulation of autoimmune arthritis by pro-inflammatory cytokines. Cytokine 98, 87–96 (2017).

95. Koch, S. & Nusrat, A. The Life and Death of Epithelia During Inflammation: Lessons Learned from the Gut. Annu. Rev. Pathol. Mech. Dis. 7, 35–60 (2012).

96. Harrison, C. & Vannucchi, A. M. Ruxolitinib: a potent and selective Janus kinase 1 and 2 inhibitor in patients with myelofibrosis. An update for clinicians. Ther. Adv. Hematol. 3, 341–54 (2012).

97. T. Virtanen, A., Haikarainen, T., Raivola, J. & Silvennoinen, O. Selective JAKinibs: Prospects in Inflammatory and Autoimmune Diseases. BioDrugs 33, 15–32 (2019).

98. Panés, J. et al. Tofacitinib for induction and maintenance therapy of Crohn's disease: Results of two phase IIb randomised placebo-controlled trials. Gut 66, 1049–1059 (2017).

99. D.M., S., M., B., M., G. & J.J., O. Type I/II cytokines, JAKs, and new strategies for treating autoimmune diseases. Nature Reviews Rheumatology 12, 25–36 (2016).

100. Sun, X.-L. et al. Optimized timing of using infliximab in perianal fistulizing Crohn's disease. World J. Gastroenterol. 26, 1554–1563 (2020).

101. Adegbola, S. O., Sahnan, K., Warusavitarne, J., Hart, A. & Tozer, P. Molecular Sciences Anti-TNF Therapy in Crohn's Disease. Int. J. Mol. Sci. 19, 1–21 (2018).

102. Rogler, G., Herfarth, H., Hibi, T. & Nielsen, O. H. Anti-tumor necrosis factor therapy in inflammatory bowel disease. Anti-Tumor Necrosis Factor Therapy in Inflammatory Bowel Disease (2015).

103. Schiller, J. H., Bittner, G., Storer, B. & Willson, J. K. V. Synergistic Antitumor Effects of Tumor Necrosis Factor and γ-Interferon on Human Colon Carcinoma Cell Lines. Cancer

Res. 47, 2809–2813 (1987).

104. Campbell, I. L., Iscaro, A. & Harrison, L. C. IFN-gamma and tumor necrosis factor-alpha. Cytotoxicity to murine islets of Langerhans. J. Immunol. 141, 2325–9 (1988).

105. Macdonald, T. T., Hutchings, P., Choy, M.-Y., Murch, S. & Cooke, A. Tumour necrosis factor-alpha and interferon-gamma production measured at the single cell level in normal and inflamed human intestine. Clin. exp. Immunol 81, (1990).

106. Ruggiero, V., Tavernier, J., Fiers, W. & Baglioni, C. Induction of the synthesis of tumor necrosis factor receptors by interferon-gamma. J. Immunol. 136, 2445–2450 (1986).

107. Wesemann, D. R. & Benveniste, E. N. STAT-1 and IFN- as Modulators of TNF- Signaling in Macrophages: Regulation and Functional Implications of the TNF Receptor 1:STAT-1 Complex. The Journal of Immunology 171, 5313–5319 (2014).

108. Jiang, Y. et al. STAT1 mediates transmembrane TNF-alpha-induced formation of death-inducing signaling complex and apoptotic signaling via TNFR1. Cell Death Differ. 24, 660–671 (2017).

109. Fulda, S. & Debatin, K. M. IFNγ sensitizes for apoptosis by upregulating caspase-8 expression through the Stat1 pathway. Oncogene 21, 2295–2308 (2002).

110. Hitomi, J. et al. Identification of a molecular signaling network that regulates a cellular necrotic cell death pathway by a genome wide siRNA screen.

111. Chen, J., Kuroki, S., Someda, M. & Yonehara, S. Interferon-g induces the cell surface exposure of phosphatidylserine by activating MLKL in the absence of caspase-8 activity. J. Biol. Chem. jbc.RA118.007161 (2019).

112. Tanzer, M. C. et al. Combination of IAP antagonist and IFN γ activates novel caspase-10- and RIPK1-dependent cell death pathways. 24, 481–491 (2017).

113. Mandal, P. et al. RIP3 induces apoptosis independent of pro-necrotic kinase activity

HHS Public Access. Mol Cell 56, 481–495 (2014).

114. Wang, H. et al. Mixed Lineage Kinase Domain-like Protein MLKL Causes Necrotic Membrane Disruption upon Phosphorylation by RIP3. Mol. Cell 54, 133–146 (2014).

115. Guo, D., Dunbar, J. D., Yang, C. H., Pfeffer, L. M. & Donner, D. B. Induction of Jak/STAT signaling by activation of the type 1 TNF receptor. J. Immunol. 160, 2742–2750 (1998).

116. Wang, Y., Wu, T. R., Cai, S., Welte, T. & Chin, Y. E. Stat1 as a Component of Tumor Necrosis Factor Alpha Receptor 1-TRADD Signaling Complex To Inhibit NF-kappa B Activation. Mol. Cell. Biol. 20, 4505–4512 (2002).

117. Tumor Necrosis Factor □ (TNF-□) Activates Jak1□Stat3-Stat5B Signaling through TNFR-1 in Human B Cells1.pdf.

118. Kumar, A., Commane, M., Flickinger, T. W., Horvath, C. M. & Stark, G. R. Defective TNF-α-induced apoptosis in STAT1-null cells due to low constitutive levels of caspases. Science 278, 1630–1632 (1997).

119. Kimura, A., Naka, T., Nagata, S., Kawase, I. & Kishimoto, T. SOCS-1 suppresses TNF-α-induced apoptosis through the regulation of Jak activation. Int. Immunol. 16, 991–999 (2004).

120. Newton, K. et al. Activity of caspase-8 determines plasticity between cell death pathways. Nature (2019).

121. Mandal, R., Barrón, J. C., Kostova, I., Becker, S. & Strebhardt, K. Caspase-8: The double-edged sword. Biochimica et Biophysica Acta - Reviews on Cancer 1873, (2020).

122. Pop, C., Hakem, R., Salvesen, G. S. & Green, D. R. Catalytic of caspase-8-FLIPL complex inhibits RIPK3-dependent necrosis. Nature 471, 363–367 (2011).

123. Kaiser, W. J. et al. RIP3 mediates the embryonic lethality of caspase-8-deficient mice. Nature 471, 368–72 (2011).

124. Alvarez-Diaz, S. et al. The Pseudokinase MLKL and the Kinase RIPK3 Have Distinct Roles in Autoimmune Disease Caused by Loss of Death-Receptor-Induced Apoptosis. Immunity 45, 513–526 (2016).

125. Alvarez-Diaz, S. et al. The Pseudokinase MLKL and the Kinase RIPK3 Have Distinct Roles in Autoimmune Disease Caused by Loss of Death-Receptor-Induced Apoptosis.

126. Henry, C. M. & Martin, S. J. Caspase-8 Acts in a Non-enzymatic Role as a Scaffold for Assembly of a Pro-inflammatory "FADDosome" Complex upon TRAIL Stimulation. Mol. Cell 65, 715-729.e5 (2017).

127. Chun, H. J. et al. Pleiotropic defects in lymphocyte activation caused by caspase-8 mutations lead to human immunodeficiency. 419, 395–399 (2002).

128. Lehle, A. S. et al. Intestinal Inflammation and Dysregulated Immunity in Patients With Inherited Caspase-8 Deficiency. Gastroenterology 156, 275–278 (2019).

129. Horn, S. et al. Caspase-10 Negatively Regulates Caspase-8-Mediated Cell Death, Switching the Response to CD95L in Favor of NF-κB Activation and Cell Survival. Cell Rep. 19, 785–797 (2017).

130. Moriwaki, K., Bertin, J., Gough, P. J. & Chan, F. K.-M. A RIPK3–Caspase 8 Complex Mediates Atypical Pro–IL-1β Processing. J. Immunol. 194, 1938–1944 (2015).

3. Chapter 3: Identification of the Mechanisms Underpinning Concentration Dependent Effects of IFN-γ and TNF-α on Epithelial Cell Death Decisions

3.1. Abstract

IFN-γ and TNF-α are pro-inflammatory cytokines, which are essential for protection of the host against viral and bacterial infections. They are also involved in a variety of biological activities including immunomodulation, cancer surveillance, regulation of epithelial barriers, inflammation, and cell death. The cellular responses initiated by the interaction of IFN-γ and TNF-α with their cell surface receptors results in different phenotypic outcomes depending on the tissue and cellular context. We hypothesised that the phenotypic effect of IFN-γ and TNF-α signalling on intestinal epithelial cells (IECs) is dependent on both the magnitude and duration of activation of the JAK1/2-STAT1 pathway. Here we show that IFN-γ and TNF-α synergised to induce cell death in IECs in a dose-dependent manner that required a minimum threshold concentration of both cytokines for induction of cell death. Western blotting and HTRF (Homogeneous Time Resolved Fluorescence) assays confirmed that, a low concentration of both cytokines led to a transient activation of the JAK1/2-STAT1 pathway while a higher concentration led to sustained activation of the pathway. Consistent with sustained activation of the JAK1/2-STAT1 pathway and its association with cell death, inhibition of JAK1/2 activity by JAKinibs for up to 10 hours post-cytokine treatment blocked cytokine-induced cell death of IECs. RNA-Sequencing (RNA-Seq) based gene expression analysis performed on IECs treated with different concentrations of IFN-γ and TNF-α for different durations of time identified genes expressed at later time points which may be involved in activation of multiple cell death pathways. Gene ontology and pathway enrichment analysis of these unique genes showed enrichment for multiple canonical cell death pathways

along with other cellular processes including cellular metabolism, mitochondrial function, and spliceosome complex. This study provides evidence that the JAK1/2-STAT1 pathway converts the relative concentration of cytokines - stimulus strength - into different signal durations giving a so-called dose-to-duration effect in terms of STAT1 activation. Our findings suggest that the duration of STAT1 activity acts as a cell death decision switch in intestinal epithelial cells.

3.2. Introduction

In order to induce cellular responses, extracellular signalling molecules such as secreted and cell surface ligands, interact with cell surface receptors, initiate downstream signalling pathways and activate specific target transcription factors to initiate selective changes in gene expression. The effects of receptor-mediated signalling pathways on the transcriptome, proteome and cellular phenotypes are highly dependent on tissue and cellular contexts[1]. A prototypical example occurs in the case of the pro-inflammatory cytokine Interleukin-6 (IL-6) and anti-inflammatory Interleukin-10 (IL-10) signalling pathways[2,3,4], whereby these two different cytokines signal through the same transcription factor signal transducer and activator of transcription 3 (STAT3) resulting in different cellular responses[5,6,7]. By taking a computational approach, Braun et al. showed that IL-6 and IL-10 signalling lead to different durations of STAT3 activation which results into different outcomes[8]. Similarly, tumour suppressor protein p53 shows different responses towards DNA damage caused by either gamma radiation or ultraviolet (UV) radiation. Where DNA damage from gamma radiations activates pulses of p53 activation results into cell cycle arrest, while in case of exposure to UV radiation, there is a sustained wave of p53 activation which increases with dose of UV radiation and leads to apoptosis[1,9,10].

Relative concentrations of extracellular ligands, receptors, intracellular signalling molecules and the duration of signal activation play an important role in regulation of the signalling outcomes[1]. Behar et al. has described the effect of stimulus concentration and duration of signalling on cellular outcomes in yeast[11]. In the yeast *Saccharomyces cerevisiae,* the concentration of mating pheromones determines whether the cells will undergo vegetative

growth (low pheromone), chemotropic growth (medium pheromone), or mating (high pheromone). Yeast pheromone signalling involves G-protein couple receptor mediated activation of mitogen-activated protein kinases (MAPK) signalling where concentration of pheromone in the environment is translated into the duration of active MAPK pathway resulting in specific outcomes. This modulation of signal concentration in the duration of the active signal has been termed as "dose-to-duration" encoding of signal[11].

IFN-γ and TNF-α are pro-inflammatory cytokines and are associated with wide range of biological activities[12,13]. But depending on the context, they have been shown to mediate several opposing and paradoxical responses. For instance, both IFN-γ and TNF-α are well known to orchestrate anti-tumour immune responses against cancer[14,15]. However, mounting evidence suggest that IFN-γ and TNF-α also have significant tumour supporting functions contributing towards cancer development[15–19]. IFN-γ and TNF-α are associated with increased cell death of intestinal epithelial cells and epithelial barrier dysfunction during in inflammatory bowel disease (IBD)[20]. However, there are also studies highlighting their role in maintaining epithelial homeostasis and gut barrier function[21,22,23].

Nava et al. have described the role of IFN-γ in the regulation of protein kinase B (AKT)-β-catenin and Wnt-β-catenin signalling in a temporally distinct fashion, where a short exposure of IFN-γ results into increased IEC proliferation and epithelial homeostasis while an extended exposure can result into epithelial apoptosis and damage[21]. Both homeostatic and apoptotic effects are potentiated by the addition of TNF-α, demonstrating the synergy of IFN-γ of TNF-α in activation of AKT-β-catenin pathway[21]. The crucial pro-survival role of TNF-α signalling has been highlighted by activation of NF-κB signalling in IECs, because the inhibition of NF-κB in IECs can lead to apoptosis of colonic epithelial cells and translocation of bacteria into the

mucosa[24,25]. Exogenous administration of TNF-α in IECs increased the cell death, but it also increased the production of mucin-2 and other components of the mucin layer providing protective barrier to the intestinal epithelium[26,27]. The studies from Polk et al. have shown that Eerb-B2 receptor tyrosine kinase 4 (ErbB4) is elevated in the damaged epithelium of IBD patients and promotes colonic epithelial cell survival[28]. Further studies performed by the same research group elicit the role of TNF-α in the transactivation of ErbB4 through a TNF-α converting enzyme (TACE)-mediated release of heparin-binding EGF-like growth factor (HB-EGF) from the cells[29]. This transactivation of ErbB4 by TNF-α is necessary to protect colonic epithelial cells from cytokine-induced apoptosis[29].

IFN-γ can also mediate temporal regulation of transcription factor and gene expression to elucidate biological activities[30]. In human pancreatic cells IFN-γ mediates a high and sustained activation of STAT1, which upregulate expression of nicotinamide adenine dinucleotide phosphate (NADPH) family members - Dual Oxidase 2 (Duox2) and Dual Oxidase A2 (DuoxA2) for increased production of both intracellular reactive oxygen species (ROS) and extracellular hydrogen peroxide (H_2O_2) production resulting in cell death[31].

These context dependent effects of IFN-γ and TNF-α in different cellular, tissue, and pathological states suggests that we need to understand in more detail how their respective signalling pathways encode and decode variables such as cytokine concentration and time and how this affects the cellular responses. In this study we show for the first time that the JAK1/2-STAT1 signalling pathway acts as a 'dose-to-duration' signalling pathway to encode and decode concentration-

dependent effects of IFN-γ/TNF-α on JAK1/2-STAT1 pathway activation and downstream gene regulation and cell death decisions.

3.3. Methods and material

3.3.1. Cell culture

Human CRC cell lines - HT-29 (ATCC® HTB-38), DLD-1 (ATCC® CCL-221), LoVo (ATCC® CCL-229), Colo-205(ATCC® CCL-222), HCT-15(ATCC® CCL-225), SW-48(ATCC® CCL-231) and SW-948(ATCC® CCL-237) were obtained from American Type Culture Collection (ATCC). HT-29 cells were cultured in McCoy's5A medium (Sigma-Aldrich #M9309), DLD-1 cells were cultured in RPMI-1640 medium (Sigma-Aldrich #R8758) and LoVo cells were cultured in Kaighn's Modification of Ham's F-12 medium (ATCC #30-2004). All media were supplemented with 10% FBS (Sigma-Aldrich) and 100 IU/mL penicillin (Sigma-Aldrich) and 0.1 mg/mL streptomycin (Sigma-Aldrich). SW-48 and SW-948 cell lines were grown in Hyclone Leibovitz's L-15 medium (Fisher Scientific #11566271) supplemented with 10% FBS, 100 IU/mL penicillin and 0.1 mg/mL streptomycin and 1500 mg/L sodium bicarbonate (Sigma-aldrich). All cell lines were routinely maintained in cell culture incubators at 37°C temperature and 5% CO2. The cell lines were mycoplasma free and were tested for mycoplasma status regularly (3-6 months).

3.3.2. Reagents

Recombinant human IFN-γ (Peprotech #300-02) and recombinant human TNF-α (Peprotech #300-01A) were used for cell stimulations using a 1 pg/mL - 100 ng/mL concentration range of each cytokine.

3.3.3. Cell death assays

Cell viability was measured by quantitation of ATP present in the cells using CellTiter-Glo® luminescent assay (Promega #G7570) and caspase-3 and caspase-7 activities were measured using Caspase-Glo® 3/7 assay kit (Promega #G8091) according to the manufacturer's instructions. The luminescence was recorded using Synergy2, Biotek plate reader. Raw viability data were normalised to the control wells in the absence of any treatment. For crystal violet staining, cells were fixed with 100% Methanol for 10 minutes at -20^{o}C and stained with 0.5% crystal violet stain (500 mg Crystal Violet, 25 mL Methanol, 75 mL Water for 100 mL solution) for 10 min. Plates were dried at room temperature overnight and scanned by using ODESSEY system. For cell death analysis by flow cytometry, cells were treated, harvested, and washed. Cells were stained with fixable viability dye FVe660 (BD Biosciences# 564405) for 15 minutes, protected from light and fixed with 100 ul of fixation/permeabilization buffer (BD Biosciences# 554714) for 30 minutes at 4ºC. Washed twice using 1X perm buffer (BD Biosciences# 554714). Fixed/permeabilized cells were immuno-stained for active caspase 3 for 30 minutes at 4ºC by using anti-active Caspase-3 antibody (BD Cat No# 561011) solution. Cells were washed twice using 1X BD perm buffer and resuspended in FACS buffer (PBS, 2% FBS, 5 mM EDTA). Cells were quantified using flow cytometry instrument- FACS Calibur 3CA (BD Biosciences) and data were analysed using FLOW-JO software (BD Biosciences - version-10).

3.3.4. CXCL-10 chemokine analysis

HT-29 cells were treated with IFN-γ and TNF-α for the indicated duration of time. Conditioned media were collected and stored at -20^{o}C for chemokine analysis.

Secreted chemokine levels were measured using the CXCL-10 MSD assay kit according to the manufacturer's instructions (Meso Scale Discovery).

3.3.5. RNA isolation and quantitative RT-PCR

Total RNA was isolated using the RNeasy Mini Kit (Qiagen) according to the manufacturer's instructions. Reverse transcription was performed on 500 ng of total RNA using Transcriptor Reverse Transcriptase (Roche) and random hexamer primers (Roche) following the manufacturer's protocol. All RT-qPCR assays were designed using the Universal Probe Library Assay Design Centre (Roche Applied Science). qPCR reactions containing 2×Sensi Mix II Probe Kit Reaction Mix (Bioline), 500 nM primers, 250 nM probe (Roche) and 10 ng of cDNA were performed in a Light Cycler 480 instrument. Information on PCR primer sequence is provided in table 3.1.

Table 3.1 List of RT-qPCR probe and primers used in the study

Gene Symbol	*Ensemble ID*	Probe	Forward Primer (5"-3")	Reverse Primer (5"-3")
STAT1	ENSG00000115415	74	GGATCAGCTGCAGAACTGGT	TTTCTGTTCCAATTCCTCCAA
CXCL9	ENSG00000138755	147	ATTGAGCTGGACCTCACCAA	AGGCCTGTAGGCTGATTCAA
CXCL10	ENSG00000169245	86	AAAAGGTATGCAATCAAATCTGC	AAGAATTTGGGCCCCTTG
CXCL11	ENSG00000169248	81	TTGTGTGCTACAGTTGTTCAAGG	TCTGCCACTTTCACTGCTTTTA
ICAM1	ENSG00000090339	60	AGTGATCAGGGTCCTGCAA	GGGAGGGAGTCCTCCAATAC
PDL1	ENSG00000120217	48	GGTAGCAATATGACAATTGAATGC	TGCAGCCAGGTCTAATTGTTT
CXCR3	ENSG00000186810	79	TCCATAGTCATAGGAAGAGCTGAA	CCATGGTCCTTGAGGTGAG
GAPDH	ENSMUSG00000057666	60	AGCCACATCGCTCAGACAC	AGCCACATCGCTCAGACAC
ACTB	ENSMUSG00000029580	11	ATTGGCAATGAGCGGTTC	CGTGGATGCCACAGGACT
PUMA	ENSG00000105327	68	GACCTCAACGCACAGTACGA	GAGATTGTACAGGACCCTCCA
NOXA	ENSG00000141682	16	AATGAACGACAGCCTGCAC	CCGTTGTTGGCTACAGTAGTAGG
BAK	ENSG00000030110	43	TGGTCACCTTACCTCTGCAAC	ATGTCGTCCCCGATGATG
BAX	ENSG00000087088	76	TGAGCGGTTCATTGGCATTAC	GATTGTGTCCCCACGCAC
BCL2	ENSG00000171791	54	ATTTGGGCCCCTGGTCAC	GATTGTACGCTCAGGTCAC
BCL-XL	ENSG00000171552	38	GAACGACAGCCTGGGAGGGA	GGTCACCTTACCTCGATTGTG

3.3.6. Cell lysis and immunoblotting

Cells were stimulated with indicated treatments for indicated times and washed twice with ice-cold PBS and lysed in RIPA buffer [50 mM Tris-HCl (pH 7.4), 1%NP-40, 0.25% Na deoxycholate, 150 mM NaCl, 1 mM EDTA supplemented with ASBEF and Halt cocktail inhibitor]. Protein concentrations were determined using Pierce™ BCA (bicinchoninic acid) protein assay kit (Thermo Fischer Scientific #23225). Immunoblotting was performed using 4-12% gradient gels (Thermo Fisher

#NW04125BOX) and mini gel tanks. Electrophoresis was performed as per manufacturers' instructions. Proteins were transferred from a polyacrylamide gel to a PVDF membrane (Millipore; Immobilon-FL, 0.45-mm thickness) using a mini bolt module (Thermo Fisher #B1000). After transfer, the membranes were blocked using blocking buffer - 5% bovine serum albumin (BSA) in 1X TBST (Tris Buffer Saline, 0.1% Tween-20) - for 1 hour at room temperature. Membranes were incubated with primary antibodies diluted in 5% BSA overnight at 4^{o}C followed by an incubation with secondary antibody for 1 hour at room temperature. Membranes were covered with Western Bright Quantum HRP substrate (Cat no# K-12042-D20) according to the manufacturer's instructions. Chemiluminescence detection was captured using Fujifilm LAS-3000 System.

Antibodies used for immunoblotting were as follow: STAT1 (CST #9172), anti-phospho-STAT1-Y701(rabbit-clone-58D6-CST #9167), phospho-STAT1-S727 (CST #9177), IRF1 (rabbit clone-D5E4-CST #8474) anti-GAPDH (Ambion #AM4300), anti-Beta actin (sc-47778), anti-mouse IgG (Sigma #A2554), anti-rabbit IgG (Sigma #A6154).

3.3.7. Homogeneous Time Resolved Fluorescence (HTRF assay)

This HTRF cell-based assay was used for quantitative detection of STAT1 and Phospho-STAT1 (Tyr701) levels in treated cells. HT-29 cells were seeded in a 96-well plate and stimulated with IFN-γ and TNF-α as indicated. After treatment, the media was removed, and cells were lysed with 50µl of lysis buffer provided with the HTRF assay kit (Cisbion # 63ADK026PEG). The level of STAT1 and STAT1 pY701 protein were quantified by using STAT1/p-STAT1 HTRF kit (Cisbion # 63ADK026PEG). Cell lysates were incubated with STAT1 or p-STAT1 detection antibodies for 4 hours according to

the manufacturer's guidelines. Fluorescence was measured at two different wavelengths 665nm and 620nm using Synergy2, Biotek plate reader. Phospho- and total protein levels were calculated as HTRF ratios, the ratio of fluorescence signal at 665 nm to Signal at 620 nm.

HTRF Ratio = (Signal 665 nm / Signal 620 nm) x 10^4

The relative or normalised value of signal was calculated by dividing the HRRF ratio of STAT1 pY01 to HTRF ratio of total STAT1 protein.

Normalization value (P/T) = (Phospho HTRF Ratio / Total HTRF Ratio) x 100

3.3.8. Cellular fractionation experiments

HT-29 cells were stimulated with cytokines as indicated and washed twice with ice-cold PBS. Cells were lysed using buffer A (10 mM HEPES (pH 7.9), 10 mM KCl, 1.5 mM MgCl2, 0.34 M sucrose, 10% glycerol, 1 mM DTT, 0.1% Triton X-100 and protease inhibitors) by incubating with buffer A for 10 minutes and centrifuged at 4000 rpm at 4ºC for 5 min. Cell supernatant (containing the cytoplasmic fraction) was collected. The pellet (containing the nuclear fraction with cell debris) was washed 3 times with buffer A without Triton X-100. The nuclear pellet was resuspended in lysis buffer B containing 0.2 mM EGTA (pH 8), 3 mM EDTA (pH 8), 1 mM DTT and incubated overnight with intermittent vigorous vortexing. The resuspended pellet was centrifuged at 10,000 rpm for 5 minutes and the supernatant was collected as the nuclear fraction.

3.3.9. Total RNA extraction and RNA-Sequencing

HT-29 cells were seeded in 12-well plates ($3.5x10^5$ cells/well) for 24 hours and stimulated with 1 ng/mL and 10 ng/mL concentration of IFN-γ + TNF-α for 4 hours,

10 hours and 16 hours. Cells were washed with ice-cold PBS and stored at -80°C. RNA was isolated from the cells using RNeasy mini kit (74106, Qiagen) and eluted in 50 µl of nuclease free water. RNA concentration was estimated by using Qubit 4 fluorometer (Thermo Fisher Scientific) and 6 µg of total RNA was DNA digested using RNA Clean and Concentrator-5 Kit (Zymo research). The eluted RNA was sent for RNA sequencing. Briefly, libraries were generated from polyA+ selected RNA utilising the Illumina® TruSeq™ Stranded mRNA-seq library preparation kit and sequenced on an Illumina® NovaSeq Platform – 2 x 100 paired end run. Dual-indexed library generation and sequencing was carried out at the Edinburgh Genomics NGS facility in Scotland.

3.3.10. RNA-Seq data analysis

The RNA-Seq data was processed through a differentially expressed data analysis pipeline to identify genes that are differentially expressed at various time points compared to the untreated samples. The pipeline involved checking the quality of the sequences using FastQC[32], trimming using fastp[33], pseudo alignment to the transcriptome using kallisto[34] aggregating to the gene level counts using tximport[35] differential expression at transcript level using Sleuth[36,37] gene ontology and functional enrichment analysis using EnrichR[38] and KEGG pathway visualization using Pathview[39].

3.3.11. Principal Component Analysis

For Deseq2 principal component analysis (PCA), variance stabilizing transformation (vsd) normalization was performed on the aggregated gene level transcripts per million (TPM) counts. plotPCA R function was used on the dataset to generate PCA plot.

3.3.12. Differential Expression (DE) Analysis

For DE analysis, standard pairwise comparison was performed comparing untreated samples to treated samples at different concentrations and duration of cytokine treatment. Sleuth Wald Test was used for pairwise comparison. Six pairwise comparisons were performed comparing untreated to 1 ng/mL at 4 hours, 1 ng/mL at 10 hours, 1 ng/mL at 16 hours, 10 ng/mL at 4 hours, 10 ng/mL at 10 hours, 10 ng/mL at 16 hours. After multiple testing, adjusted p.value (q-value) filter of 0.01 was used as a threshold for calling genes that were differentially expressed.

3.3.13. Pathway analysis

EnrichR was used to identify enriched gene ontologies and KEGG pathways in the genes lists from the different comparisons that were differentially expressed at 10 ng/mL at 16 hours and those that were unique to this comparison. Nominal p-value cut-off of 0.05 was used to filter for enriched pathways and visualized using bar graph. The pathways were identified and visualized using EnrichR (https://amp.pharm.mssm.edu/Enrichr) 'combined score' metric, which is a combination of p-value and z-score and reported to provide best rankings. Expression profile of genes from the enriched pathways in the unique dataset was visualized in the form of heatmap and cluster gram. Pathview (https://pathview.uncc.edu/) was used to visualize the KEGG pathways overlaying genes that were DE at 10 ng/mL at 16 hours and those that were unique to 10 ng/mL at 16 hours denoting the directionality of expression in the pathways.

3.3.14. Statistical Analysis

Statistical analysis was done using GraphPad prism 7 (GraphPad Software, Inc., La Jolla, CA, USA). Data are presented as mean ± SEM, and statistical analysis of the data was performed using 1-way-ANOVA or 2-way-ANOVA followed by multiple comparisons between individual groups. Statistically significant differences were identified at p value < 0.01.

3.4. Results

3.4.1. IFN-γ and TNF-α synergise to induce cell death in colorectal cancer cell lines in a concentration-dependent manner.

Elevated levels of the pro-inflammatory cytokines IFN-γ and TNF-α are associated with increased epithelial cell death and barrier dysfunction in IBD[40,41,42]. To investigate the dependency of epithelial cell death on the relative cytokine concentration, HT-29 cells were stimulated with a range of concentrations (1 pg/mL - 100 ng/mL) of IFN-γ + TNF-α for 72 hours and assayed for cell viability (Figure 3.1A). There was no decrease in cell viability observed up to 1 ng/mL of IFN-γ + TNF-α treatment, but synergistic cell death was observed at a concentration higher than 1 ng/mL (Figure 3.1A). The data revealed a concentration-dependent switch from cell viability to cell death between 1 and 10 ng/mL of cytokines (in HT-29 cells) with cells exhibiting a drastic drop in relative viability at 10 ng/mL (80% decrease) compared to 1 ng/mL (Figure 3.1A). To further pin-point on the impact of concentration, HT-29 cells were treated with 2.5 and 5 ng/mL of IFN-γ + TNF-α. Even though there was a small decrease in the viability of cells at these concentrations, the level of cell death was varying between runs (data not shown).

The results were further confirmed by estimating the effects of cytokines on cell viability and cell death by crystal violet staining and flow cytometry (Figure 3.1B-D). Even though flow cytometry data demonstrated a slight activation of caspase-3 in the cells treated with 1 ng/mL concentration of cytokines, this was not associated with significant cell death in HT-29 cells (Figure 3.1D).

To further investigate the role of cytokine concentration on cell death, a panel of six non-isogenic, IFN-γ + TNF-α sensitive CRC cell lines were exposed to a concentration range of IFN-γ + TNF-α (1 pg/mL - 100 ng/mL) and assayed for cell viability (Figure 3.2). Even though there were differences in the relative sensitivity of the different cell lines to different concentrations of cytokines, the overall concentration-dependent effects of the cytokines on cell death were consistent across the lines. Similar to HT-29 cells, the other cell lines DLD-1, HCT-15, SW-48 and SW-948 (Figure 3.2 A-D) underwent a cell death switch between 1 and 10ng/mL of cytokines while the LoVo cell line was more sensitive to the treatment and underwent cell death between 0.1 ng/mL and 1ng/mL concentration of the two cytokines (Figure 3.2 E). Colo-205 did not show any cell death sensitivity until 100 ng/mL of the cytokines was used. (Figure 3.2 F)

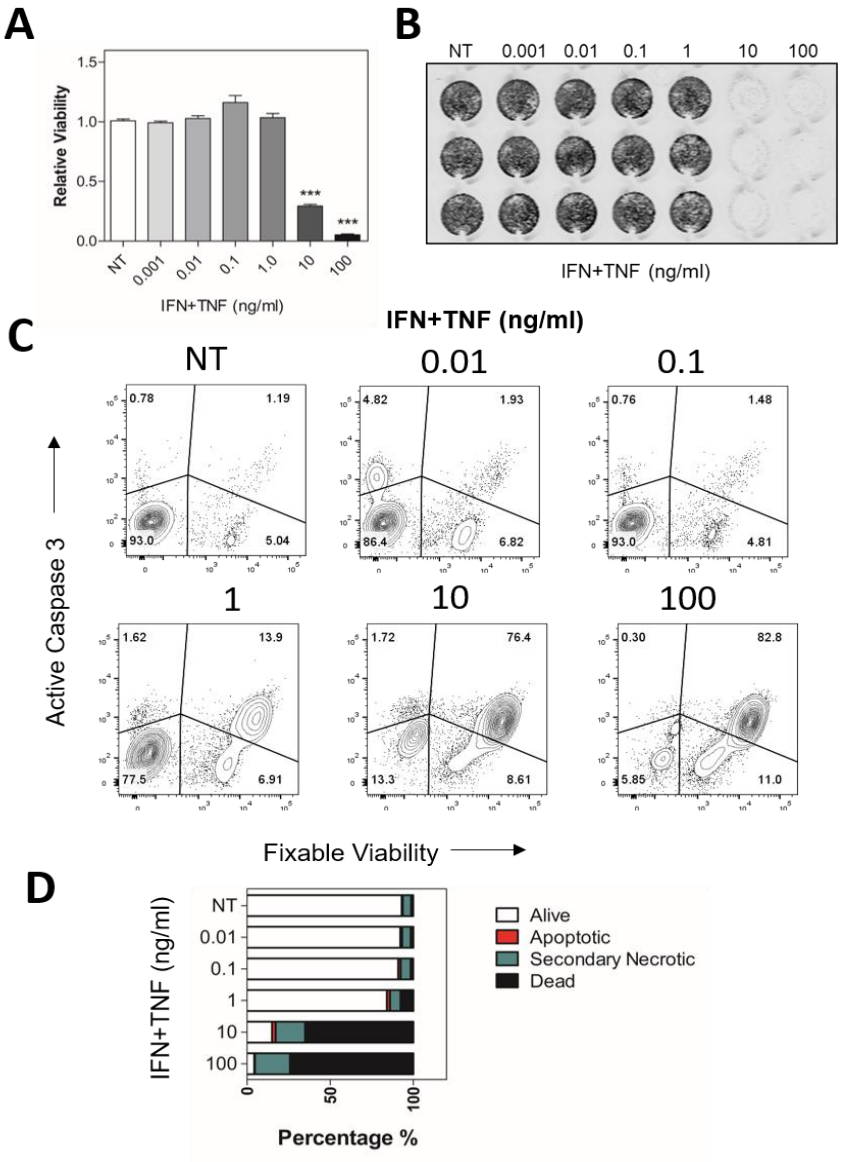


Figure 3.1. IFN-γ and TNF-α synergised to induce cell death in HT-29 cells in a concentration dependent manner

(A-D) HT-29 cells were co-stimulated with 1 pg/mL - 100 ng/mL of IFN-γ and TNF-α for 72 hours and cell viability was quantified (A) by measuring ATP level by cell titre-glo assay. Data shown are the mean ± S.E.M of n = 3 independent experiments in triplicates (B) by crystal violet assay. Image is representative of 1 out of 3 experiments. (C) by measurement of cells positive for active caspase-3 and FV-660 positive dead cells by using flow cytometry. The data is representative of one out of three experiment in duplicate. (D) Bar chart representation of flow cytometry data with combined value of 3 independent runs in triplicate. Data was plotted as mean ± S.E.M. ***p < 0.0001 (one-way ANOVA followed by Dunnett's multiple comparisons test vs. non-treated cells). NT=non-treated cells

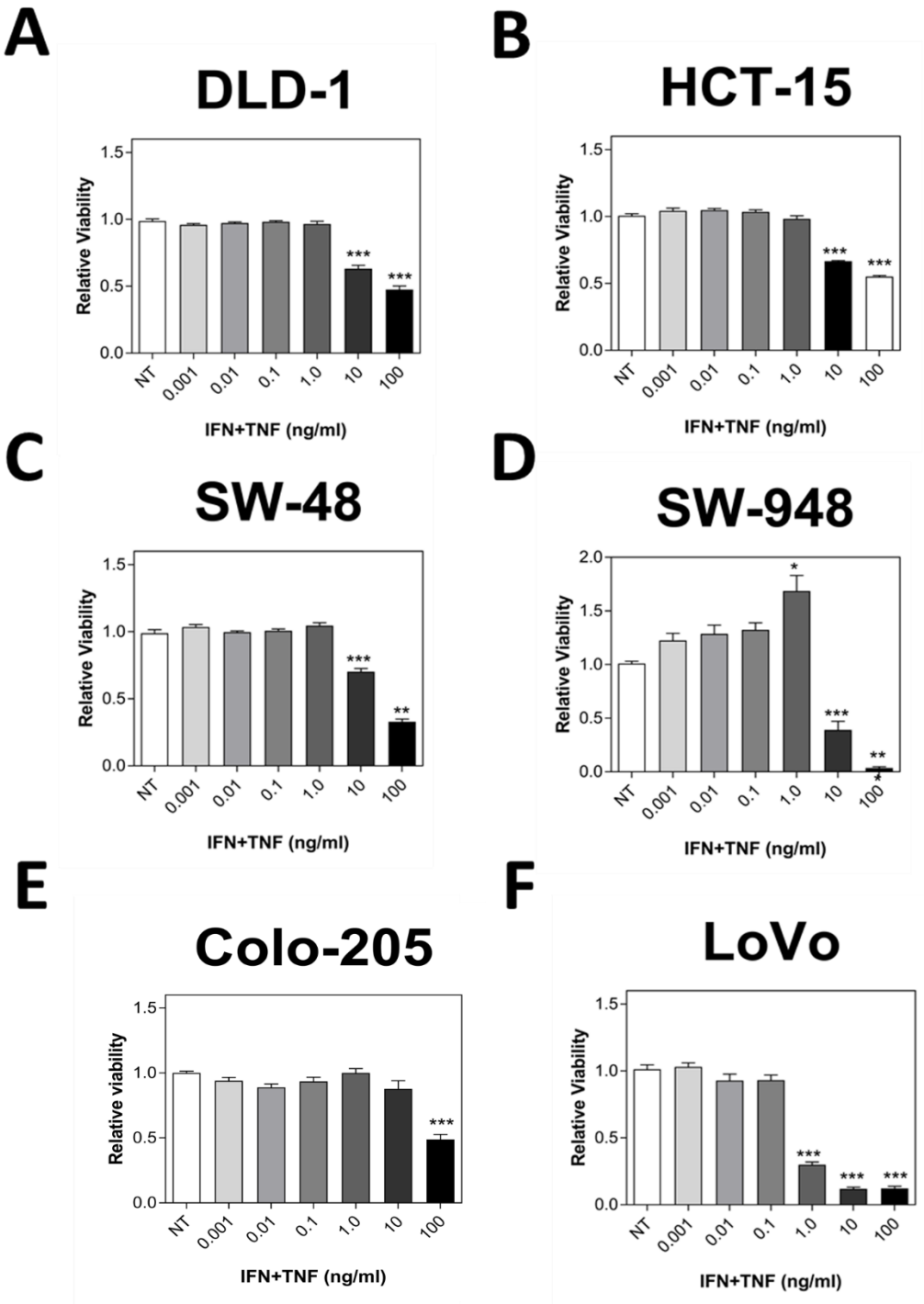


Figure 3.2. IFN-γ and TNF-α induced cell death in a panel of colorectal cancer cell lines in a concentration dependent manner

A-F) Panel of 6 non-isogenic CRC cell lines (as labelled) were co-stimulated with 1 pg/mL - 100 ng/mL of IFN-γ + TNF-α for 72 hours measured for cell viability by cell titer-glo assay. Data shown are the mean ± S.E.M of n = 3 independent experiments in triplicate. *p < 0.01, **p < 0.001 and ***p < 0.0001 (one-way ANOVA followed by Dunnett's multiple comparisons test vs. non-treated cells) NT=non cytokine treated cells

3.4.2. IFN-γ and TNF-α induced expression of pro-inflammatory and pro-apoptotic genes in a concentration dependent manner

To investigate the effect of cytokine concentration on gene expression and cell death the relative expression of different pro-inflammatory genes and pro-apoptotic genes was measured 8 hours post cytokine stimulation by RT-qPCR. The expression of immune regulatory and pro-inflammatory genes Programmed death-ligand 1 (*PDL1),* Intercellular Adhesion Molecule 1 (*ICAM1),* C-X-C Motif Chemokine Ligand 9 *(CXCL9), CXCL10, CXCL11* and C-X-C Motif Chemokine Receptor 3 *(CXCR3)* increased significantly with increasing concentration of cytokines (Figure 3.3A). There was a five to ten-fold increase in the relative expression of pro-apoptotic genes - p53 upregulated modulator of apoptosis (*PUMA),* Phorbol-12-myristate-13-acetate-induced protein 1 *(NOXA),* BCL2 Antagonist/Killer 1 *(BAK1)* with increasing concentration of cytokines (Figure 3.3B). There was no significant change in the expression level of pro-apoptotic gene BCL2 Associated X *(BAX)*. No significant differences were observed in the expression of the anti-apoptotic gene (B cell lymphoma 2 (*BCL2)* and BCL2 like 1 (*BCL-XL)* up to 10 ng/ml IFN-γ + TNF-α treatment. Although, a slight decrease in *BCl2* expression was observed at 100 ng/ml treatment (Figure 3.3B).

To further investigate the regulation of inflammatory gene expression and cell death in temporal manner, a time course experiment was performed to estimate CXCL-10 levels and cell viability in IFN-γ + TNF-α treated cells over time. Secreted CXCL-10 chemokine could be detected within 2 hours of IFN-γ + TNF-α treatment and this increased further over time (Figure 3.4 A). But cell death was a late process and a

significant level of cell death was detected only after 24 hours of cytokine treatment and at a concentration of 10 ng/mL or higher of cytokines (Figure 3.4 B).

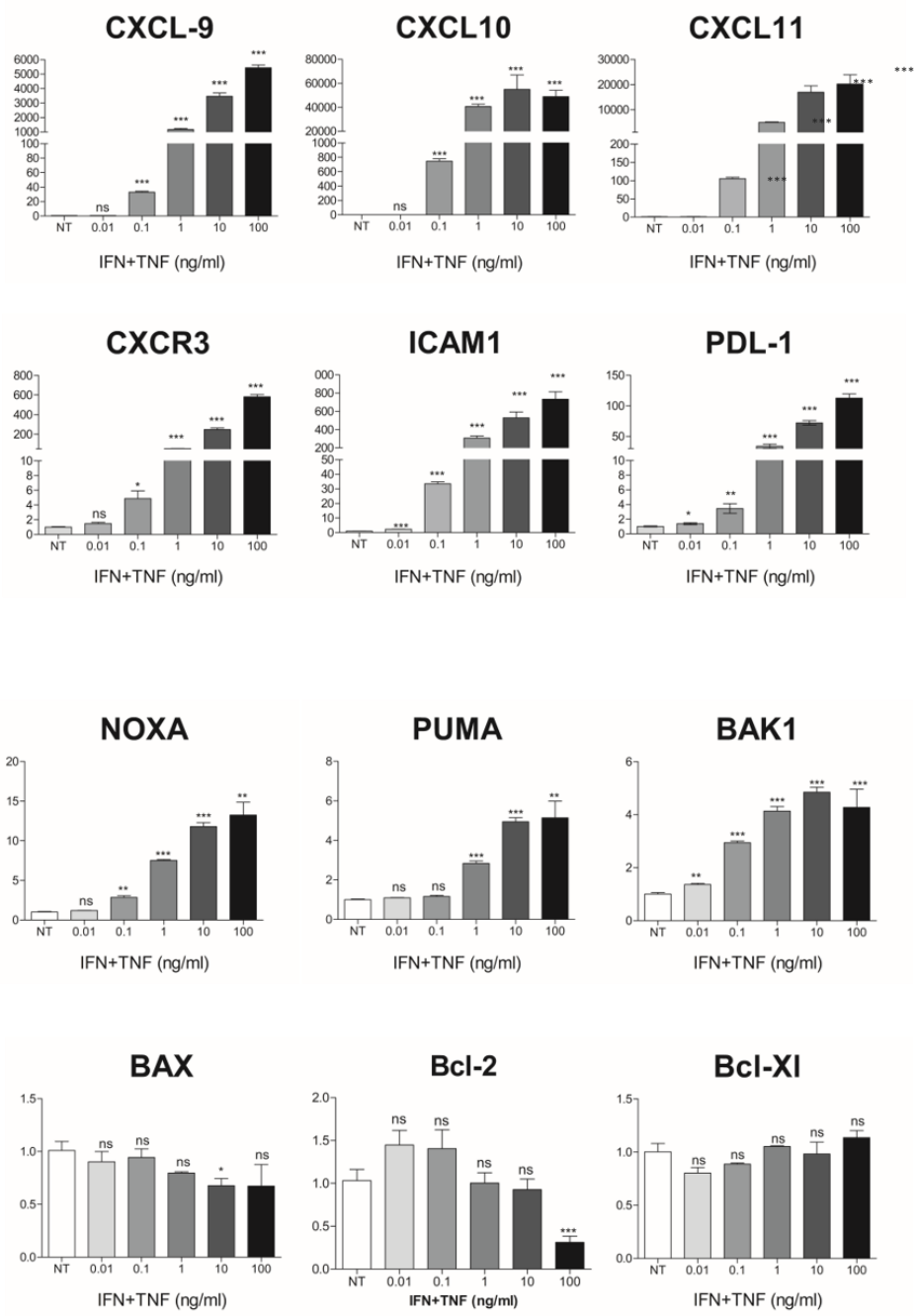


Fig 3.3 IFN-γ +TNF-α trigger the expression of pro-inflammatory and pro-apoptotic genes in a concentration dependent manner

HT-29 cells were co-stimulated with 1 pg/mL -100 ng/mL of IFN-γ and TNF-α for 8 hours and relative mRNA levels were measured by RT-qPCR for indicated genes. GAPDH and beta Actin were used as reference genes for normalisation of data. Data shown are the mean ± S.E.M of n = 2 independent experiments in triplicate. *p < 0.01, **p < 0.001 and ***p < 0.0001 (one-way ANOVA followed by Dunnett's multiple comparisons test vs. non-treated cells) NT=non cytokine treated cells

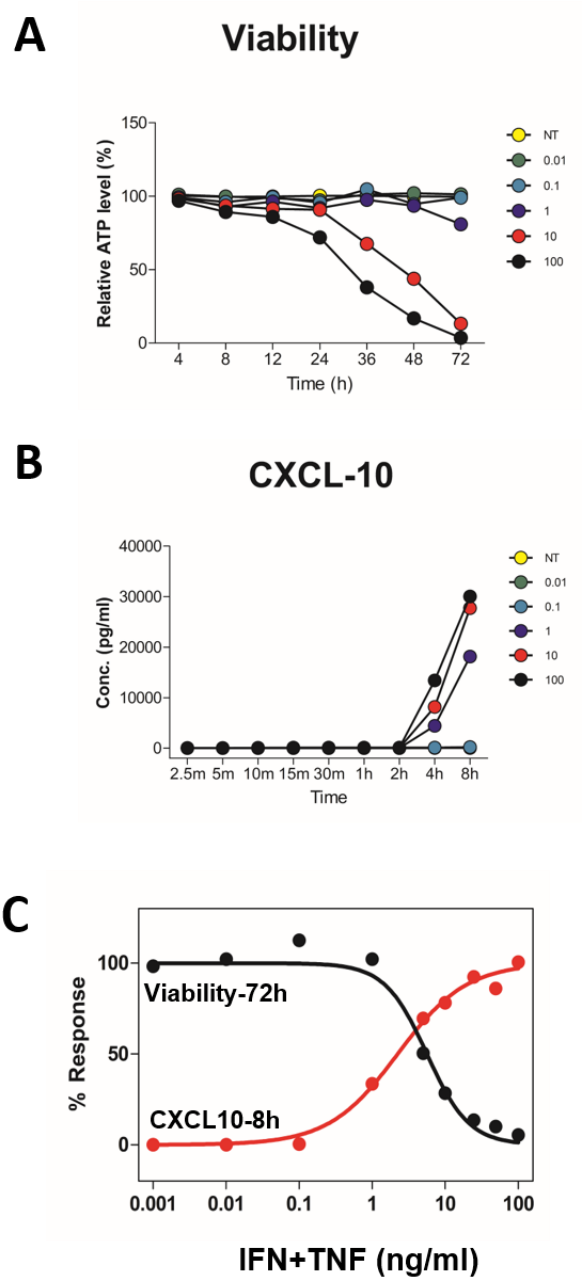


Fig 3.4. IFN-γ +TNF-α induce the production of CXCL-10 and cell death in a concentration and time dependent manner

(A-B) HT-29 cell line was co-stimulated with 1 pg/mL -100 ng/mL of IFN-γ and TNF-α and (A) cell viability was quantified by cell titer glo assay at indicated time points (B) CXCL-10 levels were measured using MSD CXCL-10 detection kit at indicated time points. C) Graph indicating relative level of CXCL-10 and viability at different concentrations of IFN-γ + TNF-α. Data shown are the mean ± S.E.M of n = 3 independent experiments in triplicate. NT=non cytokine treated cells

3.4.3. JAK1/2-STAT1 signalling induced by the combination of IFN-γ + TNF-α follows a dose-to-duration pattern.

We had already established that IFN-γ and TNF-α induced cell death of CRC cells through a JAK1/2-STAT1-dependent signalling pathway (Chapter-2). To explore the effect of different cytokine concentrations on STAT1 activation, the expression level of *STAT1* was measured at 8 hours after IFN-γ + TNF-α treatment. Even though there was an increase in *STAT1* expression level with increased cytokine concentrations, there was no significant difference observed in *STAT1* expression level between 1 ng/mL (non-cytotoxic) and 10 ng/mL (cytotoxic) treatment (Figure 3.5A). To further investigate this, we measured STAT1 and phospho-STAT1 - STAT1 pY701 and STAT1 S727 - protein levels after treatment of cells with different concentrations of cytokines for 8 hours. Consistent with the RT-qPCR data, there was no difference in total STAT1 levels in the 1, 10 and 100 ng/mL IFN-γ + TNF-α treatment groups, but a significant difference was observed in STAT1 pY701 levels between the different groups (Figure 3.5B). The level of STAT1 pY701 phosphorylation was much higher at the cytotoxic concentration (10 and 100 ng/mL) in comparison to non-cytotoxic concentrations (0.01, 0.1 and 1 ng/mL). A similar pattern was observed in STAT1 S727 levels as well (Figure 3.5 B).

To further understand the effect of the cytokine concentration-response on STAT1 phosphorylation temporally, protein and phospho-protein levels were compared between the 1 and 10 ng/mL treatment group over a time course of 15 minutes - 24 hours (Figure 3.5 C). Within 15 minutes of IFN-γ + TNF-α treatment, a very high level of STAT1 pY701 phosphorylation could be observed in both 1 and 10 ng/mL conditions (Figure 3.5 C). At earlier time points (up to 4 hours) the STAT1

pY701 levels were comparable between both 1 ng/mL and 10 ng/mL treatment conditions but at 8 hours it started to decrease in the 1 ng/mL treatment group and was almost diminished at 24-hour time point. On the other hand, in the 10 ng/mL treatment groups, the levels of STAT1 pY701 phosphorylation were sustained at the 8-hour time point and started to go down from this time onwards (Figure 3.5 C).

To confirm this observation, the more quantitative HTRF (Homogeneous Time Resolved Fluorescence) assay was performed. The HTRF Phospho-STAT1 (Tyr701) assay uses 2 labelled antibodies: one with a donor fluorophore which binds to the to the Phospho-STAT1 (Tyr701) and second with acceptor molecule which binds to STAT1 independent of its phosphorylation state. Protein phosphorylation brings the donor fluorophore into close proximity to the acceptor, thereby generating a FRET signal. The intensity of FRET signal determines the level of phosphorylation on the protein.

HTRF phospho-STAT1 (Tyr701) assay performed on lysates from cells treated with IFN-γ, TNF-α or the combination of both cytokines at a range of different concentrations (10 pg/mL to 100 ng/mL) over a time course and the level of STAT1 and STAT1 pY701 were measured (Figure 3.6). In case of IFN-γ treatment groups there was an increase in total STAT1 levels with time in concentration groups (Figure 3.6 A). Increased STAT1 pY701 could be observed at all concentrations within 15 minutes after treatment. The effect of concentration difference could be observed both in magnitude and duration of STAT1 pY701 levels, as the STAT pY701 levels were very low at 0.1 and 0.01 ng/mL IFN-γ treatment and reduced to basal level after some time. At 1 ng/mL and 10 ng/mL IFN-γ treatment, initially STAT1 and STAT1 pY701 levels were comparable, but with time there was prolonged activation of STAT1

pY701 levels at 10 ng/mL treatment group compared to 1 ng/mL (Figure 3.6 A). In the case of TNF-α, no significant increase could be observed in STAT1 and STAT1-pY701 levels (Figure 3.6 A). The STAT1 activation kinetics in IFN-γ +TNF-α treated cells was very similar to IFN-γ treated cells. There was an increase in total STAT1 protein with time with no significant difference between 0.1, 1 and 10 ng/mL treatment groups. Very high level of STAT1 pY701 levels could be observed after 15 minutes of IFN-γ+TNF-α treatment. As previously observed by western blotting (Figure 3.5 C), initially there were comparable levels of STAT1 pY701 at 1 and 10 ng/mL concentration, but there was a drop in the STAT1-pY701 levels within 8 hours in 1 ng/mL treatment group while there was a sustained activation of STAT1 pY701 observed in 10 ng/mL treatment group. Thus, the comparison of the activation profile of STAT1 pY701 in 1 ng/mL and 10ng/mL suggests a dose to duration response for STAT1 phosphorylation.

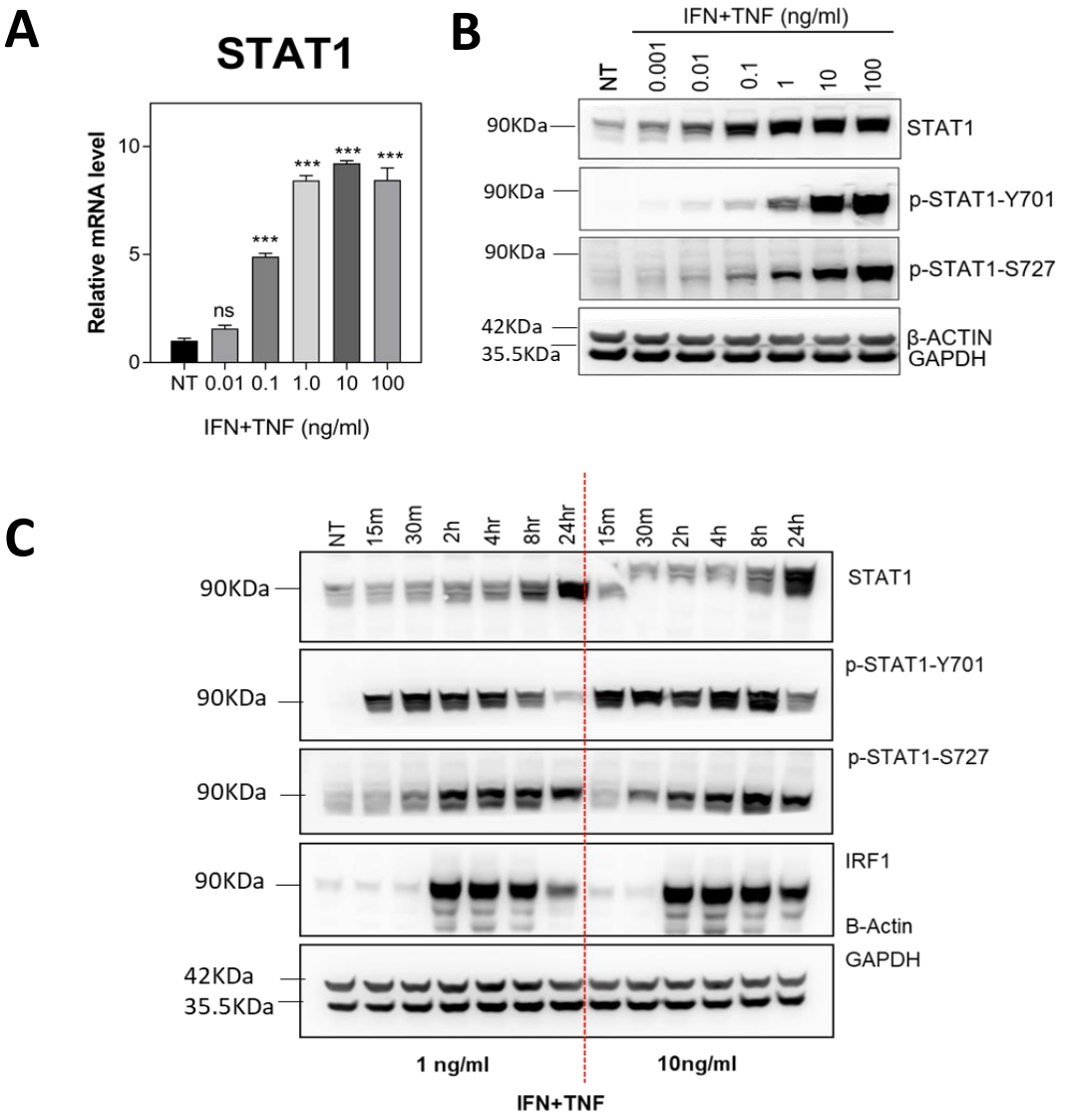


Fig 3.5. Effect of cytokine concentration on STAT1 gene expression, protein levels and phosphorylation status

(A-B) HT-29 cells were co-stimulated with 1 pg/mL - 100 ng/mL of IFN-γ and TNF-α for 8 hours and analysed for (A) relative mRNA level of *STAT1*. GAPDH and beta Actin were used as reference genes for normalisation of data. Data was plotted as mean ± S.E.M of n = 2 independent experiments in triplicates (B) the protein level of STAT1, STAT1-pY701 and STAT1-pS727 by western blotting. Image is representative of 1 out of 2 experiments (C) HT-29 cells were treated with 1 ng/mL and 10 ng/mL concentration of IFN-γ + TNF-α for the indicated duration of time and analysed for STAT1, STAT1-pY701 and STAT1-pS727 levels by western blotting. Image is representative of 1 out of 2 experiments ***p <

0.0001 (one-way ANOVA followed by Dunnett's multiple comparisons test vs. non-treated cells). NT=non-treated cells

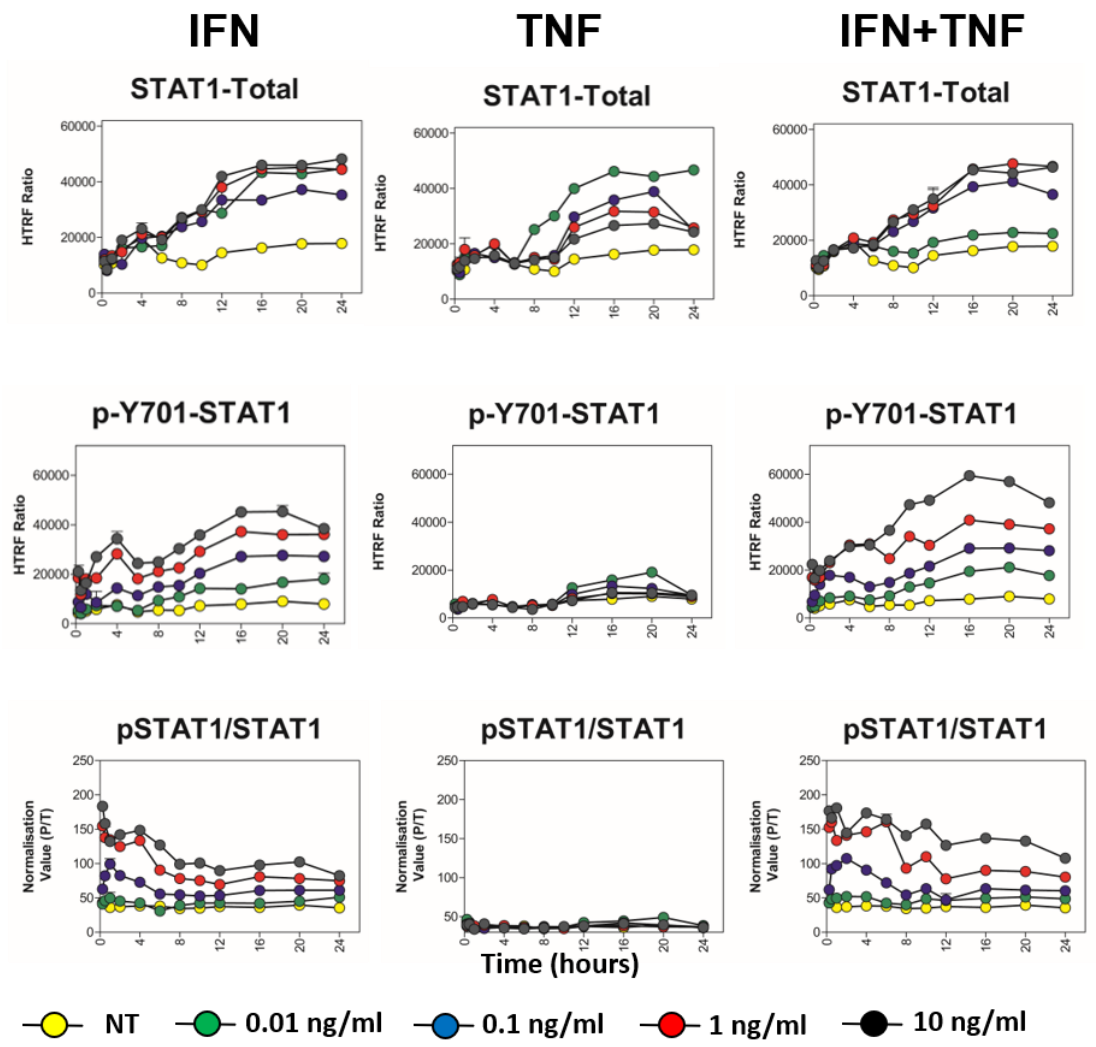


Fig 3.6. The combination of IFN-γ + TNF-α induced concentration-dependent effects on the kinetics of JAK1/2-STAT1 pathway activation

HT-29 cells were stimulated with 1 pg/mL -100 ng/mL of IFN-γ alone, TNF-α alone or combination of both cytokines for a 24-hour time course. The protein levels of STAT1 and STAT1-pY701 were estimated by performing the HTRF assay. The relative phosphorylation of STAT1-pY701 was calculated by normalising the data in terms of STAT1 pY701/ STAT1 ratio (Section-3.3.7). The data is representative of 1 out of 2 experiments.

3.4.4. The combination of IFN-γ + TNF-α at high concentrations induced sustained activation of STAT1 in both the cytoplasm and nucleus of colorectal cancer cells

As STAT1 is a transcription factor, its translocation to the nucleus is essential for its functional activity. The nuclear localization of STAT1 requires its phosphorylation at Y701 residue and STAT1 homo-dimerization[43]. Therefore, we investigated the kinetics of STAT1 phosphorylation both in the nucleus and cytoplasm of cytokine treated cells. HT-29 cells were stimulated with the combination of IFN-γ + TNF-α at 1 ng/mL or 10 ng/mL concentration over a 16-hour timeframe. Cytoplasmic and nuclear proteins were isolated by cellular fractionation as described in Figure 3.7A. The ponceau staining confirmed that a comparable amount of protein was loaded onto the gels for both the cytoplasmic and nuclear fractions (Figure 3.7B). The relative purity of the fractions was validated by western blotting for Poly ADP-ribose polymerase (PARP - control for nuclear fraction) and alpha-tubulin (control for cytoplasmic fraction) in both the fractions (Figure 3.7 C). Consistent with previous data, the level of total STAT1 protein increased in both the 1 ng/mL and 10 ng/mL treated cells and were comparable at both concentrations (Figure 3.7 C). Although detectable, relatively little STAT1 protein was detected in the nuclear fraction. STAT1 tyrosine 701 phosphorylation was also similar as the previous experiment showing a comparable amount of phosphorylation level at an early time point which further increased in case of 10 ng/mL treatment but reduced significantly in 1 ng/mL treatment condition both in nucleus and cytoplasm (Figure 3.7 C). This confirmed the sustained activation of STAT1 both in the nucleus and cytoplasm at higher cytotoxic concentrations (10 ng/mL) of both cytokines.

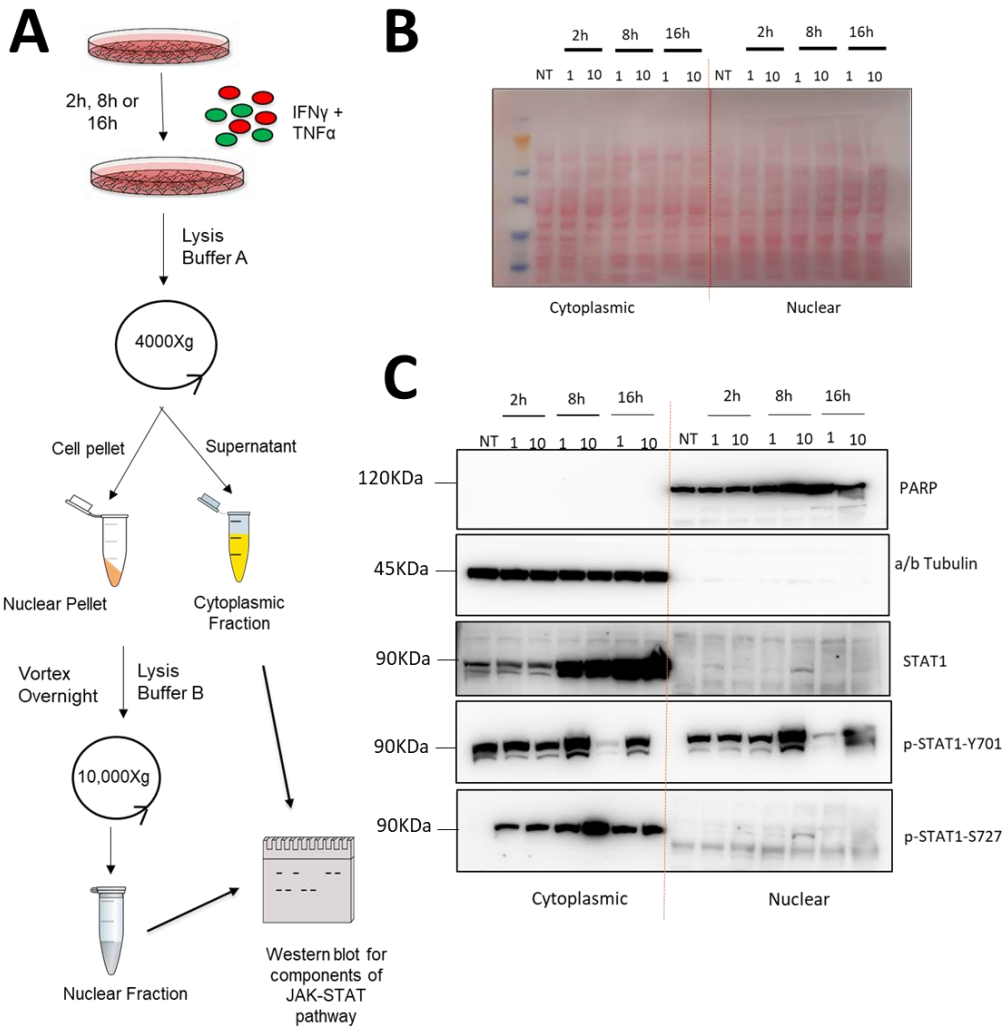


Figure 3.7. The combination of IFN-γ + TNF-α at higher concentrations induced sustained activation of STAT1 in both the cytoplasm and nucleus of HT-29 cells

(A) Schematic representation of cellular fractionation protocol. (B-C) HT-29 cells were co-stimulated with 1 ng/mL or 10 ng/mL of IFNγ + TNFα for 2 hours, 8 hours or 16 hours and protein lysates were analysed by western blotting. (B) Ponceau red stained PVDF membrane after western blotting of cytoplasmic and nuclear fractions. (C) Protein lysates from the cytoplasmic and nuclear fractions were measured for levels of total STAT1, STAT1 pY701 and STAT1 pS727 by western blotting. The data shown is representative of 1 out of 2 experiments.

3.4.5. Sustained activation of JAK1/2-STAT1 pathway is essential for the induction of cell death in HT-29 cells

To understand the role and requirement for sustained activation of the JAK1/2-STAT1 pathway in cytokine-induced cell death of CRC cells, we first analysed the kinetics of cell death in HT-29 cells treated with the combination of IFN-γ + TNF-α over a 24 hour period. The detection of alive and dead cells was performed by measurement of protease activities in the cells using the GF-AFC substrate (live-cell protease substrate from Promega) and bis-AAF-R110 Substrate (dead-cell protease substrate from Promega). In parallel, cellular ATP levels were also measured in the cells using cell-titre-glo assay. The results obtained from measuring relative cell viability and relative ATP level were identical showing a ~10% decrease in cell viability after 12-14 hours of IFN-γ + TNF-α treatment which further decreased up to ~30% at 24 hours (Figure 3.8A). The cytotoxic effect of IFN-γ + TNF-α could be observed after 12 hours of IFN-γ + TNF-α treatment and increased thereafter (Figure 3.8A). In addition to the cytotoxicity, we also measured the level of caspase- 3 and 7 activity in the cells. Caspase 3/7 activation was initially detected between 10-12 hours post-cytokine treatment and it subsequently increased with time thereafter (Figure 3.8A).

As discussed earlier, IFN-γ + TNF-α signalling induced activation of JAK1 and JAK2 to mediate the phosphorylation and sustained activation of STAT1 (Figure 3.5 & 3.6). As per the kinetics of cell death observed in IFN-γ + TNF-α treated cells activation of executioner caspases (caspase-3 & 7) was detectable between 10-12 hours of cytokine treatment immediately preceding cell death. To understand the role of sustained JAK1/2-STAT1 pathway activation on cell death, we performed a kinetic

JAK1/2 activity perturbation experiment for up to 10 hours of IFN-γ + TNF-α treatment. The JAK1/2-STAT1 pathway was activated by treating the cells with IFN-γ + TNF-α and the signalling was perturbed periodically using the JAK1 and JAK2 inhibitor baricitinib (Figure 3.8 B).

HT-29 cells treated with IFN-γ + TNF-α (10 ng/mL of each) showed a ~90% reduction in the cell viability compared to non-treated cells after 72 hours of cytokine treatment. As previously observed (Figure 2.6), 1-hour pre-treatment (represented as -1 hour) with baricitinib completely rescued the cells from IFN-γ + TNF-α induced cell death (Figure 3.8B). Baricitinib was added to the cells every two hours post-cytokine treatment up to 10 hours post-cytokine treatment. Surprisingly, blocking JAK1 and JAK2 activity with addition of baricitinib as late as 10 hours post-IFN-γ + TNF-α treatment could completely rescue the cell death phenotype (Figure 3.8 B). These data indicate that it is the sustained activation of the JAK1/2-STAT1 pathway for more than 10 hours that is associated with and required for cytokine-induced cell death of CRC cells.

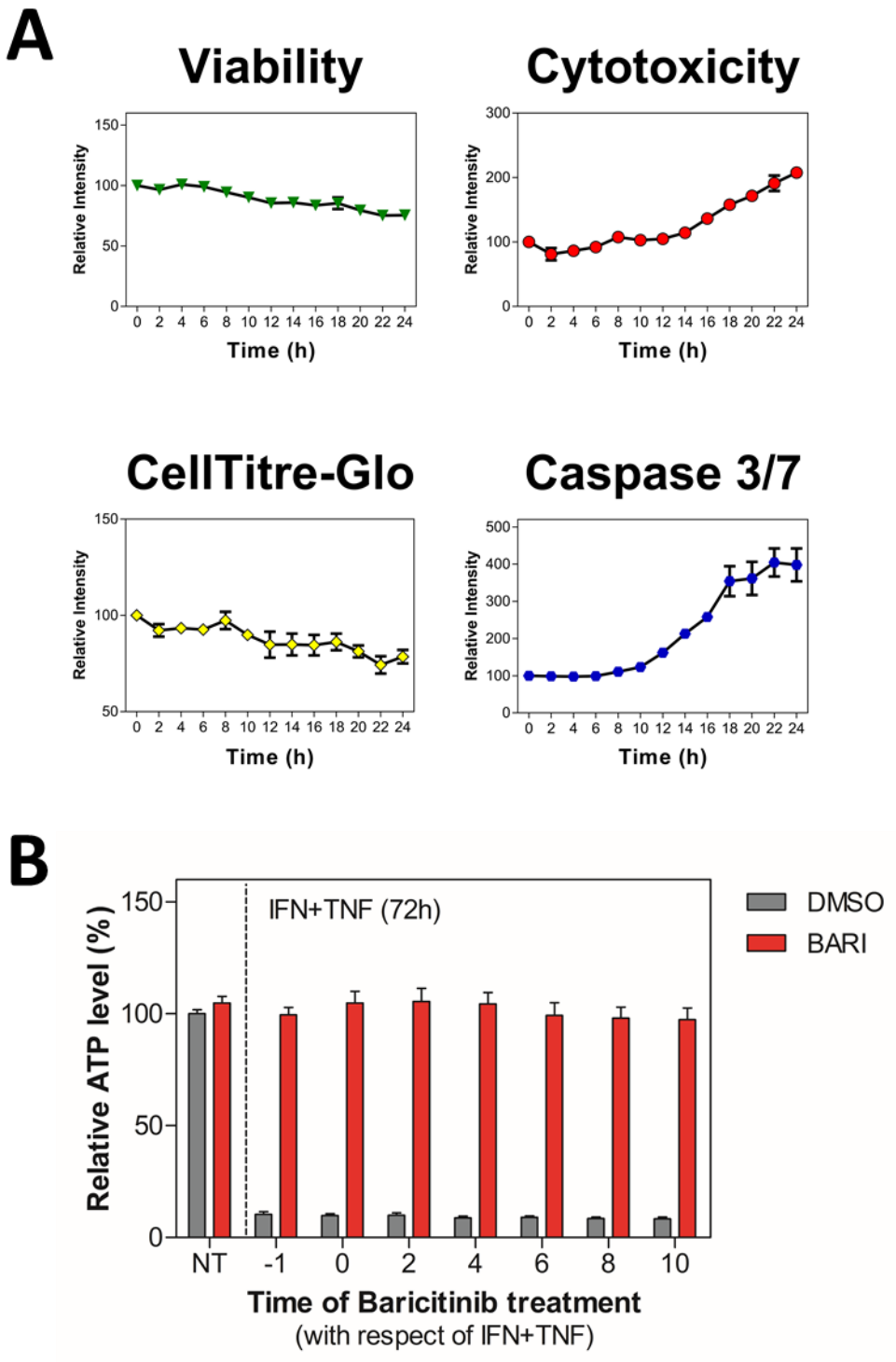


Figure 3.8. Sustained activation of the JAK1/2-STAT1 pathway is essential for IFN-γ + TNF-α induced cell death of colorectal cancer cells

(A) HT-29 cells were co-treated with IFN-γ and TNF-α at 10 ng/mL concentration for the indicated time points and measured for viability (by using live-cell protease substrate from Promega) and cytotoxicity (dead-cell protease substrate from Promega) active caspase 3/7 level (caspase 3/7 assay from

Promega) and cellular ATP levels- CTG (Cell titer glo assay from Promega). Data was plotted as mean ± S.E.M of n = 2 independent experiments in triplicates (B) HT-29 cells were treated with IFN-γ and TNF-α at 10 ng/mL concentration followed by baricitinib (1 μM) treatment at indicated interval of times. The duration represents the time of addition of baricitinib after IFN-γ + TNF-α treatment. Cell viability was measured 72 hours after IFN-γ + TNF-α treatment. ***p < 0.0001 (one-way ANOVA followed by Dunnett's multiple comparisons test vs. non-treated cells). NT= cells not treated with cytokines

3.4.6. RNA-Seq analysis identifies differentially expressed genes which are associated with the concentration of cytokines and the duration of cytokine treatment

IFN-γ + TNF-α at cytotoxic concentration (10 ng/mL) induced sustained activation of JAK1/2-STAT1 pathway and inhibition of the late phase of JAK1/2-STAT1 pathway activation blocked cytokine induced cell death. These data suggested that changes in gene expression mediated by the late sustained phase of STAT1 activation could be associated with and required for cell death. To identify potential late genes, global gene expression analysis was performed using RNA-Seq.

HT-29 cells were treated with 1 ng/mL and 10 ng/mL concentration of IFN-γ + TNF-α for the duration of 4 hours, 10 hours, and 16 hours. Total RNA was isolated from all the samples and sequenced for single-end sequencing using 100 bp length sequencing metrics. An average of 23 million reads per sample were obtained. After analysing the quality of sequences by FAST-QC, low quality reads were filtered out using FAST-p. The filtered reads were pseudo-aligned to human transcriptome and an average of 91% of reads mapped to the human genome (Pipeline for data handling-Fig 3.9).

Principal Component Analysis (PCA) plot was used to show the differentially expressed gene aggregation, clustered based on cytokine concentration and duration of cytokine treatment (Figure 3.14 A). PCA showed that the cytokine treated groups (both 1 ng/mL and10 ng/mL) clustered apart from the non-treated samples (control group), indicating the strong responses in gene expression with cytokine treatment. Intriguingly, both 1 ng/mL and 10 ng/mL cytokine treatment groups clustered closely together at early time point (4 hour) but away from each other at later time points

(10 hours and 16 hours), indicating that the higher dose of cytokine treatment induced a distinct gene expression profile or transcriptome at later time points. In accordance with our previous results (Figure 3.10), the distinct transcriptional profile may be due to differences in STAT1 pY701 levels with concentration and time.

A total of 11,604 genes were found to be differentially expressed (DE) in the pair-wise comparisons between untreated and IFN-γ + TNF-α treated cells. The pair wise comparison with untreated cells identified 4105 DE at 1 ng/mL treatment and 7499 genes at 10 ng/mL treated with an overlap of total 3757 genes between the two cytokine treatment concentrations. Pairwise comparison of DE genes in a temporal manner identified 1527 genes DE at 4 hours, 1570 at 10 hours and 3733 after 16 hours of treatment at 1 ng/mL of IFN-γ + TNF-α (Figure 3.10 B). Compared to 1 ng/mL treatment, there were increased numbers of DE genes detected (approximately twice) at corresponding time points in the 10 ng/mL cytokine treatment group, with 2851 genes at 4 hours, 3525 at 10 hour and 6006 DE at 16-hour time point (Figure 3.10 B). To understand the significance and directionality of these differentially expressed genes, volcano plots were created with protein coding DE genes at both 1 and 10 ng/mL concentration and for individual time points (Figure 3.11 & 3.12). The DE genes were sorted after using a threshold q value (FDR < 0.01) and beta value (1) and visualised in red and the genes exclusively expressed at specific time point and cytokine concentration were highlighted in blue in the volcano plots and named as 'Unique' genes to that time point (Figures 3.11 and 3.12).

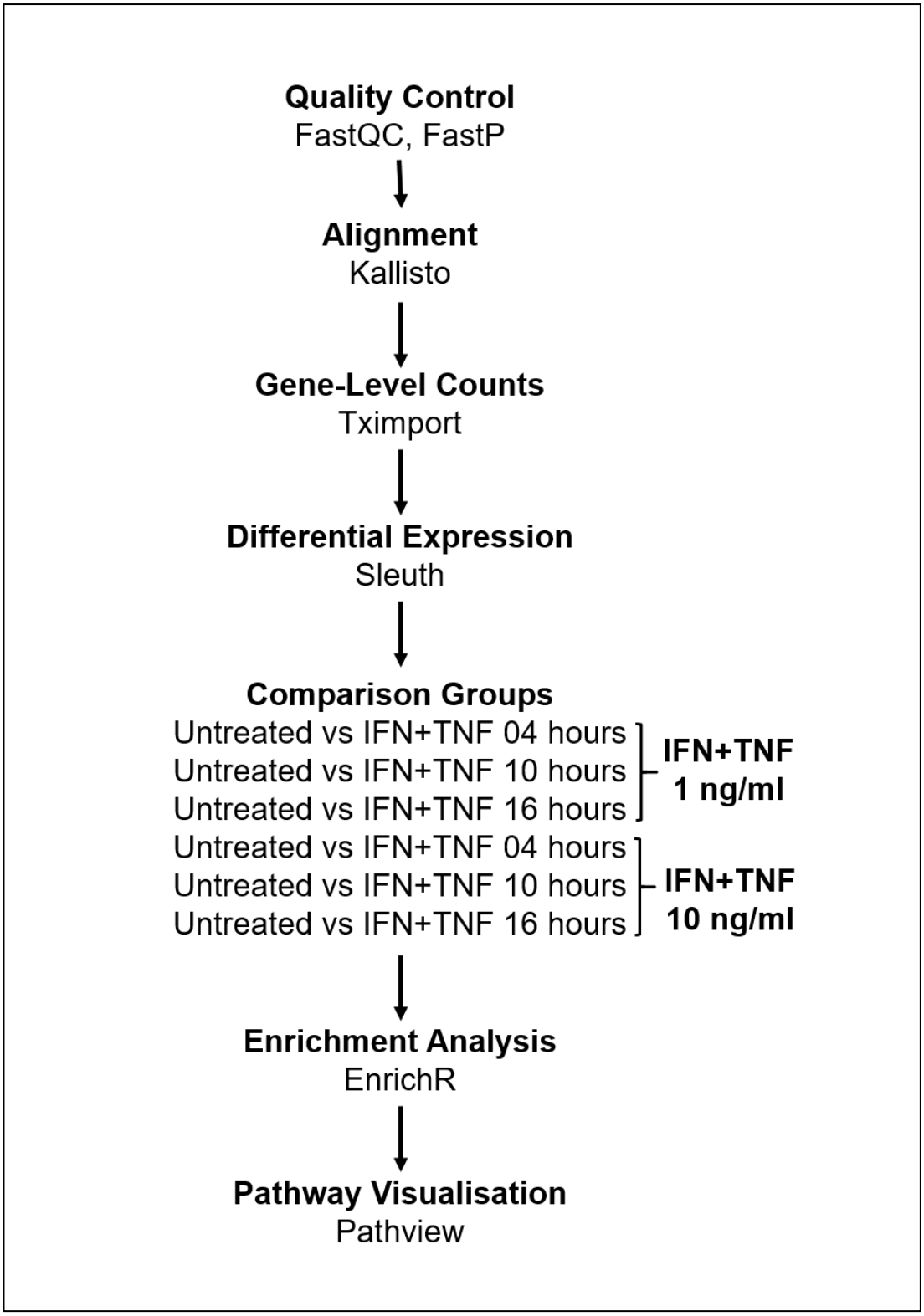


Figure 3.9 Bioinformatics pipeline describing the workflow and software used to identify differentially expressed genes from the RNA-Seq dataset

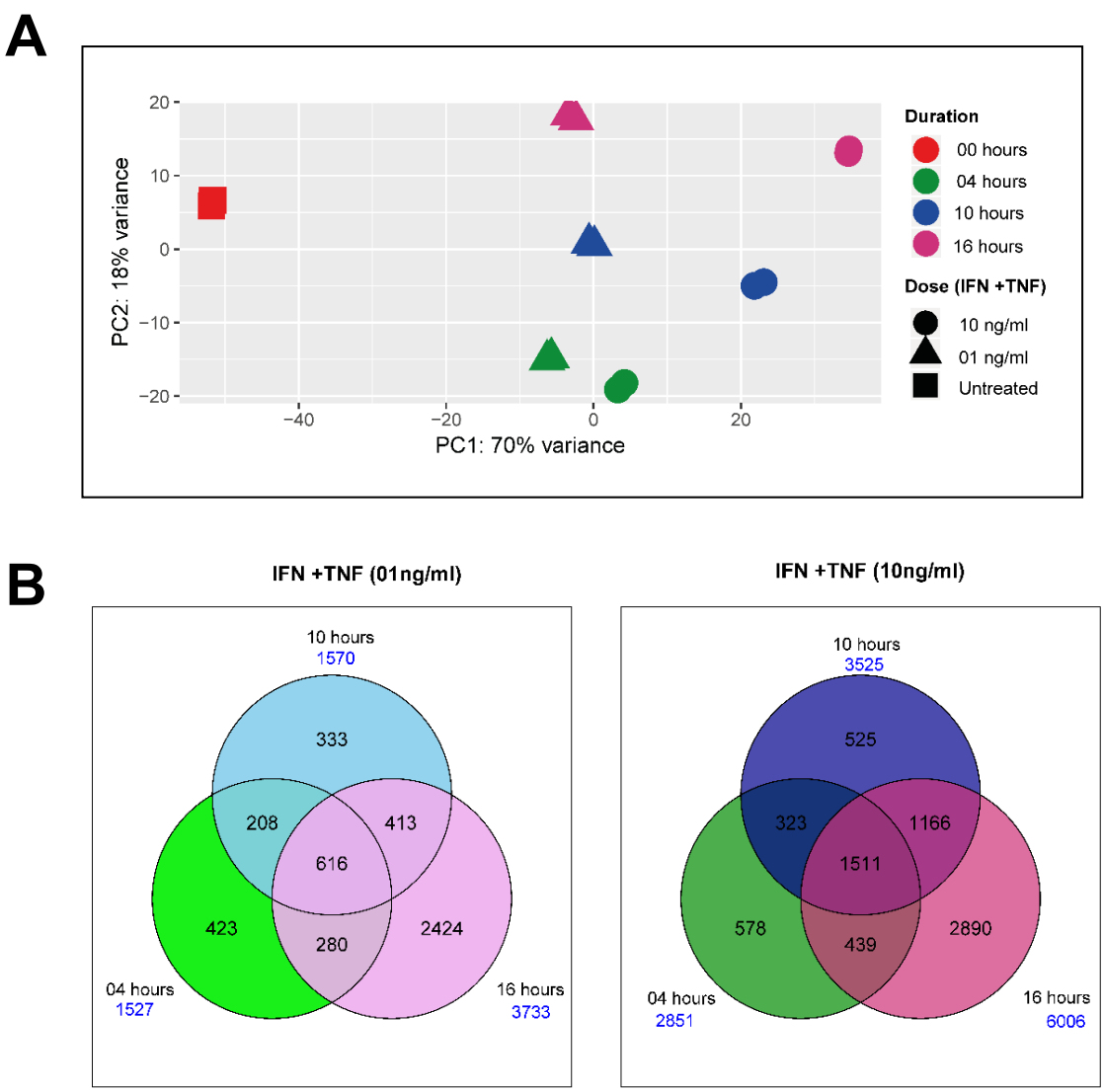


Figure 3.10 RNA-Seq identifies differences in gene regulation with cytokine concentration and duration of treatment

(A) Principal component analysis of differentially expressed genes in HT-29 cells with spatial representation of untreated and IFN-γ +TNF-α treated cells with respect of concentration and duration of treatment. Left, untreated cells were represented by Red, square. Circles represent 1 ng/mL treatments and triangles represent 10 ng/mL treatment. Duration of IFN-γ +TNF-α treatment was presented by green (4 hours), Blue (10 hours) and Magenta (16 hours) colours. The first principal component (PC1, X axis) explains 70.0% of the total variance of the dataset, while the second principal component (PC2, Y axis) explains 18% of the total variance of the dataset. (B) Venn diagram overlaps of genes differentially expressed at the q-value filter of 0.01 across different pairwise comparisons for 1 ng/mL and 10 ng/mL IFN-γ + TNF-α compared to the untreated samples.

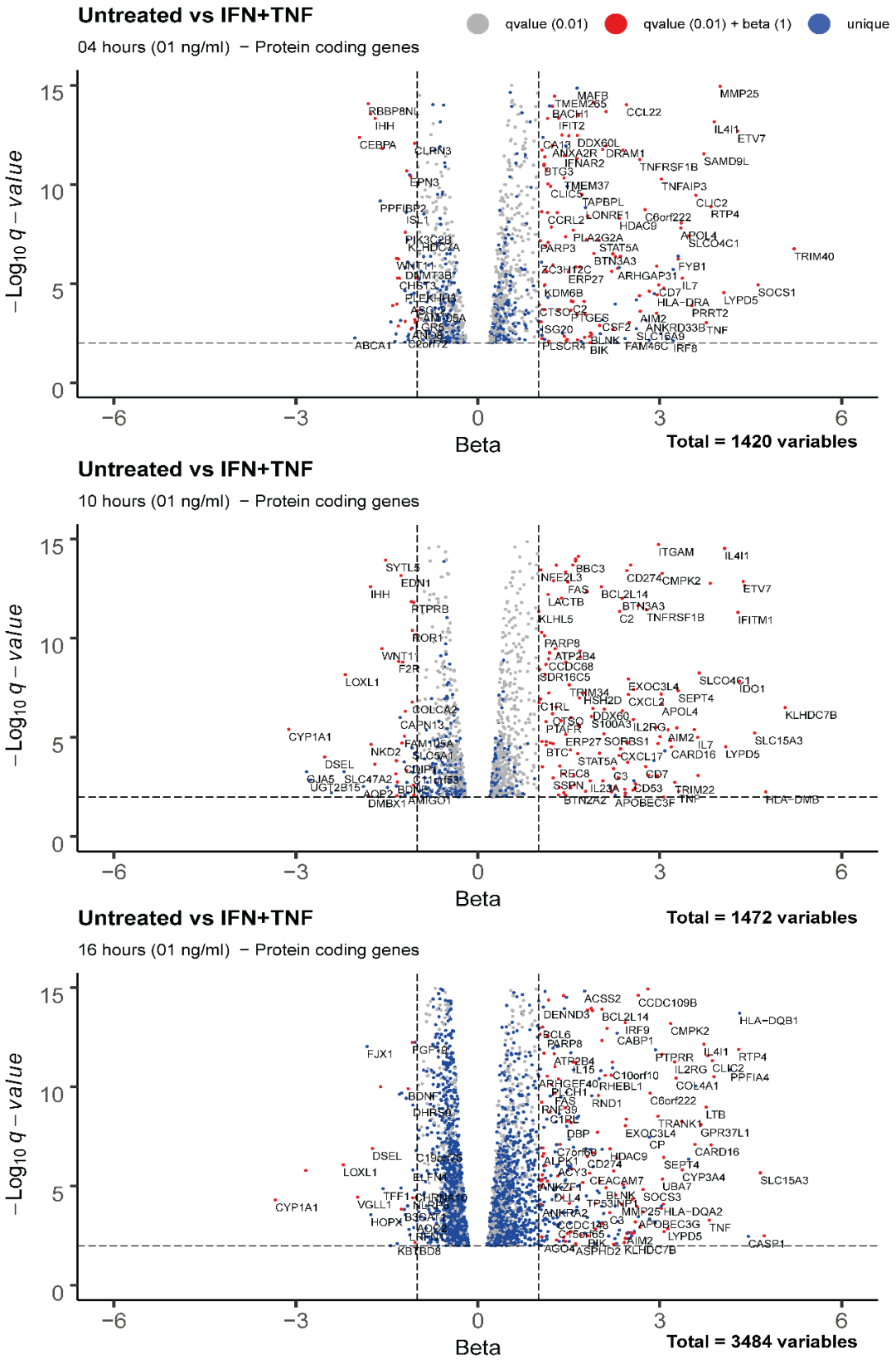


Figure 3.11 Volcano plots showing the differentially expressed protein-coding genes expressed at 04, 10, 16 hours after 1 ng/mL cytokine treatment

The differentially expressed genes obtained from pairwise comparison between 1 ng/mL treatment at 4 hours (top), 10 hours (centre) and 16 hours (bottom), compared with untreated cells were plotted as volcanic plot. The q value cut off <0.01 and beta value cut-off of 1 was used as a threshold. Genes coloured red represents genes that pass both the q-value and beta cut-offs. Whereas grey coloured genes have passed only the q-value cut off and not the beta value. The genes coloured in blue are those genes that are unique to this pairwise comparison from Figure 3.10B.

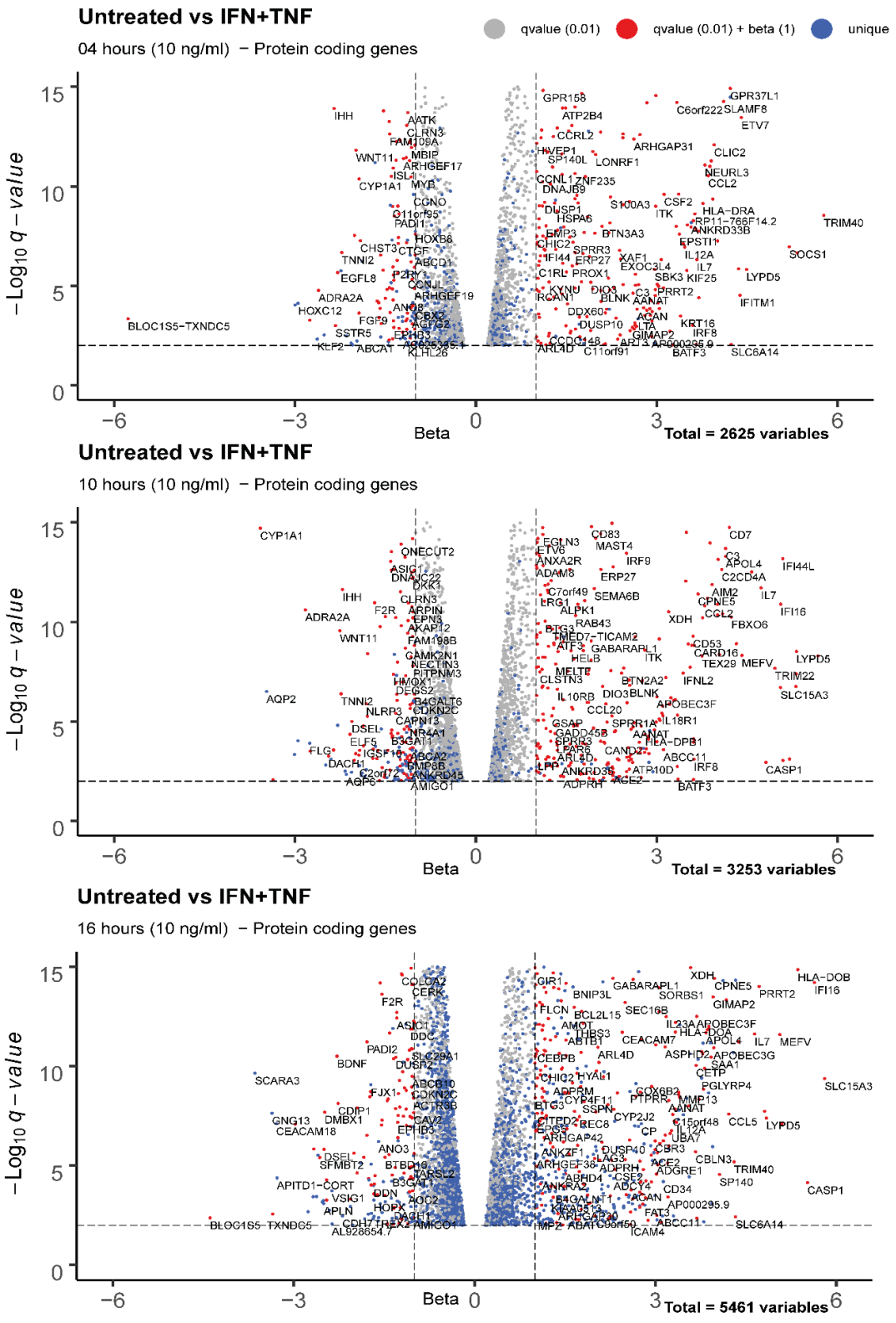


Figure 3.12. Volcano plots showing differentially expressed protein-coding genes expressed at 4, 10, 16 hours after 10 ng/mL cytokine treatment

The differentially expressed genes obtained from pairwise comparison between 10 ng/mL treatment at 4 hours (top), 10 hours (centre) and 16 hours (bottom), compared with untreated cells were plotted as volcanic plot. The q value cut off <0.01(Y-axis) and beta value cut-off (X-axis) of 1 was used as a threshold. Genes coloured red represents genes that pass both the q-value and beta cut-offs. Whereas grey coloured genes have passed only the q-value cut off and not the beta value. The genes coloured in blue are those genes that are unique to this pairwise comparison from Figure 3.10B.

3.4.7. The cytotoxic concentration of cytokines induced the differential expression of a unique set of genes at later time points post-cytokine treatment

To further explore the relationship of differentially expressed genes in a time and dose dependent manner, two different type of pairwise comparisons were performed. First pairwise comparison was performed across the time series in the same concentration group (comparing DE expressed at 4 vs 10 vs 16 hours for each concentration). Second comparison was performed for each time point across different concentration (e.g. comparing 1 ng/mL vs 10 ng/mL at 4, 10 or 16 hours). The Venn diagram in Figure 3.13A, represents overlaps of all DE gene comparisons within different time and concentration groups. As stated earlier, there was a substantial overlap observed between 1 and 10 ng/mL treatments with very a smaller number of genes exclusively expressed at low (1 ng/ml) concentration. While there were 3757 genes differentially expressed with 10 ng/mL treatment group (exclusive to 10 ng/ml treatment) and were not expressed at low concentration.

Comparing the DE genes at 10 ng/mL treatment in a time dependent manner identified a maximum number of genes expressed at late point (6006 DE genes), where there were 1451 DE genes unique to 16 hours of the 10 ng/mL IFN-γ+TNF-α treatment group (Figure 3.13A). Further separating these genes identified that there were 1223 protein coding genes among these 1451 unique genes. These uniquely expressed protein coding genes were plotted as a volcanic plot (q value cut off (<0.01) and beta value (=1)) to understand the directionality and expression level. As we have previously observed that prolonged activation of STAT1 pY701 is crucial for the

induction of CRC cell death, we focused our analysis to identify the role or involvement of these late uniquely expressed genes in cell death.

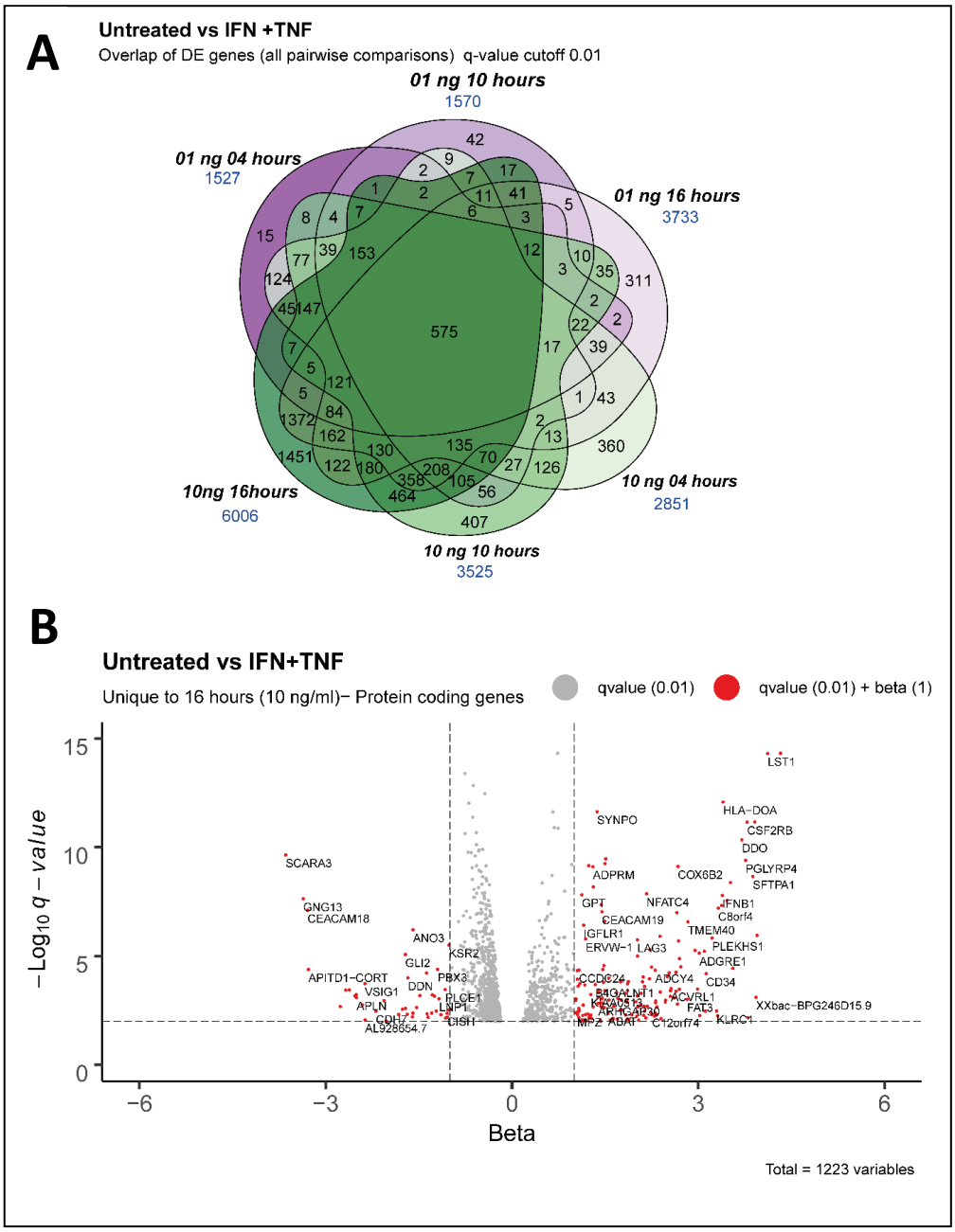


Figure 3.13 RNA-Seq identified expression of unique set of genes at 16-hour time point with 10 ng/mL concentration of IFN-γ + TNF-α

A) Venn diagram representing the overlap of differentially expressed genes obtained by pairwise comparison of cells treated with different treatments groups as indicated (i.e. 1 ng/mL and 10 ng/mL IFN-γ + TNF-α at 4 hour, 10 hour and 16 hour time point) with untreated cells. B) Volcano plot showing the differentially expressed protein coding genes (q-value filter 0.01) unique to 16 hours treatment with 10 ng/mL IFN-γ + TNF-α treatment.

3.4.8. IFN-γ and TNF-α induced late genes are associated with the induction of multiple cell death pathways

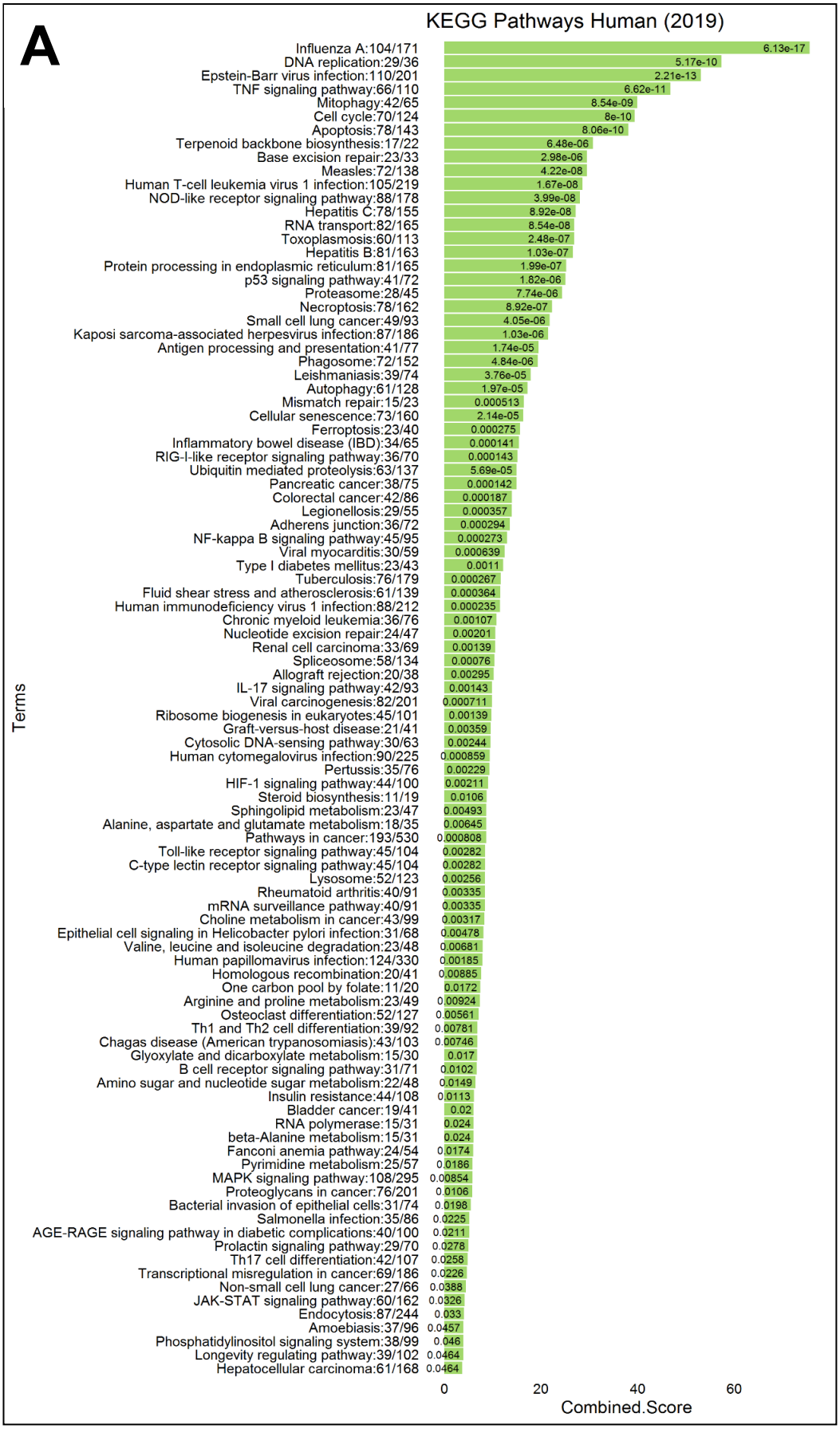
We have already shown that sustained activation of the JAK1/2-STAT1 pathway is essential for cytokine-induced CRC cell death. Therefore, to understand whether this sustained activation of STAT1 is associated with the activation and suppression of biologically relevant late genes, **all late genes** (the genes differentially expressed after 16 hours treatment with 10 ng/mL and of IFN-γ + TNF-α treatment) and **unique late genes** (genes differentially expressed exclusively at 16-hour time point with 10 ng/mL IFN-γ + TNF-α treatment) were subjected to gene ontology analysis and KEGG pathway enrichment analysis (Figure. 3.12 A & B). KEGG pathway analysis identified the involvement of late differentially expressed genes in multiple classical cell death pathways including apoptosis, necroptosis, ferroptosis, and related pathways such as autophagy, protein processing in endoplasmic reticulum, phagosome and lysosome functions and mitophagy. The late genes involved in these cell death pathways were further visualised by using clustergram and Pathview pathways (Figure 3.13 & 3.14).

Notably, several genes associated with these cell death pathways were differentially expressed at the 16-hour time point in the 10 ng/mL cytokine treatment group only. For instance, the expression of anti-apoptotic protein *Bcl-2* was downregulated at late time points. Other than that several other important genes such as ferritin light chain-*FTL* (necroptosis and ferroptosis), solute carrier family 25 member 1- *SLC25A,* heat shock protein-90 - *HSP90AA* (necroptosis), voltage-dependent anion channel-*VDAC* (ferroptosis), *ATG3* (autophagy), FUN14 domain containing-1 -*FUNDC1* and casein kinase-2 alpha -*CK2α* (mitophagy) were downregulated uniquely at 16h. while, transient receptor potential melastatin

related-7 -*TRPM7,* (necroptosis), autophagy-related 7- *ATG7*, *ATG16* (autophagy) spermidine/spermine N1-acetyltransferase family member-2 - *SAT2* (ferroptosis), major histocompatibility complex, class II, DO Alpha - HLA-DOA, neutrophil cytosolic factor-2 - NCF2, NCF4 and surfactant srotein-A1- SFTPA1 (NADPH oxidation during phagosome formation) were upregulated only at 16 hour time point in 10 ng/mL IFN-γ +TNF a treatment (Figure 3.16 I-VI).

Furthermore, the KEGG pathway analysis of unique genes expressed at late time point (Figure 3.14B) identified their association with tricarboxylic acid cycle (TCA) cycle, oxidative phosphorylation, cellular metabolism, and mitochondrial activity. There were 7 genes out of 30 genes associated with TCA cycle and 16 genes out of 133 genes associated with oxidative phosphorylation that were differentially expressed at 16-hour time point in 10 ng/mL treatment group. Most of these genes were downregulated in response to IFN-γ + TNF-α treatment suggesting impaired mitochondrial functions and cellular activities at late time points. (Fig 3.16 VII-IX). Other than that, the clustering of these unique genes was also noted in the formation of spliceosome complex. 23 out of 134 genes associated with spliceosome complex were observed to be differentially expressed at late time point in cytokine treated cells. Interestingly, several genes associated with different components of spliceosome complex including Small Nuclear Ribonucleoprotein Polypeptide F (SNRPF), Small Nuclear Ribonucleoprotein Polypeptide C (SNRPC), Splicing Factor 3b Subunit 4 (SF3B4), DExD-Box Helicase 39B (DDX39B), U6 snRNA-associated Sm-like protein (LSM5) and Ubiquitin Specific Peptidase 9 (USP9) etc. were upregulated in the cells treated with higher concentration of IFN-γ + TNF-α for 16 hours, suggesting an enhanced transcriptional activity in the cells in response of cytokine treatment

and in turn sustained activation of JAK-STAT signalling pathway. Taken together, sustained activation of STAT1 mediates expression of unique gene set at late time point associated with downregulation of metabolic activity and upregulation of several cell death pathways.


A
KEGG Pathways Human (2019)
Terms
Influenza A:104/171 6.13e-17
DNA replication:29/36 5.17e-10
Epstein-Barr virus infection:110/201 2.21e-13
TNF signaling pathway:66/110 6.62e-11
Mitophagy:42/65 8.54e-09
Cell cycle:70/124 8e-10
Apoptosis:78/143 8.06e-10
Terpenoid backbone biosynthesis:17/22 6.48e-06
Base excision repair:23/33 2.98e-06
Measles:72/138 4.22e-08
Human T-cell leukemia virus 1 infection:105/219 1.67e-08
NOD-like receptor signaling pathway:88/178 3.99e-08
Hepatitis C:78/155 8.92e-08
RNA transport:82/165 8.54e-08
Toxoplasmosis:60/113 2.48e-07
Hepatitis B:81/163 1.03e-07
Protein processing in endoplasmic reticulum:81/165 1.99e-07
p53 signaling pathway:41/72 1.82e-06
Proteasome:28/45 7.74e-06
Necroptosis:78/162 8.92e-07
Small cell lung cancer:49/93 4.05e-06
Kaposi sarcoma-associated herpesvirus infection:87/186 1.03e-06
Antigen processing and presentation:41/77 1.74e-05
Phagosome:72/152 4.84e-06
Leishmaniasis:39/74 3.76e-05
Autophagy:61/128 1.97e-05
Mismatch repair:15/23 0.000513
Cellular senescence:73/160 2.14e-05
Ferroptosis:23/40 0.000275
Inflammatory bowel disease (IBD):34/65 0.000141
RIG-I-like receptor signaling pathway:36/70 0.000143
Ubiquitin mediated proteolysis:63/137 5.69e-05
Pancreatic cancer:38/75 0.000142
Colorectal cancer:42/86 0.000187
Legionellosis:29/55 0.000357
Adherens junction:36/72 0.000294
NF-kappa B signaling pathway:45/95 0.000273
Viral myocarditis:30/59 0.000639
Type I diabetes mellitus:23/43 0.0011
Tuberculosis:76/179 0.000267
Fluid shear stress and atherosclerosis:61/139 0.000364
Human immunodeficiency virus 1 infection:88/212 0.000235
Chronic myeloid leukemia:36/76 0.00107
Nucleotide excision repair:24/47 0.00201
Renal cell carcinoma:33/69 0.00139
Spliceosome:58/134 0.00076
Allograft rejection:20/38 0.00295
IL-17 signaling pathway:42/93 0.00143
Viral carcinogenesis:82/201 0.000711
Ribosome biogenesis in eukaryotes:45/101 0.00139
Graft-versus-host disease:21/41 0.00359
Cytosolic DNA-sensing pathway:30/63 0.00244
Human cytomegalovirus infection:90/225 0.000859
Pertussis:35/76 0.00229
HIF-1 signaling pathway:44/100 0.00211
Steroid biosynthesis:11/19 0.0106
Sphingolipid metabolism:23/47 0.00493
Alanine, aspartate and glutamate metabolism:18/35 0.00645
Pathways in cancer:193/530 0.000808
Toll-like receptor signaling pathway:45/104 0.00282
C-type lectin receptor signaling pathway:45/104 0.00282
Lysosome:52/123 0.00256
Rheumatoid arthritis:40/91 0.00335
mRNA surveillance pathway:40/91 0.00335
Choline metabolism in cancer:43/99 0.00317
Epithelial cell signaling in Helicobacter pylori infection:31/68 0.00478
Valine, leucine and isoleucine degradation:23/48 0.00681
Human papillomavirus infection:124/330 0.00185
Homologous recombination:20/41 0.00885
One carbon pool by folate:11/20 0.0172
Arginine and proline metabolism:23/49 0.00924
Osteoclast differentiation:52/127 0.00561
Th1 and Th2 cell differentiation:39/92 0.00781
Chagas disease (American trypanosomiasis):43/103 0.00746
Glyoxylate and dicarboxylate metabolism:15/30 0.017
B cell receptor signaling pathway:31/71 0.0102
Amino sugar and nucleotide sugar metabolism:22/48 0.0149
Insulin resistance:44/108 0.0113
Bladder cancer:19/41 0.02
RNA polymerase:15/31 0.024
beta-Alanine metabolism:15/31 0.024
Fanconi anemia pathway:24/54 0.0174
Pyrimidine metabolism:25/57 0.0186
MAPK signaling pathway:108/295 0.00854
Proteoglycans in cancer:76/201 0.0106
Bacterial invasion of epithelial cells:31/74 0.0198
Salmonella infection:35/86 0.0225
AGE-RAGE signaling pathway in diabetic complications:40/100 0.0211
Prolactin signaling pathway:29/70 0.0278
Th17 cell differentiation:42/107 0.0258
Transcriptional misregulation in cancer:69/186 0.0226
Non-small cell lung cancer:27/66 0.0388
JAK-STAT signaling pathway:60/162 0.0326
Endocytosis:87/244 0.033
Amoebiasis:37/96 0.0457
Phosphatidylinositol signaling system:38/99 0.046
Longevity regulating pathway:39/102 0.0464
Hepatocellular carcinoma:61/168 0.0464
0
20
40
60
Combined.Score

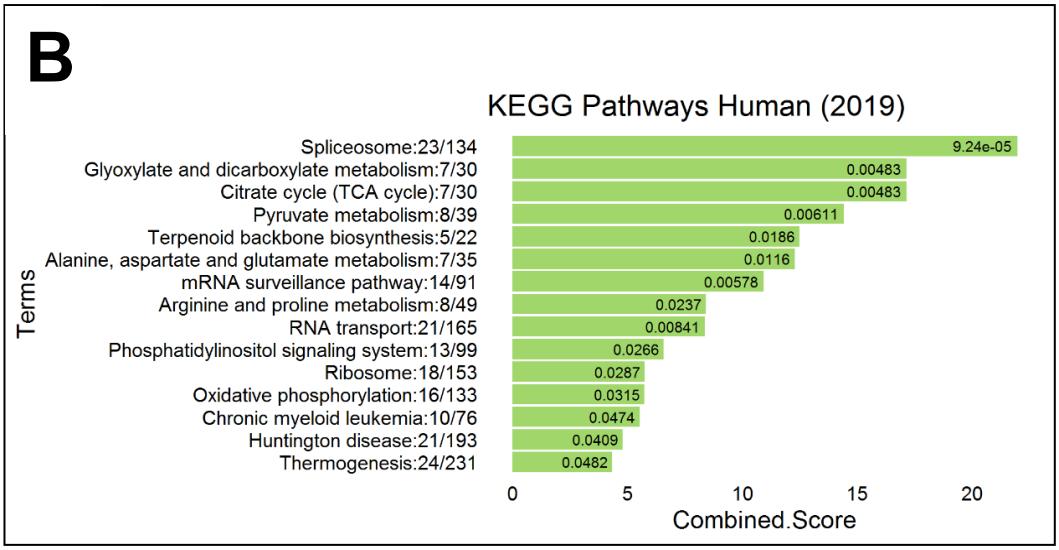


Figure 3.14. Functional analysis of genes differentially expressed at late time point (16-hour) with 10 ng/mL IFN-γ +TNF-α treatment

(A) All differentially expressed genes identified from RNA-Seq after 16 hours with 10ng/mL IFN-γ + TNF-α treatment (B) Differentially expressed genes identified as unique to 16 hour time point and 10 ng/mL treatment, were evaluated for functional enrichment using KEGG pathway analysis. The enriched pathways were filtered with a nominal p value cut-off of 0.05. The pathways are sorted based on combined score metric of EnrichR with the best ranking enriched pathway at the top. The number specified beside the KEGG terms represents the number of gene overlap by total number of genes in the term. The numbers displayed on the bar represent nominal p.value.

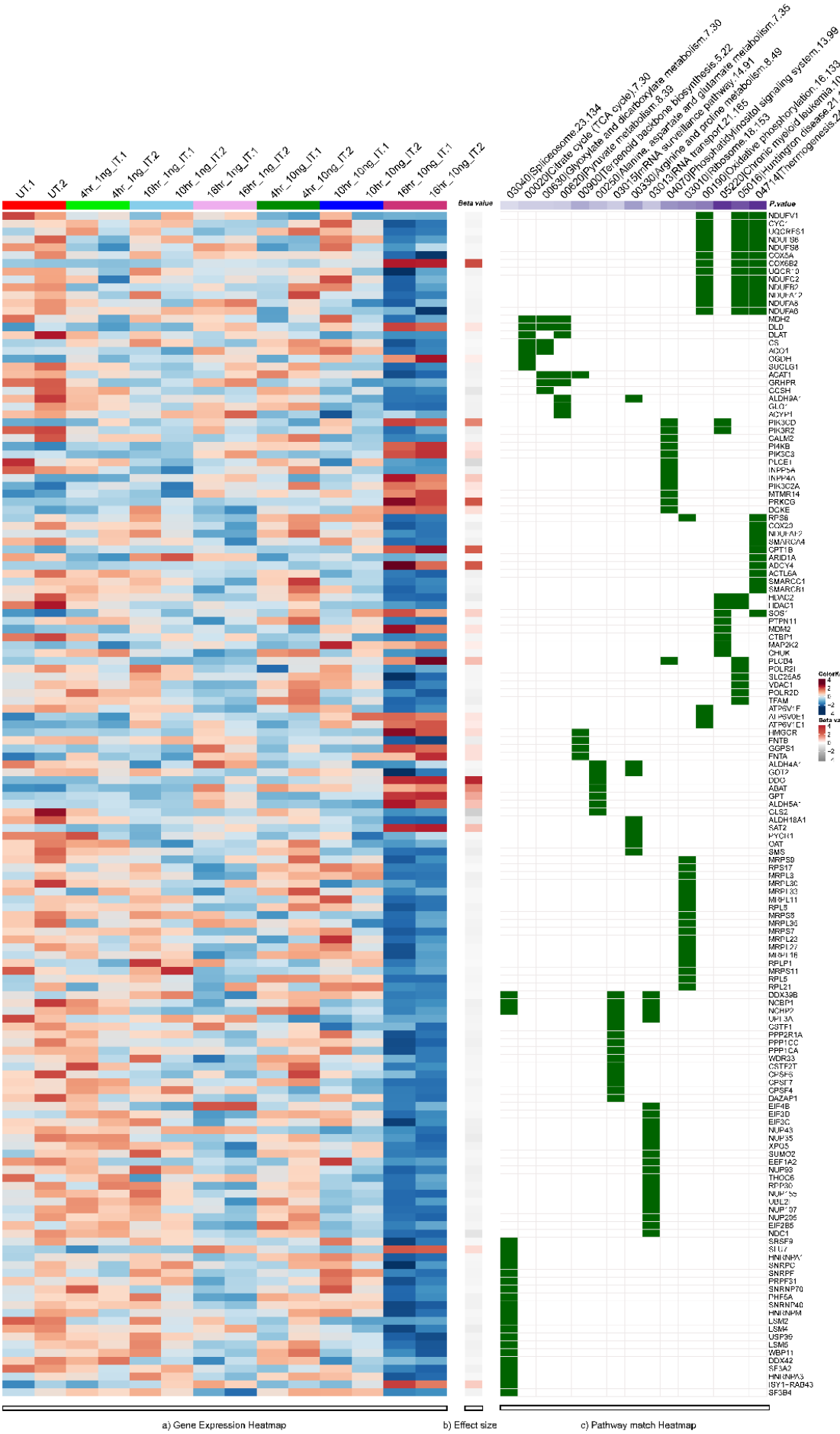

UT.1
UT.2
4hr_1ng_IT.1
4hr_1ng_IT.2
10hr_1ng_IT.1
10hr_1ng_IT.2
16hr_1ng_IT.1
16hr_1ng_IT.2
4hr_10ng_IT.1
4hr_10ng_IT.2
10hr_10ng_IT.1
10hr_10ng_IT.2
16hr_10ng_IT.1
16hr_10ng_IT.2
Beta value
P.value
03040|Spliceosome,23,134
00020|Citrate cycle (TCA cycle),7,30
00630|Glyoxylate and dicarboxylate metabolism,8,39
00620|Pyruvate metabolism,8,33
00900|Terpenoid backbone biosynthesis,5,22
00250|Alanine, aspartate and glutamate metabolism,7,30
03015|mRNA surveillance pathway,14,91
00330|Arginine and proline metabolism,8,49
03013|RNA transport,21,165
04070|Phosphatidylinositol signaling system,13,99
03010|Ribosome,18,153
05220|Chronic myeloid leukemia,16,133
00190|Oxidative phosphorylation,16,133
05016|Huntington disease,21,193
04714|Thermogenesis,24,231
NDUFV1
CYC
UQCRFS1
NDUFS6
NDUFS8
COX5A
COX6B2
UQCR10
NDUFC2
NDUFB7
NDUFA2
NDUFA8
NDUFA6
MDH2
DLD
DLAT
CS
ACO2
OGDH
SUCLG1
ACAT1
GRHPR
CCSH
ALDH9A1
GLO1
AOXP1
PIK3CD
PIK3R2
CALM2
PI4KB
PIK3C3
PLCE1
INPP5A
INPP4A
PIK3CA
MTMR14
PRKCB
DCKE
RPS6
COX20
NDUFA12
SMARCA4
CPT1B
ARID1A
ADCY4
ACTL6A
SMARCC1
SMARCB1
HDAC2
HDAC1
SOS1
PTPN11
MDM2
CTBP1
MAP2K2
CHUK
PLCD4
POLR2I
SLC25A5
VDAC1
POLR2D
TFAM
ATP5VF
ATP5VD1
ATP5VC1
HMGCR
FNTB
GGPS1
FNTA
ALDH4A1
GOT2
DDC
ADAT
GPT
ALDH5A1
CLS2
ALDH18A1
SAT2
PYCR1
OAT
SMS
MRPS9
RPS17
MRPL3
MRPL30
MRPL33
MRPL11
RPL8
MRPS5
MRPL39
MRPS7
MRPL23
MRPL27
MRPL16
RPLP1
MRPS11
RPL5
RPL21
DDX39B
NCBP1
NCHP2
UPF3A
GSTF1
PPP2R1A
PPP1CC
PPP1CA
WDR33
CSTF2T
CPSF6
CPSF7
CPSF4
DAZAP1
EIF4B
EIF3D
EIF2C
NUP43
NUP35
XPO5
SUMO2
EEF1A2
NUP93
THOC5
RPP30
NUP155
UBL3
NUP107
NUP205
EIF2B5
NDC1
SRSF9
SNRPB
SNRPC
SNRPF
PRPF31
SNRNP70
PHF5A
SNRNP40
LSM2
LSM4
USP39
LSM5
WBP11
DDX42
SF3A2
ISY1-RAB43
SF3B4
ColorKey
samples
Beta value
P.value
Pathway-match
a) Gene Expression Heatmap
b) Effect size
c) Pathway match Heatmap

Figure 3.15 Multipaneled heatmap representing the expression profile of unique genes expressed at 16-hour time point with 10 ng/mL treatment

(Left) from the enriched pathways in the unique dataset (Figure 7), heatmap of beta values (middle) from DE pairwise comparison of untreated vs 10ng.16h, clustergram (right) denoting the presence or absence of these genes in the enriched pathways.

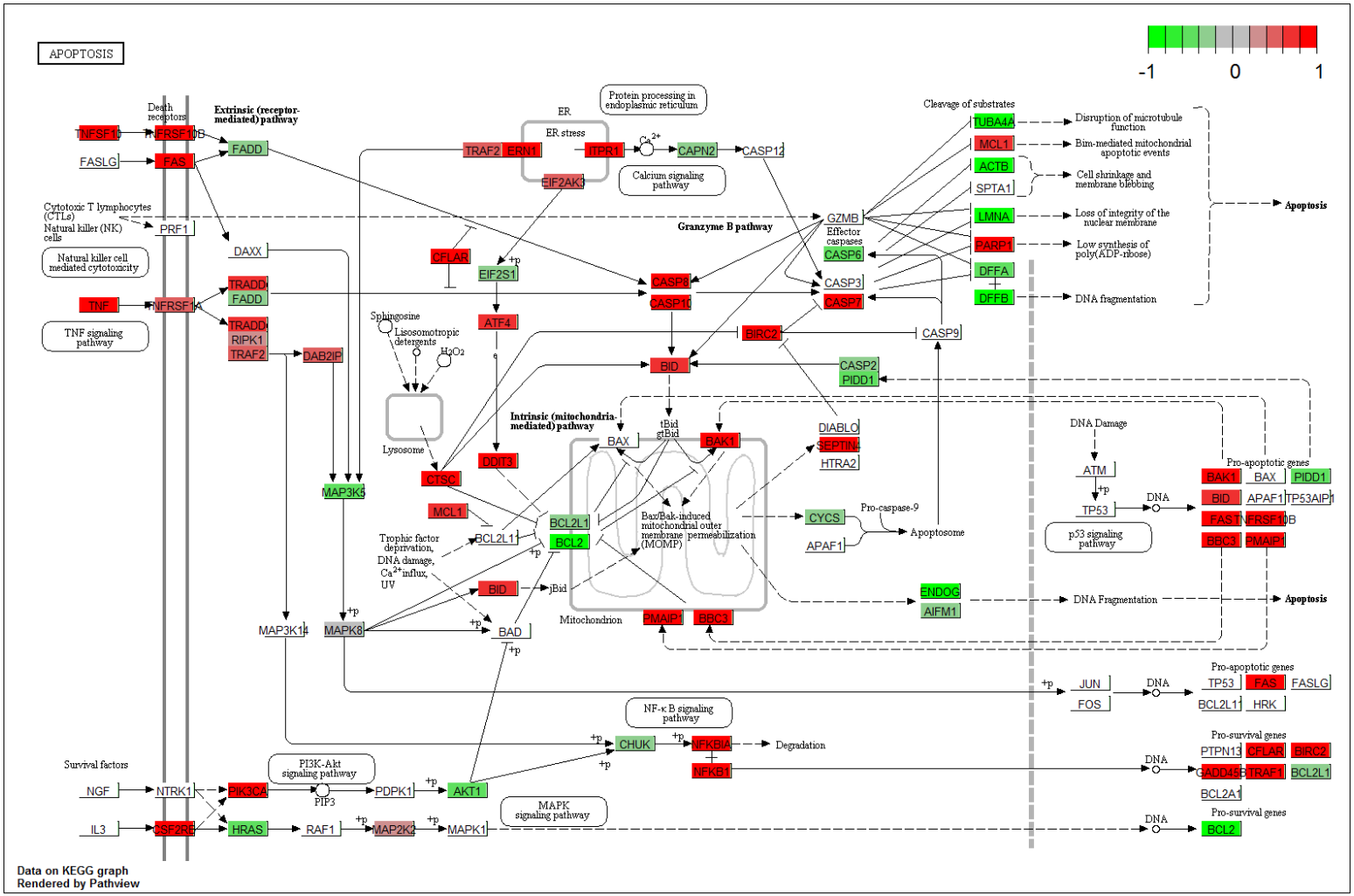


Figure 3.16 (I) APOPTOSIS: (A) Apoptosis pathway in HT-29 cells treated with 10 ng/mL IFN+TNF for 16 hours. Expression changes of target genes are mapped by colours; green colour—statistically significant increase in expression, red colour—statistically significant decrease in expression, grey colour—expression statistically insignificant

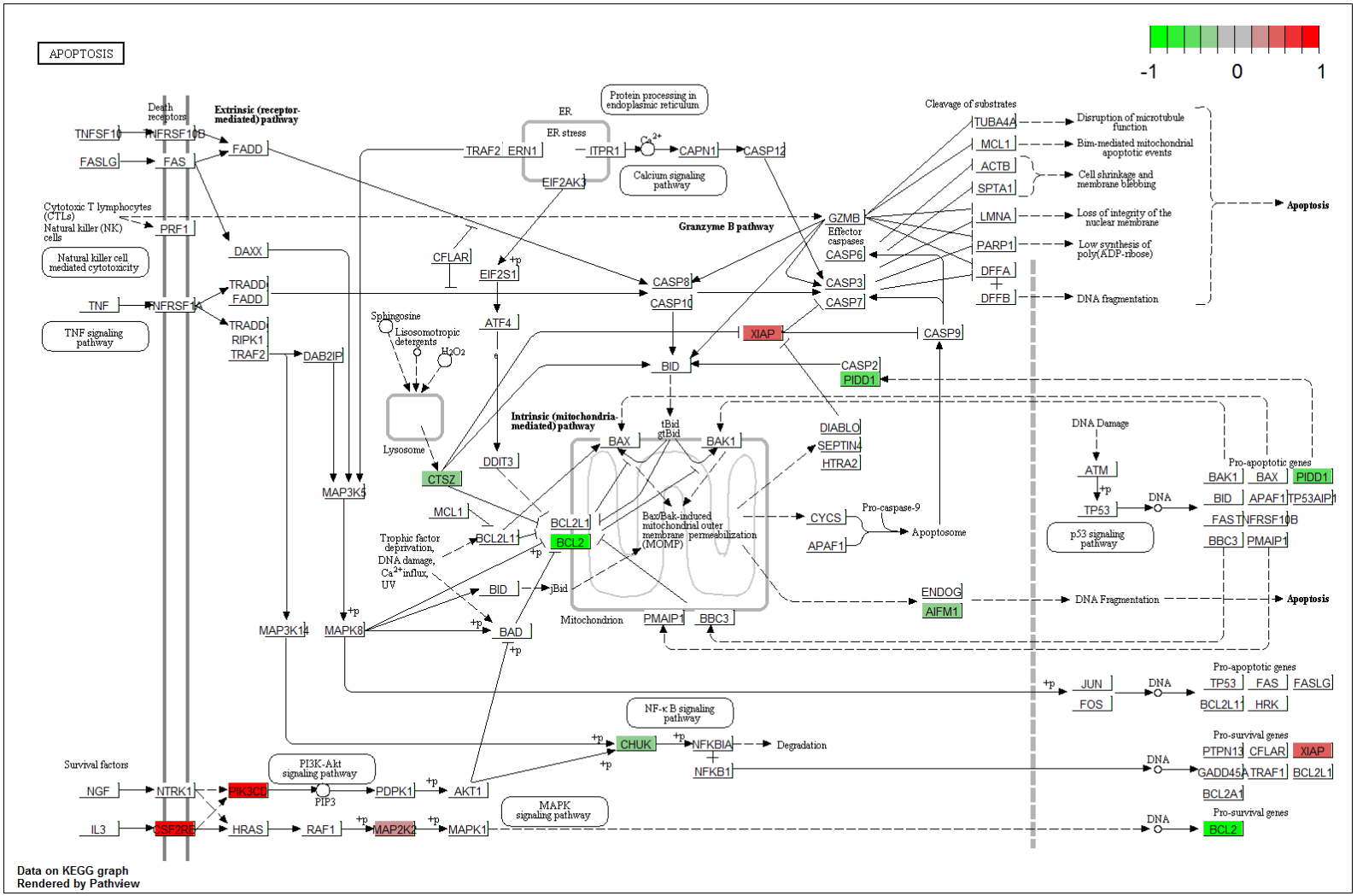


Figure 3.16 (I) APOPTOSIS: (B) Apoptosis pathway in HT-29 cells treated with 1 ng/mL IFN+TNF for 16 hours. Expression changes of target genes are mapped by colours; green colour—statistically significant increase in expression, red colour—statistically significant decrease in expression, grey colour—expression statistically insignificant

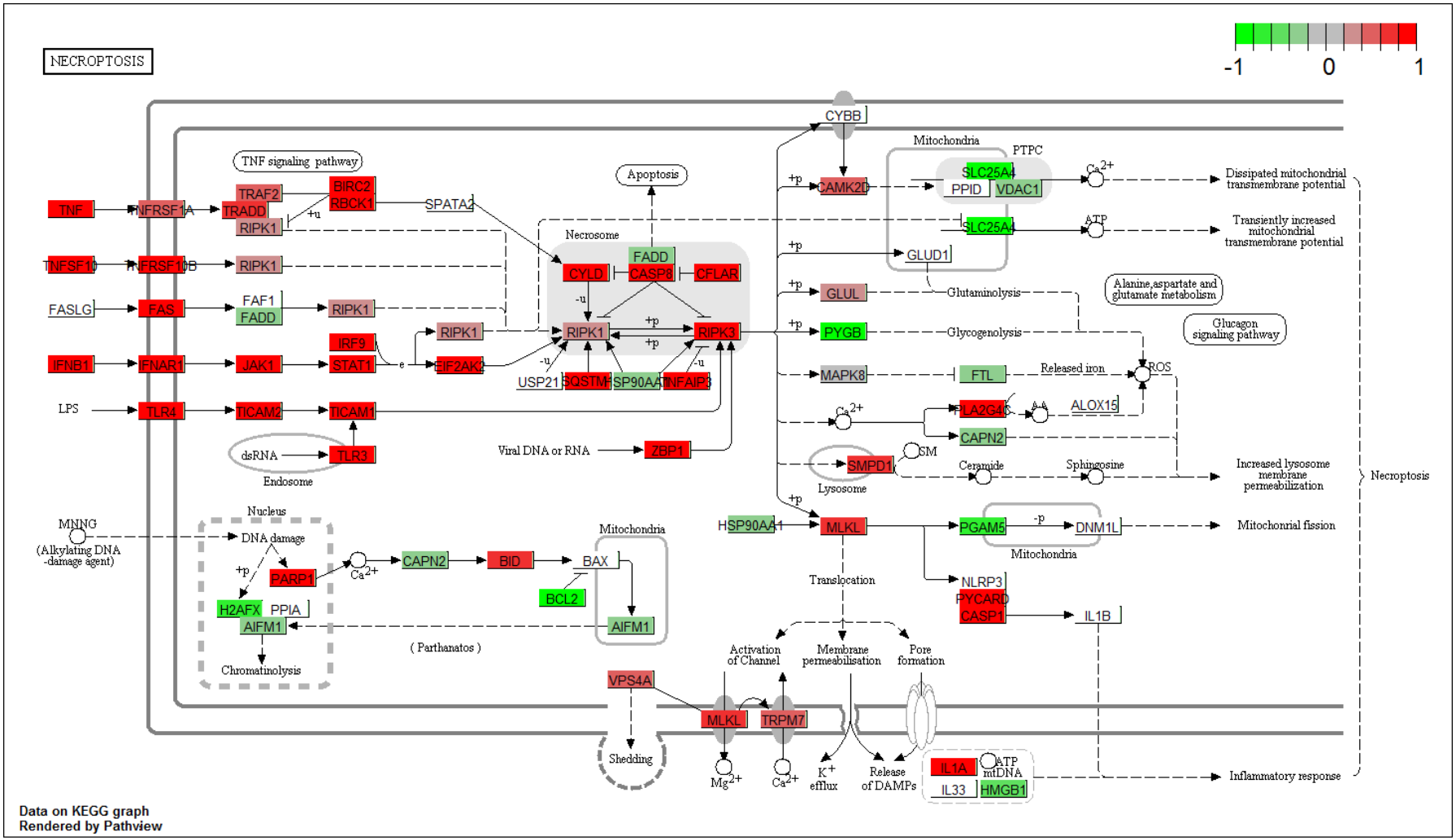


Figure 3.16 (II) NECROPTOSIS: (A) Necroptosis pathway in HT-29 cells treated with 10 ng/mL IFN+TNF for 16 hours. Expression changes of target genes are mapped by colours; green colour—statistically significant increase in expression, red colour—statistically significant decrease in expression, grey colour—expression statistically insignificant

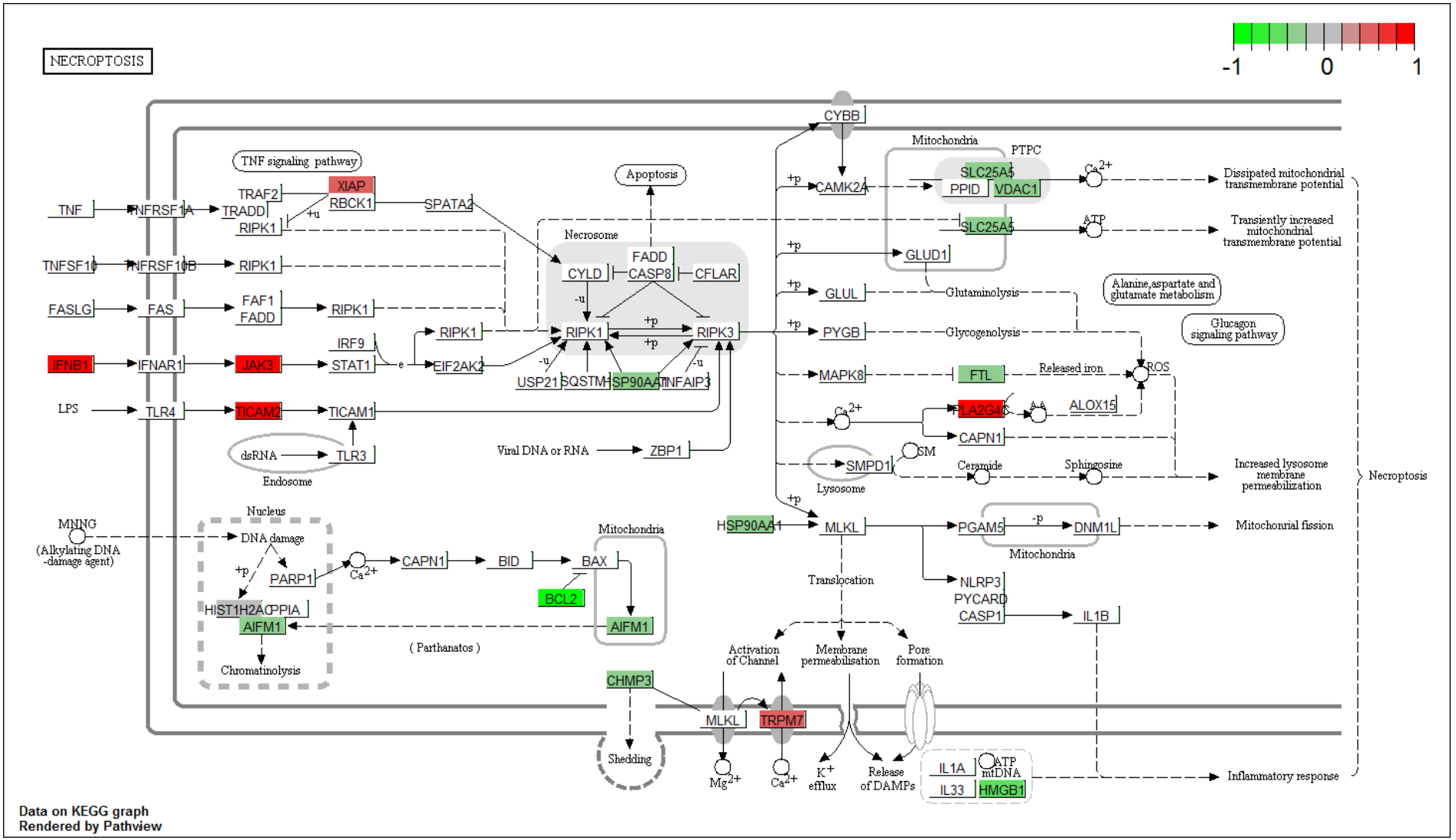


Figure 3.16 (II) NECROPTOSIS: (B) Necroptosis pathway in HT-29 cells treated with 1 ng/mL IFN+TNF for 16 hours. Expression changes of target genes are mapped by colours; green colour—statistically significant increase in expression, red colour—statistically significant decrease in expression, grey colour—expression statistically insignificant

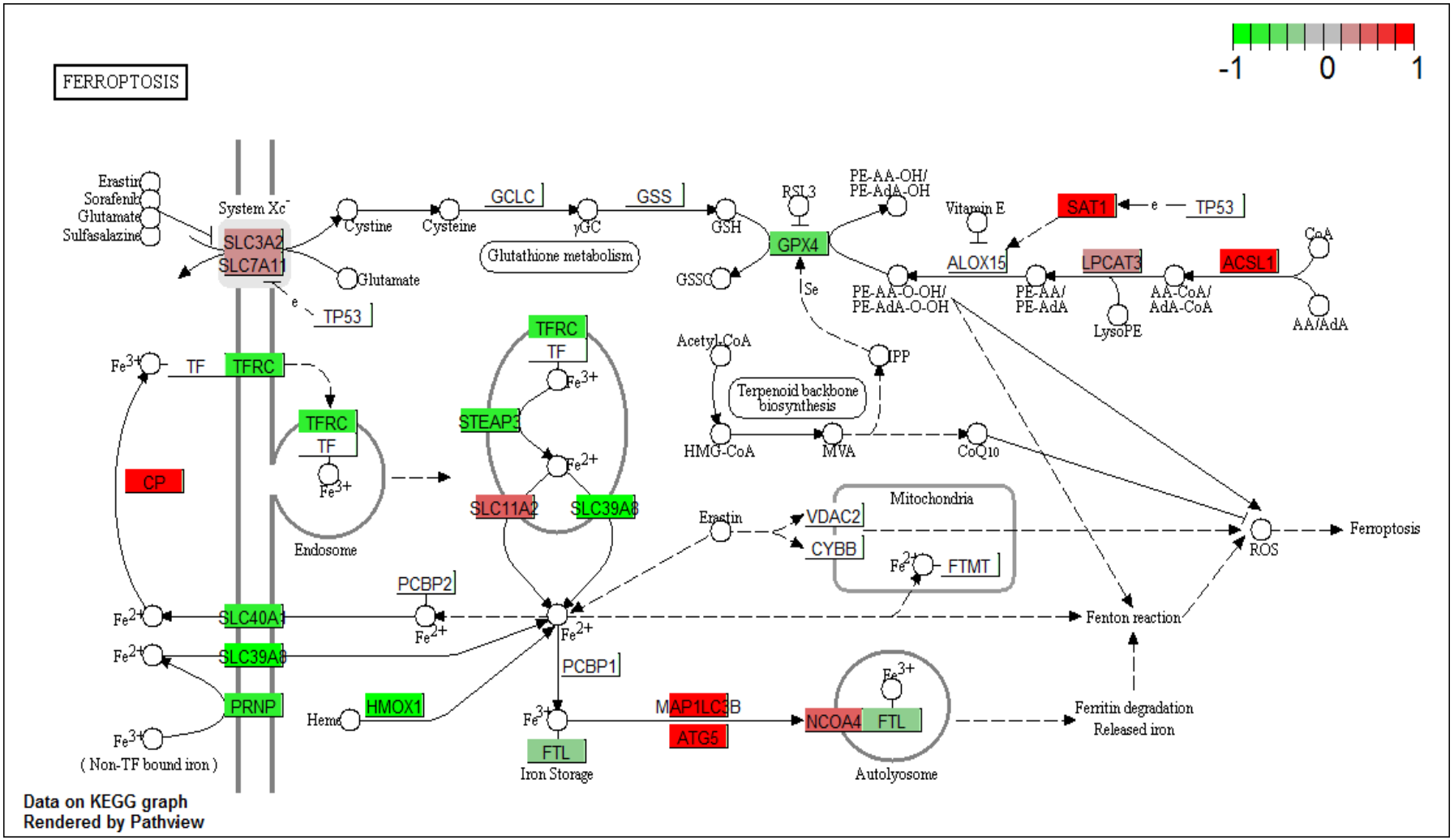


Figure 3.16 (III) FERROPTOSIS: (A) Ferroptosis pathway in HT-29 cells treated with 10 ng/mL IFN+TNF for 16 hours. Expression changes of target genes are mapped by colours; green colour—statistically significant increase in expression, red colour—statistically significant decrease in expression, grey colour—expression statistically insignificant

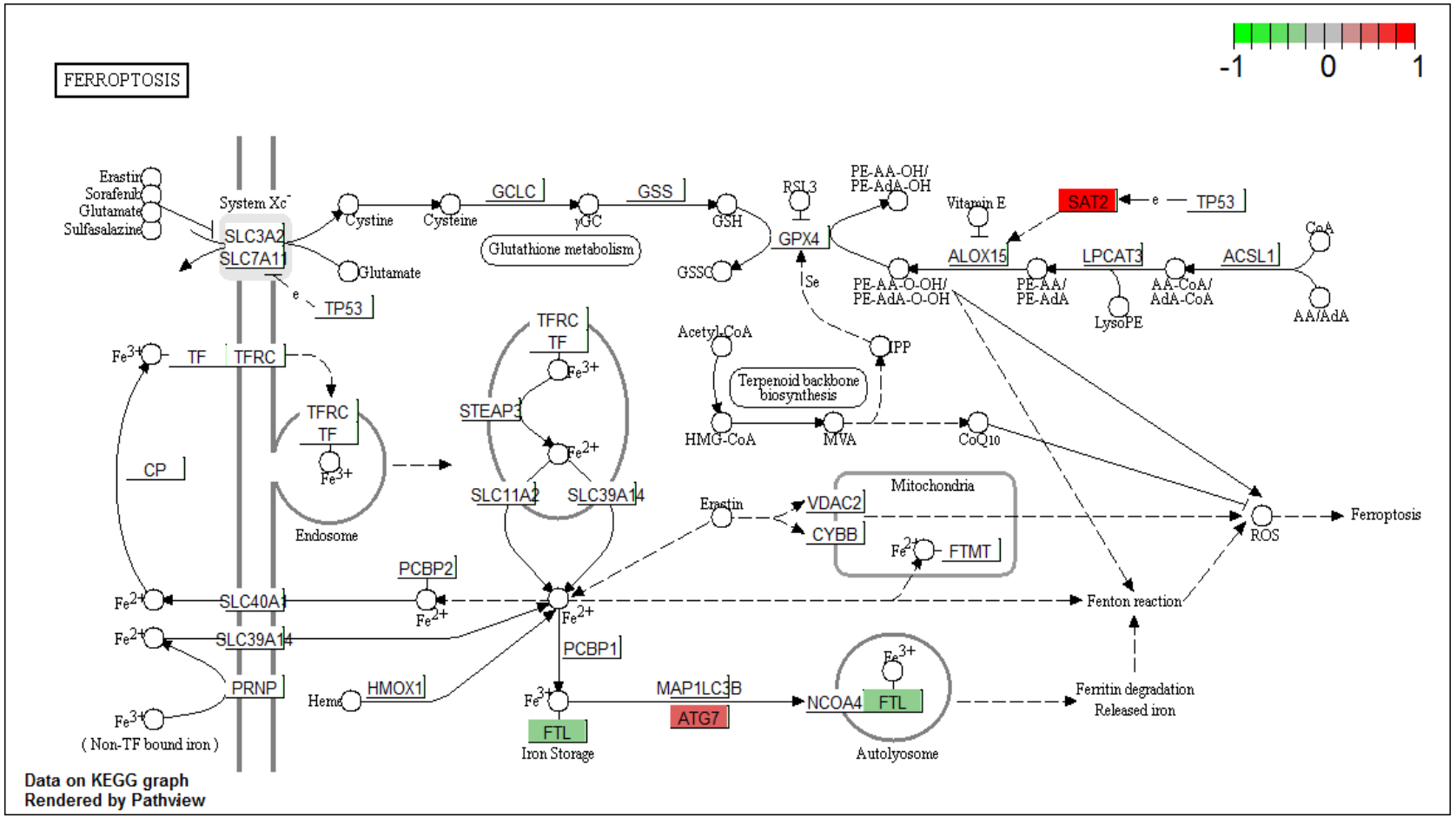


Figure 3.16 (III) FERROPTOSIS: (B) Ferroptosis pathway in HT-29 cells treated with 1 ng/mL IFN+TNF for 16 hours. Expression changes of target genes are mapped by colours; green colour—statistically significant increase in expression, red colour—statistically significant decrease in expression, grey colour—expression statistically insignificant

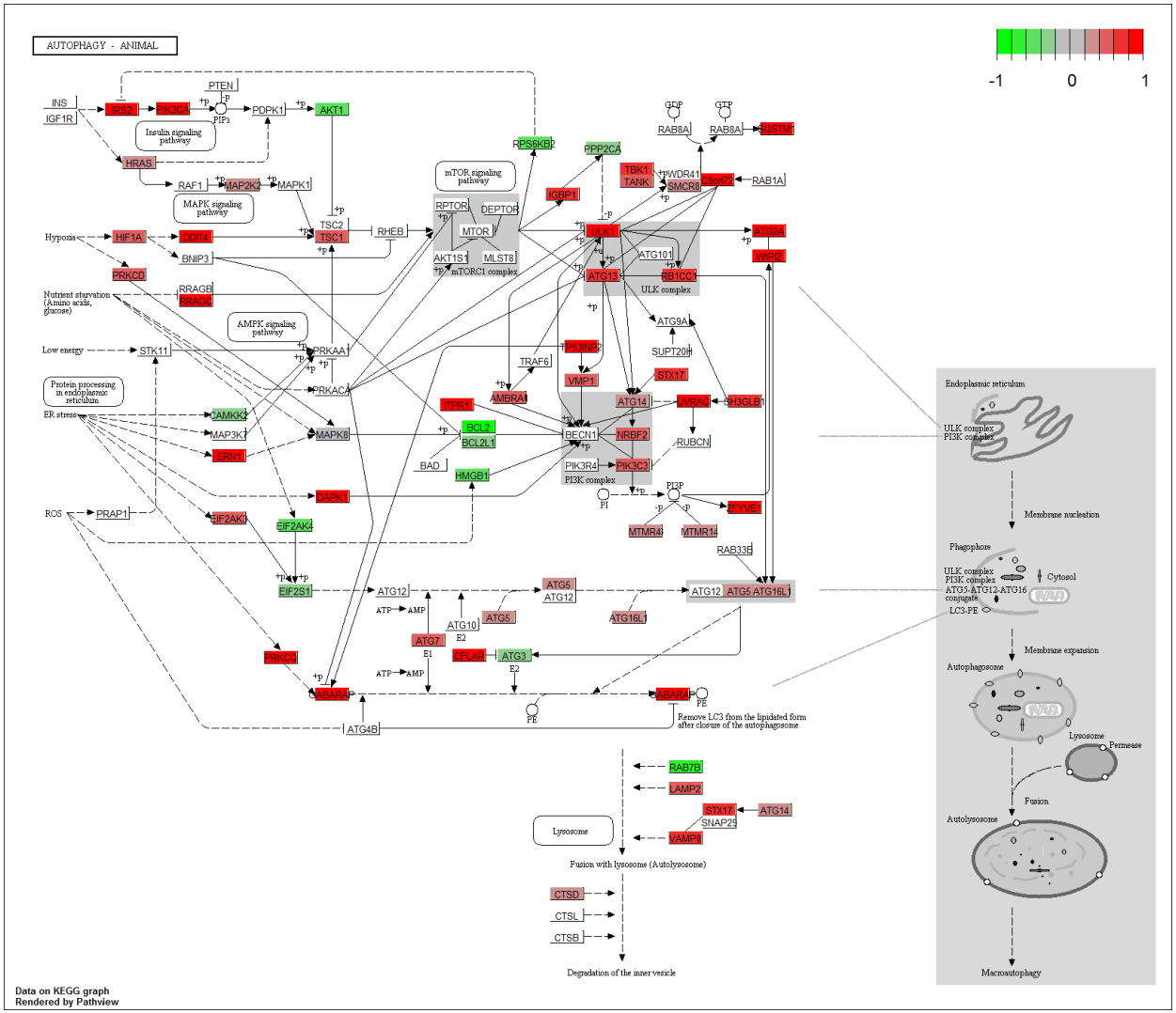


Figure 3.16 (IV) AUTOPHAGY: (A) Autophagy pathway in HT-29 cells treated with 10 ng/mL IFN+TNF for 16 hours. Expression changes of target genes are mapped by colours; green colour—statistically significant increase in expression, red colour—statistically significant decrease in expression, grey colour—expression statistically insignificant

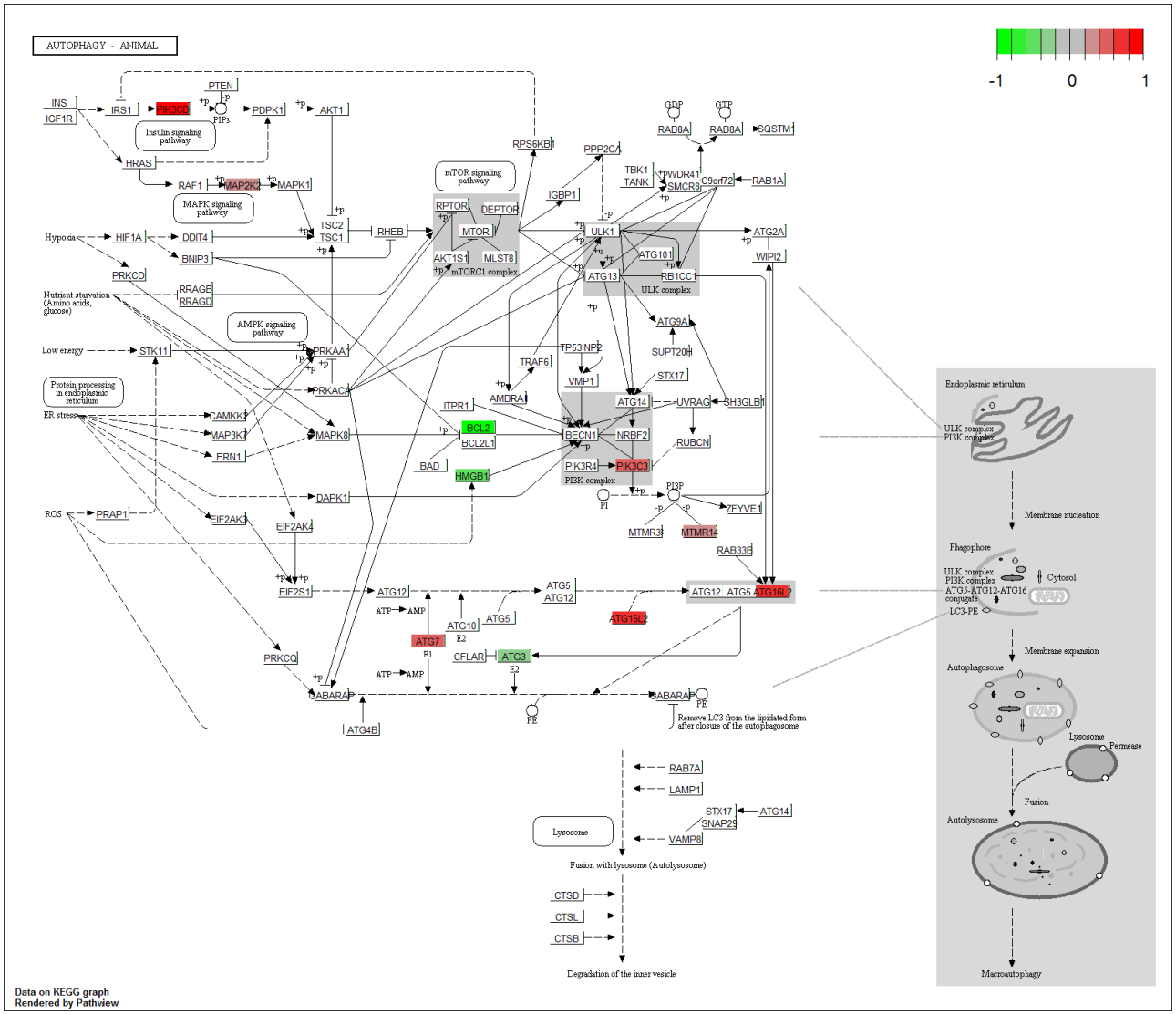


Figure 3.16 (IV) AUTOPHAGY: (B) Autophagy pathway in HT-29 cells treated with 1 ng/mL IFN+TNF for 16 hours. Expression changes of target genes are mapped by colours; green colour—statistically significant increase in expression, red colour—statistically significant decrease in expression, grey colour—expression statistically insignificant

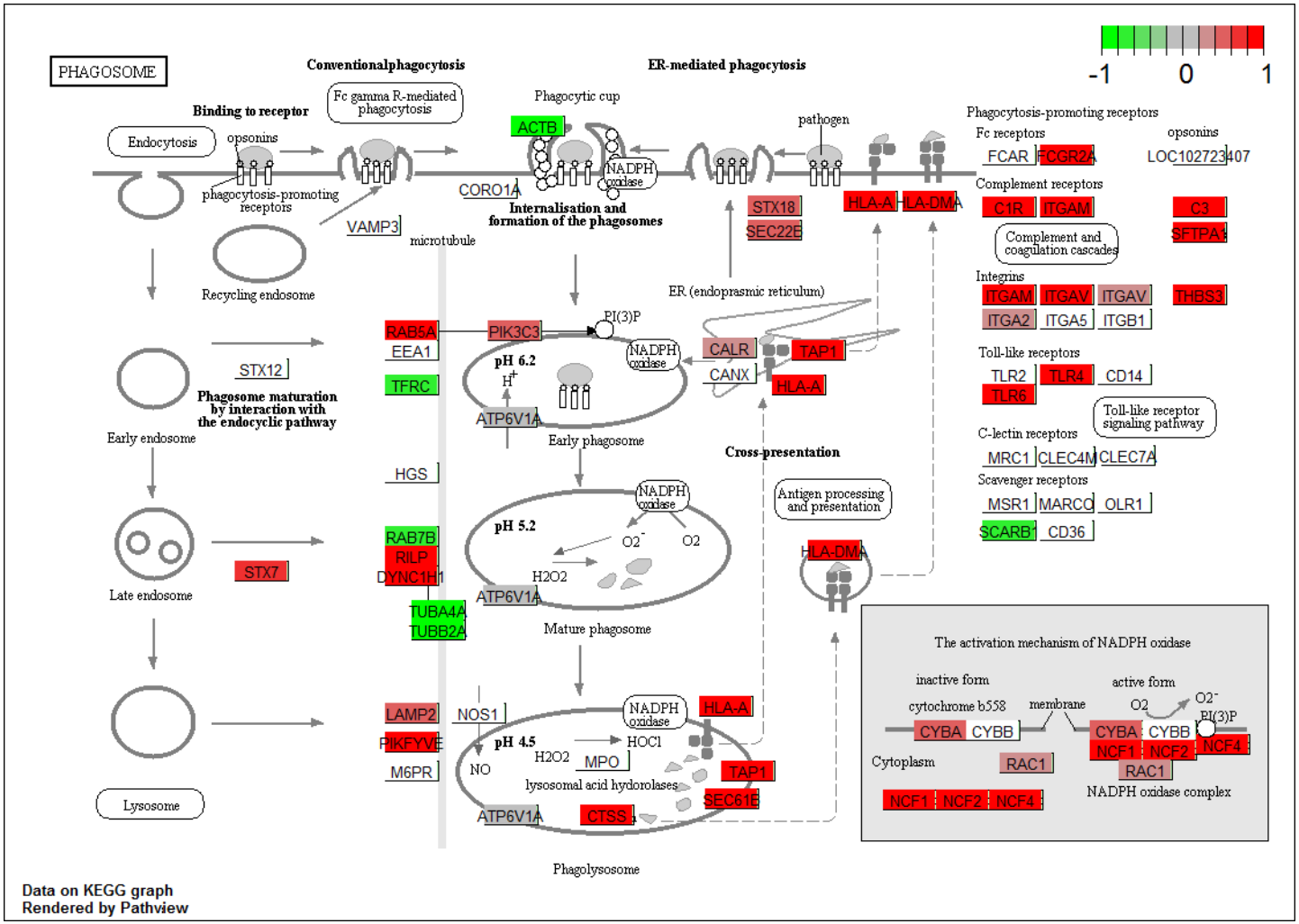


Figure 3.16 (V) PHAGOSOME FORMATION: (A) Phagosome pathways in HT-29 cells treated with 10 ng/mL IFN+TNF for 16 hours. Expression changes of target genes are mapped by colours; green colour—statistically significant increase in expression, red colour—statistically significant decrease in expression, grey colour—expression statistically insignificant

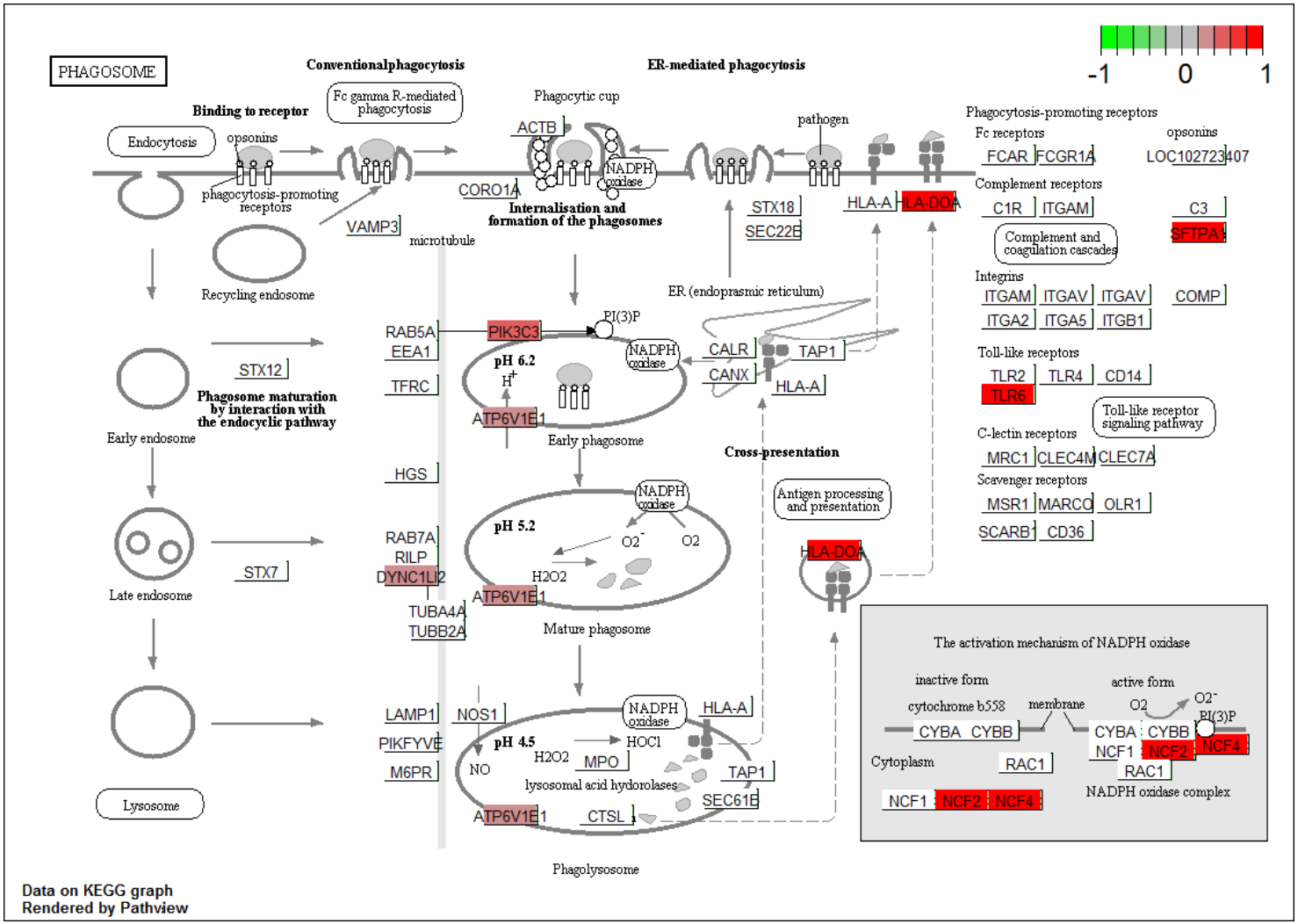


Figure 3.16 (V) PHAGOSOME FORMATION: (B) Phagosome pathway in HT-29 cells treated with 1 ng/mL IFN+TNF for 16 hours. Expression changes of target genes are mapped by colours; green colour—statistically significant increase in expression, red colour—statistically significant decrease in expression, grey colour—expression statistically insignificant

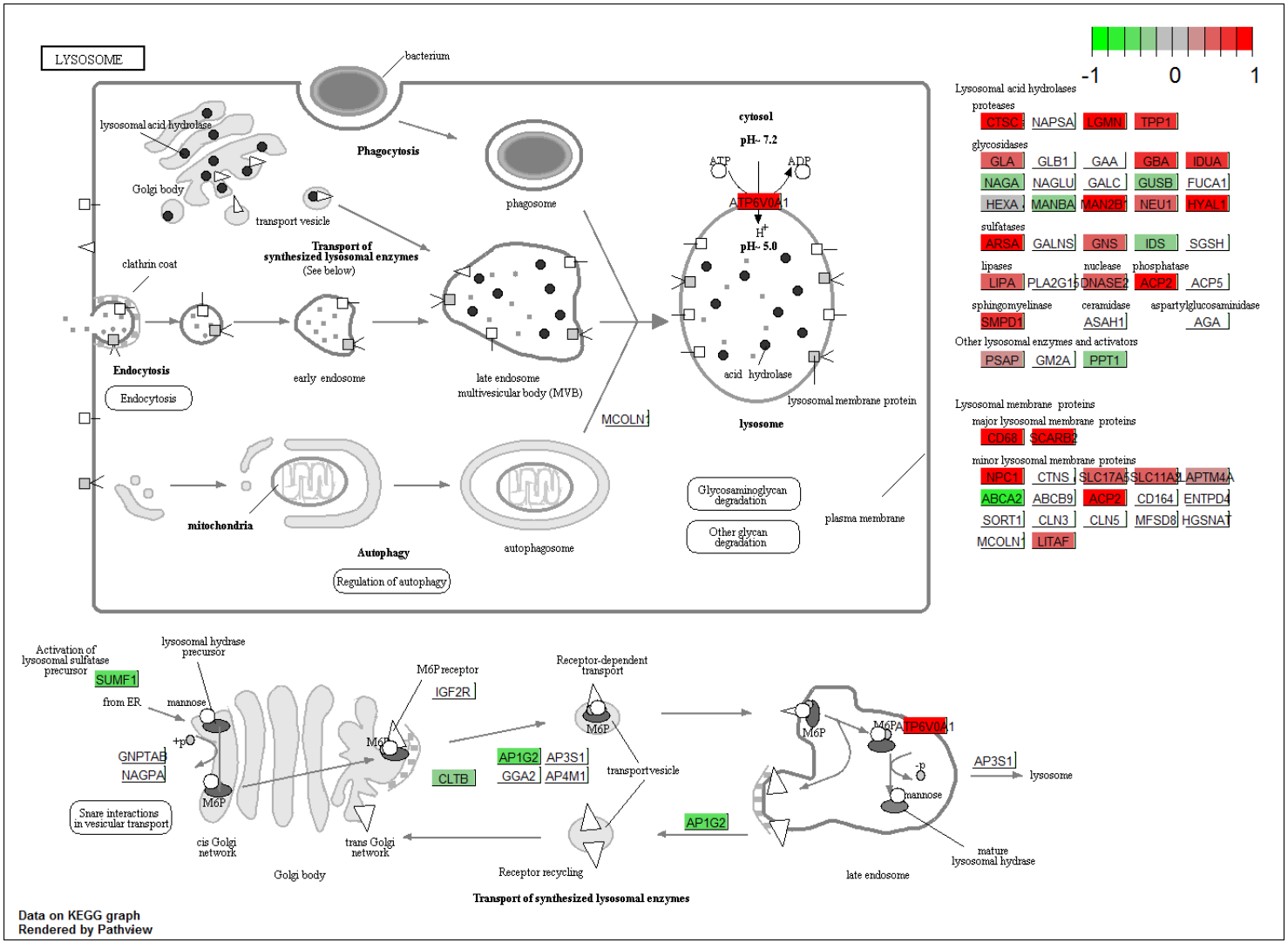


Figure 3.16 (VI) LYSOSOME FORMATION: (B) Lysosome associated pathway in HT-29 cells treated with 10 ng/mL IFN+TNF for 16 hours. Expression changes of target genes are mapped by colours; green colour—statistically significant increase in expression, red colour—statistically significant decrease in expression, grey colour—expression statistically insignificant

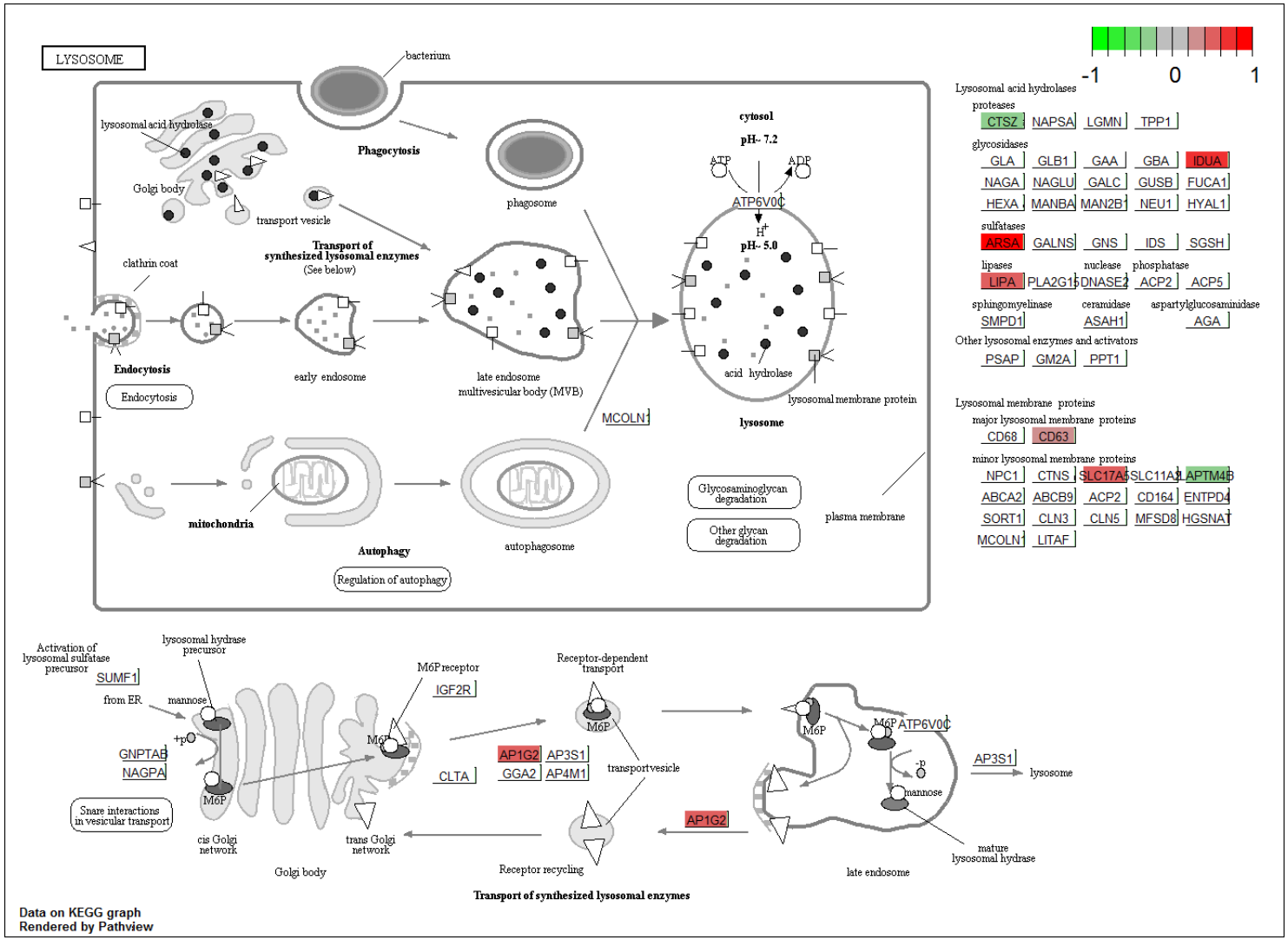


Figure 3.16 (VI) LYSOSOME FORMATION: (B) Lysosome associated pathway in HT-29 cells treated with 1 ng/mL IFN+TNF for 16 hours. Expression changes of target genes are mapped by colours; green colour—statistically significant increase in expression, red colour—statistically significant decrease in expression, grey colour—expression statistically insignificant

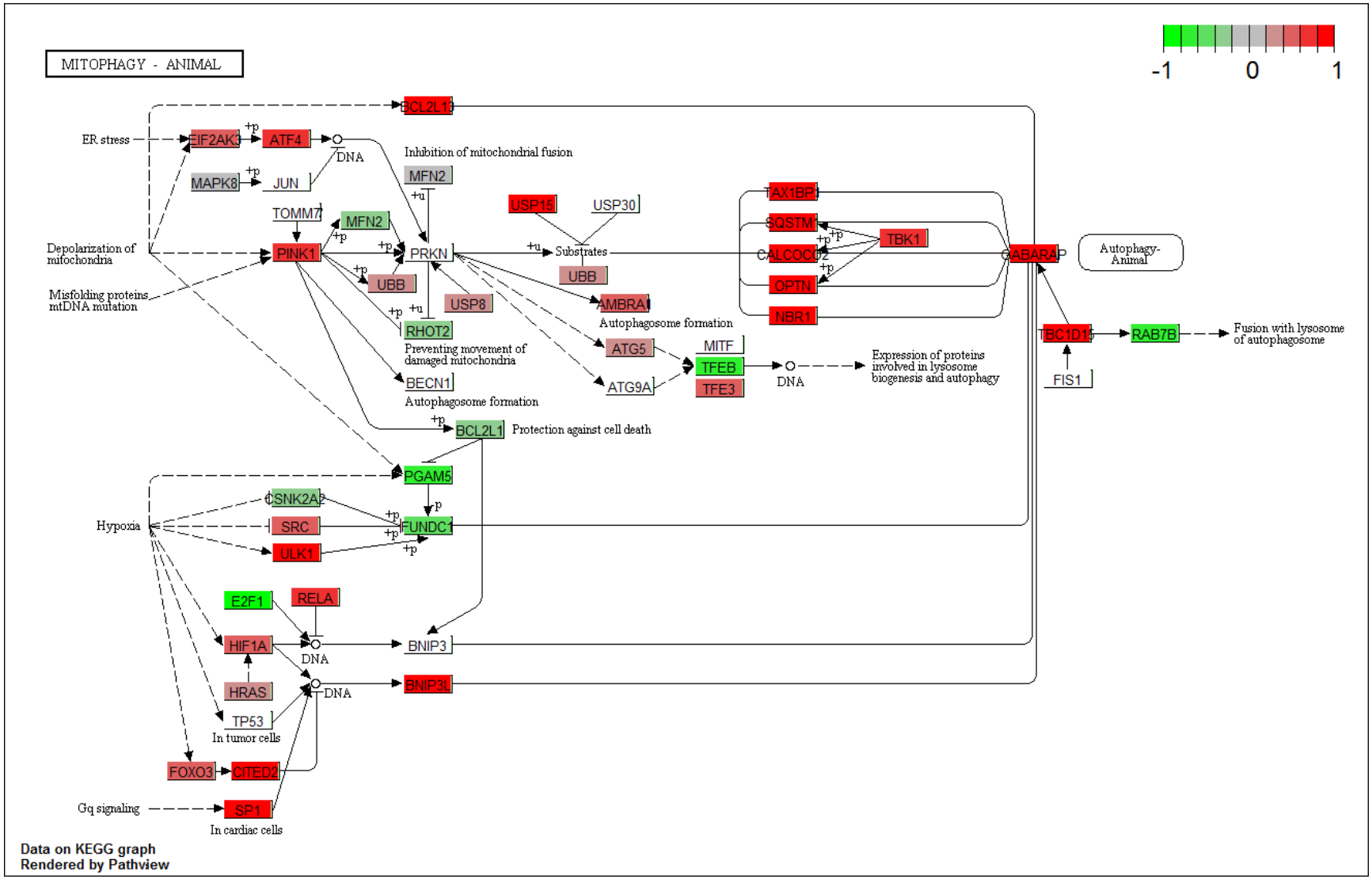


Figure 3.16 (VII) MITOPHAGY: (A) Mitophagy pathway in HT-29 cells treated with 10 ng/mL IFN+TNF for 16 hours. Expression changes of target genes are mapped by colours; green colour—statistically significant increase in expression, red colour—statistically significant decrease in expression, grey colour—expression statistically insignificant

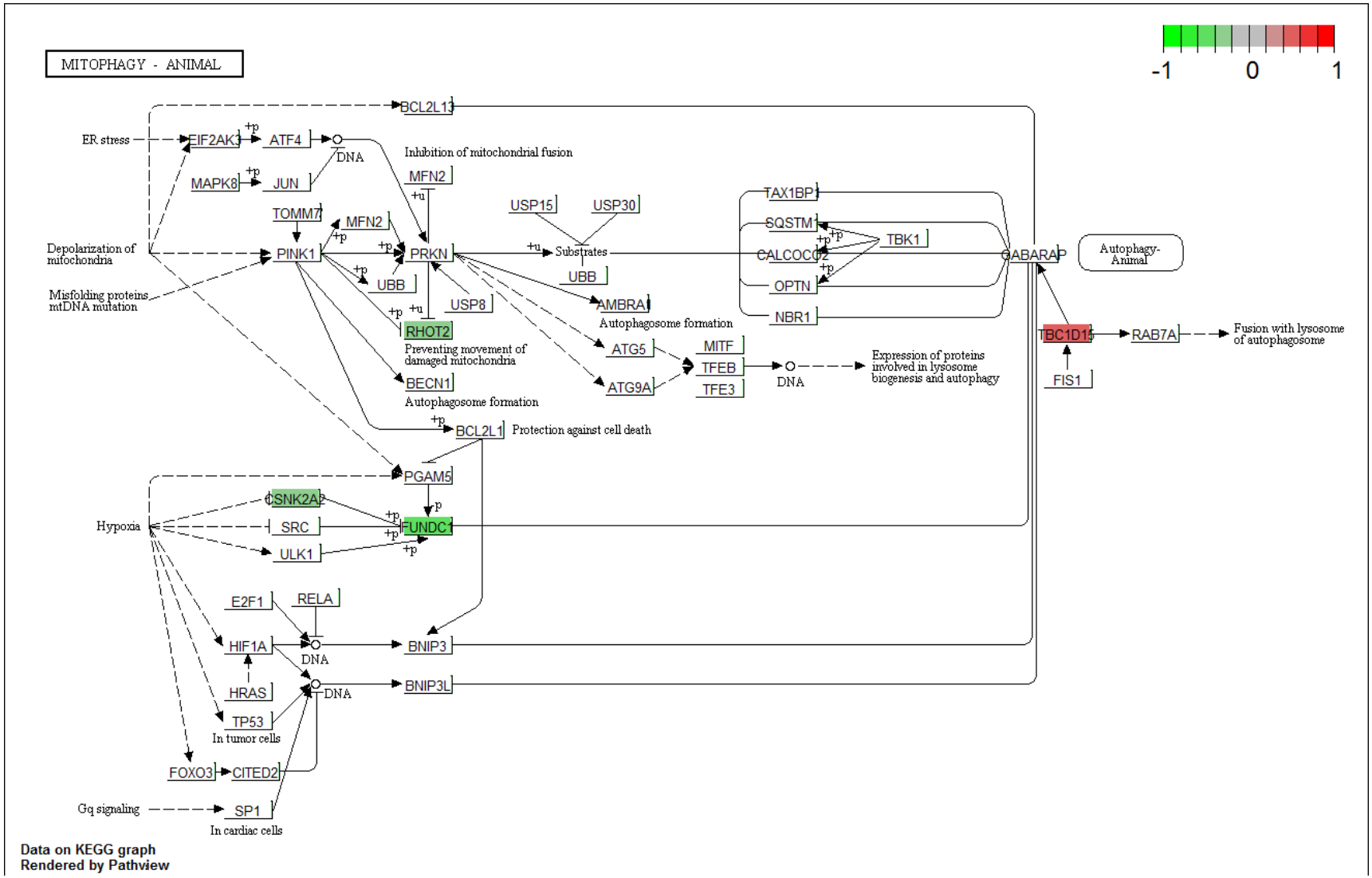


Figure 3.16 (VII) MITOPHAGY: (B) Mitophagy pathway in HT-29 cells treated with 1 ng/mL IFN+TNF for 16 hours. Expression changes of target genes are mapped by colours; green colour—statistically significant increase in expression, red colour—statistically significant decrease in expression, grey colour—expression statistically insignificant

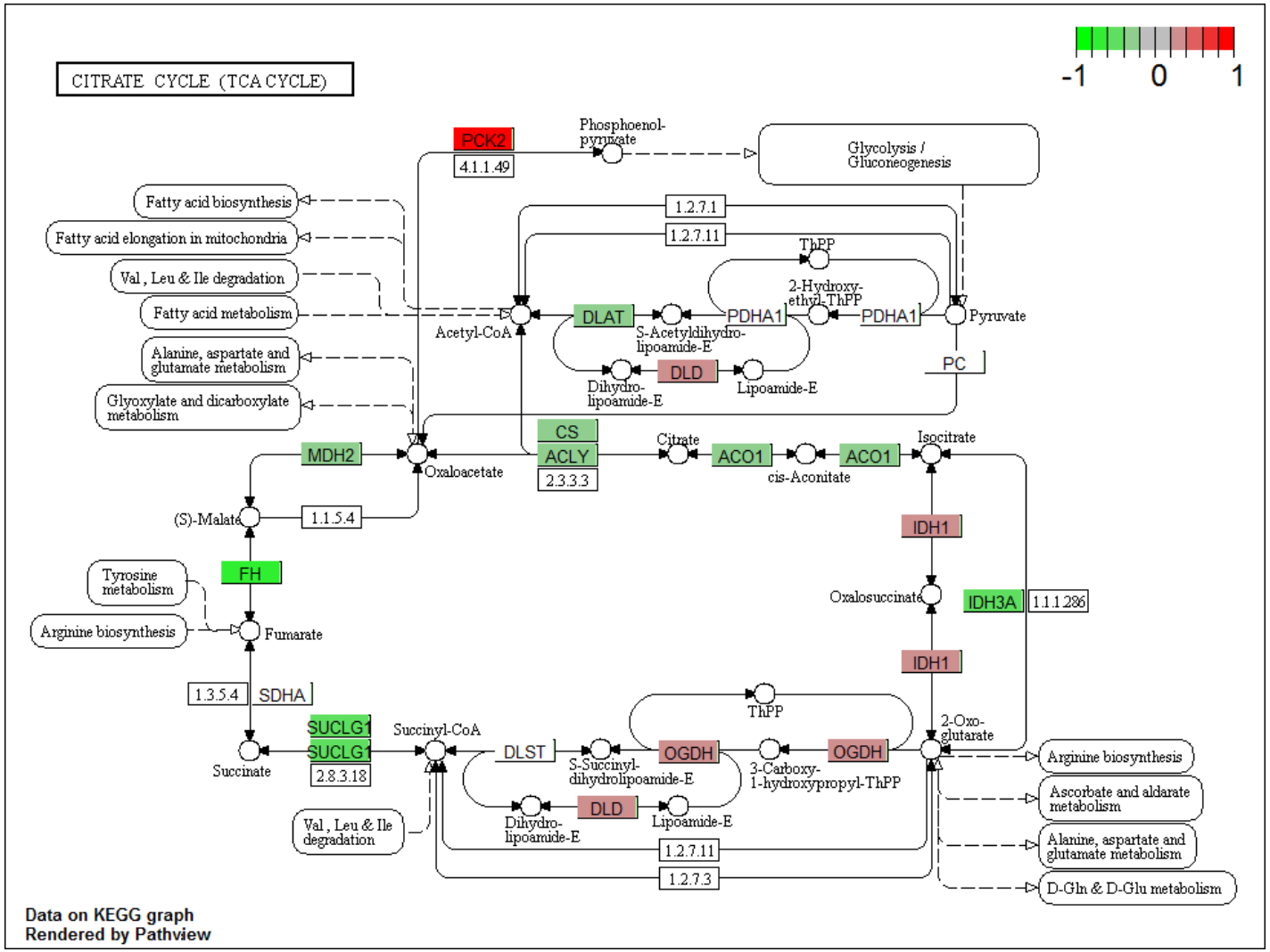


Figure 3.16 (VIII) Tricaroboxylic acid Cycle (TCA) (A) TCA Cycle in HT-29 cells treated with 10 ng/mL IFN+TNF for 16 hours. Expression changes of target genes are mapped by colours; green colour—statistically significant increase in expression, red colour—statistically significant decrease in expression, grey colour—expression statistically insignificant

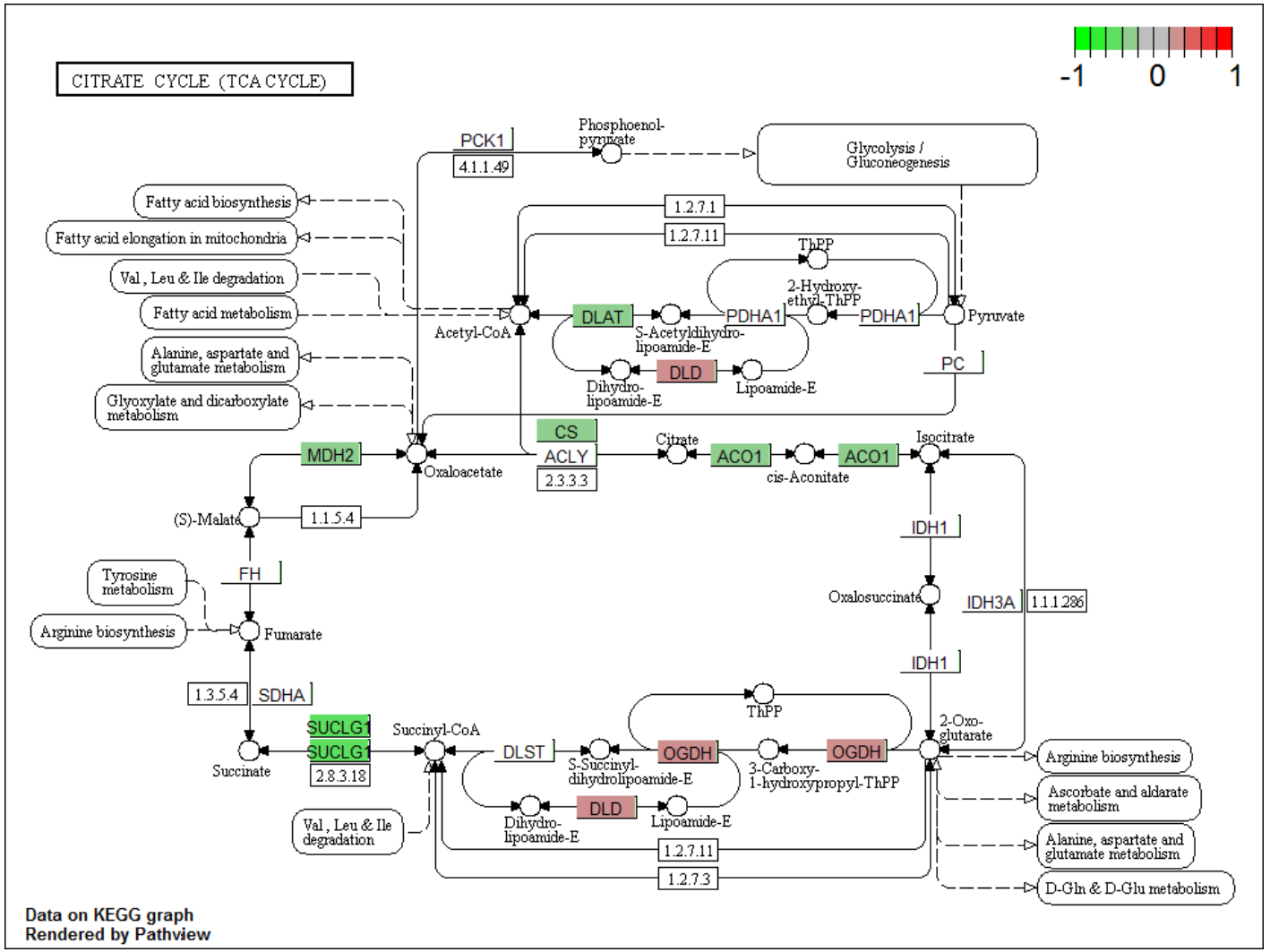


Figure 3.16 (VIII) Tricarboxylic acid Cycle (TCA) (B) TCA Cycle in HT-29 cells treated with 1 ng/mL IFN+TNF for 16 hours. Expression changes of target genes are mapped by colours; green colour—statistically significant increase in expression, red colour—statistically significant decrease in expression, grey colour—expression statistically insignificant

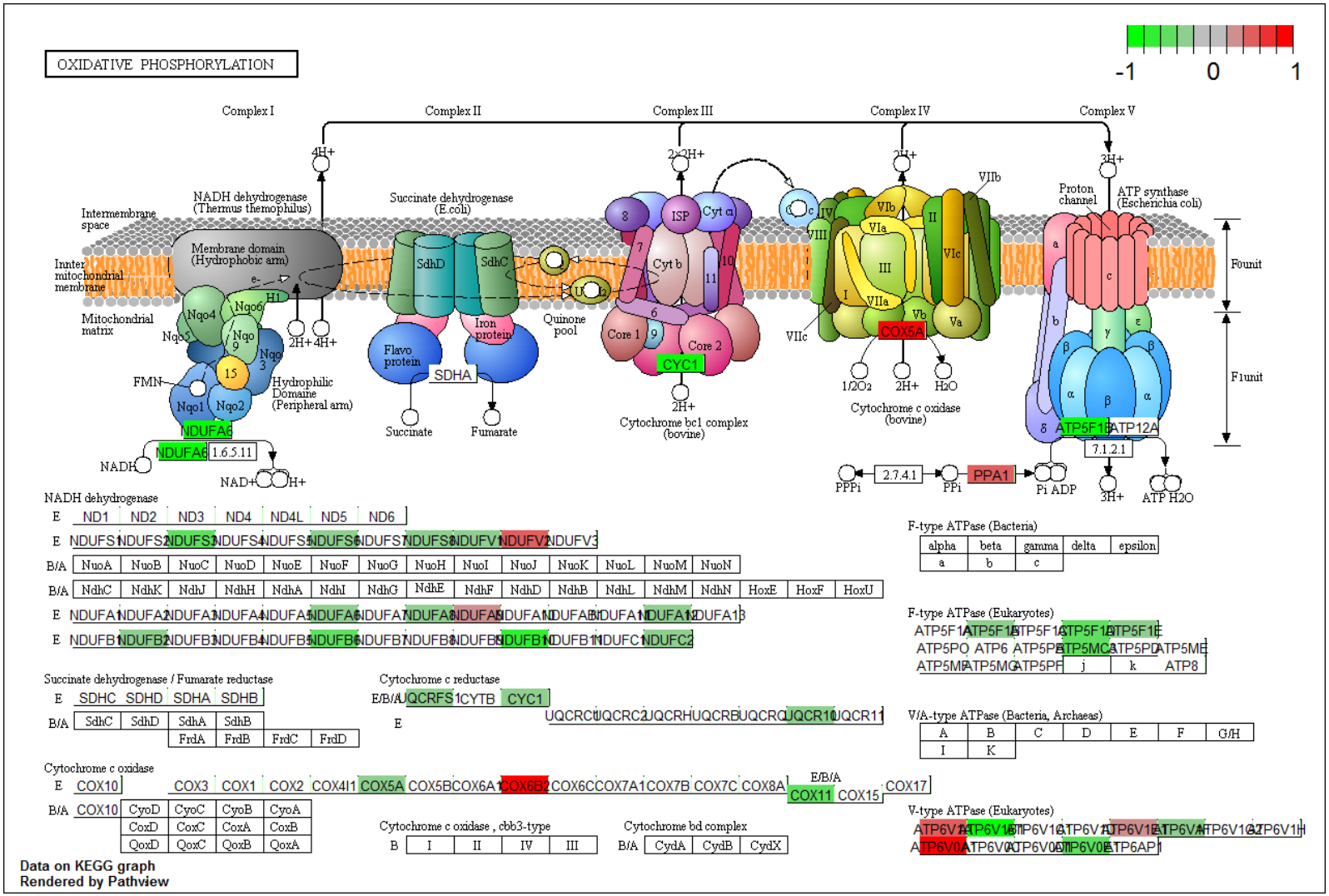


Figure 3.16 (IX) OXIDATIVE PHOSPHORYLATION: (A) Oxidative phosphorylation pathway in HT-29 cells treated with 10 ng/mL IFN+TNF for 16 hours. Expression changes of target genes are mapped by colours; green colour—statistically significant increase in expression, red colour—statistically significant decrease in expression, grey colour—expression statistically insignificant

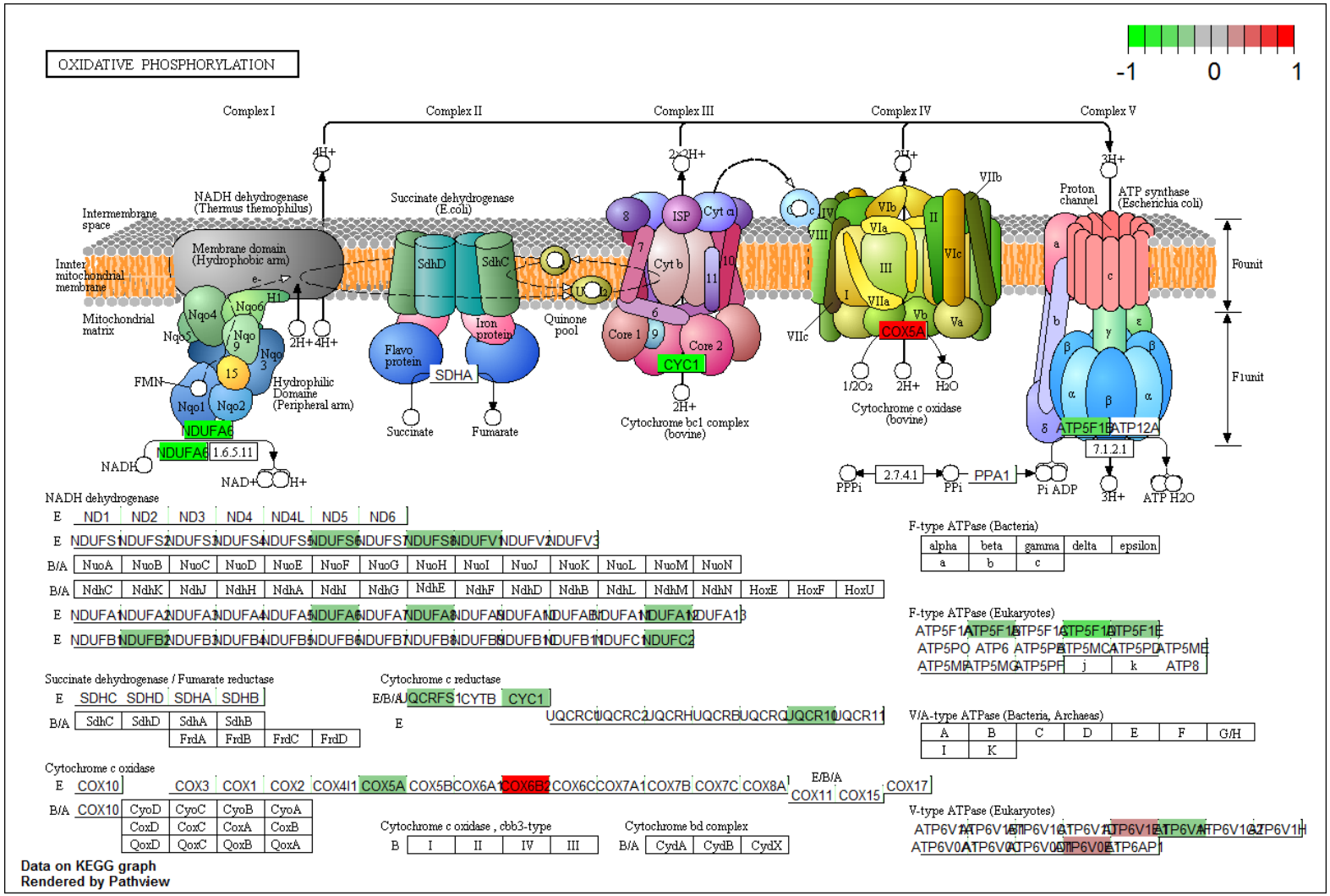


Figure 3.16 (IX) OXIDATIVE PHOSPHORYLATION: (B) Oxidative phosphorylation pathway in HT-29 cells treated with 1 ng/mL IFN+TNF for 16 hours. Expression changes of target genes are mapped by colours; green colour—statistically significant increase in expression, red colour—statistically significant decrease in expression, grey colour—expression statistically insignificant

Figure 3.16 (I-IX) KEGG pathway diagrams representing the role of late genes associated with 10 ng/mL IFN-γ+TNF-α treatment

KEGG Pathway analysis providing the overview of affected cell death pathways and metabolic pathways in HT-29 cells treated with different concentration of IFN-γ+TNF-α for the duration of 16 hours. The major affected pathways included (I-IX) – apoptosis, necroptosis, ferroptosis, autophagy, phagosome, lysosome, mytophagy, TCA cycle and oxidative phosphorylation. Each pathway is represented as two graphs each based on the concentration of IFN-γ+TNF-α treatment. (A) KEGG pathway diagrams generated by Pathview, highlighting the involvement of all genes differentially expressed at 16 hours, 10 ng/mL IFN-γ+TNF-α treatment. (B) KEGG pathway diagrams generated by Pathview, highlighting the involvement of differentially expressed genes unique to 16 hours, 10 ng/mL IFN-γ+TNF-α treatment. The statistical significance of the differentially expressed genes was estimated in terms of beta values scaled from -1 to 1. Expression changes of target genes were mapped by colours; green colour—statistically significant increase in expression, red colour—statistically significant decrease in expression, grey colour—expression statistically insignificant.

3.5. Discussion

IFN-γ and TNF-α are two major proinflammatory cytokines primarily associated with response against bacterial and viral infections[44–51]. Increased levels of these cytokines can contribute to the pathogenesis of several autoimmune diseases[52–56]. In this part of the project, we analysed the effect of cytokine concentration on epithelial cell death and gene expression profiles in CRC cell lines. Here we demonstrate that IFN-γ and TNF-α synergised to induce cell death in CRC cells in a concentration dependent manner. For the first time we show that IFN-γ +TNF-α induced cell death is associated with a dose-to-duration pattern of downstream STAT1 signalling where signalling strength in terms of increasing cytokine concentration is converted into a prolonged duration of active signal. We demonstrate that the sustained/prolonged activation of JAK-STAT signalling pathway is crucial for the induction of cell death. We also investigated differences in the gene regulation profile associated with increasing concentrations of IFN-γ + TNF-α in time dependent manner. Altogether, this study provides important insights into concentration and time dependent effect of cytokines on cell fate.

We show that IFN-γ + TNF-α synergistically induce both cell death and inflammatory gene expression in a concentration dependent manner. Our data suggests that, for induction of cell death in CRC cells, a minimum threshold concentration of IFN-γ + TNF-α is necessary, below this concentration no cell death was observed. Kracikova et al has previously described a similar cell death mechanism in p53 dependent cell death of mammary epithelial cells where the cells required a minimum threshold level of p53 for the induction of apoptosis[57]. Below

this threshold there was induction of cell cycle arrest, but it was not sufficient for apoptosis[57].

Moving forward, this concentration dependent cell death switch was confirmed in different cancer cell lines, although the threshold concentration of IFN-γ and TNF-α required for induction of cell death was different for different cell lines. IFN-γ + TNF-α synergistically induced the expression of both pro-inflammatory and pro-apoptotic genes in a concentration dependent manner, where the gene expression level increased with increasing cytokine concentration. This also suggests that even though both cell death and CXCL-10 production are synergistically regulated[58–61], the mode of activation of the two pathways may be different.

We then investigated the kinetics of activation of the JAK1/2-STAT1 signalling pathway in response to increasing cytokine concentration. While both the non-cytotoxic low concentration or cytotoxic high concentration of IFN-γ and TNF-α were able to activate STAT1 pY701 phosphorylation within a few minutes to the same magnitude the duration of signalling was different. At low IFN-γ + TNF-α concentration STAT1 pY701 phosphorylation was transient and dissipated while at the higher concentration there was a sustained activation of the pathway. A similar pattern of dose-to-duration signalling has been reported in case of MAPK signalling pathway in yeast *Saccharomyces cerevisiae* for adaptation to environmental conditions[62,11].

Next, we tested the significance of sustained activation of the JAK1/2-STAT1 pathway in regulation of epithelial cell death. We disrupted the sustained activation of the pathway by blocking JAK1/2 activity at different time intervals post-cytokine treatment. Even though treatment of cells with IFN-γ + TNF-α could induce JAK1/2-

STAT1 pathway activation and gene expression within the first hour blocking the pathway after 10 hours of cytokine treatment completely rescued the cell death phenotype. The data suggested that a sustained activation of the JAK-STAT pathway is essential for induction of cell death. The importance of temporal regulation of signalling pathways can be observed in other signalling pathways as well. For instance, treatment with TNF-α induces frequent shuttling of NF-κB in and out of the nucleus resulting into transient nuclear accumulation of NF-κB[63]. This transient accumulation triggers the expression of inflammatory response genes[64,65]. While treatment with lipopolysaccharide (LPS) can maintain NF-κB levels in the nucleus leading to a prolonged wave of NF-κB activity required for activation of different cytokines and chemokines to establish adaptive immune responses[65,66]. In case of neuronal precursor cells, a transient activation of ERK pathway by epidermal growth factor (EGF) can result into proliferation of cells while a sustained activation leads to differentiation of precursor cells into neurons[1]. Along with our findings, these studies confirm the importance of duration of signalling pathways on the outcome of biological activities and cellular fate[1].

To further investigate the effect of different concentrations of IFN-γ + TNF-α on gene regulation over time we performed an RNA-Seq experiment. Interestingly, at early time points the gene expression profiles between low and high concentrations of IFN-γ + TNF-α were broadly similar while there was a diversion in the gene expression profile at later time points. Interestingly, the comparison of differentially expressed genes after different durations of cytokine treatment identified a unique set of genes, differentially expressed only with high concentration of cytokines and at the later time point. Because cell death was induced at later time

after cytokine treatment, we focused our analysis on these 'late genes' to identify different biological activities associated with cell death. The functional analysis of these genes identified their role in several cell death pathways, cellular metabolism, and in reactive oxygen species generation.

Our work and previous reports have shown that IFN-γ + TNF-α induces the activation of components of both the intrinsic and extrinsic apoptotic pathways[58,59,67]. The expression of different caspases; *CASP8*, *CASP10* and *CASP7*, component of TNF-α apoptotic complex; TNF receptor-1 (*TNFRSF1A*), TNFR1-associated death domain protein (*TRADD)*, Receptor-interacting-protein kinase 1 (RIPK1), expression of *FAS* ligands, pro-apoptotic genes such as *PARP*, BH3 Interacting Domain Death Agonist (*BID*), *BAK1* were increased after 16 hours of IFN-γ + TNF-α treatment. Notably, the expression of the key anti-apoptotic gene *BCL2* was decreased at the later time point. Previous studies have reported the role of caspase 8 and the death-inducing signalling complex (DISC) in IFN-γ + TNF-α induced cell death[68,69]. IFN-γ has also been reported to synergise with tumour necrosis factor superfamily member 14 (TNFSF14/LIGHT) to induce cell death in HT-29 cells which was partially rescued by rescued by PARP inhibitors[70]. Increased expression of *PARP* and caspase 1, 8 and 3 has been reported in IFN-γ treated cells in erythroid progenitor cells[71]. BCL-2 family members play an important role in the regulation of intrinsic apoptotic pathways. Pro-apoptotic proteins such as BAK1 and BAX increase the outer membrane permeabilization of mitochondria (MOMP) to release cytochrome C for activation of caspase 9 and mitochondria mediated apoptosis[72,73]. On the other hand, anti-apoptotic genes BCL-2, BCL-xl and myeloid cell leukaemia 1 (MCL-1) negatively regulate these activities[74]. Previous studies have also reported the role of Bcl-2 in

IFN-γ + TNF-α induced cell death[75,76] STAT1 mediated down-regulation of Bcl-2 expression has been reported to contribute to IFN-γ/TNF-α induced apoptosis in NIT-1 cells[75]. Intriguingly, our RNA-Seq data also identified downregulation of *BCL2* gene expression only at the late time point with high concentration of IFN-γ + TNF-α, suggesting the regulation of *BCL2* expression by IFN-γ + TNF-α in a time dependent manner. While, the increased expression of BAK1 and a decrease in Bcl-2 expression level suggested a positive role towards induction of apoptosis, IFN-γ + TNF-α treatment also increased the expression of X-linked inhibitor of apoptosis protein (XIAP) and MCL-1, both negative regulators of apoptosis[77,78,79]. MCL-1 has been shown to interact with truncated BID to suppress the activation of the intrinsic cell death pathway[80]. TNF-α has been reported to increase expression of XIAP via NF-κB [81,] IFN-γ has been reported to increase the level of MCL-1 in umbilical-cord-blood-derived eosinophils to increase the cell survival[82]. IFN-γ and TNF-α also play inhibitory effects in FAS mediated apoptosis in melanocytes by increasing the expression of anti-apoptotic molecules c-FLIP and MCL1[81]. Thus, the cytokines induced the expression of both pro-apoptotic and anti-apoptotic genes while decreasing the expression of the anti-apoptotic gene *BCL2*.

In addition to apoptosis, there was a significant increase in the expression of genes involved in necroptosis. As expected, the expression level of members of TNFR1 necroptotic complex (TNFR1, RIPK1, RIPK3 and Mixed Lineage Kinase Domain Like Pseudo kinase (MLKL)) were upregulated in IFN-γ +TNF-α treated cells. The observations were in line with several studies describing the role of IFN-γ and TNF-α in activation of necroptosis. Other than key necroptotic proteins, there were a few other genes identified to be expressed at late time point. For instance, Toll Like

Receptor Adaptor Molecule 1 (TICAM1) and TICAM2 are associated with Toll like receptor 3 (TLR3) signalling pathway and play important role in inflammasome formation in response to bacterial infections[83]. Other than that TLR3/TICAM-1 axis has been reported to play an important role in tumour cell necroptosis in RIP3-dependent manner and activation of innate immunity by release of Damage-associated molecular patterns (DAMPs)[84,85]. We also observed an increased expression of *TRPM7* at later time points. For induction of necroptosis, the oligomerisation and membrane localisation of MLKL is crucial for induction of membrane permeabilization and influx of Ca2+ ions into cells[73]. TRPM7 is the downstream target for MLKL and is required for the mediation of Ca2+ influx in the cells[86], suggesting its role in IFN-γ + TNF-α induced cell death[87,88]. Curiously, the expression of TICAM2 and TRPM7 was observed only at late time points after cytokine treatment, suggesting their temporal regulation in IFN-γ + TNF-α treated cells. HSP90AA, acts as a chaperon for MLKL transport to plasma membrane and supports necroptosis [89,90] Curiously, HSP90AA was downregulated only at late time point. Other than that, we observed the negative regelation of genes involved in suppression of necroptosis. For instance, pro survival gene glycogen phosphorylase *(PYGB)*[91,92] and inducer of cell survival signalling and vacuolar Protein Sorting 4 *(VSP4)*, a negative regulator of necroptosis were supressed at late time point[93].

IFN-γ + TNF-α induced late genes were also involved in the regulation of ferroptosis[94] and reactive oxygen species (ROS) generation. There was an upregulation of genes supporting ferroptosis and ROS generation including spermidine N1-acetyltransferase 1 (*SAT1*), *SAT2, ATF7, SLC7A11* while there was a downregulation of *FTL,* Glutathione peroxidase 4 *(GPX4)*, solute carrier proteins

SLC39 & SLC40 important molecules involved in the regulation of ferroptosis and regulated by IFN-γ + TNF-α in a temporal manner. SAT1 is rate limiting enzyme in polyamine catabolism and is an important transcriptional target for p53 induced ferroptosis and lipid peroxidation[95,96]. Also, there was a upregulation of *ATG7* which supports the induction of ferroptosis in cells[97]. GPX4 is a phospholipid hydro peroxidase which protects cells from membrane lipid peroxidation. It is a key suppressor of ROS generation and ferroptosis in cells[98]. The depletion or suppression of GPX4 induced cell death and damage in different model system. Mice lacking *Gpx4* showed severe cell death by ferroptosis resulting into renal faliure[99] While overexpression of GXP4 in B-cell resulted suppression of ROS production and ferroptosis leading to B cell lymphoma[100]. The studies highlight the role of IFN-γ + TNF-α in ferroptosis by decreasing the expression of *GPX4* in the cells. FTL is a component of the ferritin complex which plays an important role in storing of iron in cells the decrease in *FTL* expression can result into release of iron from heme complex resulting into ferroptosis[98]. Our transcriptional analysis also identified the upregulation of *NCF2* and *NCF4* which encode for neutrophil cytosolic factor 2 (NCF2) and NCF4 respectively. NCF2 and NCF4 are associated with formation of the NADPH complex, which is required for ROS production and phagocytosis during microbial infections[101–103]. Studies have reported the role of NCF2/4 and NAPDH oxidase complex in generating inflammatory response in intestinal epithelial cells of patients with IBD[104–106]. In addition to genes associated with regulated cell death pathways, KEGG pathway analysis also highlighted potential roles for spliceosome complex, oxidative phosphorylation, and Tricarboxylic acid (TCA) cycle. Most of these genes

were downregulated at late time point suggesting impaired cellular metabolic and mitochondrial activities in IFN-γ + TNF-α treated cells at later time point.

Taken together, we show that the JAK1/2-STAT1 pathway follows a dose-to-duration pattern of signalling where the concentration of cytokines present in the extracellular environment is decoded into different durations of JAK-STAT signalling associated with different cellular responses. Inflammatory gene expression was an early process and required a low concentration of cytokines but as the concentration of cytokines increased this resulted in sustained activation of STAT1 and late gene expression. This sustained activation of STAT1 was also associated with impaired cellular functions and activation of multiple cell death pathways. Even though, several genes and several pathways were identified to be involved in the regulation of IFN-γ + TNF-α induced cell death further validation work is required to understand the cell death mechanisms at play.

3.6. References

1. Purvis, J. E. & Lahav, G. Encoding and decoding cellular information through signaling dynamics. *Cell* **152**, 945–956 (2013).
2. Ataie-Kachoie, P., Pourgholami, M. H. & Morris, D. L. Inhibition of the IL-6 signaling pathway: A strategy to combat chronic inflammatory diseases and cancer. *Cytokine and Growth Factor Reviews* (2013).
3. Nishimoto, N. & Kishimoto, T. Inhibition of IL-6 for the treatment of inflammatory diseases. *Current Opinion in Pharmacology* (2004). doi:10.1016/j.coph.2004.03.005
4. Ip, W. K. E., Hoshi, N., Shouval, D. S., Snapper, S. & Medzhitov, R. Anti-inflammatory effect of IL-10 mediated by metabolic reprogramming of macrophages. *Science (80-.).* (2017).
5. Niemand, C. *et al.* Activation of STAT3 by IL-6 and IL-10 in Primary Human Macrophages Is Differentially Modulated by Suppressor of Cytokine Signaling 3. *J. Immunol.* (2003).
6. Grivennikov, S. *et al.* IL-6 and Stat3 Are Required for Survival of Intestinal Epithelial Cells and Development of Colitis-Associated Cancer. *Cancer Cell* **15**, 103–113 (2009).
7. Murray, P. J. Understanding and exploiting the endogenous interleukin-10/STAT3-mediated anti-inflammatory response. *Current Opinion in Pharmacology* (2006).
8. Braun, D. A., Fribourg, M. & Sealfon, S. C. Cytokine response is determined by duration of receptor and signal transducers and activators of transcription 3 (STAT3) activation. *J. Biol. Chem.* **288**, 2986–2993 (2013).
9. Batchelor, E., Mock, C. S., Bhan, I., Loewer, A. & Lahav, G. Recurrent Initiation: A Mechanism for Triggering p53 Pulses in Response to DNA Damage. *Mol. Cell* (2008). doi:10.1016/j.molcel.2008.03.016

10. Purvis, J. E. *et al.* p53 dynamics control cell fate. *Science (80-.).* (2012). doi:10.1126/science.1218351

11. Behar, M., Hao, N., Dohlman, H. G. & Elston, T. C. Dose-to-duration encoding and signaling beyond saturation in intracellular signaling networks. *PLoS Comput. Biol.* **4**, (2008).

12. Mechanisms and consequences of Jak–STAT signaling in the immune system. (2017). doi:10.1038/ni.3691

13. Kalliolias, G. D. & Ivashkiv, L. B. TNF biology, pathogenic mechanisms and emerging therapeutic strategies. *Nat. Rev. Rheumatol.* **12**, 49–62 (2016).

14. Israeli, E. T helper-1 cell cytokines drive cancer into senescence. *Isr. Med. Assoc. J.* (2013).

15. Shen, J. *et al.* Anti-cancer therapy with TNFα and IFNγ: A comprehensive review. *Cell Prolif.* **51**, e12441 (2018).

16. Zaidi, M. R. The Interferon-Gamma Paradox in Cancer. doi:10.1089/jir.2018.0087

17. Aqbi, H. F., Wallace, M., Sappal, S., Payne, K. K. & Manjili, M. H. IFN-γ orchestrates tumor elimination, tumor dormancy, tumor escape, and progression. *Journal of Leukocyte Biology* (2018). doi:10.1002/JLB.5MIR0917-351R

18. Waters, J. P., Pober, J. S. & Bradley, J. R. Tumour necrosis factor and cancer. *Journal of Pathology* (2013).

19. Castro, F. *et al.* Interferon-gamma at the crossroads of tumor immune surveillance or evasion. *Front. Immunol.* **9**, 1–19 (2018).

20. Neurath, M. F. Targeting immune cell circuits and trafficking in inflammatory bowel disease. *Nature Immunology* (2019).

21. Nava, P. *et al.* IFN gamma regulates intestinal epithelial homeostasis through

converging Beta-catenin signaling pathways. *Immunity* **32**, 392–402 (2010).

22. Leppkes, M., Roulis, M., Neurath, M. F., Kollias, G. & Becker, C. Pleiotropic functions of TNF-α in the regulation of the intestinal epithelial response to inflammation.

23. Ruder, B., Atreya, R. & Becker, C. Tumour necrosis factor alpha in intestinal homeostasis and gut related diseases. *Int. J. Mol. Sci.* **20**, (2019).

24. Gupta, S. A decision between life and death during TNF-α-induced signaling. *Journal of Clinical Immunology* **22**, 185–194 (2002).

25. Nenci, A. *et al.* Epithelial NEMO links innate immunity to chronic intestinal inflammation. *Nature* (2007).

26. Iwashita, J. *et al.* mRNA of MUC2 is stimulated by IL-4, IL-13 or TNF-α through a mitogen-activated protein kinase pathway in human colon cancer cells. *Immunol. Cell Biol.* (2003).

27. Arnold, J. W., Klimpel, G. R. & Niesel, D. W. Tumor necrosis factor (TNFα) regulates intestinal mucus production during salmonellosis. *Cell. Immunol.* (1993).

28. Frey, M. R., Edelblum, K. L., Mullane, M. T., Liang, D. & Polk, D. B. The ErbB4 Growth Factor Receptor Is Required for Colon Epithelial Cell Survival in the Presence of TNF. *Gastroenterology* **136**, 217–226 (2009).

29. Hilliard, V. C., Frey, M. R., Dempsey, P. J., Peek, R. M. & Polk, D. B. TNF-α converting enzyme-mediated ErbB4 transactivation by TNF promotes colonic epithelial cell survival. *Am. J. Physiol. - Gastrointest. Liver Physiol.* **301**, G338 (2011).

30. Majoros, A. *et al.* Canonical and Non-Canonical Aspects of JAK–STAT Signaling: Lessons from Interferons for Cytokine Responses. *Front. Immunol.* **8**, 29 (2017).

31. Wu, Y. *et al.* Up-regulation and sustained activation of Stat1 are essential for interferon-γ (IFN-γ)-induced dual oxidase 2 (Duox2) and dual oxidase A2 (DuoxA2) expression in

human pancreatic cancer cell lines. *J. Biol. Chem.* **286**, 12245–12256 (2011).

32. Wingett, S. W. & Andrews, S. FastQ Screen: A tool for multi-genome mapping and quality control. *F1000Research* **7**, 1338 (2018).

33. Chen, S., Zhou, Y., Chen, Y. & Gu, J. Fastp: An ultra-fast all-in-one FASTQ preprocessor. in *Bioinformatics* **34**, i884–i890 (Oxford University Press, 2018).

34. Bray, N. L., Pimentel, H., Melsted, P. & Pachter, L. Near-optimal probabilistic RNA-seq quantification. *Nat. Biotechnol.* **34**, 525–527 (2016).

35. Soneson, C., Love, M. I. & Robinson, M. D. Differential analyses for RNA-seq: Transcript-level estimates improve gene-level inferences. *F1000Research* **4**, (2016).

36. Pimentel, H., Bray, N. L., Puente, S., Melsted, P. & Pachter, L. Differential analysis of RNA-seq incorporating quantification uncertainty. *Nat. Methods* **14**, 687–690 (2017).

37. Pimentel, H. J., Bray, N., Puente, S., Melsted, P. & Pachter, L. *Supplementary materials for " Differential analysis of RNA-Seq incorporating quantification uncertainty " Overview of sleuth workflow*. *bioRxiv* (Cold Spring Harbor Labs Journals, 2016).

38. Kuleshov, M. V. *et al.* Enrichr: a comprehensive gene set enrichment analysis web server 2016 update. *Nucleic Acids Res.* **44**, W90–W97 (2016).

39. Luo, W., Pant, G., Bhavnasi, Y. K., Blanchard, S. G. & Brouwer, C. Pathview Web: User friendly pathway visualization and data integration. *Nucleic Acids Res.* **45**, W501–W508 (2017).

40. Koch, S. & Nusrat, A. The Life and Death of Epithelia During Inflammation: Lessons Learned from the Gut. *Annu. Rev. Pathol. Mech. Dis.* **7**, 35–60 (2012).

41. Vitale, S. *et al.* Cytokine production profile in intestinal mucosa of paediatric inflammatory bowel disease. (2017).

42. Bruewer, M. *et al.* Proinflammatory cytokines disrupt epithelial barrier function by

apoptosis-independent mechanisms. *J. Immunol.* **171**, 6164–72 (2003).

43. Bousoik, E. & Montazeri Aliabadi, H. "Do We Know Jack" About JAK? A Closer Look at JAK/STAT Signaling Pathway. *Front. Oncol.* **8**, 1–20 (2018).

44. Ika Krisnawati, D. *et al.* Blockade Effects of Anti-Interferon-(IFN-) γ Autoantibodies on IFN-γ-Regulated Antimicrobial Immunity. (2019). doi:10.1155/2019/1629258

45. Kak, G., Raza, M. & Tiwari, B. K. Review Open Access Interferon-gamma (IFN-γ): Exploring its implications in infectious diseases. (2018). doi:10.1515/bmc-2018-0007

46. Kang, S., Brown, H. M. & Hwang, S. Direct antiviral mechanisms of interferon-gamma. *Immune Network* **18**, (2018).

47. Ning, Y.-J. *et al.* Interferon-γ-Directed Inhibition of a Novel High-Pathogenic Phlebovirus and Viral Antagonism of the Antiviral Signaling by Targeting STAT1. *Front. Immunol.* **10**, 1182 (2019).

48. Hakim, M. S. *et al.* TNF-α exerts potent anti-rotavirus effects via the activation of classical NF-κB pathway. *Virus Res.* **253**, 28–37 (2018).

49. Alejo, A. *et al.* Chemokines cooperate with TNF to provide protective anti-viral immunity and to enhance inflammation. *Nat. Commun.* **9**, 1–16 (2018).

50. Rocha, F. A. C. *et al.* Tumor necrosis factor prevents Candida albicans biofilm formation. *Sci. Rep.* **7**, 1–7 (2017).

51. Harris, J., Hope, J. C. & Keane, J. Tumor Necrosis Factor Blockers Influence Macrophage Responses to Mycobacterium tuberculosis. *The Journal of Infectious Diseases* **198**, 1842–1850

52. Muzes, G., Molnár, B., Tulassay, Z. & Sipos, F. Changes of the cytokine profile in inflammatory bowel diseases. *World J. Gastroenterol.* **18**, 5848–5861 (2012).

53. Vitale, S. *et al.* Cytokine production profile in intestinal mucosa of paediatric

inflammatory bowel disease. (2017).

54. Qiao, Y. C. *et al.* The change of serum tumor necrosis factor alpha in patients with type 1 diabetes mellitus: A systematic review and meta-analysis. *PLoS ONE* **12**, e0176157–e0176157 (2017).

55. Kunz, M. & Ibrahim, S. M. Cytokines and Cytokine Profiles in Human Autoimmune Diseases and Animal Models of Autoimmunity. *Artic. ID* **979258**, 20 (2009).

56. Li, P., Zheng, Y. & Chen, X. Drugs for autoimmune inflammatory diseases: From small molecule compounds to anti-TNF biologics. *Frontiers in Pharmacology* **8**, 460 (2017).

57. Kracikova, M., Akiri, G., George, A., Sachidanandam, R. & Aaronson, S. A. A threshold mechanism mediates p53 cell fate decision between growth arrest and apoptosis. *Cell Death Differ.* **20**, 576–588 (2013).

58. Mukherjee, S. & Biswas, T. Activation of TOLLIP by porin prevents TLR2-associated IFN-γ and TNF-α-induced apoptosis of intestinal epithelial cells. *Cell. Signal.* **26**, 2674–2682 (2014).

59. Woznicki, J. A. *et al.* Human BCL-G regulates secretion of inflammatory chemokines but is dispensable for induction of apoptosis by IFN-γ and TNF-α in intestinal epithelial cells. doi:10.1038/s41419-020-2263-0

60. Monocytes, H. T.- *et al.* Essential Involvement of Cross-Talk Between IFN- g and TNF- a in CXCL10 Production in human THP-1 monocytes. 690–697 (2009).

61. Clarke, D. L. *et al.* TNFα and IFNγ synergistically enhance transcriptional activation of CXCL10 in human airway smooth muscle cells via STAT-1, NF-κB, and the transcriptional coactivator CREB-binding protein. *J. Biol. Chem.* **285**, 29101–10 (2010).

62. English, J. G. *et al.* MAPK feedback encodes a switch and timer for tunable stress adaptation in yeast. **8**, 1–29 (2015).

63. Nelson, D. E. *et al.* Oscillations in NF-κB signaling control the dynamics of gene expression. *Science (80-.).* (2004).

64. Werner, S. L. *et al.* Encoding NF-κB temporal control in response to TNF: Distinct roles for the negative regulators IκBα and A20. *Genes Dev.* (2008).

65. Werner, S. L., Barken, D. & Hoffmann, A. Stimulus specificity of gene expression programs determined by temporal control of IKK activity. *Science (80-.).* (2005).

66. Lee, T. K. *et al.* A noisy paracrine signal determines the cellular NF-κB response to lipopolysaccharide. *Sci. Signal.* (2009).

67. Fulda, S. & Debatin, K. M. IFNγ sensitizes for apoptosis by upregulating caspase-8 expression through the Stat1 pathway. *Oncogene* **21**, 2295–2308 (2002).

68. Li, J. H. *et al.* Interferon-γ augments CD95(APO-1/Fas) and pro-caspase-8 expression and sensitizes human vascular endothelial cells to CD95-mediated apoptosis. *Am. J. Pathol.* **161**, 1485–1495 (2002).

69. Peteranderl, C. & Herold, S. The impact of the interferon/TNF-related apoptosis-inducing ligand signaling axis on disease progression in respiratory viral infection and beyond. *Frontiers in Immunology* **8**, 1 (2017).

70. Chang, Y.-H., Chao, Y., Hsieh, S.-L. & Lin, W.-W. Mechanism of LIGHT/interferon-?-induced cell death in HT-29 cells. *J. Cell. Biochem.* **93**, 1188–1202 (2004).

71. Dai, C. & Krantz, S. B. *Interferon Induces Upregulation and Activation of Caspases 1, 3, and 8 to Produce Apoptosis in Human Erythroid Progenitor Cells*.

72. Cosentino, K. & García-Sáez, A. J. Bax and Bak Pores: Are We Closing the Circle? *Trends in Cell Biology* **27**, 266–275 (2017).

73. Tang, D., Kang, R., Berghe, T. Vanden & Vandenabeele, P. The molecular machinery of regulated cell death. *Cell Res.* (2019).

74. Warren, C. F. A., Wong-Brown, M. W. & Bowden, N. A. BCL-2 family isoforms in apoptosis and cancer. *Cell Death and Disease* **10**, 1–12 (2019).

75. Cao, Z. *et al.* STAT1-Mediated Down-Regulation of Bcl-2 Expression Is Involved in IFN-γ/TNF-α–Induced Apoptosis in NIT-1 Cells. *PLoS One* **10**, e0120921 (2015).

76. Cao, Z. *et al.* Caspase-3 is Involved in IFN-γ- and TNF-α-Mediated MIN6 Cells Apoptosis via NF-κB/Bcl-2 Pathway. *Cell Biochem. Biophys.* **67**, 1239–1248 (2013).

77. Mi, C. *et al.* Immunopharmacology and Immunotoxicology Amorfrutin A inhibits TNF-α induced JAK/STAT signaling, cell survival and proliferation of human cancer cells Amorfrutin A inhibits TNF-a induced JAK/STAT signaling, cell survival and proliferation of human cancer cells. (2017).

78. Kim, H. S., Kim, S. & Lee, M.-S. IFN-gamma sensitizes MIN6N8 insulinoma cells to TNF-alpha-induced apoptosis by inhibiting NF-kappaB-mediated XIAP upregulation. *Biochem. Biophys. Res. Commun.* **336**, 847–53 (2005).

79. Probst, B. L. *et al.* Smac mimetics increase cancer cell response to chemotherapeutics in a TNF-α-dependent manner. *Cell Death Differ.* **17**, 1645–1654 (2010).

80. Thomas, L. W., Lam, C. & Edwards, S. W. Mcl-1; the molecular regulation of protein function. *FEBS Letters* **584**, 2981–2989 (2010).

81. Jimbo, H., Nagai, H., Fujiwara, S., Shimoura, N. & Nishigori, C. Fas-FasL interaction in cytotoxic T cell-mediated vitiligo: The role of lesional expression of tumor necrosis factor-α and interferon-γ in Fas-mediated melanocyte apoptosis. *Exp. Dermatol.* **29**, 61–70 (2020).

82. Druilhe, A., Arock, M., Le Goff, L. & Pretolani, M. Human eosinophils express Bcl-2 family proteins: Modulation of Mcl-1 expression by IFN-γ. *Am. J. Respir. Cell Mol. Biol.* **18**, 315–322 (1998).

83. Majumdar, T. *et al.* Tryptophan-kynurenine pathway attenuates β-catenin-dependent pro-parasitic role of STING-TICAM2-IRF3-IDO1 signalosome in Toxoplasma gondii infection. *Cell Death Dis.* **10**, (2019).

84. Seya, T. *et al.* TLR3/TICAM-1 signaling in tumor cell RIP3-dependent necroptosis. *Oncoimmunology* **1**, 917–923 (2012).

85. Kaiser, W. J. *et al.* Toll-like receptor 3-mediated necrosis via TRIF, RIP3, and MLKL. *J. Biol. Chem.* **288**, 31268–31279 (2013).

86. Cai, Z. *et al.* Plasma membrane translocation of trimerized MLKL protein is required for TNF-induced necroptosis. *Nat. Cell Biol.* **16**, 55–65 (2014).

87. Jiancheng Chen ‡ §, Shunsuke Kuroki ‡ ¶, M. S. ‡ § & and Shin Yonehara ‡ § *. Interferon-g induces the cell surface exposure of phosphatidylserine by activating MLKL in the absence of caspase-8 activity.

88. Chang, I. *et al.* - Role of Calcium in Pancreatic Islet Cell Death by IFN- /TNF. *J. Immunol.* **172**, 7008–7014 (2014).

89. Jacobsen, A. V *et al.* HSP90 activity is required for MLKL oligomerisation and membrane translocation and the induction of necroptotic cell death. *Cell Death Dis.* **7**, e2051 (2016).

90. Zhao, X. M. *et al.* Hsp90 modulates the stability of MLKL and is required for TNF-induced necroptosis. *Cell Death Dis.* **7**, e2089 (2016).

91. Wang, Z., Han, G., Liu, Q., Zhang, W. & Wang, J. Silencing of PYGB suppresses growth and promotes the apoptosis of prostate cancer cells via the NF-κB/Nrf2 signaling pathway. *Mol. Med. Rep.* **18**, 3800–3808 (2018).

92. Xia, B., Zhang, K. & Liu, C. PYGB Promoted Tumor Progression by Regulating Wnt/β-Catenin Pathway in Gastric Cancer. *Technol. Cancer Res. Treat.* **19**, (2020).

93. Gong, Y. N., Guy, C., Crawford, J. C. & Green, D. R. Biological events and molecular signaling following MLKL activation during necroptosis. *Cell Cycle* **16**, 1748–1760 (2017).

94. Mou, Y. *et al.* Ferroptosis, a new form of cell death: opportunities and challenges in cancer.

95. Ou, Y., Wang, S. J., Li, D., Chu, B. & Gu, W. Activation of SAT1 engages polyamine metabolism with p53-mediated ferroptotic responses. *Proc. Natl. Acad. Sci. U. S. A.* **113**, E6806–E6812 (2016).

96. Li, J. *et al.* Ferroptosis: past, present and future. *Cell Death and Disease* **11**, 1–13 (2020).

97. Hou, W. *et al.* Autophagy promotes ferroptosis by degradation of ferritin. *Autophagy* **12**, 1425–1428 (2016).

98. Lei, P., Bai, T. & Sun, Y. Mechanisms of ferroptosis and relations with regulated cell death: A review. *Front. Physiol.* **10**, (2019).

99. Friedmann Angeli, J. P. *et al.* Inactivation of the ferroptosis regulator Gpx4 triggers acute renal failure in mice. *Nat. Cell Biol.* **16**, 1180–1191 (2014).

100. Kinowaki, Y. *et al.* Glutathione peroxidase 4 overexpression inhibits ROS-induced cell death in diffuse large B-cell lymphoma. *Lab. Investig.* **98**, 609–619 (2018).

101. Dvoriantchikova, G., Grant, J., Santos, A. R. C., Hernandez, E. & Ivanov, D. Neuronal NAD(P)H oxidases contribute to ROS production and mediate RGC death after Ischemia. *Investig. Ophthalmol. Vis. Sci.* **53**, 2823–2830 (2012).

102. Alanazi, I., Hoffmann, P. & Adelson, D. L. MicroRNAs Are Part of the Regulatory Network that Controls EGF Induced Apoptosis, Including Elements of the JAK/STAT Pathway, in A431 Cells. *PLoS One* **10**, (2015).

103. Winter, S., Hultqvist Hopkins, M., Laulund, F. & Holmdahl, R. A Reduction in Intracellular

Reactive Oxygen Species Due to a Mutation in NCF4 Promotes Autoimmune Arthritis in Mice. *Antioxidants Redox Signal.* **25**, 983–996 (2016).

104. Ramonaite, R. *et al.* Influence of NADPH oxidase on inflammatory response in primary intestinal epithelial cells in patients with ulcerative colitis. *BMC Gastroenterol.* **13**, 159 (2013).

105. Muise, A. M. *et al.* NADPH oxidase complex and IBD candidate gene studies: Identification of a rare variant in NCF2 that results in reduced binding to RAC2. *Gut* **61**, 1028–1035 (2012).

106. Somasundaram, R., Deuring, J. J., Van Der Woude, C. J., Peppelenbosch, M. P. & Fuhler, G. M. Linking risk conferring mutations in NCF4 to functional consequences in Crohn's disease. *Gut* **61**, 1097 (2012).

4. Chapter 4: Phospho-tyrosine Proteomics Analysis Identifies JAK 1/2 Substrates in Cytokine Treated Intestinal Epithelial Cells

4.1. Abstract

The Janus kinase (JAK) family of tyrosine kinases are central components of the signal transduction cascades downstream of type I and type II cytokine receptors. In terms of canonical JAK-STAT signalling, JAKs phosphorylate the STAT family of transcription factors on phospho-tyrosine residues leading to their dimerization and activation. In addition to the direct phosphorylation and activation of STATs, JAKs have also been shown to phosphorylate other proteins leading to the activation of additional cellular pathways such as PI3K/AKT, Ras/Raf/MAPK/ERK and FAK/MEK pathway.[1] In our work to date we have identified JAK1 and JAK2 as the sole kinases required for IFN-γ/TNF-α induced cell death in intestinal epithelial cells and have shown that this cell death is associated with sustained activation of the JAK1/2 target transcription factor STAT1 and the regulation of late genes in these cells. In this present study we investigated the contribution of sustained JAK1/2 activation to cytokine induced cell death by blocking the late phase of JAK1/2 activity using the JAK1/2 inhibitor baricitinib. Blocking JAK1/2 activity 10 hours post-cytokine (IFN-γ/TNF-α) treatment completely rescued cell death showing the requirement for sustained and late JAK kinase activity for the cell death decision. To identify additional JAK1/2 target proteins associated with the late sustained phase of JAK1/2 kinase activity we performed phospho-tyrosine post-translational modification (p-Y PTM) proteomics. We identified 45 potential late target substrates associated with JAK1 and JAK2 kinase activity. These included 16 previously known JAK targets and 29 potential new substrates for JAK1/2. Gene ontology and KEGG pathway analysis identified a role of JAKs and their targets in the regulation of transcription, cellular structure, cell adhesion and cell-cell interaction. This data gives further insight into the potential molecular mechanisms through

which the combination of IFN-γ/TNF-α signalling through the JAK pathway can affect life and death decisions in intestinal epithelial cells.

4.2. Introduction

The integrity of intestinal epithelial cells and the epithelium is essential for gut barrier function. Increased epithelial cell death and/or impairment of epithelial barrier function is a common manifestation of inflammatory diseases which affect the gastrointestinal tract. These include inflammatory bowel diseases (IBD), graft versus host disease (GVHD) and necrotizing enterocolitis (NEC)[2–4]. The integrity of the epithelial barrier is determined by different adhesive multiprotein complexes which form apical junctional complexes between adjacent epithelial cells.[5] AJCs consists of apical tight junctions (TJs) and adherens junctions (AJs) establishing tight cell-cell contacts and interactions[6,7] TJs and AJs control the permeability of the intestinal epithelium to the entry of nutrients, essential ions and bacterial toxins. In addition to performing this gate and fence function, these complexes are also involved in maintenance of epithelial homeostasis and signal transduction.[8,9,10] TJs are composed of occludens, claudins, junctional adhesion molecules (JAM) and peripheral membrane proteins, zona occludens ((ZO), ZO-1, ZO-2 & ZO-3).[2] Current evidence indicates that the disruption of AJs and TJs can result into increased epithelial permeability, decreased gut barrier function and can contribute to the pathogenesis of gastrointestinal inflammatory diseases .[11, 12,13]

Pro-inflammatory cytokines IFN-γ & TNF-α have been shown to disrupt epithelial barrier function by diverse mechanisms[14,15,16,17]. The cytokines induce apoptosis independent disruption of barrier by downregulation of ZO-1 and JAM expression[18]. TNF-α on its own has been shown to induce barrier dysfunction by disassembly of AJCs[19,20]. In ductal pancreatic epithelium IFN-γ and TNF-α synergise to increase epithelial permeability and downregulate the expression of AJs and TJs[21]. Naydenov et al. showed that this epithelial permeability and

disassembly of AJs and TJs was reduced by blocking the kinase activity of JAK2 and protein kinase D (PKD)[21].

JAKs are a family of proteins responsible for downstream signal transduction from wide range of membrane receptors[22]. Signal transducer and activator of transcription (STATs) are the major transcription factors associated with JAK signalling which in turn regulate the expression of various genes involved in proliferation, survival, and cell death. But JAK signalling is not limited to just the JAK-STAT axis, JAKs are also involved in the intracellular signalling independent of STAT1[1]. For instance, JAK2 has been shown to contribute to the activation of the PI3K and MAPK signalling pathways in the context of myeloproliferative disorders and Alzheimer's disease.[23, 24] There is also evidence of IFN mediated activation of PI3K and MAPKs by JAK2 dependent phosphorylation of guanine-nucleotide-exchange factors (GEFs).[25] β-catenin is a direct substrate for JAK3[26]. JAK3 mediates phosphorylation of β-catenin at three tyrosine residues (Tyr30, Tyr64, and Tyr86). This phosphorylation plays an important role in the regulation of epithelial-mesenchymal transition, organisation of apical junctions and epithelial barrier functions[26].There is also evidence of direct interaction of JAK1 with tight junction protein ZO-2 in vascular smooth muscle cells[27].

However, while much has been reported about the effects of the proinflammatory cytokines IFN-γ and TNF-α on disruption of the epithelial barrier the direct mechanisms of action and target molecules involved have yet to be identified[5]. In this study, we show that cell death of intestinal epithelial cells induced by the synergistic combination of IFN-γ and TNF-α requires sustained late-phase activation of JAK1 and JAK2. Furthermore, by using a phospho-tyrosine post-translational modification (p-Y PTM) proteomics approach we have identified 45 JAK1/2 target substrates associated with this sustained late-phase of JAK1 and JAK2 kinase activity. Out of 45 JAK1/2 targets we identified 16 proteins which have previously been

reported to be associated with JAK1/2 signalling pathway directly or indirectly. There were also 29 novel targets identified in the study which were associated with the regulation of epithelial cell structure, cellular integrity, and cell-cell interaction. Our study suggests that sustained activation of JAK1 and JAK2 by the cytokine combination of IFN-γ and TNF-α leads to the phosphorylation of target proteins involved in regulation of transcription, cellular structure, cell adhesion and cell-cell interaction. These results provide a potential mechanistic basis for the cytotoxic and epithelial barrier disruptive properties of these cytokines.

4.3. Methods and material

4.3.1. Cell culture

The human CRC cell line HT-29 (ATCC® HTB-38) was obtained from the American Type Culture Collection (ATCC) and cultured in McCoy's5A medium (Sigma-Aldrich #M9309). Medium supplemented with 10% FBS ((Sigma-Aldrich) and 100 IU/mL penicillin (Sigma-Aldrich) and 0.1 mg/mL streptomycin (Sigma-Aldrich). Cells were cultured and maintained in cell and tissue culture incubators at 37ºC temperature and 5% CO_2 conditions at all the time. The cell line was tested for mycoplasma status was mycoplasma free.

4.3.2. Reagents

Recombinant human IFNγ (Peprotech # 300-02) and recombinant human TNFα (Peprotech # 300-01A) were used for cell stimulation using 10 ng/mL concentration of each. JAK inhibitors Filgotinib (Selleckchem #S7605), Fedratinib (Selleckchem #S2736), Upadacitinib (Insightbio #HY-19569), BMS-911543 (Bertin Pharma #21088), Baricitinib (Selleckchem #S2851) and Ruxolitinib (Selleckchem #S2851) were used at 1µM final concentration. Antibodies used for immunoblotting were as follow: STAT1 (CST #9172), anti-phospho-STAT1-Y701 (rabbit-clone-58D6-CST #9167), phospho-STAT1-S727 (CST #9177), STAT3 (CST #9139), Phospho-Stat3 (Tyr705) (rabbit clone D3A7) (CST #9145), DAPP1/BAM32 (CST #13598) Phospho-DAPP1/BAM32 (Tyr139) (rabbit clone D7G4G) (CST #13703), PDX-1, phospho-PRDX1 (Tyr194) (rabbit clone D1T9C) (CST #14041), phospho-FAK (CST #3281), phospho-FAK (CST #3284), FAK (CST #13009), JNK (CST #92587), phospho-JNK (CST #9251), Src (CST #2107), phospho-Src (CST #21 , phospho-Src (CST #6949), Src (CST #2123) anti-GAPDH (Ambion, AM4300), anti-Beta actin (sc-47778), anti-mouse IgG (Sigma #A2554), anti-rabbit IgG (Sigma #A6154).

4.3.3. Cell death assays

Cell viability was measured by quantitation of ATP present in the cells using CellTiter-Glo® luminescent assay (Promega # G7570) and caspase-3 and -7 activities were measured by using Caspase-Glo® 3/7 assay kit (Promega #G8091) according to the manufacturer's instructions. The luminescence was recorded using Synergy2, Biotek plate reader. Raw viability data were normalised to the control wells in the absence of any treatment.

4.3.4. Cell lysis and immunoblotting

Cells were stimulated with indicated treatments for indicated times and washed twice with ice-cold PBS (phosphate buffer saline) and lysed in RIPA buffer (50 mM Tris-HCl (pH 7.4), 1%NP-40, 0.25% Na deoxycholate, 150 mM NaCl, 1 mM EDTA) supplemented with broad spectrum serine protease inhibitor (AEBSF-HCl) (Stratech #S7378-SEL) and HaltTM protease & phosphatase cocktail inhibitor-100X (Thermo scientific #78446). Protein concentrations were determined with the Pierce™ BCA (bicinchoninic acid) protein assay kit (Thermo Fischer Scientific #23225). Electrophoresis was performed using 4-12% Bis-Tris gradient gels (Thermo Fisher #NW04125BOX) and mini gel tanks as per manufacturers' instructions. Proteins were transferred to a 0.45-micron PVDF membrane (Millipore; Immobilon-FL) using mini bolt module (Thermo Fisher #B1000) as suggested by the manufacturer. The membranes were blocked in 1X TBST (Tris Buffer Saline, 0.1% Tween-20) containing 5% Bovine serum albumin (BSA) for 1hour at room temperature. Membranes were incubated with primary antibodies diluted in 5% BSA over-night at 4°C. Secondary antibody incubation was performed for 1h at room temperature. The blots were developed using Western Bright Quantum HRP substrate (Cat no# K-12042-D20) according to the manufacturer's instructions. Chemiluminescence detection was captured using Fujifilm LAS-3000 System.

4.3.5. Homogeneous Time Resolved Fluorescence (HTRF) assay

HT-29 cells were seeded in 96 well plates and stimulated with IFN-γ and TNF-α as indicated. The treatment media was removed, and cells were lysed using lysis buffer provided with the HTRF kit (Cisbio # 63ADK026PEG). Level of STAT1 and STAT1 pY701 protein were quantified by using STAT1/p-STAT1 HTRF kit (Cisbio # 63ADK026PEG). Cell lysates were incubated with STAT1 or p-STAT1 detection antibodies for 4 hours according to the manufacturer's guidelines. Fluorescence were measure at two different wavelengths 665nm and 620nm using Synergy2, Biotek plate reader. Phospho- and total protein levels were calculated as HTRF ratios, the ratio of fluorescence signal at 665 nm to Signal 620 nm. The relative or normalised values were calculated by calculating the ratio of the HTRF ratio of STAT1 pY701 to the HTRF ratio of STAT1.

HTRF Ratio = (Signal 665 nm / Signal 620 nm) x 10^4

Normalization value (P/T) = (Phospho HTRF Ratio / Total HTRF Ratio) x 100

4.3.6. Phospho-tyrosine Post-translational Modification (p-Y PTM) Proteomics

HT-29 cells were plated in 15 cm cell culture dishes at a density of 9x10^6 cells/dish in McCoy 5A media supplemented with 10% FBS and 1% Penstrep and grown for 24 hours. Media was removed and cells were washed twice with prewarmed PBS. For phospho-PTM profiling, four treatment conditions were performed using 10 culture dishes per treatment condition. 1. HT-29 cells treated with condition media for 10 hours followed by treatment with DMSO (1:10,000 times diluted in condition media) for 15 minutes. 2. HT29 cells treated with culture media supplemented with IFN-γ+TNF-α (10 ng/mL of each) for 10 hours followed by treatment with condition media with DMSO (1:10,000 times diluted) and IFN-γ + TNF-α (10 ng/mL of each) for 15 minutes 3. HT-29 cells treated with culture media for 10 hours followed by treatment with

condition media with the JAK1/2 inhibitor baricitinib (1μM) for 15 minutes, 4. HT-29 cells treated with condition media supplemented with IFN-γ+TNF-α (10 ng/mL of each) for 10 hours followed by treatment with culture media with baricitinib (1μM) and IFN-γ+TNF-α (10 ng/mL of each) for 15 minutes. Cells were washed with 1X PBS and lysed using 5 mL of Urea lysis buffer (20 mM HEPES, 9 M Urea, 1 mM activated sodium orthovanadate and 2.5 mM of sodium pyrophosphate) for 5 minutes and scraped out. The lysate from all treatment dishes per condition was pooled together. Lysate were snap-frozen for 4 minutes using liquid nitrogen and stored at -80^{o}C until processed. Subsequent steps were performed at Cell Signalling Technology (CST) as per their protocol. Briefly, the cell lysates were subjected to post translational modification analysis by using PTM Scan phospho-tyrosine pY-1000 Motif Antibody (CST #8803). Cell lysates were protease digested and extracted by using C-18 phase extraction kit. Peptides were immobilised by using protein A agarose column and immunoprecipitated using pY-1000 motif antibody . Eluted peptides were subjected to mass spectroscopy (LC-MS/MS). LC-MS/MS Analysis was performed using Orbitrap-Fusion Lumos, ESI-HCD. MS/MS spectra were evaluated using SEQUEST[28].

4.3.7. PTM Scan data analysis

For the analysis of PTMScan data the cut offs used in each step were minimum fold-change, intensity and % CV. A minimum of 2.5-fold cut of was used as significant for fold changes. Any peptide with a fold change greater than 2.5 that had a Max Intensity less than 500,000 were excluded. Secondly the peptides with a Max % CV > 50% on the duplicates were also removed. From the remaining, the peptides with at least 1.5-fold decrease in pY signal after Baricitinib treatment (in Baricitinib + IFN-γ/TNF-α sample) compared to DMSO+IT were selected. This produced a final list of bona fide “late” JAK targets.

4.3.8. Gene Ontology (GO) analysis and pathway analysis

Protein-protein interaction networks were generated using STRING protein interaction study tool (STRING-db.org). The list of selected proteins was inputted to the STRING software and default parameter setting was used for the generation of interaction maps. Pathway and GO analysis were performed by using online tool Metascape (Metascape.org). The list of selected proteins was inputted into Metascape followed by a pathway and process enrichment. Parameters used: Min Overlap: 3, p value cut off: 0.01, Min Enrichment: 1.5. Gene Prioritization by Evidence Counting (GPEC) were selected. KEGG pathways and structural complex (GO cellular components) were identified.

4.3.9. Statistical Analysis

Statistical analysis was done using GraphPad prism 7.0 (GraphPad Software, Inc., La Jolla, CA, USA). Data are presented as mean ± SEM, and statistical analysis of the data was performed using unpaired t-test or ANOVA followed by multiple comparison test. Statistically significant differences were selected at $p < 0.01$.

4.4. Results

4.4.1. Sustained activation of the JAK1/2-STAT1 pathway is required for cytokine-induced cell death of colorectal cancer cells

IFN-γ and TNF-α synergised to induce cell death in CRC cells in a JAK1/2-STAT1 dependent manner and this cell death could be rescued by blocking the kinase activity of either JAK1 or JAK2 or both (Chapter-2). However, IFN-γ is the main activator of the JAK1/2-STAT1 pathway, it induced only a moderate cytotoxic effect on its own compared to the combined treatment of cells with IFN-γ and TNF-α. Therefore, to understand the differences in activation and regulation of the JAK1/2-STAT1 signalling pathway by IFN-γ+TNF-α individually or together, we investigated the kinetics of STAT1 activation in response to cytokine treatment. HT-29 cells were treated with IFN-γ or TNF-α alone or co-treated with both cytokines for a duration of 5 minutes to 24 hours and immunoblotted for STAT1, STAT1 pY701 and STAT1 pS727 (Figure 4.1A).

In IFN-γ treated cells, there was an increase in total STAT1 levels observed 8 hours after IFN--γ treatment which further increased with time. Increased STAT1 pY701 phosphorylation was observed within 5 minutes of IFN-γ treatment and was sustained until 4-8 hours. After 8 hours there was a significant drop in STAT1 pY701 phosphorylation levels which further decreased after 24 hours of treatment. Unlike STAT1 pY701 phosphorylation, STAT1 pS727 phosphorylation could be observed only after 30 minutes of IFN-γ treatment and the levels increased with time. There was no reduction in STAT1 pS727 levels for the duration of 24 hours. For TNF-α treatment, the total STAT1 level was comparable to untreated cells and did not change significantly for the duration of 24 hours. Similarly, the level of STAT1 pY701 did not change with TNF-α treatment up to 12 hours. But there was a sudden increase in STAT1 pY701

level observed at 24-hour time point. Interestingly the STAT1 pS727 phosphorylation was regulated by TNF-α treatment at early time points. A wave of STAT1 pS727 phosphorylation could be observed between 15 minutes – 2 hours of TNF-α treatment and it reduced to the basal level afterwards. The activation profile of STAT1 in IFN-γ +TNF-α treated cells was very similar to IFN-γ treated cells. There was an accumulation of total STAT1 protein 8 hours after IFN-γ +TNF-α treatment which increased after 24 hours of treatment. Increased STAT pY701 phosphorylation was observed 5 minutes after cytokine treatment and increased afterwards. The maximum level of STAT1 pY701 phosphorylation was observed 8 hours after IFN-γ +TNF-α treatment and decreased afterwards. STAT1 pS727 phosphorylation could be seen 30 minutes after IFN-γ +TNF-α treatment and the level further increased over 24 hours. Even though the activation kinetics of IFN-γ alone and IFN-γ +TNF-α co-treatment were very similar, the magnitude of STAT1 pY701 and pS727 phosphorylation seemed to be higher and more sustained in cells treated IFN-γ +TNF-α with compared to IFN-γ treatment. But as the samples for all three conditions were run of different immunoblots, the quantitative differences in STAT1 and STAT1 pY701 or pS727 levels among these treatment groups could not be confirmed. Therefore, to further analyse the quantitative differences between individual or combined IFN-γ and TNF-α treatment, total STAT1 and STAT1 pY01 levels were compared between IFN-γ or TNF-α individual treatment alone and IFN-γ + TNF-α combined treatment by using Homogeneous Time Resolved Fluorescence (HTRF) assay (Figure 4.2)

Consistent with the western blotting data, HTRF assay also showed an increase in total STAT1 levels in IFN-γ treated cells with time. High level of STAT1 pY701 levels were detected in IFN-γ treated cells 15 min after treatment and was sustained until 4 hours of IFN-γ treatment. There was a drop in STAT1 pY701 level observed after 4 hours of treatment. For TNF-α alone, no significant change in STAT1 or STAT1 pY701 levels were observed. In cells treated with

combination of IFN-γ +TNF-α, high STAT1 pY701 levels were observed after treatment and were sustained until 12 hours of IFN-γ +TNF-α treatment and started to decrease afterwards. Even though there was a gradual decrease in the STAT1 pY701 levels with time in all groups, there was an unexpected peak observed at 20-hour time point. Taken together, there was a sustained activation of STAT1 in cells treated with IFN-γ+TNF-α, compared to the two individual cytokines alone. As described previously in chapter 3, both the magnitude and duration of activation of the JAK1/2-STAT1 pathway play an important role in the cell death decision, thus this difference in the duration of STAT1 activity could explain the differences between the cytotoxic potential of IFN-γ compared with IFN-γ + TNF-α co-treatment.

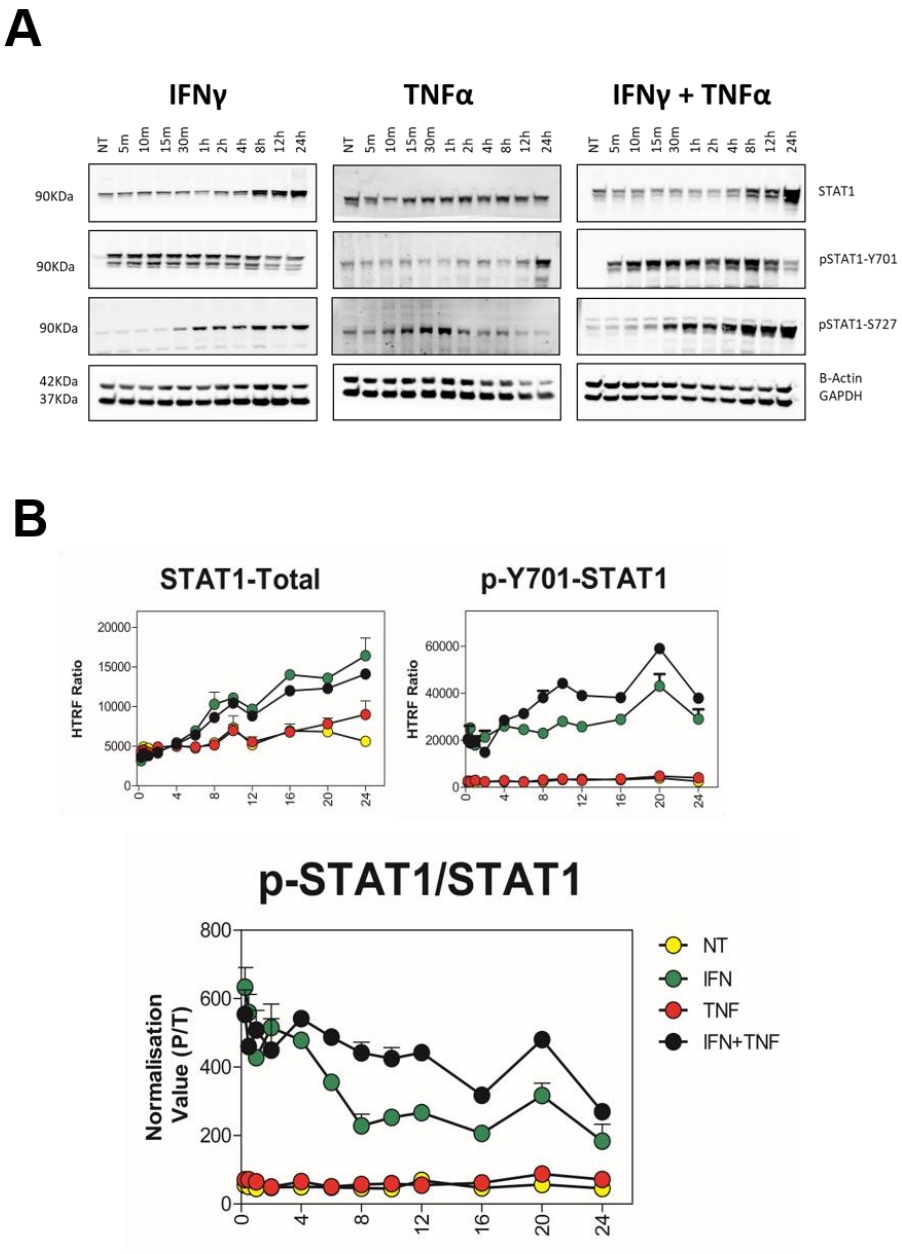


Figure 4.1. Kinetics of JAK1/2-STAT2 Pathway Activation in IFN-γ/TNF-α treated cells

(A-B) HT-29 cells were treated with 10 ng/mL of IFN-γ, TNF-α or co-treated with IFN-γ + TNF-α (10ng/mL of each) for indicated duration of time (5 minutes -24 hours). (A) Level of STAT1, STAT pY701, and STAT1 pS727 levels were analyzed by western blotting. The data is representative of 1 out of 2 experiments. (B) HTRF ratio were calculated for total STAT1 and STAT1 pY701. The normalised value for STAT1 pY701 phosphorylation level was calculated by dividing the HTRF ratio of STAT pY701 by the HTRF ratio of total STAT1 (bottom). The data is representative of one out of two experiments performed in duplicate.

4.4.2. IFN-γ + TNF-a dependent synergistic cell death is dependent on the sustained and late phase kinase activity of JAK1 and JAK2

Previously we observed that sustained activation of the JAK1/2-STAT1 pathway is crucial for the induction of cell death in CRC cells (Chapter 3). Blocking the kinase activity of JAK1 and JAK2 using the JAK1/2 inhibitor baricitinib before IFN-γ + TNF-α treatment (Figure 4.2A) or even 10 hours post IFN-γ + TNF-α treatment (Figure 4.2B) rescued the cells from cytokine induced cell death. This suggests that the sustained activation and the late phase of JAK1 and JAK2 kinase activity in particular is crucial for the induction of cell death in epithelial cells by cytokines.

.

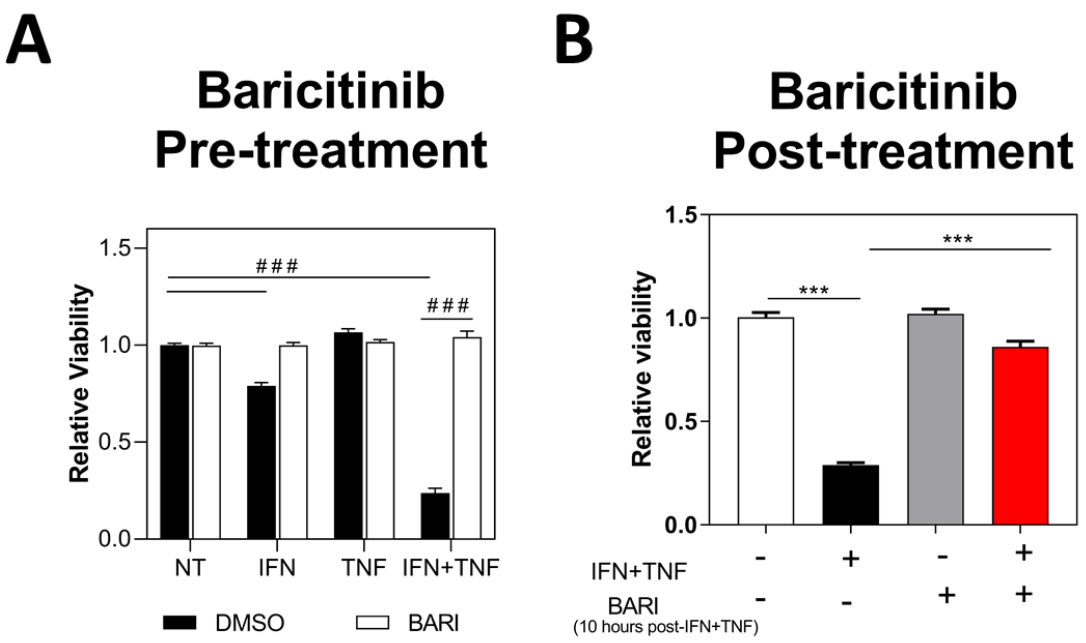


Figure 4.2 Late phase of JAK1 and JAK2 kinase activity is required for IFN-γ + TNF-α induced epithelial cell death

(A) HT-29 cells were pre-treated with 1µM baricitinib or equivalent amount of DMSO for 1 hour, followed by treatment with IFN-γ, TNF-α or IFN-γ+TNF-α (10 ng/mL of each) with or without baricitinib (1µM). Cell viability was assayed 72 hours after cytokine treatment. Data was plotted as mean ± S.E.M of n = 3 independent experiments in triplicates (B) HT-29 cells were treated with IFN-γ + TNF-α (10 ng/mL of each) for 10 hours followed by treatment with IFN-γ + TNF-α (10 ng/mL of each) with or without baricitinib (1µM). Cell viability was estimated 72 hours after cytokine treatment. Data was plotted as mean ± S.E.M of n = 2 independent experiments in triplicate. # # #p < 0.0001 (two-way ANOVA followed by Tukey's multiple comparisons test as indicated). ***p < 0.0001 (one-way ANOVA followed by Tukey's multiple comparisons test as indicated). NT=non-cytokine treated cells, Bari= JAK1/2 inhibitor baricitinib.

4.4.3. Blocking JAK1 and JAK2 kinase activity results in rapid dephosphorylation of STAT1 p-Y701

IFN-γ and TNF-α treatment increased STAT1 phosphorylation (STAT1 pY701) in HT-29 cells and we observed it to be sustained and maximum at 8-10 hours post IFN-γ + TNF-α treatment (Figure 3.3.5). Blocking the kinase activity of JAK1 and JAK2 using selective JAK inhibitors such as baricitinib can block STAT1 pY701 phosphorylation. To identify the minimum time required for STAT1 dephosphorylation upon addition of JAK 1/2 selective inhibitor[29,22,30] baricitinib we performed a kinetic experiment in HT-29 cells. Cells were treated with IFN-γ and TNF-α for 10 hours followed by co-treatment with baricitinib and IFN-γ + TNF-α (Figure 4.3A). Cells were collected subsequently each hour post baricitinib treatment for next 5 hours and STAT1 pY701 and STAT1 pS727 phosphorylation levels were analysed by immunoblotting. The cells treated with only vehicle control (DMSO) or IFN-γ + TNF-α + baricitinib for 10 hours exhibited similar level of STAT1 phosphorylation, confirming complete dephosphorylation of STAT1 with 10 hours of baricitinib, even in the presence of IFN-γ + TNF-α (Figure 4.3B). In cells treated with IFN-γ + TNF-α there was a significant increase in STAT1 expression, STAT1 pY701 and STAT1 pS727 phosphorylation after 10 hours. In contrast, in cells treated with IFN-γ + TNF-α for 10 hours followed by baricitinib treatment there was a reduction in STAT1 p-Y701 to baseline level at 1 hours post-baricitinib treatment and STAT1 pS727 decreased 2 hours post-baricitinib treatment (Figure 4.3B).

Because 1 hour post-baricitinib treatment was sufficient for phosphatase-mediated dephosphorylation of STAT1 pY701 we repeated the experiment with shorter durations of baricitinib treatment (15 minutes – 1 hour) to identify a minimum time for STAT1 pY701 dephosphorylation post-baricitinib treatment (Figure 4.3C). The data showed that STAT1 p-Y701 was dephosphorylated to baseline levels 15 min post-baricitinib treatment. These data

confirmed that blocking JAK1/2 tyrosine kinase activity with the selective JAK1/2 inhibitor baricitinib resulted in rapid dephosphorylation of STAT1 pY701 (Figure 4.3D).

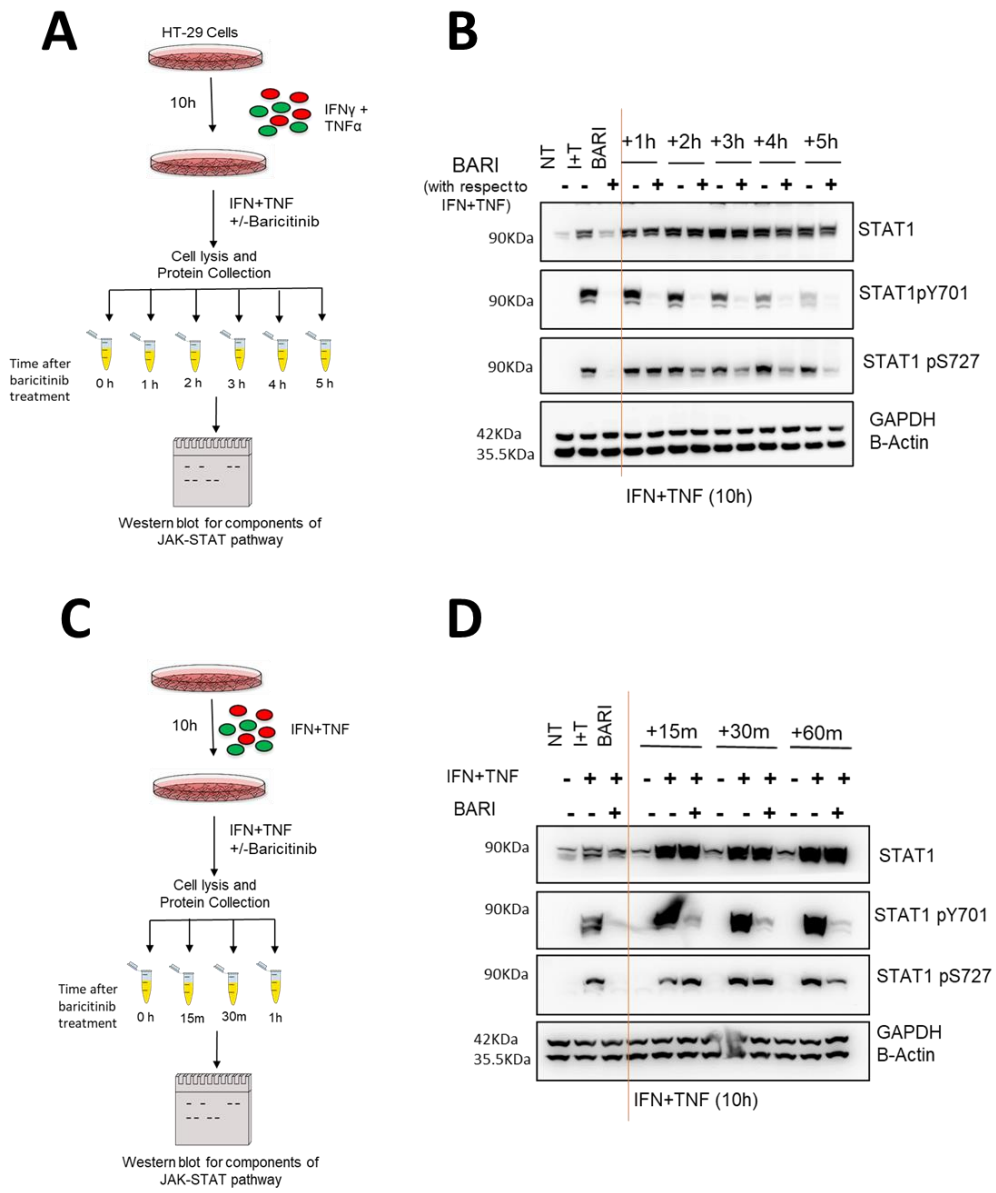


Figure 4.3. Blocking JAK1 and JAK2 kinase activity results in rapid dephosphorylation of STAT1 pY701 in cytokine treated cells

(A) & (C) Schematic representing experimental plan. HT-29 cells were treated with 10 ng/mL of IFN-γ + TNF-α for 10 hours followed by indicated duration of baricitinib treatment. Cell lysates were analysed for level of STAT1 and p-STAT1. (B) Cells were treated with baricitinib for 0-5 hours of baricitinib treatment and STAT1, STAT1 pY701 and STAT1 pS727 were analysed (D) Cells were treated with baricitinib for 0-1 hour of baricitinib treatment and STAT1, STAT1 pY701 and STAT1 pS727 were analyzed. The image is representative of 1 out of 2 independent experiments. NT= non cytokine treated cells, BARI= JAK1/2 inhibitor baricitinib, h= hours, m= minutes.

4.4.4. Identification of "late phase" JAK1/2 target substrates by phospho-tyrosine post-translational modification (p-Y PTM) proteomics

Because we found that the sustained activation of JAK1/2 and in particular the late phase activity of these kinases was critical for the induction of cell death by IFN-γ and TNF-α we decided to investigate additional phosphorylation substrates of JAK1 and JAK2. We reasoned that this approach could give us a deeper understanding of the potential kinase substrates and hence mechanisms - in addition to STAT1 regulation - through which JAK1 and JAK2 were dictating the cell death decision. To do this we decided to take a targeted phospho-tyrosine proteomics approach[31,32].

With the goal of identifying new late phase targets for JAK1/2 activity in response to IFN-γ + TNF-α treatment, a phospho-tyrosine (p-Y) PTM profiling experiment was performed as outlined in workflow (Figure 4.4). HT-29 cells were stimulated with 10 ng/mL of IFN-γ + TNF-α for 10 hours and then JAK1/2 activity was blocked using the selective JAK1/2 inhibitor baricitinib for 15 minutes[29](Figure 4.4A). Cells were washed, lysed and the lysates were flash frozen using liquid nitrogen. Next, the cell extracts were trypsin digested, and cellular proteins were extracted using C18 solid phase extraction. The peptides obtained from different samples were immuno-adsorbed to protein A/G agarose using anti-pY1000 motif antibodies. The p-Y peptides were immunoprecipitated and quantified using LC-MS/MS and spectral analysis (Figure 4.3 B). To ensure the specificity of the technique, the screen was performed in two technical runs, with each run-in duplicate.

Overall analysis from pY-PTM profiling identified 45 proteins corresponding to a total of 54 tyrosine residues modulated in response to late phase JAK1/2 activity. The selected proteins exhibited either complete dephosphorylation or more than 1.5-fold reduction in phosphorylation at their tyrosine residues upon baricitinib treatment. The results from pY

phospho-PTM findings are summarised in table 4.1 and 4.2; as list of target proteins, Sequence of peptide and p-Y sites modified and fold change in p-Y level in response to baricitinib treatment are included. There was an reproducible overlap of 33 proteins (70.2%) proteins observed between the two MS runs with 6 proteins observed unique to each independent MS experiment (Table 4.3). Basic function of each target protein is described in Table 4.4 (generated by STRING database).

Certain previously described substrates of JAK1/JAK2 such as JAK1, JAK2, STAT1, STAT3 and STAT5 were major hits in the pY-PTM screen and served as the validating targets[22]. To further understand the functionality of identified proteins and their regulation by JAK1 and JAK2, the target proteins were divided into two categories based on the knowledge from previously reported studies. (A) Known substrates of JAK1/JAK2 signalling (B) Novel targets associated with JAK1/JAK2 signalling (Table 4.4). There were 16 proteins identified as known targets of JAK1 or JAK2 in the literature. It was not surprising that the major categories of these proteins belonged to the JAK-STAT signalling pathway; with modulation in STAT1 pY701, STAT3 pY705, STAT5B pY694, STAT6 pY641, SOCS3 pY204, SHP-2 pY542 and pY546 phosphorylation[1,33,34,35]. In addition, we also observed the phosphorylation of components of several other cytokine signalling pathway e.g. JNK1 pY185 & pY223, SHIP-1 pY1022, SHIP-2 pY986, HSG pY289 & pY334 and STAM2 pY374[36]. Components of tight junction ZO-1 and ZO-2, and DSG-2 were also regulated by late phase activity of JAK1 and JAK2, which was in line with the studies showing JAK-STAT dependent regulation of these proteins[27,37,10]. Other than known substrates of JAK1 and JAK2, the pY-PTM screen identified 26 novel targets of JAK1/2 late phase activity. Interestingly some of these proteins contained 2 or more phospho-tyrosine sites regulated by JAK1 and JAK2. For example, in CDA2P (pY361, pY541, pY548) and in ZDHHC5 (pY354, pY358 and pY630) three novel sites were identified. Moving forward, to

further analyse the biological relevance of these JAK1/2 novel targets, in silico protein-protein interaction analysis and pathway analysis were performed.

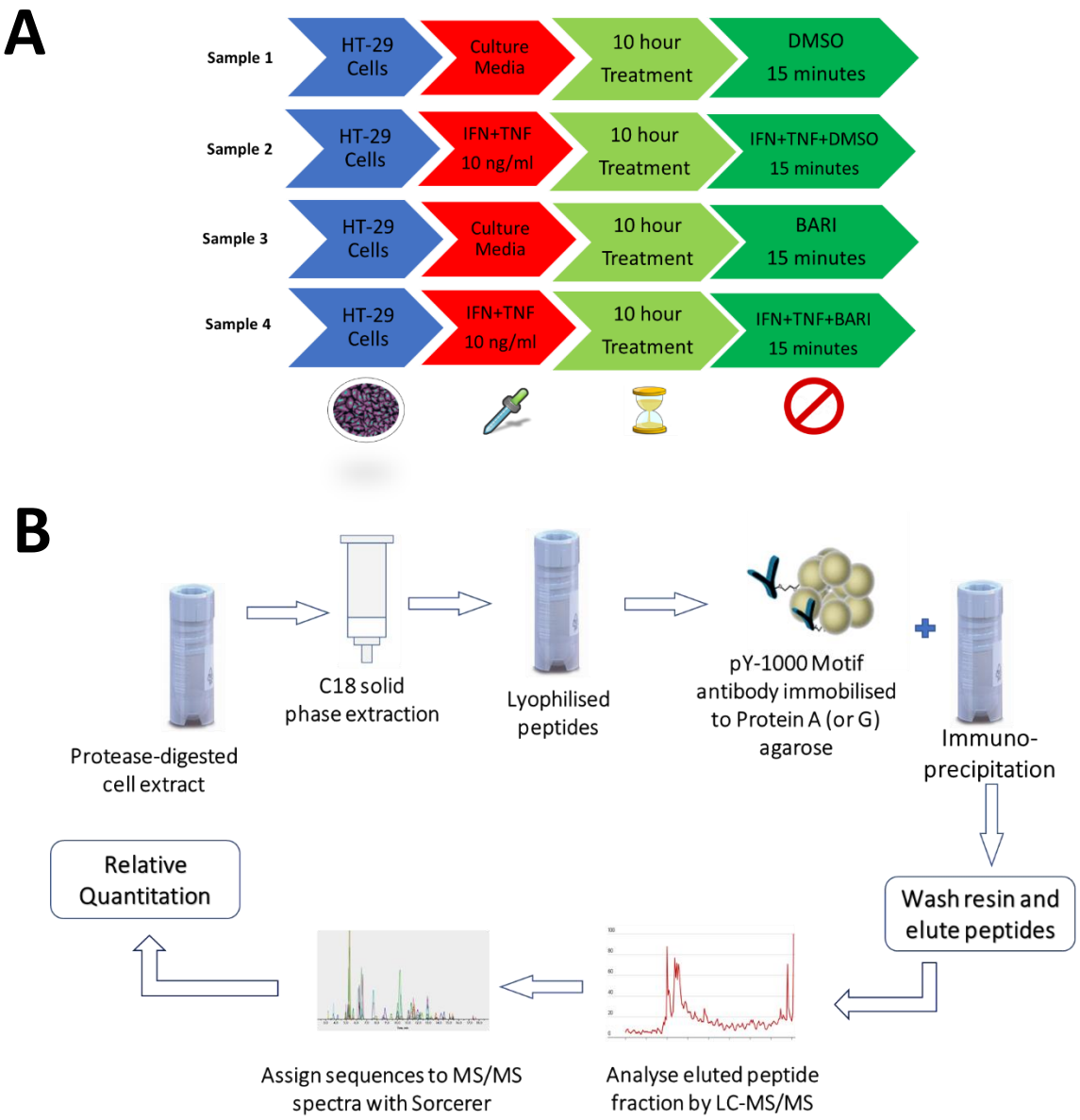


Figure 4.4 Workflow for Phospho-PTM proteomic screen to discover novel JAK1 and JAK2 phospho-tyrosine substrates

(A) Schematic representing workflow of sample preparation for pY-PTM screen. HT-29 cells were treated with 10 ng/mL of IFN-γ+TNF-α or untreated for 10 hours followed by treatment with IFN-γ+TNF-α with DMSO or baricitinib for 15 minutes. Cells were lysed with Urea based buffer lysis buffer and snap frozen in liquid nitrogen. (B) Schematic representing workflow of phospho-tyrosine proteomic screen. Cell lysate were digested into tryptic peptides and immunoprecipitated using anti-pY-1000 motif antibodies. Eluted peptide fraction were run on LC-MS/MS in duplicates. Relative quantification of MS spectra was performed.

Table 4.1: JAK1/2 late phase targets identified by PTMscan analysis (RUN-1)

	Protein Name	Peptide	Ratio BARI: DMSO	Ratio DMSO+IT: DMSO	Ratio BARI+IT: DMSO	Ratio DMSO+IT: BARI+IT
1	CHIC2	Y*SPDPVVVR	-1.1	12.4	1.6	**7.56**
2	BAG3	GY*ISIPVIHEQNVTRPAAQPSFHQAQK	-1.2	14.0	2.0	**7.01**
3	STAT1	EAPEPM#ELDGPKGTGY*IK	-1.0	411164.0	62201.4	**6.61**
4	SOCS3	KTVNGHLDSY*EK	1.3	28.6	4.7	**6.14**
5	STAT1	EAPEPMELDGPKGT*GYIKTELISVSEVHPSR	4.7	5146.6	924.3	**5.57**
6	TPD52L2	SWHDVQVSSAY*VK	-1.1	7.2	1.3	**5.52**
7	CHST8	NTVHY*GSALKR	1.1	5.4	1.1	**4.79**
8	SEPT2	QQPTQFINPETPGY*VGFANLPNQVHR	1.1	11.4	2.5	**4.60**
9	FLVCR1	GY*LPLPR	1.1	9.7	2.2	**4.36**
10	STAT3	YCRPESQEHPEADPGSAAPY*LK	-1.3	263.7	71.2	**3.71**
11	STAT5B	AVDGY*VKPQIK	-1.0	74.7	20.3	**3.69**
12	STAT3	YCRPESQEHPEADPGAAPY*LK	1.2	262.0	76.1	**3.44**
13	EPLIN	Y*PHIKDGEDLKDHSTESK	-1.1	4.3	1.5	**2.82**
14	DSG2	VIQPHGGGSNPLEGTQHLQDVPY*VMVR	1.1	2.7	1.1	**2.44**
15	SHIP	NAGDTLPQEDLPLTKPEMFENPLY*GSLSSFPKPAPR	1.7	3.4	1.4	**2.40**
16	ZO1	FTPKPY*TSSARPFER	-1.3	3.0	1.3	**2.38**
17	JAK2	GM#EY*LGTKR	-2.1	6.9	3.6	**1.95**
18	ZDHHC5	Y*RPGYSSSSTSAAMPHSSSAK	-1.4	2.8	1.5	**1.87**
19	ZDHHC5	YRPGY*SSSSTSAAMPHSSSAK	-1.4	2.8	1.5	**1.87**
20	SLC7A11	GGY*LQGNVNGR	-1.5	2.9	1.7	**1.68**
21	JAK1	AIETDKEY*Y*TVKDDR	-1.0	5264.5	3133.8	**1.68**
22	UBE2F 7	NKVDDY*IKR	-1.2	6.4	4.2	**1.53**
23	JNK1	TAGTSFMMTPY*VVTR	1.3	4.3	2.8	**1.53**
24	RAPH1	AGYGGSHISGY*ATLR	-1.0	3.0	2.0	**1.52**
25	SHIP-2	NSFNNPAY*YVLEGVPHQLLPPEPPSPAR	1.7	9.1	6.0	**1.51**
26	ZO2	RGY*YGQSAR	-3.5	5.9	-8.8	**-0.67**
27	PRDX1; PRDX2	SKEY*FSK	-5.7	3.4	-3.5	**-0.98**
28	EPB41L2	QKSY*TLVVAK	-1.2	2.8	-1.9	**-1.50**
29	SNAP23	GPVTNGQLQQPTTGAASGGY*IKR	-1.8	3.3	-2.2	**-1.51**
30	STAT6	GY*VPATIK	-5.4	2.8	-1.6	**-1.80**
31	ZDHHC5	GVGSPEPGPTAPY*LGR	-11.9	2.9	-1.6	**-1.81**
32	FLOT2	LKAEAY*QK	-2.0	3.5	-1.7	**-2.08**
33	Afadin	DLQY*ITVSKEELSSGDSLSPDPWKR	1.4	4.1	-1.8	**-2.22**
34	HRS	YLNRNY*WEK	-1.7	4.4	-1.8	**-2.48**
35	HRS2	STYTSY*PK	-2.0	7.2	-2.8	**-2.62**
36	SHP-2	RKGHEY*TNIK	-1.0	3.5	-1.3	**-2.62**
37	DAPP1	KVEEPSIY*ESVR	1.5	11.8	-4.4	**-2.70**
38	MISP	VTRY*PILGIPQAHR	-1.2	5.0	-1.8	**-2.72**
39	SNCG	EGVM#Y*VGAK	-1.1	4.7	-1.6	**-2.85**
40	CD2AP	Y*FSLKPEEKDEK	-1.4	4.0	-1.2	**-3.48**
41	CD2AP	DTCY*SPKPSVYLSTPSSASK	-1.8	7.0	-1.3	**-5.42**
42	CD2AP	DTCYSPKPSVY*LSTPSSASK	-1.8	7.0	-1.3	**-5.42**
43	Zyxin	VSSGY*VPPPVATPFSSK	1.5	14.0	-2.0	**-6.90**
44	CGI-38	QDILDDSGY*VSAYK	1.2	10.4	-1.1	**-9.09**

Table 4.1 The amino acid with asterisk (*) represent the phosphorylation of tyrosine residue impacted in response to IFN+TNF treatment. The Ratio provided is the relative fold-change between the integrated peak area of the experimental (numerator) and control (denominator) conditions. A positive value denotes a decrease in phosphorylation while a negative value suggests a decrease resulting a value lower than control.

Table 4.2: JAK1/2 late targets identified by PTMscan analysis (RUN-2)

	Protein Name	Peptide	Ratio BARI: DMSO	Ratio DMSO+IT: DMSO	Ratio BARI+IT: DMSO	Ratio DMSO+IT: BARI+IT
1	STAM2	LVNEAPVYSVY*SK	1.5	19.4	1.1	**17.9**
2	ZDHHC5	GVGSPEPGPTAPY*LGR	-4.4	18.6	1.6	**11.4**
3	CHIC2	Y*SPDPVVVR	-1.7	26.8	2.6	**10.3**
4	CD2AP	DTCY*SPKPSVYLSTPSSASK	1.3	13.9	1.6	**8.52**
5	CD2AP	DTCYSPKPSVY*LSTPSSASK	1.3	13.9	1.6	**8.52**
6	BAG3	GY*ISIPVIHEQNVTRPAAQPSFHQAQK	-1.5	9.2	1.3	**7.16**
7	SOCS3	KTVNGHLDSY*EK	1.8	17.8	2.8	**6.25**
8	STAT1	EAPEPM#ELDGPKGTGY*IK	1.2	383226.2	62365.0	**6.14**
9	PLEKHA7	LQQSSTIAPY*VTLR	1.0	8.5	1.5	**5.77**
10	STAT1	EAPEPMELDGPKGT*GYIKTELISVSEVHPSR	1.7	8827.8	1623.5	**5.4**
11	STAT1	GTGY*IKTELISVSEVHPSR	3.5	408.8	78.2	**5.2**
12	DAPP1	KVEEPSIY*ESVR	1.6	13.3	2.7	**5.0**
13	SEPT2.	QQPTQFINPETPGY*VGFANLPNQVHR	-1.0	8.6	1.9	**4.47**
14	TPD52L2	SWHDVQVSSAY*VK	-1.7	9.0	2.3	**3.91**
15	STAT3	YCRPESQEHPEADPGSAAPY*LK	-1.4	202.1	57.6	**3.51**
16	DSG2	VIQPHGGGSNPLEGTQHLQDVPY*VMVR	-1.7	5.0	1.5	**3.23**
17	ZO-1	FTPKPY*TSSARPFER	-1.2	3.7	1.2	**3.12**
18	PXN	LLLELNAVQHNPPGFPADEANSSPP LPGALSPLY*GVPETNSPLGGK	1.5	3.7	1.2	**2.96**
19	STAT5B	AVDGY*VKPQIK	-1.3	72.1	24.5	**2.95**
20	STAT3	YCRPESQEHPEADPGAAPY*LK	-2.0	158.7	54.6	**2.91**
21	ZDHHC5	Y*RPGYSSSSTSAAMPHSSSAK	-2.0	3.0	1.2	**2.39**
22	ZDHHC5	YRPGY*SSSSTSAAMPHSSSAK	-2.0	3.0	1.2	**2.39**
23	RANBP1	ICANHY*ITPMMELKPNAGSDR	1.1	3.4	1.5	**2.31**
24	JAK2	REVGDY*GQLHETEVLLK	-2.8	30.2	15.7	**1.93**
25	LMO7	SRQPSY*VPAPLRK	1.1	2.6	1.4	**1.86**
26	SLC7A11	GGY*LQGNVNGR	-1.1	4.2	2.4	**1.74**
27	UBE2F	NKVDDY*IKR	-1.1	5.6	3.4	**1.66**
28	JAK1	AIETDKEY*Y*TVKDDR	1.2	4362.6	2840.1	**1.54**
29	ZO-2	RGY*YGQSAR	-4.2	3.0	-16.9	**-0.18**
30	PRDX1 PRDX2	SKEY*FSK	-4.8	4.6	-3.8	**-1.22**
31	SHP-2	RKGHEY*TNIK	-1.2	3.4	-1.9	**-1.77**
32	ZNF185	GILFVKEY*VNASEVSSGKPVSAR	1.3	3.1	-1.7	**-1.79**
33	STAT6	GY*VPATIK	-4.0	2.8	-1.5	**-1.86**
34	Zyxin	VSSGY*VPPPVATPFSSK	1.2	8.5	-3.8	**-2.22**
35	FLOT2	LKAEAY*QK	-1.7	4.5	-2.0	**-2.27**
36	eplin	Y*PHIKDGEDLKDHSTESK	-1.3	2.8	-1.1	**-2.5**
37	ADD3	WLNSPNTY*MK	-1.5	3.2	-1.3	**-2.58**
38	MISP	VTRY*PILGIPQAHR	1.2	3.1	-1.1	**-2.9**
39	CHST8	NTVHY*GSALKR	1.2	4.1	-1.4	**-2.95**
40	CD2AP	Y*FSLKPEEKDEK	-1.1	4.4	-1.0	**-4.29**
41	SNAP23	GPVTNGQLQQPTTGAASGGY*IKR	-1.6	6.9	-1.5	**-4.50**
42	HRS	YLNRNY*WEK	-1.8	4.8	-1.1	**-4.54**
43	TPPP3	QDILDDSGY*VSAYK	-1.1	6.4	-1.1	**-5.65**
44	Afadin	RQEEGY*YSRLEAER	-1.3	7.4	-1.0	**-7.4**
45	FLVCR1	GY*LPLPR	1.0	8.2	-1.1	**-7.53**

Table 4.2 The amino acid with asterisk (*) represent the phosphorylation of tyrosine residue impacted in response to IFN+TNF treatment. The Ratio provided is the relative fold-change between the integrated peak area of the experimental (numerator) and control (denominator) conditions. A positive value denotes a decrease in phosphorylation while a negative value suggests a decrease resulting a value lower than control.

Table 4.3: JAK1/2 late phase targets identified in both pY-PTMscan analysis runs (run 1 & run2)

	Protein Name	Peptide	Ratio DMSO+IT: BARI+IT (RUN-1)	Ratio DMSO+IT: BARI+IT (RUN-2)
1	CHIC2	Y*SPDPVVVR	**7.56**	**10.3**
2	BAG3	GY*ISIPVIHEQNVTRPAAQPSFHQAQK	**7.01**	**7.16**
3	STAT1	EAPEPM#ELDGPKGTGY*IK	**6.61**	**6.14**
4	SOCS3	KTVNGHLDSY*EK	**6.14**	**6.25**
5	STAT1	EAPEPMELDGPKGT*GYIKTELISVSEVHPSR	**5.57**	**5.4**
6	TPD52L2	SWHDVQVSSAY*VK	**5.52**	**3.91**
7	CHST8	NTVHY*GSALKR	**4.79**	**-2.95**
8	SEPT2	QQPTQFINPETPGY*VGFANLPNQVHR	**4.60**	**4.47**
9	FLVCR1	GY*LPLPR	**4.36**	**-7.53**
10	STAT3	YCRPESQEHPEADPGSAAPY*LK	**3.71**	**3.51**
11	STAT5B	AVDGY*VKPQIK	**3.69**	**2.95**
12	STAT3	YCRPESQEHPEADPGAAPY*LK	**3.44**	**2.91**
13	EPLIN	Y*PHIKDGEDLKDHSTESK	**2.82**	**-2.5**
14	DSG2	VIQPHGGGSNPLEGTQHLQDVPY*VMVR	**2.44**	**3.23**
15	ZO1	FTPKPY*TSSARPFER	**2.38**	**3.12**
16	ZDHHC5	Y*RPGYSSSSTSAAMPHSSSAK	**1.87**	**2.39**
17	ZDHHC5	YRPGY*SSSSTSAAMPHSSSAK	**1.87**	**2.39**
18	SLC7A11	GGY*LQGNVNGR	**1.68**	**1.74**
19	JAK1	AIETDKEY*Y*TVKDDR	**1.68**	**1.54**
20	UBE2F 7	NKVDDY*IKR	**1.53**	**1.66**
21	ZO2	RGY*YGQSAR	**-0.67**	**-0.18**
22	PRDX1; PRDX2	SKEY*FSK	**-0.98**	**-1.22**
23	SNAP23	GPVTNGQLQQPTTGAASGGY*IKR	**-1.51**	**-4.5**
24	STAT6	GY*VPATIK	**-1.80**	**-1.86**
25	ZDHHC5	GVGSPEPGPTAPY*LGR	**-1.81**	**11.4**
26	FLOT2	LKAEAY*QK	**-2.08**	**-2.27**
27	HRS	YLNRNY*WEK	**-2.48**	**-4.54**
28	SHP-2	RKGHEY*TNIK	**-2.62**	**-1.77**
29	DAPP1	KVEEPSIY*ESVR	**-2.70**	**5.0**
30	MISP	VTRY*PILGIPQAHR	**-2.72**	**-2.9**
31	CD2AP	Y*FSLKPEEKDEK	**-3.48**	**-4.29**
32	CD2AP	DTCY*SPKPSVYLSTPSSASK	**-5.42**	**8.52**
33	CD2AP	DTCYSPKPSVY*LSTPSSASK	**-5.42**	**8.52**
34	Zyxin	VSSGY*VPPPVATPFSSK	**-6.90**	**-2.22**
35	CGI-38	QDILDDSGY*VSAYK	**-9.09**	**-5.65**

Table 4.4 The description of late protein targets generated by STRING protein interaction software.

Query Item	Uniprot Identifier	Annotation	Description
ADD3	Q9UEY8	Gamma-adducin;	Membrane-cytoskeleton-associated protein that promotes the assembly of the spectrin-actin network. Plays a role in actin filament capping. Binds to calmodulin; Belongs to the aldolase class II family. Adducin subfamily
Afadin/ MLLT4	P55196	Afadin	Belongs to an adhesion system, probably together with the E-cadherin-catenin system, which plays a role in the organization of homotypic, interneuronal and heterotypic cell-cell adherens junctions (AJs). Nectin- and actin-filament-binding protein that connects nectin to the actin cytoskeleton
BAG3	O95817	BAG family molecular chaperone regulator 3;	Co-chaperone for HSP70 and HSC70 chaperone proteins. Acts as a nucleotide-exchange factor (NEF) promoting the release of ADP from the HSP70 and HSC70 proteins thereby triggering client/substrate protein release. Nucleotide release is mediated via its binding to the nucleotide-binding domain (NBD) of HSPA8/HSC70 whereas the substrate release is mediated via its binding to the substrate-binding domain (SBD) of HSPA8/HSC70. Has anti-apoptotic activity. Plays a role in the HSF1 nucleocytoplasmic transport;
CD2AP	Q9Y5K6	CD2-associated protein	Seems to act as an adapter protein between membrane proteins and the actin cytoskeleton. In collaboration with CBLC, modulates the rate of RET turnover and may act as regulatory checkpoint that limits the potency of GDNF on neuronal survival. Controls CBLC function, converting it from an inhibitor to a promoter of RET degradation (By similarity). May play a role in receptor clustering and cytoskeletal polarity in the junction between T-cell and antigen-presenting cell
CGI-38 or TPPP3	Q9BW30	Tubulin polymerization-promoting protein family member 3;	Binds tubulin and has microtubule bundling activity. May play a role in cell proliferation and mitosis; Tubulin polymerization promoting proteins
CHIC2	Q9UKJ5	Cysteine-rich hydrophobic domain-containing protein 2	Cysteine rich hydrophobic domain 2; Belongs to the CHIC family
CHST8	Q9H2A9	Carbohydrate sulfotransferase 8;	Catalyses the transfer of sulphate to position 4 of non- reducing N-acetyl galactosamine (GalNAc) residues in both N-glycans and O-glycans. Required for biosynthesis of glycoprotein hormones lutropin and thyrotropin, by mediating sulfation of their carbohydrate structures. Only active against terminal GalNAcbeta1, GalNAcbeta. Not active toward chondroitin; Belongs to the sulfotransferase 2 family
DAPP1	Q9UN19	Dual adapter for phosphotyrosine and 3-phosphotyrosine and 3-phosphoinositide;	May act as a B-cell-associated adapter that regulates B- cell antigen receptor (BCR)-signalling downstream of PI3K;

DSG2	Q14126	Desmoglein-2;	Component of intercellular desmosome junctions. Involved in the interaction of plaque proteins and intermediate filaments mediating cell-cell adhesion
Eplin or LIMA1	Q9UHB6	LIM domain and actin-binding protein 1;	Binds to actin monomers and filaments. Increases the number and size of actin stress fibres and inhibits membrane ruffling. Inhibits actin filament depolymerization. Bundles actin filaments, delays filament nucleation and reduces formation of branched filaments.
FLOT2	Q14254	Flotillin-2	May act as a scaffolding protein within caveolar membranes, functionally participating in formation of caveolae or caveolae-like vesicles. May be involved in epidermal cell adhesion and epidermal structure and function; Belongs to the band 7/mec-2 family.
FLVCR1	Q9Y5Y0	Feline leukaemia virus subgroup C receptor-related protein 1; Isoform 1:	Heme transporter that exports cytoplasmic heme. It can also export coproporphyrin and protoporphyrin IX, which are both intermediate products in the heme biosynthetic pathway. Does not export bilirubin. Heme export depends on the presence of HPX and is required to maintain intracellular free heme balance, protecting cells from heme toxicity. Heme export provides protection from heme or ferrous iron toxicities in liver, brain, sensory neurons and during erythropoiesis, a process in which heme synthesis intensifies.
HRS/ HGS	O14964	Hepatocyte growth factor-regulated tyrosine kinase substrate;	Involved in intracellular signal transduction mediated by cytokines and growth factors. When associated with STAM, it suppresses DNA signaling upon stimulation by IL-2 and GM-CSF. Could be a direct effector of PI3-kinase in vesicular pathway via early endosomes and may regulate trafficking to early and late endosomes by recruiting clathrin. May concentrate ubiquitinated receptors within clathrin-coated regions. Involved in down- regulation of receptor tyrosine kinase via multivesicular body (MVBs) when complexed with STAM
JAK1	P23458	Tyrosine-protein kinase JAK1;	Tyrosine kinase of the non-receptor type involved in the IFN-alpha/beta/gamma signal pathway. Kinase partner for the interleukin (IL)-2 receptor; FERM domain containing
JAK2	O60674	Tyrosine-protein kinase JAK2;	Non-receptor tyrosine kinase involved in various processes such as cell growth, development, differentiation, or histone modifications. Mediates essential signalling events in both innate and adaptive immunity. In the cytoplasm, plays a pivotal role in signal transduction via its association with type I receptors such as growth hormone (GHR), prolactin (PRLR), leptin (LEPR), erythropoietin (EPOR), thrombopoietin (THPO); or type II receptors including IFN-alpha, IFN-beta, IFN-γamma and multiple interleukins.
LMO7	Q8WWI1	LIM domain only protein 7	
MISP	Q8IVT2	Mitotic interactor and substrate of PLK1;	Plays a role in mitotic spindle orientation and mitotic progression. Regulates the distribution of dynactin at the cell cortex in a PLK1-dependent manner, thus stabilizing cortical and astral microtubule attachments required for proper mitotic spindle positioning. May link microtubules to the actin cytoskeleton and focal adhesions. May be required for directed cell migration and centrosome orientation. May also be necessary for proper stacking of the Golgi apparatus; Belongs to the MISP family

PLEKHA7	Q61Q23	Pleckstrin homology domain-containing family A member 7;	Required for zonula adherens biogenesis and maintenance. Acts via its interaction with KIAA1543/Nezha, which anchors microtubules at their minus-ends to zonula adherens, leading to the recruitment of KIFC3 kinesin to the junctional site; Pleckstrin homology domain containing
PRDX1	P35700	Peroxiredoxin-1;	Thiol-specific peroxidase that catalyses the reduction of hydrogen peroxide and organic hydroperoxides to water and alcohols, respectively. Plays a role in cell protection against oxidative stress by detoxifying peroxides and as sensor of hydrogen peroxide-mediated signalling events. Might participate in the signalling cascades of growth factors and tumour necrosis factor-alpha by regulating the intracellular concentrations of H_2O_2. Reduces an intramolecular disulphide bond in GDPD5 that gates the ability to GDPD5 to drive postmitotic motor neuron differentiation
PRDX2	P32119	Peroxiredoxin-2	Thiol-specific peroxidase that catalyses the reduction of hydrogen peroxide and organic hydroperoxides to water and alcohols, respectively. Plays a role in cell protection against oxidative stress by detoxifying peroxides and as sensor of hydrogen peroxide-mediated signalling events. Might participate in the signalling cascades of growth factors and tumour necrosis factor-alpha by regulating the intracellular concentrations of H(2)O(2); Belongs to the peroxiredoxin family.
PXN	P49023	Paxillin	Cytoskeletal protein involved in actin-membrane attachment at sites of cell adhesion to the extracellular matrix (focal adhesion); Belongs to the paxillin family
RANBP1	P43487	Ran-specific GTPase-activating protein;	Inhibits GTP exchange on Ran. Forms a Ran-GTP-RANBP1 trimeric complex. Increase GTP hydrolysis induced by the Ran GTPase activating protein RANGAP1. May act in an intracellular signalling pathway which may control the progression through the cell cycle by regulating the transport of protein and nucleic acids across the nuclear membrane
SEPT2.	Q15019	Septin-12;	Filament-forming cytoskeletal GTPase (By similarity). Involved in spermatogenesis. Involved in the morphogenesis of sperm heads and the elongation of sperm tails probably implicating the association with alpha- and beta-tubulins. Forms a filamentous structure with SEPT7, SEPT6, SEPT2 and probably SEPT4 at the sperm annulus which is required for the structural integrity and motility of the sperm tail during post meiotic differentiation. May play a role in cytokinesis (Potential); Belongs to the TRAFAC class TrmE-Era-EngA-EngB-Septin- like GTPase superfamily.
SHP-2	Q06124	Tyrosine-protein phosphatase non-receptor type 11;	Acts downstream of various receptor and cytoplasmic protein tyrosine kinases to participate in the signal transduction from the cell surface to the nucleus. Positively regulates MAPK signal transduction pathway. Dephosphorylates GAB1, ARHGAP35 and EGFR. Dephosphorylates ROCK2 at 'Tyr-722' resulting in stimulation of its RhoA binding activity. Dephosphorylates CDC73; Protein tyrosine phosphatases, non-receptor type
SLC7A11	Q9UPY5	Solute Carrier Family 7 Member 11	Cystine/glutamate transporter; Sodium-independent, high-affinity exchange of anionic amino acids with high specificity for anionic form of cystine and glutamate; Belongs to the amino acid-polyamine-organocation (APC) superfamily. L-type amino acid transporter (LAT) (TC 2.A.3.8) family
SNAP23	O00161	Synaptosomal-associated protein 23;	Essential component of the high affinity receptor for the general membrane fusion machinery and an important regulator of transport vesicle docking and fusion; Belongs to the SNAP-25 family

SOCS3	O14543	Suppressor of cytokine signalling 3;	SOCS family proteins form part of a classical negative feedback system that regulates cytokine signal transduction. SOCS3 is involved in negative regulation of cytokines that signal through the JAK/STAT pathway. Inhibits cytokine signal transduction by binding to tyrosine kinase receptors including gp130, LIF, erythropoietin, insulin, IL12, GCSF and leptin receptors. Binding to JAK2 inhibits its kinase activity. Suppresses foetal liver erythropoiesis. Regulates onset and maintenance of allergic responses mediated by T-helper type 2 cells.
STAM2	O75886	Signal transducing adapter molecule 2;	Involved in intracellular signal transduction mediated by cytokines and growth factors. Upon IL-2 and GM-CSL stimulation, it plays a role in signalling leading to DNA synthesis and MYC induction. May also play a role in T-cell development. Involved in down-regulation of receptor tyrosine kinase via multivesicular body (MVBs) when complexed with HGS (ESCRT-0 complex). The ESCRT-0 complex binds ubiquitin and acts as sorting machinery that recognizes ubiquitinated receptors and transfers them to further sequential lysosomal sorting/trafficking process
STAT1	P42224	Signal transducer and activator of transcription 1-alpha/beta;	Signal transducer and transcription activator that mediates cellular responses to interferons (IFNs), cytokine KITLG/SCF and other cytokines and other growth factors. Following type I IFN (IFN-alpha and IFN-beta) binding to cell surface receptors, signalling via protein kinases leads to activation of Janus kinases (TYK2 and JAK1) and to tyrosine phosphorylation of STAT1 and STAT2. The phosphorylated STATs dimerize and associate with ISGF3G/IRF-9 to form a complex termed ISGF3 transcription factor, that enters the nucleus.
STAT3	P40763	Signal transducer and activator of transcription 3;	Signal transducer and transcription activator that mediates cellular responses to interleukins, KITLG/SCF, LEP and other growth factors. Once activated, recruits' coactivators, such as NCOA1 or MED1, to the promoter region of the target gene. May mediate cellular responses to activated FGFR1, FGFR2, FGFR3 and FGFR4. Binds to the interleukin-6 (IL-6)-responsive elements identified in the promoters of various acute-phase protein genes. Activated by IL31 through IL31RA.
STAT5B	P51692	Signal transducer and activator of transcription 5B	Carries out a dual function: signal transduction and activation of transcription. Mediates cellular responses to the cytokine KITLG/SCF and other growth factors. Binds to the GAS element and activates PRL-induced transcription. Positively regulates hematopoietic/erythroid differentiation
STAT6	P42226	Signal transducer and activator of transcription 6;	Carries out a dual function: signal transduction and activation of transcription. Involved in IL4/interleukin-4- and IL3/interleukin-3-mediated signalling; SH2 domain containing
TPD52L2	O43399	Tumour protein D52 like 2	
UBE2F	Q969M7	NEDD8-conjugating enzyme UBE2F;	Accepts the ubiquitin-like protein NEDD8 from the UBA3- NAE1 E1 complex and catalyses its covalent attachment to other proteins. The specific interaction with the E3 ubiquitin ligase RBX2, but not RBX1, suggests that the RBX2-UBE2F complex neddylates specific target proteins, such as CUL5
ZDHHC5	Q9C0B5		Palmitoyl acyltransferase for the G-protein coupled receptor SSTR5. Also, palmitoylates FLOT2 (By similarity); Zinc fingers DHHC-type

ZNF185	O15231	Zinc finger protein 185;	May be involved in the regulation of cellular proliferation and/or differentiation; LIM domain containing
ZO1/ TJP1	Q07157	Tight junction protein ZO-1	The N-terminal may be involved in transducing a signal required for tight junction assembly, while the C-terminal may have specific properties of tight junctions. The alpha domain might be involved in stabilizing junctions. Plays a role in the regulation of cell migration by targeting CDC42BPB to the leading edge of migrating cells; Belongs to the MAGUK family
ZO2 /TJP2	Q9UDY2	Tight junction protein ZO-2	Plays a role in tight junctions and adherens junctions; Belongs to the MAGUK family
Zyxin / ZYX	Q15942	Zyxin	Adhesion plaque protein. Binds alpha-actinin and the CRP protein. Important for targeting TES and ENA/VASP family members to focal adhesions and for the formation of actin-rich structures. May be a component of a signal transduction pathway that mediates adhesion-stimulated changes in gene expression

Table 4.5 Classification of JAK1/2 late targets based on their association with JAK1 and JAK2 in literature.

JAK1/2 known target (Direct or Indirect)	JAK1, JAK2, STAT1, STAT3, STAT5B, STAT6, SHP-2, SHIP-1, SOCS3, STAM2, SLC7A11, ZO-1, ZO-2, HRS, DSG-2,
JAK1/2 associated Novel targets	AFDN, ADD3, BAG3, CD2AP, TPPP3, CHIC2, CHIST8, DAPP1, EPLIN, FLOT2, FLVCR1, LMO7, MISP, PRDX1, PRDX2, PLEKHA7, PXN, RANBP1, SEPT2, TPD52L2, UBE2F, ZDHHC5, ZNF185, ZYX, SNCC, EPB4IL2

4.4.5. Functional analysis of "late phase" JAK1/2 target substrates identifies their role in cellular integrity and cell-cell interaction

To understand the biological functions and protein-protein signalling interactions of 45 late phase JAK1/JAK2 targets, the proteins were analysed by STRING software and interaction maps were generated. The STRING interaction analysis of 45 late targets displayed their major clustering into 4 categories including; cytokine signalling (JAK1, JAK2 and STAT1, STAT3, STAT5B, STAT6, SOCS3 & SHP-2), cell junction complex and cell adhesion (ZO-1, ZO-2, PXN, ZYX, FLOT-2, Afadin, DSG-2), cytoskeleton (BAG3, MAPK8 (JNK1), ZDHHC5, LIMA1 etc) and plasma membrane bound projections (RANBP1, TPPP3, STAM2, SNAP23, SEPT2) (Figure 4.5). In order to gain more information about additional protein-protein interaction partners and the biological signalling networks to which these proteins might participate in 10 additional potential interaction nodes were included in the STRING analysis which allowed further grouping of proteins into endoplasmic vesicle formation and vesicular transport (STAM2, SEPT2, SNAP23) (Figure 4.6).

To further investigate the biological pathways which the 45 identified late JAK target substrates were aligned with, we performed KEGG pathways analysis and structural component analysis by using gene annotation software Metascape (metascape.org). Pathway analysis identified enrichment of these proteins with 16 different biological processes. (Figure 4.7, Table 4.6). Other than cytokine signalling; cleavage of adhesion proteins, apoptosis, and oxidative stress ranked among the significantly enriched pathways regulated by late JAK targets. There was also enrichment of biological processes associated with membrane permeabilization and cell structure organisation (Figure 4.8, Table 4.7). Furthermore, GO analysis for cellular components and molecular functions for these proteins showed their enrichment into categories, cellular junctions, anchorage junctions, tight junctions, actin

cytoskeleton, cell cortex, brush border, membrane raft and perinuclear cytoplasm. The data indicated the role of late activity of JAK1/2 in the regulation of epithelial barrier. (Fig 4,8B, Table 4.4).

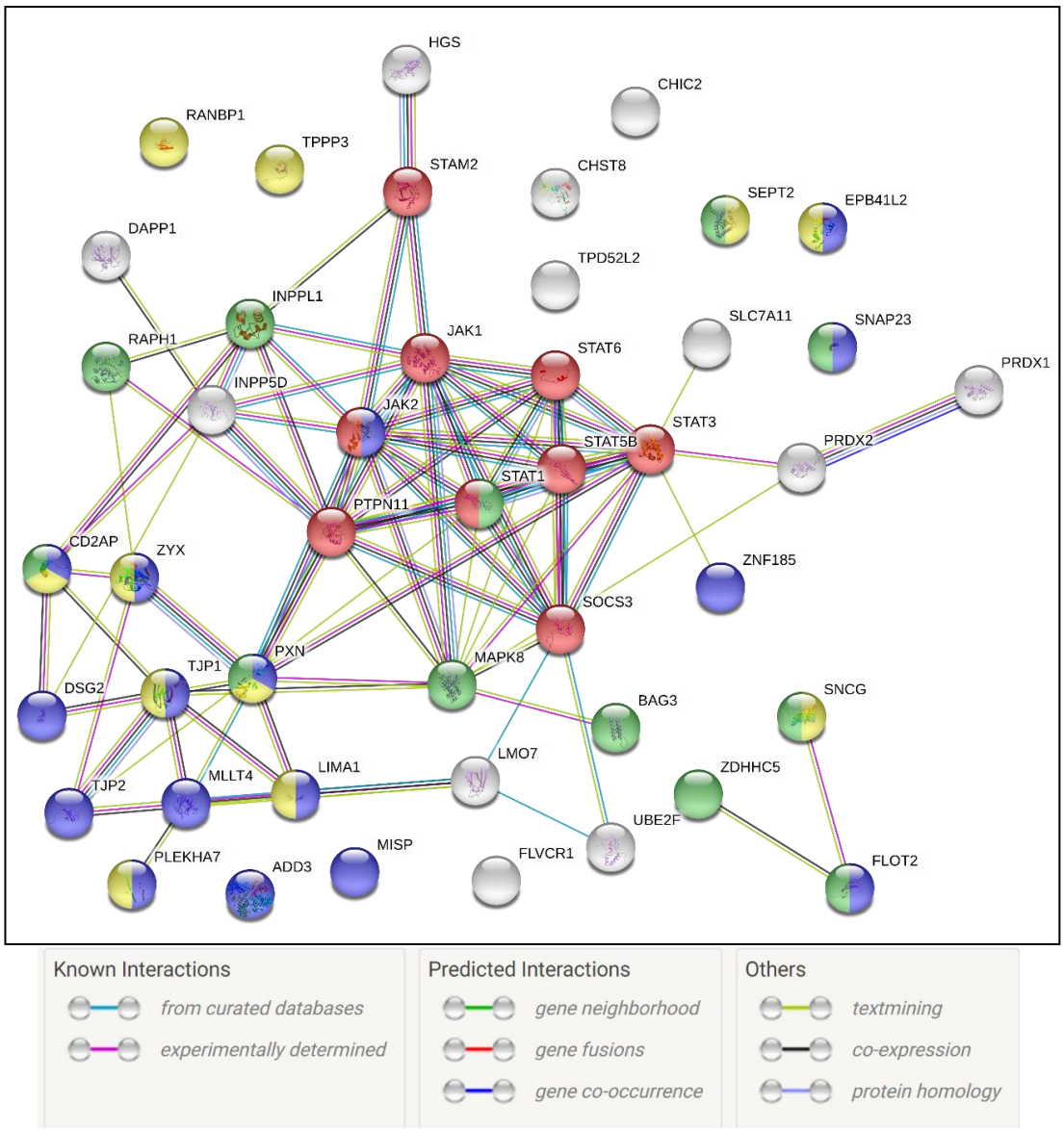


Figure 4.5 Protein-protein interaction study of late JAK targets using STRING software (No. of Nodes=45)

Protein-protein interaction analysis of 45 late phase JAK1/2 target was performed using STRING database (https://string-db.org/). Protein interaction identified in four main categories were colour coded as indicated. Connectivity are experimentally determined (Purple lines), or via curated datasets (light blue lines) as indicated.

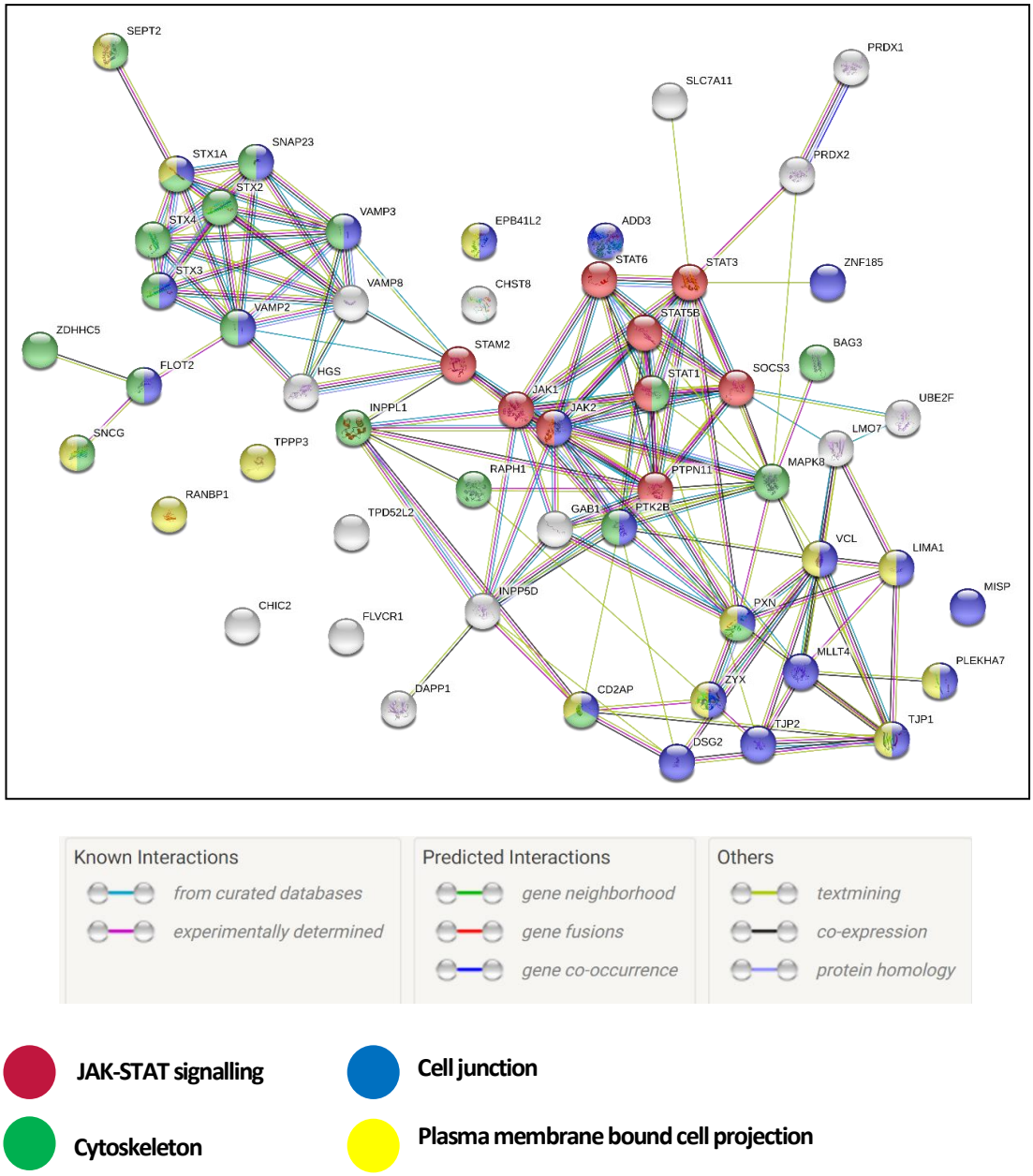


Figure 4.6. Protein-protein interaction study of late JAK targets along with 10 additional nodes generated by STRING software (No. of Nodes=55)

Along with 45 late phase JAK1/2 targets, 10 additional nodes were added by using expand/add protein feature of STRING database (https://string-db.org/). Protein-protein interaction analysis of 55 protein was performed. Protein interaction identified in four main categories were colour coded as indicated. Connectivity are experimentally determined (Purple lines), or via curated datasets (light blue lines) as indicated.

KEGG/Reactome/Canonical pathway Analysis

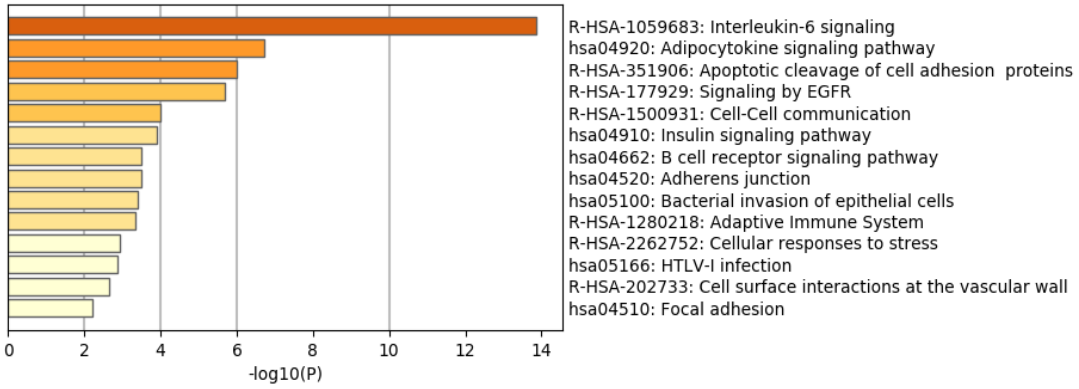


Table 4.6 KEGG pathway analysis of late JAK targets by using Metascape

GO Term	Description	Symbols
R-HSA-1280218	Adaptive Immune System	INPP5D, LMO7, PTPN11, SNAP23, SOCS3, DAPP1, UBE2F
hsa04520	Adherens junction	LMO7, AFDN, TJP1
hsa04920	Adipocytokine signalling pathway	JAK2, MAPK8, PTPN11, STAT3, SOCS3, PXN, TJP1
R-HSA-351906	Apoptotic cleavage of cell adhesion proteins	DSG2, TJP1, TJP2, MAPK8, STAT3, AFDN
hsa04662	B cell receptor signalling pathway	INPP5D, INPPL1, DAPP1
hsa05100	Bacterial invasion of epithelial cells	SEPTIN2, PXN, CD2AP
R-HSA-202733	Cell surface interactions at the vascular wall	INPP5D, PTPN11, SLC7A11
R-HSA-1500931	Cell-Cell communication	AFDN, PTPN11, PXN, CD2AP, MAPK8
R-HSA-2262752	Cellular responses to stress	PRDX1, MAPK8, STAT3, PRDX2, BAG3
hsa01521	EGFR tyrosine kinase inhibitor resistance	JAK1, JAK2, STAT3
hsa04510	Focal adhesion	MAPK8, PXN, ZYX
hsa05166	HTLV-I infection	JAK1, MAPK8, RANBP1, STAT5B
hsa04910	Insulin signalling pathway	FLOT2, INPPL1, MAPK8, SOCS3
R-HSA-1059683	Interleukin-6 signalling	JAK1, JAK2, PTPN11, STAT1, STAT3, SOCS3, INPP5D, INPPL1, STAT5B, STAT6, STAM2, MAPK8, PXN, HGS, RANBP1

Figure 4.7. Pathway enrichment analysis of late phase JAK targets identified in pY-PTM screen

Gene ontology studies of 45 late phase JAK1/2 target by selecting KEGG pathway canonical pathway enrichment analysis by using Metascape software (Metascape.org). Bar graphs represent each enrichment term. P value cut from off =0.01 and minimum enrichment of 1.5-fold was used for the analysis. Table 4.6 indicating the proteins associated with each GO term.

Cellular Component analysis

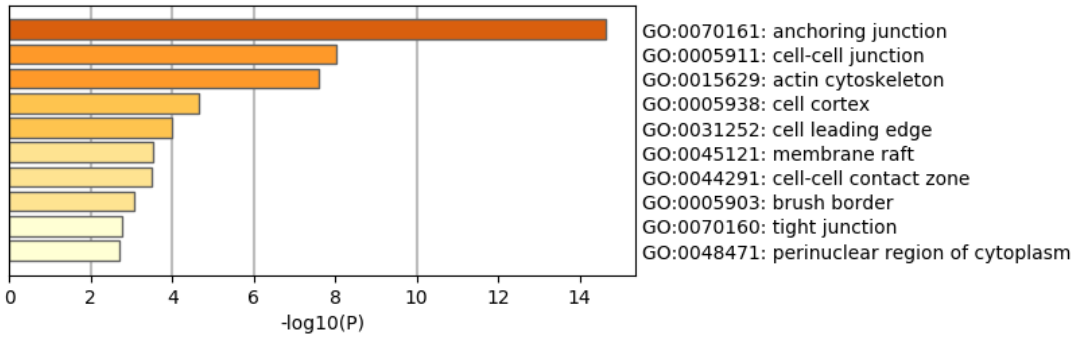


Table 4.5 Cellular component analysis of late JAK targets by using Metascape

TERM	DESCRIPTION	SYMBOLS
GO:0070161	anchoring junction	DSG2, EPB41L2, FLOT2, JAK1, JAK2, LMO7, AFDN, PXN, TJP1, ZNF185, ZYX, SNAP23, TJP2, LIMA1, MISP, PLEKHA7
GO:0005925	focal adhesion	EPB41L2, FLOT2, JAK1,JAK2,LMO7,PXN,ZNF185,ZYX,SNAP23,LIMA1,MISP
GO:0005911	cell-cell junction	ADD3,DSG2,FLOT2,AFDN,TJP1,ZYX,SNAP23,TJP2,CD2AP,PLEKHA7
GO:0015629	actin cytoskeleton	EPB41L2,FLOT2,PXN,TJP1,ZNF185,ZYX,BAG3,CD2AP,LIMA1,MISP
GO:0005938	cell cortex	ADD3,EPB41L2,FLOT2,SEPTIN2,PXN,MISP
GO:0031252	cell leading edge	FLOT2,INPPL1,PXN,CD2AP,LIMA1,RAPH1
GO:0044291	cell-cell contact	DSG2,FLOT2,AFDN,LMO7,TJP1
GO:0045121	membrane raft	ADD3,FLOT2,INPP5D,JAK2,STAT6
GO:0005903	brush border	ADD3,SLC7A11,LIMA1
GO:0070160	tight junction	AFDN,TJP1,TJP2,PLEKHA7

Figure 4.8. Cellular component enrichment analysis of late phase JAK targets identified in pY-PTM screen

Gene ontology studies of 45 late phase JAK1/2 targets by selecting cellular component enrichment analysis, using Metascape software (Metascape.org). Bar graphs represent each enrichment GO term. P value cut from off =0.01 and minimum enrichment of 1.5-fold was used for the analysis. Table 4.7 indicating the proteins associated with each GO term.

4.4.6. Identification of pathways dependent on late kinase activity of JAK1 and JAK2 in IFN-γ+TNF-α treated cells

The phospho-tyrosine proteomics screen highlighted the possible role of JAK1 and JAK2 in the disruption of the epithelial barrier by the phosphorylation of proteins involved in cellular junction and cell-cell interactions.[38] To validate these results, a similar experimental set-up as the screen was performed. HT-29 cells were treated with IFN-γ and TNF-α for 10 hours, followed by a co-treatment with cytokines IFN-γ + TNF-α +/- JAK inhibitors for 15 minutes. A panel of four different JAK inhibitors; Upadacitinib (JAK1 inhibitor), BMS-911543 (JAK2 inhibitor), Baricitinib and Ruxolitinib (JAK1/2 inhibitor) was used in the experiment.

Due to commercial unavailability of phospho-antibodies for most of the JAK 1/2 target substrates identified from the screen, this initial study had to be restricted to the validation of fewer targets identified from the screens. As detected by the screen, both STAT1 and STAT3 showed an accumulation of total protein after 10 hours of treatment. The phosphorylation of STAT1 p-Y701 was very high in cells treated with IFN-γ and TNF-α compared to control cells. Treatment of cells with JAK inhibitors was able to reduce STAT1 pY701 and STAT3 pY705 levels significantly. The dephosphorylation of STAT1 and STAT3 was observed within 15 minutes of treatment of cells with the various JAK inhibitors which validated the results from the phospho-proteomic screen.

Dual adapter for phosphotyrosine and 3-phosphotyrosine (DAPP1) was identified to be dephosphorylated with baricitinib treatment in both run1 and run 2 of the PTM screen. During the validation experiment, even though the treatment with TNF-α or IFN-γ + TNF-α induced the accumulation of DAPP1 protein in the HT-29 cells, its tyrosine phosphorylation did not change irrespective of the treatment. Pancreatic and duodenal homeobox 1 (PDX1) was another protein identified as late Phase target of JAK1/2 during phospho-proteomic screen.

But during the validation study there was no effect of IFN-γ + TNF-α treatment observed on PDX1 or PDX1 pY194 levels.

Gene ontology and pathway analysis of late phase JAK targets identified proteins associated with cell structure, cell adhesion and cell-cell interaction. JAK2 has been reported to phosphorylate other kinases such as focal adhesion kinase (FAK) and Src via STAT3 to regulate the phosphorylation and activation of cytoskeleton-linked proteins.[39, 40, 41] Hence, the late kinase activity of JAKs was tested on regulation of FAK, SRC and JNK phosphorylation. The level of total FAK or FAK pY576/Y577 did not change in any treatment group[42]. But FAK pY925 levels increased with IFN-γ, TNF-α and co-treatment. A slight decrease in the level of FAK pY925 was observed with upadacitinib and ruxolitinib treatment and baricitinib treatment decreased it to basal level[43]. But there was no effect of BMS-911543 treatment on the phosphorylation of FAK. Notably, the activation of JNK signalling pathway was observed in IFN-γ+TNF-α treated cells with an increased phosphorylation of JNK1 pY185. But there was no significant decrease in JNK1 pY185 levels observed with JAKinib treatment. Both activation (Y416) and autoinhibitory (Y527) pY sites were tested in IFN-γ+TNF-α treated cells[44,4544]. There was no effect of cytokine treatment observed on Src pY527 levels while an accumulation Src pY416 protein observed in IFN-γ+TNF-α treated cells suggests the activation of Src signalling. But there was no effect of blocking JAK activity on Src phosphorylation at either phosphosite. It suggests that either JNK1 pY185 and Src pY416 phosphorylation are not direct substrate of JAK1 and JAK2 or a 15 minutes treatment with JAK inhibitors was not enough time for dephosphorylation of these proteins.

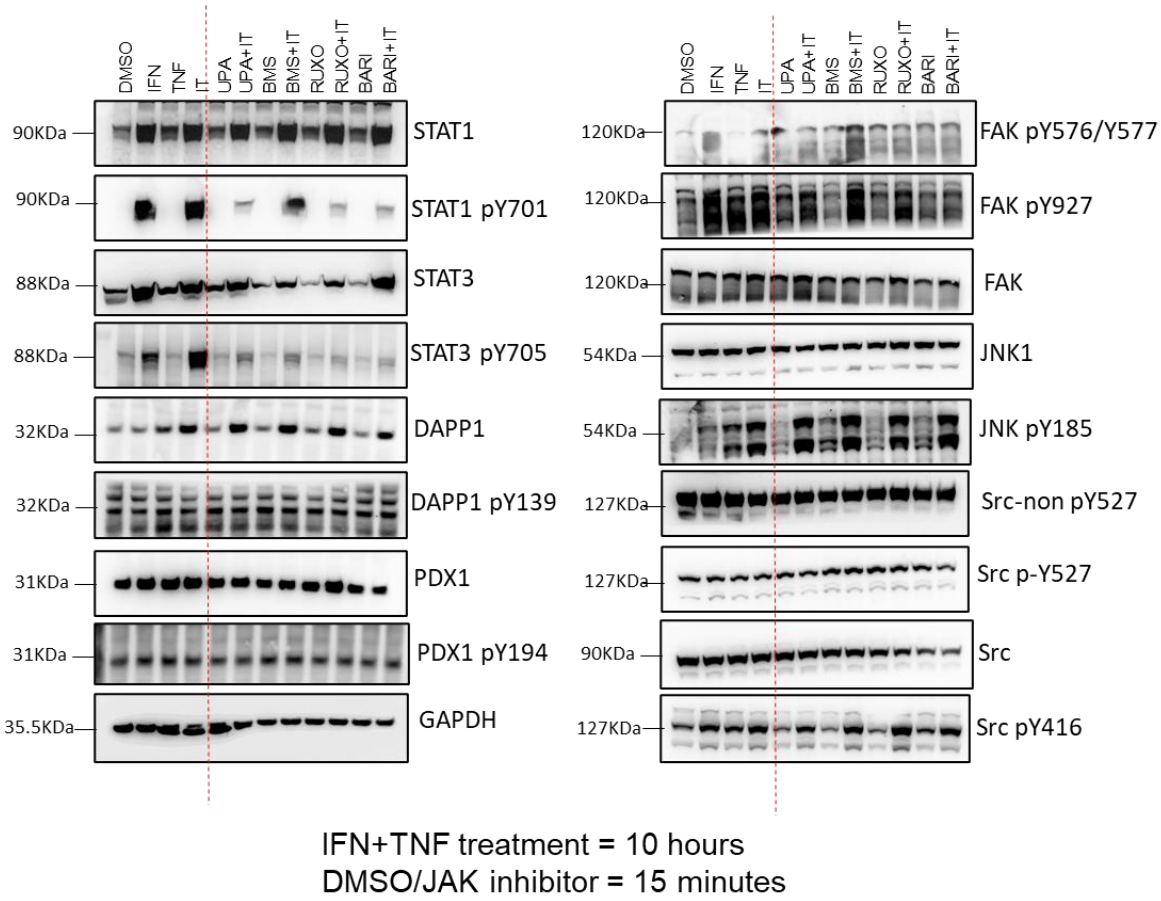


Figure 4.8 Validation and identification of the pathways dependent on late kinase activity of JAK1 and JAK2 in IFN-γ+TNF-α treated cells

HT-29 cells were treated with 10 ng/mL of IFN-γ+TNF-α or untreated for 10 hours followed by treatment with IFN-γ+TNF-α with DMSO or JAKinibs (as indicated) for 15 minutes. Cells were lysed with RIPA lysis buffer and analysed for total protein and p-Y levels for the indicated proteins by western blotting. JAKinibs; UPA- JAK1 inhibitor Upadacitinib, BMS- JAK2 inhibitor BMS-911543, RUXO- JAK1/2 inhibitor Ruxolitinib, BARI- JAK1/2 inhibitor Baricitinib, IT= IFN+TNF. The data is representative of 1 experiment.

4.5. Discussion

Epithelial barrier disruption is a major factor associated with the pathogenesis of IBD[1,2] . The two cytokines, IFN-γ and TNF-α are known to synergize to induce disruption of epithelial cell apical junction complexes contributing to barrier disruption[3,4,5]. We identified JAKs as the major kinases associated with IFN-γ + TNF-α mediated synergistic cell death of CRC cell lines (Chapter-1). We also showed that sustained activation of the JAK1/2-STAT1 pathway is essential for induction of cell death and that blocking JAK activity at later stages of signalling (10 hours post IFN-γ + TNF-α treatment) could rescue the cell death (Chapter-2). We then focussed our study on understanding the role of late phase activity of JAK1 and JAK2. Our overall goal was to uncover new targets associated with JAK1/2 'late phase' activity that might contribute to epithelial barrier dysfunction and cell death. By taking a phospho tyrosine PTM approach we identified 45 late phase JAK1/JAK2 targets. Gene ontology analysis of these late JAK targets identified the role of these proteins in focal adhesions, cell-cell junctions, tight junctions, actin cytoskeleton, in the ferroptosis cell death pathway and reactive oxygen species (ROS) generation. The regulation of these proteins by JAK1 and JAK2 suggests a possible role of late phase JAK1 and JAK2 activity in the regulation of epithelial barrier functions and epithelial homeostasis.

To begin with, we tried to resolve the long-standing molecular mystery underpinning IFN-γ + TNF-α synergism and its contribution to colonic epithelial cell death. We described (Chapter-3) that increasing concentrations of IFN-γ and TNF-α could result into prolonged activation of JAK1/2-STAT1 signalling and that this sustained activation of JAK-STAT pathway was crucial for induction of cell death (Chapter 3). Following on from these observations, we decided to try and identify novel late phase phospho-tyrosine targets for JAK1 and JAK2, which

may contribute to IFN-γ + TNF-α induced cell death or epithelial barrier dysfunction. By performing a p-Y PTM screen we identified 45 proteins that exhibited a reduced phosphorylation upon treatment of cytokine treated cells with the JAK1/2 inhibitor baricitinib. Known JAK1/2 targets numbering 16 proteins including JAK1 and JAK2 themselves and STATs were identified while 29 new targets were also identified during the screens. The GO enrichment notation category of 'cellular components' grouped these target proteins mostly into the areas of focal adhesions, cell-cell interactions, tight junctions. There were also proteins identified that play a role in the regulation of ferroptosis and reactive oxygen species generation.

Focal adhesions (FAs) are important cellular structures connecting the intracellular cytoskeleton to the extracellular matrix (ECM). Because of their crucial role in cell adhesion and cell migration, they play important role during cancer and metastasis. The association of JAK-STAT pathway and focal adhesions has previously been described in several studies[39,46,47]. The JAK/STAT3 axis has been reported to be involved in the regulation of FAK signalling[48,49]. There is also evidence of STAT3 localisation to focal adhesions along with Paxillin (PXN) and FAK[49]. A study from Xie et al showed that integrin/FAK signalling activated STAT1 but not STAT3 to reduce cell adhesion and promote cell migration in fibroblast cell lines[50]. In addition, the interaction of the JAK-STAT pathway with focal adhesions is also supported by the fact that suppressor of cytokine signalling 1 (SOCS1) and SOCS3 – which are negative regulators of JAK signalling – decrease tyrosine phosphorylation of FAK in 3T3 fibroblast cells[47]

In addition to that, our pY-PTM screen also identified the role of late phase activity of JAK1 and JAK2 in the regulation of several proteins associated with focal adhesions such as Paxillin, Zyxin, Flotillin, EPLIN and LMO7 by modulating their tyrosine phosphorylation. Paxillin (PXN) and Zyxin (ZYX) are also a major component of focal adhesions and acts as adaptors for

recruitment of different kinases, phosphatases, cofactors, and structural proteins[51]. Clinical samples from colon cancer tissues show elevated expression level of Zyxin compared with normal tissue[52]. The tyrosine phosphorylation of paxillin is important for cell migration.[53] FLOT2 or Flotillin 2 is known to be associated with important cellular processes including cytoskeletal organisation, membrane trafficking, signal transduction and pathogen entry.[54] It directly interact with γ-catenin and control cell-cell adhesion in epithelial cells.[55] Similar to ZYX and PXN, FLOT2 also performs crucial functions in cellular homeostasis and cell survival[56]. The most studied role of FLOT-2 has been described in epithelial-mesenchymal transition and metastasis.[57,58,59]. The tyrosine phosphorylation of FLOT-2 by EGFR at Y163 results into its translocation from lipid raft to endosomes[60]. Thus, the regulation of the tyrosine phosphorylation of FLOT-2 by JAK1/JAK2 suggests the importance of JAKs in regulating cell adhesion and actin dynamics[56] EPLIN is a cytoskeletal, actin-binding protein and regulates the actin dynamics in epithelial cell junctions[61].

Other than focal adhesions, JAK1 and JAK2 also regulate the phosphorylation of several proteins associated with cell structure and cell-cell junction ADD3, DSG2, AFDN, CD2AP, PLEKHA7 and SNAP23. ADD3 or Adducin-gamma is a membrane cytoskeletal protein, required for the physical support to the plasma membrane and also mediates signal transduction during several cellular physiological processes[62]. Adducin (ADD1 and ADD3) also play an important role in stabilization of epithelial junctions (AJs and TJs) and regulation of junctional remodelling in human epithelial cells[63] Dysregulation of ADD3 has been associated with several colorectal cancers[64]. DSG2 or Desmolglein-2 a major protein associated with cytoskeleton and cell-cell junctions. Previous studies have described the role of DSG2 in regulation of epithelial barrier function and epithelial homeostasis[65]. IFN-γ and TNF-α stimulation has been reported to result in the cleavage of DSG2 and apoptosis induction[37,11].

Tyrosine phosphorylation of DSG2 by EGFR has been reported to be important for DSG-2 shedding and internalisation and play specific role in epithelial remodelling[66]. Afadin is an important part of adherens junction complex and connects it with actin cytoskeleton[67]. It has been previously described as a substrate for AKT/PI3K signalling pathway during the development of breast cancers and glioblastoma[68,69].

Another important group of proteins identified from the screen are components of tight junction complexes. Previous studies have described the role of tight junctions and adherens proteins in the regulation of epithelial barrier[70, 71,72]. Tight junction proteins TJP1 and TJP2 (also known as ZO-1 and ZO-2 respectively) are components of tight junction complex and their interaction with other components of tight junctions called occludins, is required for the formation of apical junction and sealing the cells to create the primary barrier.[73] [38] Activation of epidermal growth factor (EGFR) signalling has been reported to result in the phosphorylation of TJP1 and TJP2 resulting in reorganisation of actin filament and cell structure.[74] IFN-γ and TNF-α have been reported to downregulate the expression of TJP1 and disrupt tight junctions[18,75,76] Moreover, JAK1 has been reported to induce tyrosine phosphorylation of TJP2 in smooth muscle cells[27].

PRDX 1 and PRDX2 are two major peroxidases of the PRDX family and play a major role in the regulation of lipid peroxidation[77,78]. PRDX1 and PRDX2 are located in the cytoplasm and nucleus of cells and negatively regulate ROS production. Mice lacking *PRDX1* have been shown to have high level of ROS generation and shorter life span[79,80]. The phosphorylation of PRDX1 at Y194 by SRC induced inactivation of PRDX1 and increased local hydrogen peroxide (H_2O_2) levels[81] The p-Y PTM identified the phosphorylation of PRDX1 by late phase activity of JAK1 and JAK2, suggesting its possible involvement in ROS generation or ferroptosis. FLVCR1 was another protein phosphorylated by JAK1/JAK2 and reported to be involved in ROS

generation and ferroptosis. FLVCR1 protein is a heme exporter in different type of cells, including intestinal cells and is associated with absorption of heme in the cells[82], recent studies have highlighted its role in maintaining intestinal homeostasis by exporting excess heme outside the cells[83]. Mice lacking *FLVCR1* gene exhibited an increase in cellular heme levels, ferroptotic cell death in intestinal cells and decrease in survival efficiency[83]. Furthermore, another JAK1/2 target SLC7A11, is a key component of the cystine-glutamate antiporter and plays major role in lipid peroxidation and regulation of ferroptosis[84,85] Mice lacking *SLC7A11* gene showed ferroptosis under high iron conditions[86]. Moreover, Glutathione peroxidase 4 (GPX4), a negative regulator of ferroptosis was also identified as a late JAK target[428]. The role of the JAK-STAT pathway in ROS generation and ferroptosis was also backed up by results from the RNA-Seq dataset which identifying decreased expression of *GPX4* and increased expression of *SLC7A11* at late time points (Chapter-3) and by a recent publication which showed that CD8+ T cell derived IFN-γ induced tumour cell ferroptosis during cancer immunotherapy[87,88,89,90].

Altogether, our phospho-proteomic study suggests the IFN-γ and TNF-α induced epithelial barrier disruption through multiple mechanisms in addition to or/and in parallel with induction of cell death[18]. The sustained activation of JAKs induces tyrosine phosphorylation of components of focal adhesions, apical junction complexes, cytoskeleton molecules and tight junction proteins. As these molecules play major role in keeping the barrier intact, the phosphorylation of these proteins may result in disruption of these various protein complexes, increased epithelial barrier permeability and bacterial translocation contributing to pathogenesis of IBD[70,91,92].

4.6. References

1. Bousoik, E. & Montazeri Aliabadi, H. "Do We Know Jack" About JAK? A Closer Look at JAK/STAT Signaling Pathway. *Front. Oncol.* 8, 1–20 (2018).
2. Salim, S. Y. & Söderholm, J. D. Importance of disrupted intestinal barrier in inflammatory bowel diseases. *Inflamm. Bowel Dis.* 17, 362–381 (2011).
3. Takiishi, T., Fenero, C. I. M. & Câmara, N. O. S. Intestinal barrier and gut microbiota: Shaping our immune responses throughout life. *Tissue Barriers* 5, 1–12 (2017).
4. Park, J. H., Peyrin-Biroulet, L., Eisenhut, M. & Shin, J. Il. Inflammatory Bowel Diseases (IBD) immunopathogenesis: A comprehensive review of inflammatory molecules. (2017).
5. Lechuga, S. & Ivanov, A. I. Disruption of the epithelial barrier during intestinal inflammation: Quest for new molecules and mechanisms. *Biochim. Biophys. Acta - Mol. Cell Res.* 1864, 1183–1194 (2017).
6. Vogelmann, R. & Nelson, W. J. Fractionation of the epithelial apical junctional complex: Reassessment of protein distributions in different substructures. *Mol. Biol. Cell* 16, 701–716 (2005).
7. Huber, P. Targeting of the apical junctional complex by bacterial pathogens. *Biochimica et Biophysica Acta - Biomembranes* 1862, (2020).
8. Garcia, M. A., Nelson, W. J. & Chavez, N. Cell – Cell Junctions Organize Structural. *Cold Spring Harb. Perspect. Biol.* 10, 1–28 (2017).
9. Zihni, C., Balda, M. S. & Matter, K. Signalling at tight junctions during epithelial differentiation and microbial pathogenesis. *Journal of Cell Science* 127, 3401–3413 (2014).

10. González-Mariscal, L., Tapia, R. & Chamorro, D. Crosstalk of tight junction components with signaling pathways. *Biochimica et Biophysica Acta - Biomembranes* 1778, 729–756 (2008).
11. Nava, P. *et al.* Desmoglein-2: a novel regulator of apoptosis in the intestinal epithelium. *Mol. Biol. Cell* 18, 4565–78 (2007).
12. Kohr, B., Gardet, A. & Xavier, R. J. Genetics and pathogenesis of inflammatory bowel disease. *Nature* 474, 307–317 (2011).
13. Laukoetter, M. G., Bruewer, M. & Nusrat, A. Regulation of the intestinal epithelial barrier by the apical junctional complex. *Current Opinion in Gastroenterology* 22, 85–89 (2006).
14. Sugi, K., Musch, M. W., Field, M. & Chang, E. B. Inhibition of Na+,K+-ATPase by interferon gamma down-regulates intestinal epithelial transport and barrier function. *Gastroenterology* 120, 1393–403 (2001).
15. Ferrier, L. *et al.* Stress-induced disruption of colonic epithelial barrier: role of interferon-γ and myosin light chain kinase in mice. *Gastroenterology* 125, 795–804 (2003).
16. Immunol, J. C. C. Inflammatory Mediators Contributing to Intestinal Epithelial Cell Apoptosis Inflammatory Mediators Contributing to Intestinal Epithelial Cell Apoptosis and Barrier Disruption in IBD. (2011).
17. Cao, M., Wang, P., Sun, C., He, W. & Wang, F. Amelioration of IFN-γ and TNF-α-Induced Intestinal Epithelial Barrier Dysfunction by Berberine via Suppression of MLCK-MLC Phosphorylation Signaling Pathway. *PLoS One* 8, e61944 (2013).
18. Bruewer, M. *et al.* Proinflammatory cytokines disrupt epithelial barrier function by apoptosis-independent mechanisms. *J. Immunol.* 171, 6164–72 (2003).

19. Ma, T. Y., Boivin, M. A., Ye, D., Pedram, A. & Said, H. M. Mechanism of TNF-α modulation of Caco-2 intestinal epithelial tight junction barrier: Role of myosin light-chain kinase protein expression. *Am. J. Physiol. - Gastrointest. Liver Physiol.* 288, (2005).
20. Noth, R. *et al.* Anti-TNF-α antibodies improve intestinal barrier function in Crohn's disease. *J. Crohn's Colitis* 6, 464–469 (2012).
21. Nayden G. Naydenov, 1, * somesh Baranwal, 1 & shadab Khan, 2 alex Feygin, 1 pooja Gupta1 and andrei I. Ivanov1, 3, 4. Novel mechanism of cytokine-induced disruption of epithelial barriers:Janus kinase and protein kinase D-dependent downregulation of junction protein expression. (2013).
22. Morris, R., Kershaw, N. J. & Babon, J. J. The molecular details of cytokine signaling via the JAK/STAT pathway. *Protein Science* 27, 1984–2009 (2018).
23. Levine, Ross L; Pardanani, Animesh; Tefferi, Ayalew; Gilliland, D. G. Role of JAK2 in the pathogenesis and therapy of myeloproliferative disorders. (2007). doi:10.1038/nrc2210
24. Chiba, T., Yamada, M. & Aiso, S. Targeting the JAK2/STAT3 axis in Alzheimer's disease. *Expert Opin. Ther. Targets* 13, 1155–67 (2009).
25. Platanias, L. C. Mechanisms of type-I- and type-II-interferon-mediated signalling. *Nature Reviews Immunology* (2005). doi:10.1038/nri1604
26. Mishra, J., Das, J. K. & Kumar, N. Janus kinase 3 regulates adherens junctions and epithelial mesenchymal transition through -catenin. *J. Biol. Chem.* 292, 16406–16419 (2017).
27. Tkachuk, N. *et al.* The tight junction protein ZO-2 and Janus kinase 1 mediate intercellular communications in vascular smooth muscle cells. *Biochem. Biophys. Res. Commun.* 410, 531–536 (2011).

28. Eng, J. K., McCormack, A. L. & Yates, J. R. An approach to correlate tandem mass spectral data of peptides with amino acid sequences in a protein database. *J. Am. Soc. Mass Spectrom.* 5, 976–989 (1994).

29. T. Virtanen, A., Haikarainen, T., Raivola, J. & Silvennoinen, O. Selective JAKinibs: Prospects in Inflammatory and Autoimmune Diseases. *BioDrugs* 33, 15–32 (2019).

30. Danese, S., Argollo, M., Le Berre, C. & Peyrin-Biroulet, L. JAK selectivity for inflammatory bowel disease treatment: does it clinically matter? *Gut* 68, 1893–1899 (2019).

31. Held, M. A. *et al.* Phospho-PTM proteomic discovery of novel EPO- modulated kinases and phosphatases, including PTPN18 as a positive regulator of EPOR/JAK2 Signaling. *Cell. Signal.* 69, 109554 (2020).

32. Batth, T. S. *et al.* Large-Scale Phosphoproteomics Reveals Shp-2 Phosphatase-Dependent Regulators of Pdgf Receptor Signaling Data and Software Availability PXD005803. (2018). doi:10.1016/j.celrep.2018.02.038

33. Haan, S. *et al.* Tyrosine phosphorylation disrupts elongin interaction and accelerates SOCS3 degradation. *J. Biol. Chem.* 278, 31972–31979 (2003).

34. Xu, D. & Qu, C.-K. Protein tyrosine phosphatases in the JAK/STAT pathway. *Front. Biosci.* 13, 4925–32 (2008).

35. Yu, L. *et al.* JAK2 and SHP2 Reciprocally Regulate Tyrosine Phosphorylation and Stability of Proapoptotic Protein ASK1 *. (2009).

36. Pandey, A. *et al.* Identification of a novel immunoreceptor tyrosine-based activation motif-containing molecule, STAM2, by mass spectrometry and its involvement in growth factor and cytokine receptor signaling pathways. *J. Biol. Chem.* 275, 38633–38639 (2000).

37. Yulis, M., Quiros, M., Hilgarth, R., Parkos, C. A. & Nusrat, A. Intracellular Desmoglein-2 cleavage sensitizes epithelial cells to apoptosis in response to pro-inflammatory cytokines. *Cell Death Dis.* 9, 389 (2018).

38. Elias, B. C. *et al.* Phosphorylation of Tyr-398 and Tyr-402 in occludin prevents its interaction with ZO-1 and destabilizes its assembly at the tight junctions. *J. Biol. Chem.* 284, 1559–69 (2009).

39. Zhu, T., Goh, E. L. K. & Lobie, P. E. Growth Hormone Stimulates the Tyrosine Phosphorylation and Association of p125 Focal Adhesion Kinase (FAK) with JAK2. *J. Biol. Chem.* 273, 10682–10689 (1998).

40. Zheng, Q. *et al.* JAK2/STAT3 targeted therapy suppresses tumor invasion via disruption of the EGFRvIII/JAK2/STAT3 axis and associated focal adhesion in EGFRvIII-expressing glioblastoma.

41. Macha, M. A. *et al.* Guggulsterone decreases proliferation and metastatic behavior of pancreatic cancer cells by modulating JAK/STAT and Src/FAK signaling. *Cancer Lett.* 341, 166–77 (2013).

42. Calalb, M. B., Polte, T. R. & Hanks, S. K. Tyrosine phosphorylation of focal adhesion kinase at sites in the catalytic domain regulates kinase activity: a role for Src family kinases. *Mol. Cell. Biol.* 15, 954–963 (1995).

43. Deramaudt, T. B. *et al.* FAK phosphorylation at Tyr-925 regulates cross-talk between focal adhesion turnover and cell protrusion. *Mol. Biol. Cell* 22, 964–975 (2011).

44. Okada, M. Regulation of the Src family kinases by Csk. *International Journal of Biological Sciences* 8, 1385–1397 (2012).

45. Boggon, T. J. & Eck, M. J. Structure and regulation of Src family kinases. *Oncogene* 23, 7918–7927 (2004).

46. Cho, H. J. *et al.* Ascochlorin Suppresses MMP-2-Mediated Migration and Invasion by Targeting FAK and JAK-STAT Signaling Cascades. *J. Cell. Biochem.* 119, 300–313 (2018).

47. Liu, E., Côté, J.-F. & Vuori, K. Negative regulation of FAK signaling by SOCS proteins. *EMBO J.* 22, 5036–46 (2003).

48. Swiatek-Machado, K. *et al.* Novel small molecular inhibitors disrupt the JAK/STAT3 and FAK signaling pathways and exhibit a potent antitumor activity in glioma cells. *Cancer Biol. Ther.* 13, 657–670 (2012).

49. Silver, D. L., Naora, H., Liu, J., Cheng, W. & Montell, D. J. Activated signal transducer and activator of transcription (STAT) 3: Localization in focal adhesions and function in ovarian cancer cell motility. *Cancer Res.* 64, 3550–3558 (2004).

50. Xie, B. *et al.* Focal Adhesion Kinase Activates Stat1 in Integrin-mediated Cell Migration and Adhesion. *J. Biol. Chem.* 276, 19512–19523 (2001).

51. Legerstee, K., Geverts, B., Slotman, J. A. & Houtsmuller, A. B. Dynamics and distribution of paxillin, vinculin, zyxin and VASP depend on focal adhesion location and orientation. *Sci. Rep.* 9, 1–18 (2019).

52. Zhou, J. *et al.* Zyxin promotes colon cancer tumorigenesis in a mitotic phosphorylation-dependent manner and through CDK8-mediated YAP activation. *Proc. Natl. Acad. Sci. U. S. A.* 115, E6760–E6769 (2018).

53. Oliver, B. L., Garat, C., Pytela, R. & Matthay, M. A. Protein tyrosine phosphatases mediate cell readhesion in alveolar epithelial cells mechanically separated from in vitro matrix. *Am. J. Respir. Cell Mol. Biol.* 16, 613–20 (1997).

54. Sasaki, Y. *et al.* Identification of Flotillin-2, a Major Protein on Lipid Rafts, as a Novel Target of p53 Family Members. *Mol Cancer Res* 6, 395–406 (2008).

55. Kurrle, N. *et al.* Flotillins Directly Interact with γ-Catenin and Regulate Epithelial Cell-Cell Adhesion. *PLoS One* 8, e84393 (2013).

56. Wei, S. *et al.* Flotillin-2 Modulates Fas Signaling Mediated Apoptosis after Hyperoxia in Lung Epithelial Cells. *PLoS One* (2013).

57. Wang, D., Lu, G., Shao, Y. & Xu, D. microRNA-802 inhibits epithelial-mesenchymal transition through targeting flotillin-2 in human prostate cancer. *Biosci. Rep.* 37, 20160521 (2017).

58. Zhao, L. *et al. Oncotarget 9781 www.impactjournals.com/oncotarget Flotillin-2 promotes nasopharyngeal carcinoma metastasis and is necessary for the epithelial-mesenchymal transition induced by transforming growth factor-β*. *Oncotarget* 6,

59. Wen, Q. *et al.* Increased Expression of Flotillin-2 Protein as a Novel Biomarker for Lymph Node Metastasis in Nasopharyngeal Carcinoma. *PLoS One* 9, (2014).

60. Neumann-Glesen, C., Fernow, I., Amaddii, M. & Tikkanen, R. Role of EGF-induced tyrosine phosphorylation of reggie-1/flotillin-2 in cell spreading and signaling to the actin cytoskeleton. *J. Cell Sci.* 120, 395–406 (2007).

61. Collins, R. J., Jiang, W. G., Hargest, R., Mason, M. D. & Sanders, A. J. EPLIN: a fundamental actin regulator in cancer metastasis? *Cancer Metastasis Rev.* 34, 753–764 (2015).

62. Kiang, K. M.-Y. & Leung, G. K.-K. A Review on Adducin from Functional to Pathological Mechanisms: Future Direction in Cancer. *Biomed Res. Int.* 2018, (2018).

63. Naydenov, N. G. & Ivanov, A. I. Adducins regulate remodeling of apical junctions in human epithelial cells. *Mol. Biol. Cell* (2010).

64. Luo, C. & Shen, J. Adducin in tumorigenesis and metastasis. *Oncotarget* (2017).

65. Gross, A. *et al.* Desmoglein 2, but not desmocollin 2, protects intestinal epithelia from injury. *Mucosal Immunol.* (2018).

66. Klessner, J. L., Desai, B. V., Amargo, E. V., Getsios, S. & Green, K. J. EGFR and ADAMs cooperate to regulate shedding and endocytic trafficking of the desmosomal cadherin desmoglein 2. *Mol. Biol. Cell* (2009).

67. Sawyer, J. K. *et al.* A contractile actomyosin network linked to adherens junctions by Canoe/afadin helps drive convergent extension. *Mol. Biol. Cell* 22, 2491–2508 (2011).

68. Elloul, S., Kedrin, D., Knoblauch, N. W., Beck, A. H. & Toker, A. The adherens junction protein Afadin is an AKT substrate that regulates breast cancer cell migration. *Mol. Cancer Res.* 12, 464–476 (2014).

69. Zhai, X. *et al.* PI3K/AKT/Afadin signaling pathway contributes to pathological vascularization in glioblastomas. *Oncol. Lett.* 15, 1893–1899 (2018).

70. Lee, J. Y. *et al.* Molecular pathophysiology of epithelial barrier dysfunction in inflammatory bowel diseases. *Proteomes* 6, (2018).

71. Landy, J. *et al.* Tight junctions in inflammatory bowel diseases and inflammatory bowel disease associated colorectal cancer. *World Journal of Gastroenterology* 22, 3117–3126 (2016).

72. McCole, D. F. IBD candidate genes and intestinal barrier regulation. *Inflammatory Bowel Diseases* 20, 1829–1849 (2014).

73. Furuse, M. *et al. Direct Association of Occludin with ZO-1 and Its Possible Involvement in the Localization of Occludin at Tight Junctions*.

74. Christina M. Van Itallie*, M. S. B. and J. M. A. *Epidermal growth factor induces tyrosine phosphorylation and reorganization of the tight junction protein ZO-1 in A431 cells*. (1995).

75. Ma, T. Y. *et al.* TNF-induced increase in intestinal epithelial tight junction permeability requires NF-κB activation. (2004).

76. Fengjun Wang1,2,§, Brad T. Schwarz2,§, W. Vallen Graham2, Yingmin Wang2, L. S. IFN-γ-induced TNFR2 Upregulation is Required for TNFdependent Intestinal Epithelial Barrier Dysfunction.pdf.

77. Rhee, S. G. *et al.* Intracellular messenger function of hydrogen peroxide and its regulation by peroxiredoxins. *Current Opinion in Cell Biology* (2005).

78. Lovatt, M. *et al.* Peroxiredoxin-1 regulates lipid peroxidation in corneal endothelial cells. *Redox Biol.* (2020).

79. Neumann, C. A. *et al.* Essential role for the peroxiredoxin Prdx1 in erythrocyte antioxidant defence and tumour suppression. *Nature* (2003).

80. Rani, V., Neumann, C. A., Shao, C. & Tischfield, J. A. Prdx1 deficiency in mice promotes tissue specific loss of heterozygosity mediated by deficiency in DNA repair and increased oxidative stress. *Mutat. Res. - Fundam. Mol. Mech. Mutagen.* (2012).

81. Woo, H. A. *et al.* Inactivation of Peroxiredoxin I by Phosphorylation Allows Localized H2O2 Accumulation for Cell Signaling. *Cell* (2010).

82. Keel, S. B. *et al.* A heme export protein is required for red blood cell differentiation and iron homeostasis. *Science (80-.).* 319, 825–828 (2008).

83. Fiorito, V., Forni, M., Silengo, L., Altruda, F. & Tolosano, E. Crucial Role of FLVCR1a in the Maintenance of Intestinal Heme Homeostasis. *Antioxid. Redox Signal.* 23, 1410–1423 (2015).

84. Liu, T., Jiang, L., Tavana, O. & Gu, W. The deubiquitylase OTUB1 mediates ferroptosis via stabilization of SLC7A11. *Cancer Res.* (2019).

85. Xie, Y. *et al.* Ferroptosis: Process and function. *Cell Death and Differentiation* 23, 369–379 (2016).

86. Wang, H. *et al.* Characterization of ferroptosis in murine models of hemochromatosis. *Hepatology* 66, 449–465 (2017).

87. Zitvogel, L. & Kroemer, G. Interferon-Î³ induces cancer cell ferroptosis.

88. Wang, W. *et al.* CD8+ T cells regulate tumour ferroptosis during cancer immunotherapy. *Nature* 569, 270–274 (2019).

89. Immunotherapy Activates Unexpected Cell Death Mechanism. *Cancer discovery* 9, OF2 (2019).

90. Imai, H., Matsuoka, M., Kumagai, T., Sakamoto, T. & Koumura, T. Lipid peroxidation-dependent cell death regulated by GPx4 and ferroptosis. in *Current Topics in Microbiology and Immunology* 403, 143–170 (Springer Verlag, 2017).

91. Lee, S. H. Intestinal permeability regulation by tight junction: implication on inflammatory bowel diseases. *Intest. Res.* 13, 11–8 (2015).

92. Schoultz, I. & Keita, Å. V. cells Cellular and Molecular Therapeutic Targets in Inflammatory Bowel Disease-Focusing on Intestinal Barrier Function. (2019).

5. Chapter 5: General Discussion and Future Perspectives

5.1. General Discussion and future perspectives:

The increased incidence and prevalence of autoimmune diseases has become a major issue resulting in increased morbidity and mortality in the last few decades. The dysregulation of cytokine networks, especially the imbalance between pro-inflammatory and anti-inflammatory cytokines can be a major factor in the pathogenesis of several autoimmune diseases including Inflammatory bowel disease[1,2]. T helper type-1, cytokines IFN-γ and TNF-α are major regulators of intestinal homeostasis[3,4,5]. Elevated levels of these cytokines has been observed in biopsy tissues of patients with Inflammatory bowel disease (IBD) implicating them in disease pathogenesis[5–7] Distinctive features of IBD that affect the intestinal epithelium include, reduced epithelial cell proliferation, increased epithelial cell death, dysregulated cellular junctions, and injured stem cell niche[8–12]. Many studies have described the role of both IFN-γ and TNF-α in these above activities, showing them to be drivers of inflammation and immunopathology in IBD[1,2,13–15]. Moreover, the success of anti-TNF biologics and the JAK inhibitor, Tofacitinib represents a successful translation of discoveries in basic immunology into effective therapies for patients[16–18] . It has been more than 30 years since the phenomenon of synergism between IFN-γ and TNF-α was first identified both in terms of its effect on cell death and its anti-viral effects[19–21]. Since then several studies have investigated the synergistic effect of the two cytokines in several cellular processes including cell proliferation, gene regulation, chemokine secretion, and cell death[22–26], however the mechanisms involved remain unknown. The aim of my PhD research project was to further investigate and identify the mechanisms underpinning the synergistic effects of IFN-γ and TNF-α on cell death in CRC cell lines and primary colonic epithelial organoids.

In first part of our study **(Chapter-2)** we investigated the molecular mechanisms required for IFN-γ and TNF-α induced synergistic cell death in colonic epithelial cells[27] [28] . To identify the key kinases associated with IFN-γ and TNF-α induced cell death, we performed an RNAi mediated human kinome screen by using a library of 768 siRNAs against all human kinases. Our screen identified that JAK1 and JAK2 are the major kinases responsible for IFN-γ and TNF-α mediated synergistic cell death. Intriguingly, despite the known involvement of several important kinases in TNF-α associated signalling and canonical cell death pathways[29], none of these other kinases were significant hits in our screens. Furthermore, after performing a drug repurposing screen by screening a library of 2,766 small molecules, we identified JAK inhibitors as the only drugs which could block cytokine induced cell death, confirming the role of JAK1 and JAK2 as the main players in this cell death pathway. Thereafter, we also confirmed role of JAK1 and JAK2 using a panel of 7 JAK1 and/or JAK2 inhibitors. We also observed that there was activation of both apoptotic (caspase-8, 9, 10 and 3) and necroptotic markers (p-MLKL) in IFN-γ + TNF-α treated cells [30]. Therefore, we also investigated the role of TNF receptors and TNF associated cell death complexes in IFN-γ+TNF-α induced cell death. RNAi mediated knockdown of TNF receptors (TNFR1 and TNFR2) showed that TNFR1 but not TNFR2 was essential for induction of epithelial cell death. Therefore we investigated if TNFR1 played a role in the cell death pathway by forming apoptotic and necroptotic complexes (complex II a/b or IIc)[31] [32]. Cell death mediated by TNF-α and known sensitizers to either apoptosis or necroptosis was blocked by apoptotic and necroptotic inhibitors indicating the role of TNFR1 canonical complexes, while cell death induced by IFN-γ + TNF-α was independent of TNFR-1 canonical cell death pathways could not be rescued by inhibitors of apoptosis or necroptosis. Furthermore, by performing BAK/BAX knock-down we eliminated the requirement for canonical mitochondria associated intrinsic cell death pathways in IFN-γ+TNF-α induced killing.

It was interesting to note that, even though IFN-γ+TNF-α treatment induced activation of caspases 8, 9, 10, 3 & 7 and also MLKL phosphorylation (necroptotic marker), blocking apoptosis and/or necroptosis by selective inhibitors did not rescue the cells. We also identified the accumulation of reactive oxygen species (ROS) in IFN-γ+TNF-α treated cells. Considering previous studies suggesting the role of ROS in IFN-γ+TNF-α induced cell death we investigated the role of ROS in the process[33–35] Interestingly, we observed significant generation of cytoplasmic ROS after IFN-γ+TNF-α treatment but blocking ROS generation using the ROS scavenger N-acetyl-L-cysteine (NAC) could not rescue the cells even though treatment with the JAK 1/2 inhibitor baricitinib reduced ROS level to baseline (DMSO treated cells). This data suggests that the generation of ROS may play a role in one of the multiple cell death pathways activated in response to IFN-γ+TNF-α treatment.

One of the most interesting findings in our study was the identification of a new signalling role for caspase-8. Even though we found that the catalytic activity of caspase-8 is not essential for IFN-γ+TNF-α induced cell death, the presence of procaspase-8 protein was required for cell death. By using RNAi mediated caspase 8 knock-down and HT-29 *CASP8*$^{-/-}$ cell line we identified that caspase 8 protein is an essential component of the cell death signalling pathway in IFN-γ+TNF-α treated cells, independent of its catalytic activity. Similar to caspase-8, we also identified a role for RIPK3 in the cell death pathway independent of kinase activity. Even though the human kinome RNAi screen did not show any effect of RIPK3 knockdown on cell death rescue, HT-29 *RIPK3*$^{-/-}$ cell lines were resistant to IFN-γ+TNF-α induced cell death. Therefore, further investigation is required to confirm the role of RIPK3 in cell death induced by IFN-γ+TNF-α. The non-enzymatic role of caspase 8 and RIPK3 in IFN-γ+TNF-α induced cell death suggests the possible involvement of caspase-8 and RIPK3 as scaffold molecules for the formation a unique cell death complex for the induction of cell death.

Altogether, our work performed in CRC cell lines and human colonic 3D organoid lines confirmed that IFN-γ+TNF-α synergises to induce cell death in a JAK1/2-STAT1 dependent manner and is also dependent on caspase 8 and RIPK3. Even though our study was successful in providing new insights into the underlying mechanism of IFN-γ/TNF-α induced cell death, there are still several unanswered questions to address.

- Does TNFR1 connect with the JAK-STAT signalling pathway as has been reported in several studies or does it require the formation of a novel cell death signalling complex?
- Is caspase-8 required for formation of this signalling complex and what other proteins are involved?
- Is RIPK3 required for formation of this proposed signalling complex and what additional proteins are involved?

Future planned experiments will investigate these questions using co-immunoprecipitation of Caspase-8, RIPK3, JAK1 and JAK2 and other candidate protiens. Such a strategy may give an interaction profile of proteins associated with Caspase 8 and may possibly identify the other components of this novel cell death signalling complex.

The relative concentration of IFN-γ and TNF-α plays an important role in deciding cellular outcomes. For example, high concentrations of IFN-γ and/or TNF-α are reported to deliver anti-tumour effects while lower concentrations of IFN-γ and/or TNF-α can lead to inflammatory and proliferative effects possibly contributing to their pro-tumorigenic activities. Therefore, in the second part of my PhD **(Chapter-3)** I focused on understanding the relationship between cytokine concentration and cell life-and-death decisions. Our results showed that IFN-γ+TNF-α synergised to induce cell death in CRC cells in a dose or concentration dependent manner. We found that a low concentration of IFN-γ+TNF-α was

sufficient to induce expression of pro-inflammatory genes in the cells but a certain threshold concentration of the two cytokines was required for induction of cell death. By comparing the effect of different doses of IFN-γ+TNF-α on CRC cells we identified that IFN-γ+TNF-α induced a dose-to-duration pattern of JAK1-JAK2-STAT1 signalling whereby a low cytokine concentration induced a transient activation of the JAK1/2-STAT1 signalling pathway while at higher cytokine concentration there was sustained activation of the pathway. This pattern of signalling has been described as 'dose-to-duration' signalling. To investigate the role of this sustained activation of the JAK1/2-STAT1 pathway on epithelial cell death, we blocked JAK1/2-STAT1 signalling after regular intervals of time post-cytokine treatment. We showed that blocking the JAK1/2-STAT1 pathway even 10 hours after IFN-γ+TNF-α treatment could rescue the cells from cell death. Our data suggested that sustained activation of the JAK1/2-STAT1 pathway is essential for induction of cell death. Furthermore, our results also show that there is a sustained STAT1 pY701 phosphorylation in the nucleus of cells with higher cytokine concentration suggesting a transcriptionally active STAT1 at later time points. Therefore, to investigate the effect of cytokine concentration on gene expression in a temporal manner we performed RNA-Sequencing of cells treated with IFN-γ+TNF-α at different concentrations and for different durations of time. Our results show that IFN-γ+TNF-α induced expression of a set of genes associated with different cell death pathways (apoptosis, necroptosis, ferroptosis and related pathways) and metabolic activity, at later time points. The association of these late genes with cell death and related processes further supports the importance of IFN-γ + TNF-α induced dose-to-duration signalling in cell death.

Interestingly, some of these cell deaths associated genes were only differentially expressed at the later time point with the higher concentration of cytokines. Furthermore, our study shows that at the latee time point there was downregulation of several genes associated

with the tricarboxylic acid cycle (TCA) cycle and oxidative phosphorylation, suggesting an impaired mitochondrial and cellular function at this point. Due to limitation of time for completion of my PhD, I could not perform the validation of these late genes. It will be important to investigate the importance of these differentially expressed 'late genes' on epithelial cell death and biological activities. The genes expressed only at late time point and high dose of cytokines could be relevant for understanding the mechanism of this unique form of cell death.

In final part of my thesis **(Chapter-4)**, we provided new mechanistic insights into how JAK1 and JAK2 dysregulate epithelial homeostasis and epithelial barrier function[36–38]. To investigate the role of the late phase of JAK1 and JAK2 activity, we first confirmed that late kinase activity of JAK1 and JAK2 is critical for IFN-γ and TNF-α induced cell death. We then used a phospho-proteomic approach and identified 45 proteins associated with late kinase activity of JAK1 and JAK2. By performing a thorough search through literature, I concluded that from our hit list of 45 proteins, there were 16 proteins previously reported for to be associated with JAK1 and JAK2 activity in different cellular processes, while there were 29 novel targets identified in this study. Even though their role has been reported in the literature as regulators of cell structure, cell adhesion, and cell-cell interaction, their role in IFN-γ/TNF-α biology still needs to be verified. Going through the targets individually we found that most of the known proteins from the list were associated with JAK-STAT signalling pathways. It was not surprising to see the tight junction proteins in the list, further confirming the role JAKs in regulation of epithelial barrier function. Functional analysis of these novel JAK targets identified them to be involved in focal adhesions, cytoskeleton, cell-cell junctions and ferroptosis. Even though the role of these proteins has been identified to be associated with cellular activities, the importance of tyrosine phosphorylation of these proteins has not been explored before. It will

be important to investigate the importance of tyrosine phosphorylation of these proteins and its contribution to the cell death pathway. Because many of these represent new phospho-sites, we could not avail of commercially available phospho-antibodies for most of the hits for our validation studies. So, it will be interesting to confirm the role of JAK mediated tyrosine phosphorylation on the function of these proteins and further understand their role in epithelial biology.

Overall, my PhD research has made significant discoveries in relation to the mechanisms underpinning IFN-γ + TNF-α synergism. These include (1) identification of the signalling mechanism behind IFN-γ/TNF-α induced cell death of epithelial cells, (2) identification of a dose-to-duration signalling mechanism underpinning the concentration dependent effects of IFN-γ+TNF-α on epithelial cell biology (3) identification of new protein substrates of JAK1 and JAK2 that may provide additional mechanism for epithelial barrier disruption by JAKs. In addition to deepening our understanding about IFN-γ+TNF-α synergism, our study also identified novel gene and protein targets associated with these processes. Studying these signalling mechanisms and targets and their role in the context of immune-mediated cell death, gut epithelial barrier function, chronic inflammatory diseases and tumour immunity may provide new opportunities for understanding disease biology and therapeutic development.

5.2. References

1. Park, J. H., Peyrin-Biroulet, L., Eisenhut, M. & Shin, J. Il. Inflammatory Bowel Diseases (IBD) immunopathogenesis: A comprehensive review of inflammatory molecules. (2017).
2. Vitale, S. et al. Cytokine production profile in intestinal mucosa of paediatric inflammatory bowel disease. (2017).
3. Neurath, M. F. Targeting immune cell circuits and trafficking in inflammatory bowel disease. Nature Immunology (2019).
4. Macdonald, T. T., Hutchings, P., Choy, M.-Y., Murch, S. & Cooke, A. Tumour necrosis factor-alpha and interferon-gamma production measured at the single cell level in normal and inflamed human intestine. Clin. exp. Immunol 81, (1990).
5. Hu, S. et al. TNF-α and IFN-γ synergistically inhibit the repairing ability of mesenchymal stem cells on mice colitis and colon cancer. Am J Transl Res 11, (2019).
6. Vitale, S. et al. Cytokine production profile in intestinal mucosa of paediatric inflammatory bowel disease. (2017).
7. Muzes, G., Molnár, B., Tulassay, Z. & Sipos, F. Changes of the cytokine profile in inflammatory bowel diseases. World J. Gastroenterol. 18, 5848–5861 (2012).
8. Maloy, K. J. & Powrie, F. Intestinal homeostasis and its breakdown in inflammatory bowel disease. Nature 474, 298–306 (2011).
9. Schoultz, I. & Keita, Å. V. cells Cellular and Molecular Therapeutic Targets in Inflammatory Bowel Disease-Focusing on Intestinal Barrier Function. (2019).
10. Williams, J. M. et al. Epithelial Cell Shedding and Barrier Function: A Matter of Life and Death at the Small Intestinal Villus Tip. Vet. Pathol. (2015).

11. Landy, J. et al. Tight junctions in inflammatory bowel diseases and inflammatory bowel disease associated colorectal cancer. World Journal of Gastroenterology 22, 3117–3126 (2016).
12. Ruder, B., Atreya, R. & Becker, C. Tumour necrosis factor alpha in intestinal homeostasis and gut related diseases. Int. J. Mol. Sci. 20, (2019).
13. Strober, W. & Fuss, I. J. Proinflammatory cytokines in the pathogenesis of inflammatory bowel diseases. Gastroenterology 140, 1756-1767.e1 (2011).
14. Nava, P. et al. IFN gamma regulates intestinal epithelial homeostasis through converging Beta-catenin signaling pathways. Immunity 32, 392–402 (2010).
15. Koch, S. & Nusrat, A. The Life and Death of Epithelia During Inflammation: Lessons Learned from the Gut. Annu. Rev. Pathol. Mech. Dis. 7, 35–60 (2012).
16. T. Virtanen, A., Haikarainen, T., Raivola, J. & Silvennoinen, O. Selective JAKinibs: Prospects in Inflammatory and Autoimmune Diseases. BioDrugs 33, 15–32 (2019).
17. Adegbola, S. O., Sahnan, K., Warusavitarne, J., Hart, A. & Tozer, P. Molecular Sciences Anti-TNF Therapy in Crohn's Disease. Int. J. Mol. Sci. 19, 1–21 (2018).
18. Danese, S., Argollo, M., Le Berre, C. & Peyrin-Biroulet, L. JAK selectivity for inflammatory bowel disease treatment: does it clinically matter? Gut 68, 1893–1899 (2019).
19. Williamson, B. D., Carswell, E. A., Rubin, B. Y., Prendergast, J. S. & Old, L. J. Human tumor necrosis factor produced by human B-cell lines: Synergistic cytotoxic interaction with human interferon. Proc. Natl. Acad. Sci. U. S. A. (1983).
20. Wong, G. H. W. & Goeddel, D. V. Tumour necrosis factors α and β inhibit virus replication and synergize with interferons. Nature (1986).

21. Aggarwal, B. B. & Eessalu, T. E. Induction of receptors for tumor necrosis factor-α by interferons is not a major mechanism for their synergistic cytotoxic response. J. Biol. Chem. (1987).
22. Monocytes, H. T.- et al. Essential Involvement of Cross-Talk Between IFN- g and TNF- a in CXCL10 Production in human THP-1 monocytes. 690–697 (2009).
23. Robinson, C. M., Shirey, K. A. & Carlin, J. M. Synergistic Transcriptional Activation of Indoleamine Dioxygenase by IFN-g and Tumor Necrosis Factor-a. JOURNAL OF INTERFERON & CYTOKINE RESEARCH 23, (2003).
24. Li, N. et al. Cross-talk between TNF-α and IFN-γ signaling in induction of B7-H1 expression in hepatocellular carcinoma cells. Cancer Immunol. Immunother. 67, 271–283 (2018).
25. Viard-Leveugle, I. et al. TNF-α and IFN-γ are potential inducers of fas-mediated keratinocyte apoptosis through activation of inducible nitric oxide synthase in toxic epidermal necrolysis. J. Invest. Dermatol. 133, 489–498 (2013).
26. Shen, J. et al. Anti-cancer therapy with TNFα and IFNγ: A comprehensive review. Cell Prolif. 51, e12441 (2018).
27. Kimura, M. et al. TNF combined with IFN-α accelerates NF-κB-mediated apoptosis through enhancement of Fas expression in colon cancer cells. Cell Death Differ. 10, 718–728 (2003).
28. Woznicki, J. A. et al. Human BCL-G regulates secretion of inflammatory chemokines but is dispensable for induction of apoptosis by IFN-γ and TNF-α in intestinal epithelial cells.
29. Brenner, D., Blaser, H. & Mak, T. W. Regulation of tumour necrosis factor signalling: live or let die. Nat. Rev. Immunol. 15, 362–374 (2015).
30. Murphy, J. M. et al. The pseudokinase MLKL mediates necroptosis via a molecular switch mechanism. Immunity 39, 443–453 (2013).

31. Silke, J., Rickard, J. A. & Gerlic, M. The diverse role of RIP kinases in necroptosis and inflammation. Nat. Immunol. 16, 689–697 (2015).
32. Kondylis, V., Kumari, S., Vlantis, K. & Pasparakis, M. The interplay of IKK, NF-κB and RIPK1 signaling in the regulation of cell death, tissue homeostasis and inflammation. Immunological Reviews 277, 113–127 (2017).
33. Yang, D. et al. Pro-inflammatory cytokines increase reactive oxygen species through mitochondria and NADPH oxidase in cultured RPE cells. Exp. Eye Res. 85, 462–472 (2007).
34. Chen, X. et al. Role of Reactive Oxygen Species in Tumor Necrosis Factor-alpha Induced Endothelial Dysfunction. Curr. Hypertens. Rev. 4, 245–255 (2008).
35. Wang, Y. et al. The STAT-ROS cycle extends IFN-induced cancer cell apoptosis. Int. J. Oncol. 52, 305–313 (2018).
36. Nayden G. Naydenov, 1, * somesh Baranwal, 1 & shadab Khan, 2 alex Feygin, 1 pooja Gupta1 and andrei I. Ivanov1, 3, 4. Novel mechanism of cytokine-induced disruption of epithelial barriers:Janus kinase and protein kinase D-dependent downregulation of junction protein expression. (2013).
37. Coskun, M., Salem, M., Pedersen, J. & Nielsen, O. H. Involvement of JAK/STAT signaling in the pathogenesis of inflammatory bowel disease. Pharmacol. Res. 76, 1–8 (2013).
38. Richmond, C. A. et al. JAK/STAT-1 Signaling Is Required for Reserve Intestinal Stem Cell Activation during Intestinal Regeneration Following Acute Inflammation. Stem Cell Reports (2018).

Acknowledgment

During this time, so many people have helped and supported me. I am very glad to have this opportunity to extend my gratefulness to all of them. Without them, it would not have been possible to complete this thesis. I would like to start by thanking Ireland for being such a welcoming country and for making my PhD so joyful. I am very grateful to University College Cork for giving me this opportunity and to Science foundation Ireland for providing me the funding to do my research.

Most importantly, I would like to express my sincere gratitude to my supervisor Dr. Ken Nally for the continuous support during my PhD study and related research, for his patience, motivation, and immense knowledge. His guidance helped me in all the time during my research and thesis. I would like to thank Dr. Silvia Melgar for her support and all the valuable comments and friendly behaviour. I am very grateful to Dr. Amanda Lohan as well for organising everything for my research and making it easier.

Next, I would like to thank my two amazing buddies: Ana and Sree for starting this PhD journey with me and for supporting me till the end. Sree, thank you so much for being my best friend and giving me company not only in lab but outside as well, you are irreplaceable in my life. Ana, thank you so much being such a huge emotional support and giving me the right advice, you were the only one I could always trust with all my secrets. I would like to thank Valerio, for being my stress buster in the lab. Valerio, you could always make me smile, no matter how difficult the time was and yes, we need to go for more night-outs. My great thanks to Subha for being my lab buddy for all those years. Subha, you were so helpful throughout, that I don't know how I would have survived my PhD without you. Thank you so much for helping me with all that experimental work and making my PhD a bit easier.

I am also very grateful to Jerzy for helping me get through my research and doing all the troubleshooting with me, and also thanks for continuing the project after me. My sincere thanks to Agnes, Milan and Pepi for not only helping with my research but also for being such a great motivation. Also, a big thanks to Peter for doing all that organoid hard work for me. I would also like to thank Janaki for doing all the bioinformatics work for me and especially keeping her calm even after being asked to do re-analysis the data for small things for so many times. Thanks to Ana Ramon for being such a good friend in very short time.

There is a long list of people I want to thank outside the lab and were a big part of my PhD. I would like to start with thanking Milind for being such a wonderful friend and husband. Thanks for being so patient with me and specially to bear with all my tantrum on the name of my PhD. But I am upset that soon I will lose that PhD excuse for my actions. But really, thank you so much for helping me, supporting me, loving me and most importantly helping me with all the formatting of my thesis. I would also like to thank Samreen for being my family in Ireland. Samreen, you are my stress buster, thanks for all those coffee treats, long drives, delicious food, pampering and sound advice, basically thanks for spoiling me. I would also like to thank my amazing friend Helena for always motivating me and for visiting me here in Ireland every year. Thanks to Pooja for listening to all my venting all the time and still being so supportive.

Finally, my deep and sincere gratitude to my family for their continuous and unparalleled love, help and support. Thanks to Mom and Dad for giving me the courage to chase my dream. I would like to thank my sister Poonam and Jeeju Parkash for helping me throughout my life. A huge credit of what I have achieved so far, goes to you both. Thanks to my brother Sachin and sister Neelam being there for me as a friend.

Thanks to everyone who supported me and helped me go through my PhD journey.

THANK YOU ALL!!!!